# *Wolbachia*-mediated arbovirus inhibition in *Aedes* mosquitoes

A thesis submitted for the degree of Doctor of Philosophy at the University of Glasgow

Christie Herd

Centre for Virus Research
College of Medical, Veterinary and Life Sciences
University of Glasgow

September 2018

# Abstract

Currently, *Aedes aegypti* mosquitoes carrying *Wolbachia* strains *w*Mel and *w*AlbB, both of which provide good levels of arbovirus transmission inhibition, are being used in field releases for dengue control. Other strains of*Wolbachia* might provide even stronger virus transmission inhibition in *Ae. aegypti*. *w*Au and *w*AlbA were transinfected into *Ae. aegypti* and fitness traits were characterised, as well as the ability to block arbovirus replication and transmission. These data reveal that while *w*Au provides complete viral blockage of dengue and Zika virus, it has a detrimental effect on fitness with reduced adult longevity and egg survival. Interestingly, although *w*AlbA reached a high density in the *Ae. aegypti* host, no pathogen inhibition was observed following challenge with Semliki Forest Virus.

The suitability of *w*Mel, *w*Au and *w*AlbB-infected *Ae. aegypti* for field releases was examined by exposing larvae to higher temperatures that can occur in the field. An experimental temperature cycle was based on water temperatures recorded from larval breeding sites in Trinidad and environmental temperature in Malaysia. Larvae were exposed to these temperatures, or the normal insectary rearing temperatures, and the impact this had on *Wolbachia* density was assessed. Data revealed *w*Mel and *w*Au were not stable following heat-treatment, with drops in whole-body and ovary density, leading to reductions in maternal transmission rate. On the other hand, *w*AlbB remained stable following heat-treatment. Heat-treated mosquitoes were then challenged with Semliki Forest virus, revealing no significant loss of the pathogen-inhibition phenotype.

*Aedes* cell lines infected with the high-density *w*MelPop and *w*Au *Wolbachia* strains were used to investigate the mechanism of *Wolbachia*-mediated pathogen inhibition. One hypothesis is that transinfection of *Wolbachia* into novel hosts primes the immune system against viruses by inducing oxidative stress. While *Ae. aegypti* (Aag2) *w*MelPop cells showed evidence of oxidative stress, *Ae. albopictus* (Aa23) wAu did not, yet both are strong blockers of arboviruses. Gene transcription assays indicated that *w*MelPop is interfering with the expression of protein chaperones that are involved in the folding of proteins in the endoplasmic reticulum (ER). This indicates *Wolbachia* may be modifying the ER and thereby preventing incoming virus from completing replication.

# Table of Contents

# List of Tables

# List of Figures

# Acknowledgements

Firstly I'd like to thank my parents Dave and Christine Herd, who have provided me with unconditional love and support throughout my entire PhD. Thank you to my brother David and sister-in-law Heather (the first Herd that was a Dr) that have encouraged me along the way and provided an escape with road trips and holidays- it meant a lot and kept me sane.

I cannot thank Thomas Ant enough for all the laughs and support he provided me during most of my PhD – we survived together and I know we will be friends for life. Also to the past lab members Caroline Harris and Vincent Geoghegan – you have both helped me in many ways. To the current lab members who have helped me ensure I finished this PhD in one piece and with lots of data; Mariavittoria Mancini and our never-ending virus challenges, Stephanie Rainey with her never-ending support with any lab-related question, Sara Elg and her never-ending help with rearing the mosquitoes. My PhD would not have been possible without working with a mixture of great people, so thank you.

Last but not least, thank you to my supervisor Steve for choosing me to do this PhD in the first place. For letting me join a great lab with many resources and work on exciting topics that have a real impact in the field. Thank you for providing me support when required and acknowledging my importance in the lab.

# Author's Declaration

The research reported within this thesis is my own work unless otherwise stated and has not been submitted for any other degree. A number of the experiments reported in chapter 4 were carried out jointly with Dr Thomas Ant. Some of the data included in the chapter was published in Ant TH, Herd CS, Geoghegan V, Hoffmann AA, Sinkins SP (2018) The *Wolbachia* strain *w*Au provides highly efficient virus transmission inhibition in *Aedes aegypti*. PLoS Pathog 14(1): e1006815. https://doi.org/10.1371/journal.ppat.1006815. Novel *Wolbachia* transinfections in *Ae. aegypti* were created by Thomas Ant. The rest of the experiments were carried out 50/50 with Thomas Ant, with the exception of fig.4.2.5, fig.4.2.6 and fig.4.2.7, which were performed alone. For chapter 5; larval rearing, dissections and detection of *Wolbachia* was performed jointly with Dr Mariavittoria Mancini. Part of this data is submitted (under review) in Nazni et al (2019) 'Dengue case reduction following invasion of Malaysian *Aedes aegypti* by *Wolbachia* strain wAlbB'.

Christie S Herd

# Abbreviations

| | |
|---|---|
| +ve | Positive |
| 2HPCD | 2-hydroxypropyl-beta-cyclodextrin |
| AMP | Antimicrobial peptide |
| BHK | Baby hamster kidney |
| Bti | *Bacillus thuringiensis israelensis* |
| CECD | Cecropin D |
| CECG | Cecropin G |
| CHIKV | Chikungunya virus |
| CHPx | Cumene hydroperoxide |
| CI | Cytoplasmic incompatibility |
| DC-SIGN | Dendritic-cell specific intracellular adhesion molecule |
| DCV | *Drosophila* C Virus |
| DEFC | Defensin C |
| DEGs | Driving endonuclease genes |
| DENV | Dengue virus |
| D.P.O. | Days post-eclosion |
| ER | Endoplasmic reticulum |
| ERAD | Endoplasmic-reticulum associated degradation |
| FFA | Fluorescent focus assay |
| FHV | Flock house virus |
| FISH | Fluorescent in-situ hybridisation |
| FLOW-FISH | Flow cytometry fluorescent in-situ hybridisation |
| $H_20_2$ | Hydrogen peroxide |
| HEGs | Homing endonuclease genes |
| HTH | Homothorax reference gene |
| IIV6 | Insect iridescent virus 6 |
| Imd | Immune deficiency pathway |
| IR | Insecticide resistance |
| ITN | Insecticide-treated net |
| IVM | Integrated vector management |
| JAK-STAT | Janus kinase transcription pathway |
| miRNA | Micro RNA |
| MAYV | Mayaro virus |
| MOI | Multiplicity of infection |
| NAC | N-acetyl cysteine |
| NHP | Non-human primates |
| ONNV | O'nyong yong |
| PBS | Phosphate buffer solution |
| PCR | Polymerase chain reaction |
| piRNA | Piwi-interacting RNA |
| PRR | Pattern recognition receptors |
| RT-qPCR | Reverse transcriptase quantitative PCR |
| RdRp | RNA dependent RNA polymerase |
| RIDL | Release of a dominant-lethal gene |
| ROS | Reactive oxygen species |
| SFV | Semliki forest virus |
| SINV | Sindbis virus |
| SiRNA | Small interfering RNA |
| SIT | Sterile insect technique |
| SNP | Single nucleotide polymorphism |

| | |
|---|---|
| SsRNA | Single-stranded RNA |
| TBHP | Tert-butyl hydroperoxide |
| UPR | Unfolded protein response |
| -ve | Negative |
| WHO | World Health Organisation |
| WNV | West nile virus |
| WT | Wild type |
| YFV | Yellow fever virus |
| ZIKV | Zika virus |

# Chapter 1

## Introduction

# 1. Introduction

## 1.1 The spread of Arboviruses

There are over 3000 species of mosquitoes in the world, of which several hundred bite humans. Mosquitoes are a biting nuisance to those in sub-tropical and tropical climates, but importantly mosquitoes of the *Anopheles*, *Culex* and *Aedes* genera transmit arthropod-borne viruses (arboviruses) of serious medical concern to humans. *Aedes aegypti* is the primary vector of dengue (DENV), chikungunya (CHIKV) and Zika (ZIKV) viruses. All three viruses originated in Africa and Asia but have spread to the semi-tropical and tropical Americas, recently in the case of ZIKV and CHIKV (Deilgat et al., 2014; ECDC, 2016; Zanluca et al., 2015) .

DENV, CHIKV and ZIKV have similar clinical manifestations in humans, which include fever, severe joint pain, muscle pain, fatigue and a rash. DENV (genus *Flavivirus*, family *Flaviviridae*) causes a severe flu-like illness, but a small percentage of cases develop into severe dengue, which can result in total organ shut down and death. DENV is endemic in more than 100 countries with the most affected areas occurring in the Western Pacific, the Americas and South-East Asia (CDC, 2014). DENV has had an increasing effect on human morbidity and mortality in these regions, particularly from 2010 onwards (Figure 1.1.A). There is also an increasing risk of transmission of DENV in more temperate regions, due to the expansion of the geographical range of *Ae. albopictus* (Fig.1.1.B). Colonisation of *Ae. albopictus* in Europe has resulted in local transmission of DENV in France and Croatia, with imported cases of the virus in three other countries in Europe (Rezza, 2014; WHO, 2017c).

Another arbovirus increasingly invading new territories is CHIKV (genus *Alphavirus*, family *Togaviridae*), a debilitating disease which manifests mainly as arthralgia and fatigue in a human host. As there is no cure, treatment involves trying to relieve the patient of these symptoms. CHIKV was first identified in 1952 in Africa and Asia, however following later re-emergence of the virus in 2004, cases were then identified in countries in and around the Indian Ocean, including the Americas (Yactayo et al., 2016). An outbreak of CHIKV on Reunion Island in the Indian Ocean in 2005 involved over 200,000 cases, spanning twelve months, and significantly there was a 1 in 1000 fatality rate (Josseran et al., 2006). Alarmingly,

there has been local transmission of CHIKV in France and Italy in 2017, with the latter outbreak consisting of over 100 confirmed cases (WHO, 2017b). The increasing frequency of local transmission in previously non-endemic areas shows the rapid spread of these arboviruses.

A large outbreak of Zika virus (ZIKV: genus *Flavivirus*, family *Flaviviridae*) in Brazil in 2015 highlighted the risk of complications associated with arboviral infections. Over 1 million cases of ZIKV were reported, with over 4,000 associated cases of

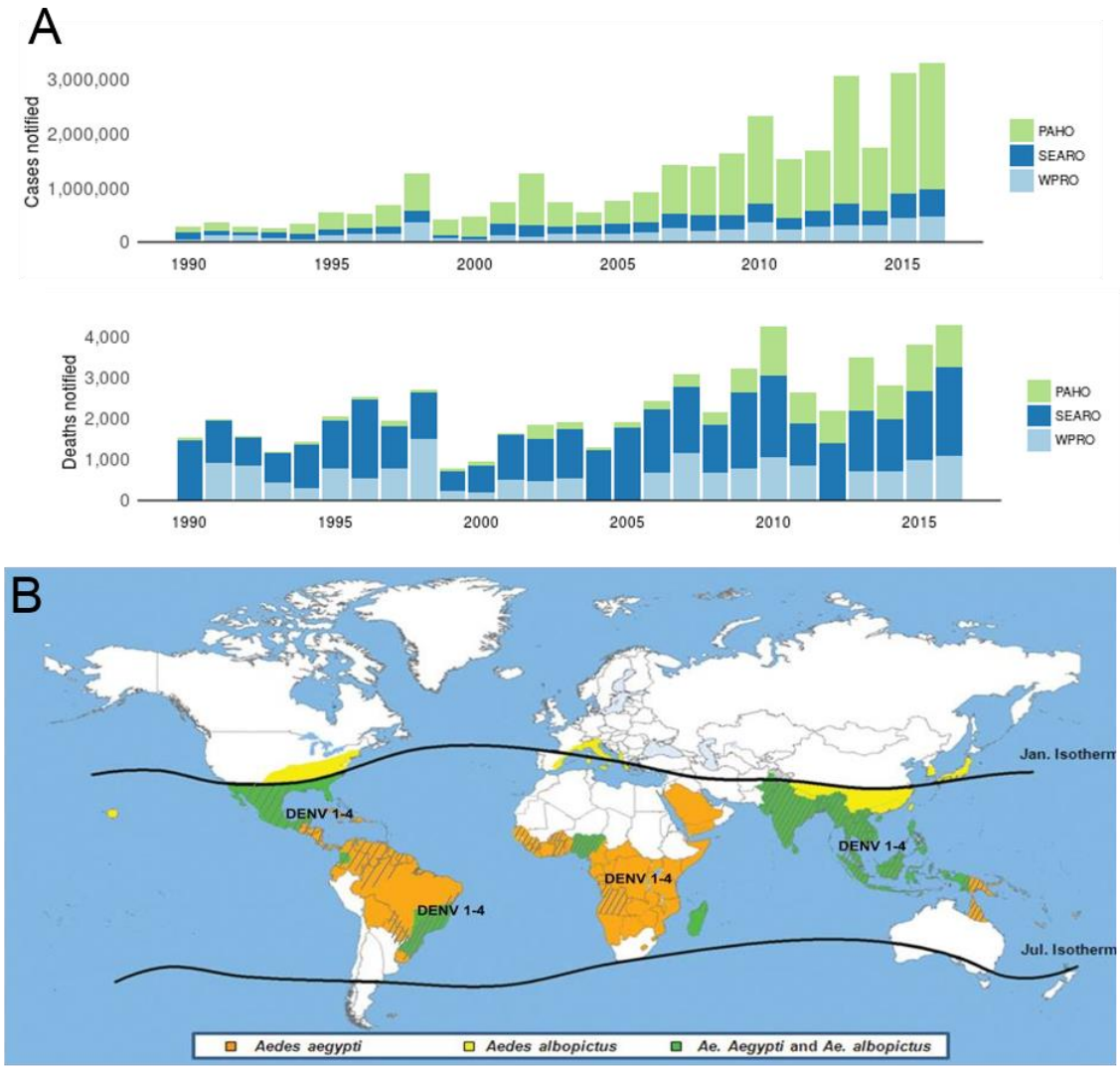


**Figure 1.1. Global burden of Dengue virus.**

Data shows a Dengue cases and deaths reported to the World Health Organisation from 1990- 2016 **(A)**. There is a general increase in Dengue cases since 2010. PAHO = The Americas, SEARO = South-East Asia, WPRO = Western Pacific. (CDC, 2017c; Deilgat et al., 2014; WHO, 2016a). Map shows equatorial belt of typical Dengue endemic areas **(B)** indicating that all four serotypes have been found there. Map also shows presence of *Aedes aegypti* (orange), *Aedes albopictus* (yellow) and both (green). Note yellow areas in North America and Europe which indicate spread of *Ae. albopictus* to temperate regions (Rezza, 2014).

microcephaly in infants born of an infected mother (Heukelbach et al., 2016). ZIKV infection can also result in the development of Guillian-Barre syndrome in adults, in which the immune system attacks the peripheral nervous system (ECDC, 2015). Towards the end of 2016, local transmission of ZIKV also occurred in the states of Texas and Florida in North America (CDC, 2017a). Although these areas are no longer at risk of local transmission, there is still potential for ZIKV to spread further in North America. The spread of arboviruses into areas with humans that have previously not been exposed to these viruses also increases the risk of serious disease complications, as they have not developed immunity from previous exposure to the virus.

*Aedes* mosquitoes also transmit Yellow fever virus (YFV) (genus *Flavivirus*, family *Flaviviridae*) which typically causes a febrile illness, however, a small proportion of those infected will develop severe symptoms including organ shutdown, which proves fatal. YFV is endemic in tropical areas of South America and Africa, but does have an effective vaccine that provides life-long immunity (WHO, 2016). However, with limited vaccine supplies and capacity to deliver this to the public, deadly outbreaks have occurred in Central/South America in recent years; one outbreak between December 2016 and March 2018 led to 500 deaths in Brazil, a country where the last documented outbreak was in 1942 (Possas et al., 2018). Due to this outbreak, travellers in Brazil then transported YFV to 7 countries in Europe in 2018; a region which had only experienced 3 cases of YFV in the previous 16 years (Barrett, 2018).

Another arbovirus increasingly imported from Central/South America to Europe is the emerging Mayaro virus (MAYV) (genus *Alphavirus*, family *Togaviridae*), which is in the same antigenic complex as Semliki Forest virus (SFV), a model alphavirus. MAYV was first documented in Trinidad in the 1950s and is commonly reported in Central/South America and the Caribbean (Izurieta et al., 2018). In severe cases, MAYV can cause paralysis, haemorrhaging and death. MAYV was previously contained in a sylvatic cycle between non-human primates and mosquitoes such as *Haemagogus janthinomys*, which is normally found in the top canopy of rainforest, with sporadic human cases occurring near forest areas. However, disturbance of the canopy by urbanisation can cause the vector to remain at ground level, increasing the chances of transmission to humans. In addition, *Ae*.

*aegypti* and 4 species of *Anopheles* mosquitoes, which are all present in North America, have been shown to be competent vectors of MAYV in laboratory settings (Brustolin et al., 2018; Long et al., 2011). MAYV has been recorded in a semi-rural area of Haiti, indicating the potential for urban spread. Imported cases of MAYV have occurred in 4 countries in Europe between 2008-12 due to returning travellers from endemic areas, showing the potential of geographical spread (Friedrich-Jänicke et al., 2014; Hassing et al., 2010; Receveur et al., 2010; Theilacker et al., 2013). The clinical symptoms of MAYV, CHIKV, DENV and ZIKV are so similar that the term "ChikDenMaZika syndrome" has been coined when diagnosing febrile illness, highlighting the difficulty of arbovirus indentification and increase in occurrence of infection in humans (Acosta-Ampudia et al., 2018).

*Anopheles* and *Culex* mosquitoes are capable of spreading arboviruses different to those spread by *Aedes* mosquitoes, enabling the opportunity for interepidemic transmission of various arboviruses. *Anopheles* mosquitoes are the main vector of the malaria parasite, *Plasmodium*, a leading cause of morbidity and mortality in sub-Saharan Africa (WHO, 2017e). *Anopheles* mosquitoes can also transmit O'nyong yong virus (ONNV) which, like most arboviruses, causes a febrile illness and arthralgia. ONNV is becoming more of a problem in East Africa as its prevalence in communities has been increasing over the past three decades, and epidemics cycle alternate to CHIKV (LaBeaud et al., 2015).

*Culex* mosquitoes are responsible for the transmission of the closely related West Nile virus (WNV) and Japanese encephalitis virus (JEV) (genus *Flavivirus*, family *Flaviviridae*). For the majority, infection with WNV is asymptomatic, but 20% of those infected develop a typical arbovirus fever. For a small percent of those infected, WNV can be fatal when it develops into a neuroinvasive disease such as encephalitis, meningitis or acute flaccid paralysis. An estimated 1 in 150 cases of WNV are fatal due to invasion of the brain (WHO, 2011). WNV is present in several continents including West Asia, the Middle East, Africa, Europe and North America. The WNV life cycle involves replication in birds, which make long migratory journeys, allowing the virus to 'piggyback' across wider territories. WNV has spread successfully to almost every state in North America and was responsible for just under 2000 deaths cumulatively from 1999-2015 (CDC, 2017b). The threat of neuroinvasive WNV is current in North America and highlights the fact that

arboviruses are not restricted to sub-tropical climates, as WNV has spread to even northerly states.

Typical symptoms of JEV include headache and mild fever and as with WNV, a small percentage develop severe symptoms which can result in encephalitis, paralysis and death. Infact, the fatality rate of people presenting with severe JEV symptoms can be as high as 30% (WHO, 2015). JEV is typically maintained in a cycle with *Culex* mosquitoes (particularly *Cx. Tritaeniorhynchus*) and vertebrates such as pigs and birds. Humans are a dead-end host of WNV and JEV, as the virus does not achieve a high enough viraemia in the blood to be transmitted to a feeding mosquito (CDC, 2015). JEV is a leading cause of encephalitis across South-East Asia; virus spread is correlated with increased agricultural development of pig farming and intensive rice cultivation. However, there is increasing cases of imported cases due to travellers and spread of JEV into new territories, even in high altitude regions (Di Francesco et al., 2018; Zhang et al., 2017). JEV has previously been considered a rural disease, however mosquitoes collected from an urban city in South Vietnam have tested positive for the virus (Lindahl et al., 2013). Although there is an effective vaccine against JEV, the unpredictable spread of the virus means there may be sporadic unexpected outbreaks of the virus and 3 billion people are currently at risk of infection (Connor and Bunn, 2017).

More people than ever are at risk of arbovirus infection and recent unpredictable outbreaks have emphasised the serious complications these diseases can have, causing permanent microcephaly in unborn children or proving fatal due to organ shutdown/invasion of the brain. In order to prevent transmission of arboviruses to humans, we must understand how an arbovirus completes its life cycle and identify stages that can be intercepted. One of these steps is control of the mosquito vector, which directly delivers arboviruses to humans through an infected bite.

### 1.1.2. Distribution of *Aedes* mosquitoes

*Ae. aegypti* has spread worldwide from its origins in sub-Saharan Africa. *Aedes* mosquitoes can breed in essentially any standing water containing suitable food in natural or man-made containers. The preference for breeding site and vertebrate blood meal differs between mosquito species (Barrera et al., 2012;

Dom et al., 2013). *Ae. aegypti* is more genetically diverse in sub-Saharan Africa, where the presumed ancestral species *Ae. formosus* is also present; these mosquitoes are morphologically darker, reside in natural containers such as tree holes, and feed on non-human animals (the sylvan form) (Mattingly and Brucechwatt, 1954; McClelland, 1960). The formation of the Sahara desert in North Africa created a dry environment and selected for diversification. The sylvan mosquitoes remained south of the Sahara, whereas those in the north were in closer contact to human settlements, and switched from zoophagy to anthropophagy (feeding on humans)(Powell and Tabachnick, 2013).

It is widely thought *Ae. aegypti* were introduced to the New World (Americas) from the Old World (Africa, Europe) on ships with conditions that were ideal for selection of a domestic type of *Aedes*. European transportation of slaves from West Africa to the New World likely accounted for a majority of this mosquito introduction, with thousands of cramped humans in damp conditions providing the ideal setting for the *Aedes* life cycle. During this time *Ae. aegypti* earned the name the 'Yellow Fever' mosquito, as it brought YFV into the western hemisphere, which reportedly caused more deaths of US soldiers in the Spanish-American war than the war itself (CDC, 2017b). Analysis of single nucleotide polymorphisms (SNPs) suggests that *Ae. aegypti* then spread west from the New World to Asia and Australia (Brown et al., 2014).

The closely related *Ae. albopictus*, also known as the Asian Tiger mosquito, is extremely invasive and has adapted to survive at colder temperatures compared to *Ae. aegypti* (Thomas et al., 2012). As the name suggests, the Asian Tiger mosquito originated in Asia but has spread to 28 countries over the past two decades. They inhabit natural and artificial containers much like *Ae. aegypti*, but it is thought they particularly utilised pools of water in used tyres for laying eggs, which are resistant to desiccation, and this led to their transportation across the globe in the used tyre trade (Benedict et al., 2007). *Ae. albopictus* is an aggressive, outdoor biter that is a secondary vector of DENV and can be an extremely efficient vector of some strains of CHIKV, the latter of which is due to multiple adaptations of virus envelope mutations which increase virus dissemination within the vector (Tsetsarkin et al., 2007; Tsetsarkin, 2011). With

*Ae. albopictus* colonising colder areas north of the equator, and *Ae. aegypti* creating endemics south of the equator (Figure 1.2.), an increasing number of people are at risk of contracting an arbovirus of medical concern.

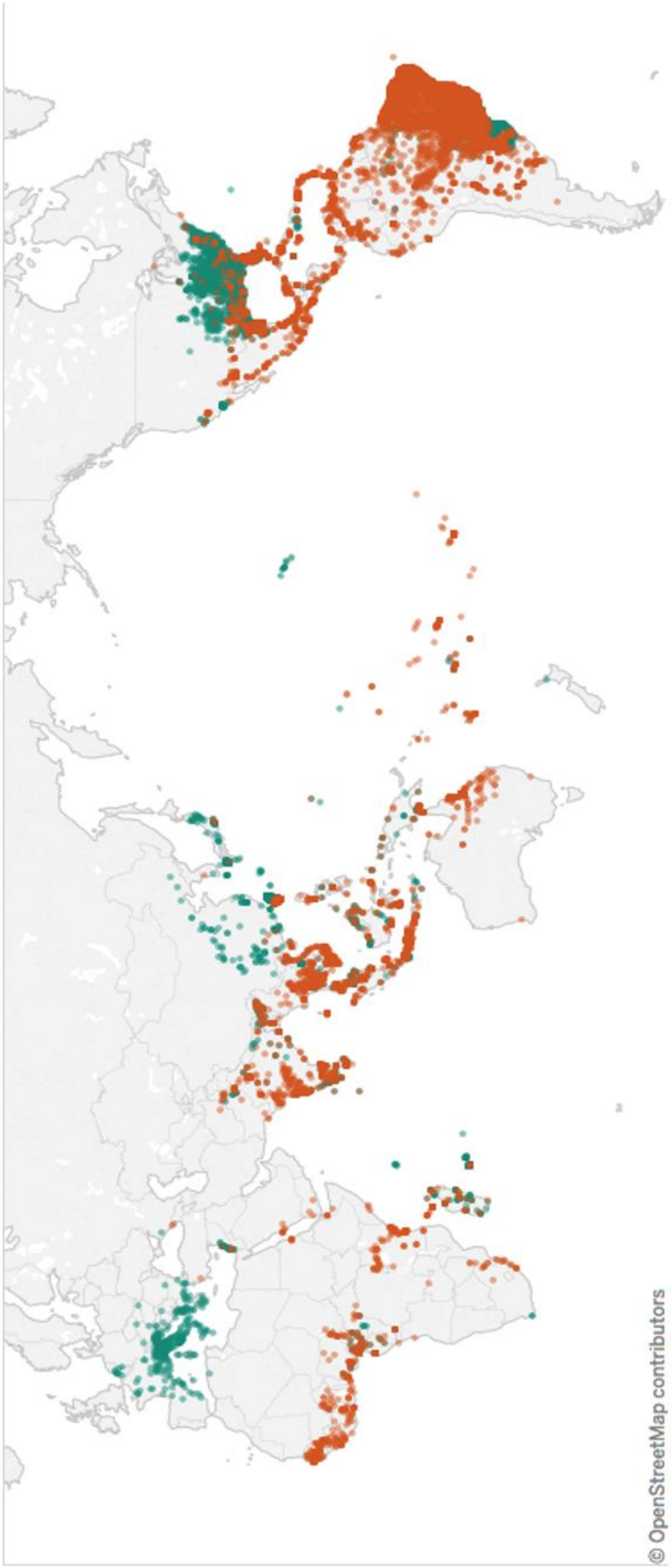


**Figure 1.2.**

**Global recorded occurences of *Ae. aegypti* and *Ae. albopictus* from 1958-2014.**

Dots represent recorded occurrence of *Ae. aegypti* (orange) and *Ae. albopictus* (green) noted in peer-reviewed literature and unpublished studies. *Ae. aegypti* colonise sub-tropical to tropical temperatures, whereas *Ae. albopictus* can extend this colonisation to temperate countries. (PHI, 2015)

### 1.1.3 Arbovirus life cycle

Different stages of the arbovirus life cycle occur in the arthropod vector and mammalian host. Mosquitoes can remain infected indefinitely with an arbovirus, as they have evolved an appropriate RNAi immune response which keeps the virus below pathogenic levels (Myles et al., 2008). Female mosquitoes transmit virus to a mammalian host when acquiring a blood meal, which is required for development of fertilised eggs. The virus replicates to high levels in the mammalian host and this viraemic state increases the chances of another biting vector acquiring the virus in a blood meal, completing the cycle (Pfeffer and Dobler, 2010).

Most arboviruses are sustained in a sylvatic cycle, from arthropod vector to non-human mammalian host, such as birds or primates, with very low morbidity and mortality in these sylvatic hosts. Humans are generally a dead-end host of most arboviruses, with some exceptions being DENV, CHIKV and ZIKV, which can sustain transmission between humans and arthropods without the need for a non-human reservoir (Gould et al., 2017). Arboviruses are not only restricted to transmission via arthropod vectors, as was highlighted in the 2015 ZIKV outbreak in Brazil; ZIKV is the first known arbovirus to be transmitted via sexual intercourse, blood transfusion and worryingly from a mother to a baby in the womb (Figure 1.3.). In fact, a recent study has computed that the risk of sexually-transmitted ZIKV is at least an order of magnitude higher than is currently estimated (Allard et al., 2017). Arboviruses can also be transmitted vertically from arthropod host to offspring; although insect-specific flaviviruses exhibit high rates of vertical transmission, dual-host flaviviruses such as DENV and ZIKV do not (Lequime et al, 2016). It is thought less than 0.1% of mosquitoes are infected with arboviruses vertically in nature (Lequime & Lambrechts, 2014).

While it is clear there can be transmission of ZIKV without the aid of mosquitoes, these vectors are responsible for the majority of arbovirus-related disease. The intrusion of ZIKV into an urban cycle highlights how humans are increasingly crossing over with the life cycle of *Aedes* mosquitoes, allowing outbreaks of previously sylvatic arboviruses to occur.

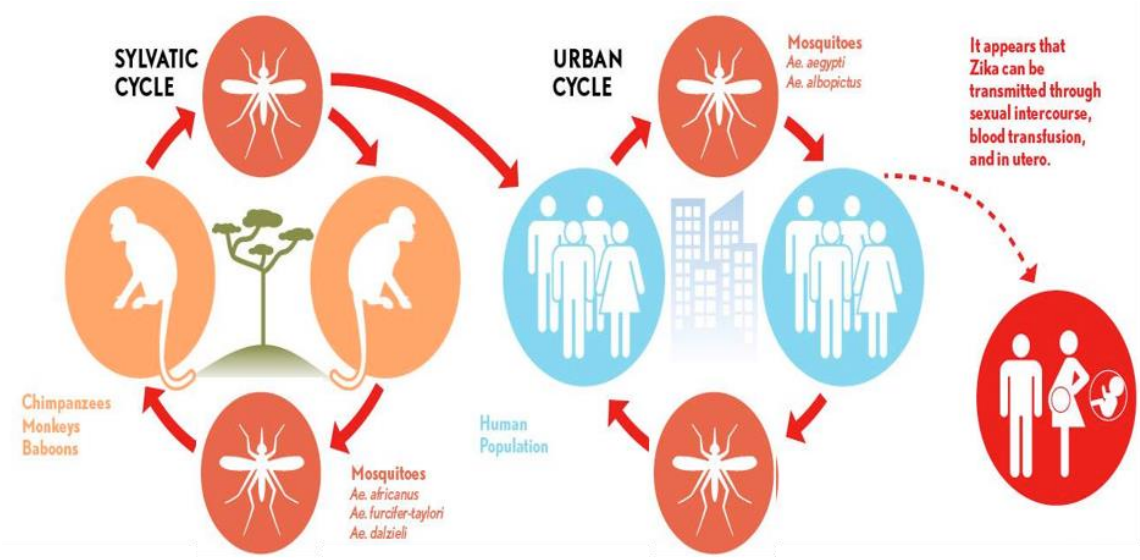


**Figure 1.3. Transmission routes of Zika virus.**

ZIKV is usually maintained in a forest environment in a sylvatic cycle between arboreal arthropods and non-human primates. ZIKV enters an urban cycle when vectors come in close contact with humans, with cycling of the virus via domesticated vectors. Zika virus can also be transmitted via sexual intercourse, blood transfusions and in utero. Adapted from Council of Foreign Relations. (Meltzer, 2016)

### 1.1.4. *Aedes* life cycle

The *Aedes* life cycle requires an aquatic and terrestrial environment and consists of 4 stages: eggs, larvae, pupae and adult (Figure 1.4.). Eggs are laid above a water line in a standing pool of water and hatch when water reaches the egg line. *Aedes* eggs are particularly resistant to desiccation (drying); *Ae. aegypti* can withstand several months of desiccation while retaining high viability, but *Ae. albopictus* can withstand up to a year even in temperate countries (Faull and Williams, 2015; Hawley et al., 1989). The larvae stage is mobile and feeds on microorganisms and nutrients within the water, shedding its skin three times through four instar stages. The third aquatic stage is the pupae, also known as 'tumblers' due to their mobility. Pupae do not feed and eclose into terrestrial adults once metamorphosis is complete; this whole process lasts 8-10 days (Clements, 1992).

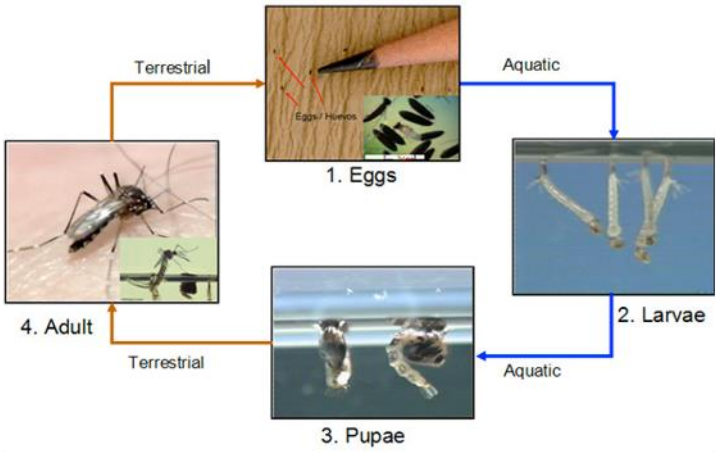


Figure 1.4. **Life cycle of *Aedes* mosquitoes.**

Eggs are laid above the water line and hatch into larvae in the presence of water. Larvae feed and develop through four instars into pupae, where metamorphosis into an adult occurs. Adults remain terrestrial. (CDC, 2012)

## 1.2. Arbovirus replication

A lot of the knowledge of virus replication in insects arose from discovering homologues to mammalian systems, therefore the study of virus replication in mammals is crucial. The replication process of arboviruses has been well studied in mammalian systems and can differ across genera, due to the composition of viral genomes. DENV, ZIKV, YF and WNV are members of the *Flavivirus* genus, one of three genera in the Flaviviridae family (Simmonds et al., 2017). CHIKV and the model virus SFV are part of the *Alphavirus* genus, of the family Togaviridae (Powers et al., 2001). All known alphaviruses and flaviviruses that cause disease in humans are transmitted via arthropods.

The composition of viral particles of both genera are similar; they contain the viral genome in the form of a positive single-stranded RNA (ssRNA) enclosed within an enveloped membrane. Both genera are spherical in shape, with the diameter of flaviviruses measuring slightly smaller (40-50nm) compared to alphaviruses (60-70nm), with a small genome of between 9-11kb (nucleotide bases) that can encode only up to 10 viral proteins (Fernandez-Garcia et al., 2009; Smit et al., 2011). The lack of replication machinery within a virion means they must exploit host-cell resources in order to multiply.

### 1.2.1. *Flavivirus* replication

*Flavivirus* virions contain one copy of the viral genome, which will encode a polyprotein that is cleaved into 7 non-structural proteins and 3 structural proteins during replication. The structural proteins of flaviviruses are the core (C), premembrane (prM) and E glycoprotein, which will form the viral particle. Non-structural proteins (NS1, NS2A, NS2B, NS3, NS4A, NS4B, NS5) will be involved in replication of viral RNA, virus assembly and modulation of host-cell responses (Fernandez-Garcia et al., 2009). Flaviviruses first bind and enter cells through receptor-mediated endocytosis. The viral glycoprotein E binds to a cellular receptor; studies have shown there can be many of these receptors including heat shock proteins 70/90, BiP, C-type lectins such as dendritic-cell specific intracellular adhesion molecule (DC-SIGN), and negatively charged glycosaminoglycan's, the latter of which are expressed on many cell surfaces (Smit et al., 2011).

Flaviviruses have been shown to enter cells by clathrin-mediated receptor endocytosis; single-particle tracking has shown DENV will select an attachment receptor preferentially if it is located at a clathrin hotspot (van der Schaar et al., 2008). The plasma membrane invaginates around the virus and is sealed with dynamin, resulting in containment of the virus within a clathrin-coated vesicle. However, a study has shown that entry into Vero cells, which are widely used in mammalian cell culture, can differ between DENV serotypes. While DENV-1 entered by classical clathrin-mediated endocytosis, DENV-2 did not, although it did require dynamin (Acosta et al., 2009). Despite the difference in internalisation, once inside both serotypes are guided by GTPases Rab 5 and Rab 7 to early and late endosomes, respectively (Acosta et al., 2012).

Once virus is trafficked to endosomes a low pH environment induces a conformation change in the glycoprotein E, inducing fusion of host and viral membranes. This results in release of the viral genome into the cell cytoplasm for replication (Sánchez-San Martín et al., 2009). The composition of the host cell membrane that the virus is being released from has been shown to be important in this process. The presence of cholesterol is important for fusion; cholesterol-depleted cells show less viral infectivity and addition of cholesterol to artificial membranes results in increased fusion of WNV (Medigeshi et al., 2008). It is

therefore thought the presence of cholesterol influences the properties and fluidity of a membrane, required for arbovirus fusion (Smit et al., 2011).

Following fusion and release of the viral genome, *Flavivirus* replication occurs on virus-induced host cell membranes within host cell organelles, such as the endoplasmic reticulum (ER). Flaviviruses use host-cell signalases and the virus-derived NS3 protease to process the viral polyprotein into three structural and seven non-structural proteins. Following translation of the viral input RNA, the non-structural RNA-dependent RNA polymerase (RdRp) NS5 protein transcribes a complimentary (-) strand to the input (+) strand. This (-) strand will then serve as a template for transcription back into the (+) form. The +ve RNA strands can then be processed for virion formation or used for further transcription (Fernandez-Garcia et al., 2009). New viral RNA is complexed with the C protein on the ER surface and packaged into a lipid bilayer with heterodimers of the E and prM, which is transported to the Golgi apparatus. This is where virus maturation occurs, with furin-mediated cleavage of the prM to the M (membrane), after which virus is released into the cytoplasm by exocytosis (Fernandez-Garcia et al., 2009).

### 1.2.2. *Alphavirus* replication

Like Flaviviruses, Alphaviruses are enveloped viruses, however the composition of virons differs and slightly alters the replication process. The structure of *Alphavirus* Sindbis virus (SINV) has been extensively studied in mammalian systems. A mature SINV virion is composed of two protein shells; the outer shell contains 240 copies of glycoproteins E1 and E2, whereas the inner shell contains the capsid protein and ssRNA. The E2 glycoprotein is involved in receptor recognition and binding to cells, whereas the E1 protein helps preserve the virion structure and mediate the infection process (Vancini et al., 2015). Alphaviruses can enter cells via clathrin-mediated endocytosis like Flaviviruses, however there is evidence the virus RNA can also enter cells through a virus-formed pore structure that penetrates the plasma membrane (Vancini et al., 2013).

As Alphaviruses are also +ve ssRNA viruses, the replication process of creating a complementary (-) strand to the input (+) strand is the same as with Flaviviruses. However, the translation of the *Alphavirus* genome is slightly different as the viral genome encodes for two open-reading frames; non-structural proteins are

translated by the larger genomic RNA region and structural proteins encoded in a smaller region by the 26S RNA promoter (Leung et al., 2011). The non-structural proteins encoded aid in the replication process, whereas the structural proteins encoded by the 26S RNA site associate with genomic RNA near the budding site (Leung et al., 2011; Wielgosz et al., 2001). *Alphavirus* replication occurs in bulb-shaped membrane invaginations of complex cytoplasmic vacuolar structures (type 1) (CPV-I), which originate from endosomes and secondary lysosomes (Jose et al., 2017). Replication complexes (RC) are formed on these spherules, which contain non-structural proteins nsP1-4, viral RNA and host proteins. 240 copies of the structural capsid protein (CP) form around a single viral RNA to form the virus core, which is presumed to be trafficked to the plasma membrane for budding by type II cytoplasmic vacuoles (CPV-II) (Jose et al., 2009; Jose et al., 2017). Much of what is known about arbovirus replication comes from studies in mammalian systems, however we can use current knowledge of how viruses manipulate mammalian-cell systems to investigate homologous systems in insects.

### 1.2.3. Arbovirus replication in mosquitoes

Arboviruses must navigate different pathways, cell types and barriers in an arthropod vector compared to in a mammalian host. Only female mosquitoes acquire a blood meal in order to gain the nutrients required for egg development. If females feed on a viraemic host, they will ingest arboviruses within the blood meal. Once a mosquito is infected with an arbovirus, it can remain infectious indefinitely, without detrimental effects to the vector (Blair, 2011). However, there is a certain degree of specificity between vector and virus, as only certain vectors can spread certain viruses. The success of a virus infecting a vector relies on the virus avoiding various immune responses within the vector, and maneuvering several bottleneck barriers to get to the salivary glands; therefore, the establishment of viruses in certain vectors is likely due to years of co-evolution (Bosio et al., 1998; Miller and Mitchell, 1991).

Viruses enter the mosquito midgut during ingestion of a viraemic blood meal from a vertebrate host. Once in the midgut, virus must enter midgut epithelial cells within 12 hours, before the peritrophic matrix forms around the gut. This is the first bottleneck for the virus, as it is estimated as little as 20% of epithelial cells are successfully infected with virus (Franz et al., 2015). Inside epithelial cells,

viruses hijack the host-cell machinery to perform viral RNA replication at the endoplasmic reticulum (ER) membrane. Following replication, virus maturation occurs within the cell at various sites depending on virus/vector; CHIKV matures at the plasma membrane in *Ae. aegypti*, whereas YFV can mature at the cisternae of the ER (Deubel et al., 1981; Vega-Rúa et al., 2015).

During blood meal digestion at 24-32 hours post blood meal, the collagen-constructed basal lamina becomes permissive, as collagenase activity increases (Dong et al., 2017). Current studies suggest virions pass through the basal lamina of the midgut epithelium to enter the hemocoel for dissemination to secondary tissues such as the fat body, nerve tissues and haemocytes (Figure.1.5.)(Franz et al., 2015). The final organ for viruses is the salivary gland, and it is thought haemocytes provide a cell to amplify in and a vehicle to transport the virus there. Arbovirus replication can also occur in the salivary glands, as budding of CHIKV has been observed in the salivary glands of *Ae. albopictus* (Vega-Rúa et al., 2015). Finally, mature virions enter the apical cavities of acinar cells in the salivary glands, and are inoculated into a vertebrate host upon feeding (Figure 1.5.).

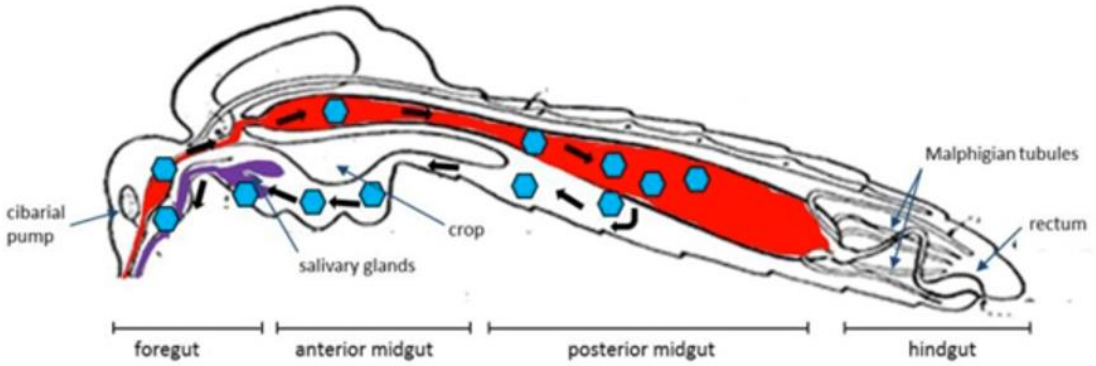


Figure 1.5. **Schematic of viral progression through a mosquito.**

Ingested virus moves to midgut, where it infects epithelial cells. Virus then escapes the basal lamina and disseminates to secondary organs, finally reaching the salivary glands. Mature virions are expectorated during the mosquito's bite. (Deilgat et al., 2014; Franz et al., 2015)

## 1.3. Mosquito immune defences to arboviruses

Dual-host arboviruses must overcome tissue barriers, humoral and cellular responses, and insect-specific viruses (ISV) that are already established within the vector.Unlike mammals, mosquitoes do not have adaptive immunity and rely on innate immune responses. Much of what is known of mosquito immunity comes

from studies in *Drosophila* with further identification of homologues in mosquitoes. There are three main conserved immune pathways in mosquitoes; the Toll, Immune deficiency (Imd) and Janus kinase (JAK) signal transducer and activator of transcription (STAT) pathways. These immune pathways are activated by identification of an invading pathogen, resulting in translocation of transcription factors, which are translated into anti-bacterial/fungi/viral effectors. The main anti-viral pathway in insects is the exogenous RNAi pathway, which operates differently to Toll, Imd and JAK-STAT, in that it directly cleaves incoming virus RNA, preventing infection. Together, these pathways collaborate to mount an effective antiviral response. In addition, there is mounting evidence that the presence of ISVs can significantly alter the vector competence of a mosquito.

### 1.3.1. RNAi

The well-characterised RNAi immune response is the major antiviral pathway in insects and is composed of three pathways; small interfering (si) RNA, piwi-interacting (pi) RNA and micro (mi) RNA pathways, the latter of which is less involved in immunity. The siRNA pathway is activated by double-stranded RNA (dsRNA) longer than 150 base pairs in length. Viruses trigger this pathway as they produce dsRNA intermediates during their replication cycle, which are then detected by the Dicer-2 protein attached to the R2D2 protein. Dicer then splices the dsRNA into smaller fragments (siRNA); these are then unwound and a guide strand is selected based on its complementarity. This guide strand is loaded onto a preRNA-induced silencing complex (preRISC) which has the RNase Argonaute-2 (Ago2) attached. Any other viral RNA strands which then pair with the guide strand are degraded by Ago2 (Kingsolver et al., 2013).

The RNAi pathway mounts such a potent antiviral response that viruses produce proteins that suppress elements of the pathway in both arthropods and mammals. Viruses in *Drosophila* (*Drosophila* C Virus (DCV) and Flock House Virus (FHV)) produce RNAi silencing suppressor (RSS) proteins that prevent the cleavage of dsRNA by Dicer. In addition, when the RSS protein B2 is knocked down in FHV there is no established infection of the virus (Han et al., 2011). Similar RSS proteins have been found in mammalian systems infected with DENV; the NS4B protein from all four DENV serotypes has been shown to suppress the RNAi pathway in mammalian

cells (Kakumani et al., 2013). There is a lack of evidence of any RSS proteins encoded by arboviruses in insect systems; it was considered that arboviruses may not require RSS proteins and tolerate the RNAi response, as there is still persistent low levels of infection. However, flaviviruses DENV and WNV have been shown to produce subgenomic flavivirus RNA (sfRNA) that inhibits RNAi, rather than viral proteins, in both insect and mammalian cells (Schnettler et al., 2012).

### 1.3.2. JAK-STAT

The antiviral pathways in mosquitoes do not necessarily work alone; rather they can work in conjunction to mount a wide cellular antiviral response. The RNAi pathway upregulates transcription of the protein Vago, which directly activates the JAK-STAT pathway. In WNV-infected *Culex* cells, Vago is upregulated and acts as an Interferon-like antiviral cytokine, activating the JAK-STAT pathway, which induces further antiviral responses. Transcription of this protein has been shown to be dependent on Dicer-2, but not other components of the RNAi pathway (Paradkar et al., 2012). Vago acts as an extracellular receptor that activates the JAK-STAT pathway however the receptor it binds with is unknown. JAK-STAT is traditionally activated by the Upd cytokine binding to transmembrane receptor Domeless (DOME). Binding of different Upd cytokines results in different genes being transcribed, either promoting developmental process or responses to bacterial challenge or septic injury. Once the Upd is bound, the Jak (Hopscotch) can phosphorylate DOME, allowing a binding site for the STAT (STAT92E). This STAT is also phosphorylated and dimerized, then translocated to the nucleus for gene transcription (Liu et al., 2017).

The JAK-STAT pathway has been shown to have an important role in virus infection in insects by activating transcription of antiviral genes. In *Drosophila*, the gene vir-1 is upregulated by JAK-STAT in response to *Drosophila* C virus infection, reducing the viral load (Myllymäki and Rämet, 2014). JAK-STAT is also activated in *Ae. aegypti* in response to DENV infection, with susceptibility to virus increased with RNAi depletion of Hop and DOME (Souza-Neto et al., 2009).

### 1.3.3. Toll

Pattern recognition receptors (PRR) detect invading pathogens and bind to a specific membrane protein to activate each pathway. The Toll pathway is activated by a range of organisms in insects, including gram-positive bacteria, fungi and viruses. The cytokine Spatzle binds to transmembrane protein Toll to activate the Toll pathway. Toll then interacts with a cascade of proteins, Myd88, Tube and Pelle, which results in translocation of transcription factor Rel1 to the nucleus. This translocation results in the production of anti-microbial peptides (AMPs), such as Defensin and Cecropin, which are anti-bacterial, fungal and viral (Liu et al., 2017). The Toll pathway has been shown to play an antiviral role in *Drosophila*, as knockdown of the pathway results in higher viral loads of RNA viruses *Drosophila* C virus and Cricket Paralysis Virus (Ferreira et al., 2014). Components of the Toll pathway such as transcription factor Rel1 and AMP Cecropin G are upregulated in *Ae. aegypti* in response to DENV infection (Xi et al., 2008). Interestingly, Xi et al also showed that the presence of naturally occurring microbiota in *Ae. aegypti* upregulates Toll-pathway components, which reduces viral load, compared to *Ae. aegypti* cleared of microbiota with antibiotics.

### 1.3.4. Imd

The Imd pathway is activated primarily by gram-negative bacteria, via the peptidoglycan-recognition protein receptors (PGRP)-LC and LG. Like Toll, this binding initiates a cascade of proteins (IMD, FADD, Dredd, Tak1 and IKK) resulting in translocation of Rel2 to the nucleus. Antimicrobial effectors are then produced which are specific for gram-negative bacteria, including Attacin and Diptericin (Liu et al., 2017). Microbiota in *Ae. aegypti* has also been shown to activate the Imd pathway, resulting in a decreased Sindbus virus (SINV) load (Barletta et al., 2017). Injection of Cricket paralysis virus into *Drosophila*, with Imd mutants, led to increases in viral loads (Costa et al., 2009).

### 1.3.5. Insect-specific viruses

To date, there have been 38 mosquito-specific flaviviruses identified, with the assumption there are many more to be discovered. ISVs are transmitted through a mosquito population vertically via the eggs, therefore a dual-host flavivirus entering the midgut following a blood-meal may encounter inhibited replication

as ISVs are already established. ISVs such as cell fusing agent virus (CFAV), phasi charoen-like virus (PCLV) and *Aedes* flavivirus (AeFV) have been detected in mosquito lab colonies and field caught *Aedes* and *Culex* mosquitoes (Cook et al., 2006; Cook et al., 2009; Yamanaka et al., 2013). Importantly, studies have shown presence of ISVs can inhibit growth of WNV, ZIKV, DENV, CHIKV and La Crosse encephalitis virus (LACV) in mosquitoes, in vitro and in vivo (Romo et al., 2018; Schultz et al., 2018). Sequencing of CFAV shows a distant relation to dual-host flaviviruses, with a high similarity of NS5 and NS3 genes (Bolling et al., 2015). The mechanism of ISV-induced flavivirus inhibition is unknown, but is theorised to be due to super-exclusion of incoming flaviviruses from cells by ISVs, preventing replication. However, the presence of ISVs may also be priming the immune system, preventing establishment of incoming flaviviruses.

## 1.4. Transmission of arboviruses to humans

Traditionally, arboviruses are contained in a sylvatic cycle within forests, between arboreal vectors and non-human mammals. Arboviruses can enter an urban cycle when vectors come in close contact with humans; this is becoming an increasing problem due to deforestation and urbanisation, resulting in intrusion into previously isolated vector habitats. The current state of many emerging arboviruses globally is not an isolated event, and rather, should be considered re-emerging arboviruses.

### 1.4.1. Re-emergence of arboviruses

YFV has been present in African forests for centuries, transmitted from arboreal *Aedes* mosquitoes such as *Ae. africanus* and *Ae. simpsoni*, to non-human primates (NHP). Small-scale epidemics of YFV occur in humans in rural and peri-domestic areas when arboreal *Aedes* mosquitoes cross over with fully domesticated *Ae. aegypti* on the outskirts of the forest, thus allowing the virus to travel into households (Gould et al., 2017). However, there has been a resurgence of YFV outbreaks in recent years, in Central/South America and Africa, with urban YFV transmission occurring (Barrett, 2018). There were over 900 confirmed cases of YFV across an outbreak in Angola, Democratic Republic of Congo and Kenya between 2016-17 (WHO, 2019). This prompted an emergency vaccination campaign with 18 million vaccines being distributed throughout these countries.

Such outbreaks highlight the need to maintain prevention strategies for arbovirus control, such as immunisation. In addition, this outbreak led to the first import of YFV into China, due to infected travellers returning from Angola (Cui et al., 2017). If there were vectors capable of spreading YFV established in China, this could have led to a widespread outbreak in a high density population with no previous exposure to the virus.

In the Americas, DENV has an endo-epidemic pattern, with outbreaks occurring every 3-5 years. There has been several stages of DENV transmission in the Americas since its introduction in the 1600s; successful eradication due to vector control, subsequent failure of mosquito eradication and increased vector dispersion and DENV-serotype circulations (Dick et al, 2012).

ZIKV has emerged and disappeared several times across the globe, only to re-emerge in a novel location. In 2007 the African lineage of ZIKV dispersed to Malaysia, and a subsequent Asian lineage is the likely origin of the strain responsible for the outbreak in Brazil in early 2015 (Gould et al, 2017). It is thought ZIKV was introduced to the Americas via the French Pacific (FP), and the cases seemed to coincide with the large influx of people during the FIFA World Cup in June-July 2014. However, no countries from the FP were competing in the cup; therefore blame turned to a FP-attended canoe race in Rio de Janeiro in August 2014. Despite these events in which people from different countries that had potentially been exposed to ZIKV may have attended, mathematical predictions estimate ZIKV was established in Brazil by infected travellers from October 2013-March 2014, before the two events (Massad et al, 2017). Following its introduction in the North-East of South America, ZIKV is thought to have spread southwards at an average speed of 47km per day due to movement of viremic hosts, with cases occurring in the South 5-6 months later (Zinszer et al, 2017). The rapid spread of ZIKV was also attributed to the 2015 El Nino event, which created optimal climactic conditions for vector-borne spread of the disease (Caminade et al., 2017).

The closely related *Ae. albopictus* also transmits DENV, but is a particularly efficient vector of CHIKV. A mutation on the viral envelope of CHIKV allows *Ae. albopictus* to transmit the 'Indian Ocean' lineage more effectively than *Ae.*

*aegypti* (Tsetsarkin et al., 2007). *Ae. albopictus* are of particular concern due to their ability to survive in colder temperatures than *Ae. aegypti*, and were responsible for outbreaks of CHIKV in Europe (Delisle et al., 2015; Grandadam et al., 2011; Paupy et al., 2009; WHO, 2017a). The expanding geographical range of *Aedes* mosquito vectors indicate the current vector control methods are not effective and novel strategies are required.

The re-emergence of these arboviruses highlights the importance of constant monitoring and control of vectors responsible for spreading disease, the lack of which can lead to re-emergence of arboviruses in regions where they have previously been eradicated (or transmission ceased naturally). With the predicted global range of *Aedes* mosquitoes set to increase (Figure 1.6.), monitoring vector control is crucial in the fight against arboviruses.

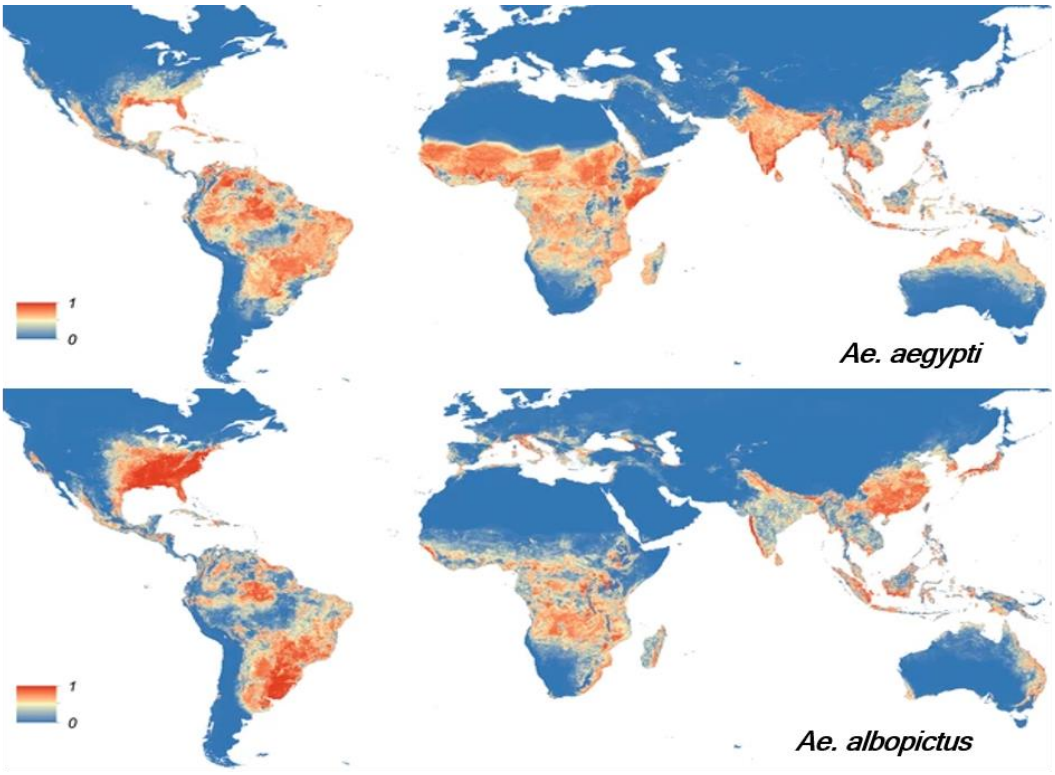


Figure 1.6. **Predicted global range of *Ae. aegypti* and *Ae.albopictus*.**

Probability map produced by advanced modelling, combining occurrence records and environmental correlates. Map shows probability of species occurring at a special resolution of 5km x 5km (blue 0 - red 1). (Kraemer et al., 2015)

### 1.4.2. Vaccine development

One way to prevent transmission of disease is the development of vaccines. Vaccine development of arboviruses is a crucial but complicated task. The success story of arbovirus-vaccination lies with YFV, a virus that mostly causes a typical febrile illness, however serious complications can occur when it infects organs. Around half of those that develop severe symptoms such as bleeding from orifices, vomiting blood and jaundice, will die from the disease (WHO, 2016). YFV is endemic in Africa and South America, however a licenced vaccine produced in the 1930s is used for immunisation worldwide, providing up to ten years of protection (CDC, 2017b).

Despite this, endemic areas can lag behind on immunisation due to the lack of the virus presence in the area. YFV has become a concern again in Brazil due to an outbreak in 2016, during which approximately 300 deaths were confirmed due to the virus. The virus had spread from rural areas to metropolitan cities of Vitoria and Rio de Janeiro, where around 12 million unvaccinated people live with YFV-competent vectors (Gómez et al., 2018).

The trouble with developing a vaccine for DENV is due to the fact there are 4 genetically distinct serotypes of the virus. If a person is infected with one serotype, they are then provided antibody-mediated protection against secondary infection of the same serotype. However, if the secondary infection is a different serotype, protection is transient and subsequently antibody-mediated immune enhancement can occur which increases the chances of severe dengue (WHO, 2018). There is one licenced vaccine for Dengue – Dengvaxia – a live recombinant tetravalent vaccine that should protect against all 4 serotypes. However, efficacy of this vaccine is not great, with 65% protection offered to those above 9 years old, and 44% to those that are younger. In addition, hospitalization rates of children given Dengvaxia have not declined relative to those not given the vaccine. In-fact, evidence suggests exposure to Dengvaxia resulted in a high risk of hospitalisation if subsequently infected with DENV, much like occurs naturally with antibody-dependent enhancement with different virus strains (Halstead, 2017; WHO, 2018).

Antibody-mediated immune enhancement is also a problem for ZIKV, which is closely related to DENV. Studies have shown there is substantial sero-cross-reactivity between DENV and ZIKV, and DENV antibodies can result in enhancement of ZIKV infection (Charles and Christofferson, 2016; Dejnirattisai et al., 2016). This means any DENV vaccine licenced for public use must take into account the effect on ZIKV pathogenesis, and vice-versa. Due to the huge outbreak of ZIKV in Brazil, a lot of effort was put in to development of a vaccine. There are currently multiple vaccine candidates, including a DNA-based vaccine that has entered phase 2 of a clinical trial in 2017. Interestingly, a vaccine is being developed which is designed to trigger an immune response to mosquito salivary proteins, which in turn will stimulate an immune response in the human against any virus, not just a specific viral antigen (NIH, 2017). Despite the efforts going in to developing vaccines for arboviruses, it is a challenging and lengthy process; meanwhile people are suffering from these preventable diseases. The main method used for arbovirus control is to target the vector to reduce population density.

## 1.5. Vector control methods

There are many methods of vector control, which include physical, chemical, biological and genetic control methods. As noted below, each type of control has its weaknesses, making it inefficient as a control method on its own. The World Health Organisation (WHO) recommends Integrated Vector Management (IVM); this means incorporating several methods at the same time to ensure efficient suppression/eradication of the vector.

### 1.5.1. Physical control

Physical control of vectors is aimed at prevention of mosquito colonisation and biting of humans; this includes the use of insecticide-coated bed nets, wearing protective clothing and removing potential man-made breeding areas. An insecticide-treated net (ITN) is a mosquito net covered in pyrethroid insecticide that disables or kills mosquitoes that come in contact with the net, typically hung over a bed to prevent biting when people are asleep. Nets can be manually dipped in a WHO-recommended insecticide or factory-treated with netting that has

insecticide incorporated within/around the fibres, known as a long-lasting insecticidal net (LLIN)(WHO, 2017d).

The use of bednets has had considerable success with regards to reducing malaria in Sub-Saharan Africa, as *Anopheles* vectors are most active at night when a person is likely to be indoors/in bed (endophilic)(Ndoen et al., 2011). However, *Ae. aegypti* and *Ae. albopictus* are aggressive day-time biters, making the use of bed nets largely useless. The use of bed nets does not ensure 100% coverage from biting vectors, as studies have shown children under 5 years old use them inconsistently and those 6-14 years old are less likely to use them at all (Bawo et al., 2012; Wanzira et al., 2016). In addition, LLIN must be checked regularly for holes, which are common with usage. Perhaps the most important problem is the increasingly widespread pyrethroid resistance observed, meaning the bed net is essentially just a physical barrier similar to wearing protective clothes (Moyes et al., 2017).

Removal of breeding sites is an important vector control method that needs to be incorporated at a community-wide scale for it to be a success. This involves removing any man-made container that may collect rain water for mosquitoes to breed in. This may prove successful in more rural areas, however in a city it is almost impossible to remove all man-made containers. In addition, the ever-resourceful *Aedes* mosquitoes can also breed in natural containers such as coconuts shells/plant axils, and in water storage tanks, gutters, drains etc., meaning the sources can never be totally eradicated.

### 1.5.2. Chemical control

The aim of chemical control is to eradicate a pre-existing colony of mosquitoes, using insecticides and larvicides. Techniques include indoor-residual spraying, outdoor fogging and addition of larvicide at breeding spots. Four classes of insecticide are currently used; carbamates, organochlorines, pyrethroids and organophosphates (EPA, 2017b). Indoor-residual spraying involves regular spraying of walls inside a residence, so when a mosquito lands on the wall it will be disabled/killed. However, this requires a lot of regulation to ensure this is being

done regularly and efficiently. This method is also ineffective against *Ae. albopictus*, which prefers to reside outdoors.

Outdoor fogging involves widescale spraying of insecticide from a vehicle and is usually implemented for vector control once an epidemic has already begun, in an attempt to reduce further transmission. However, the effectiveness of peridomestic space spraying, with regards to disease transmission, is not known. While some studies report short-term reduction in mosquito population, most do not investigate any effect on disease transmission (Esu et al., 2010).

A number of plant-based compounds are toxic to mosquitoes at several life stages, being used as adulticides, larvicides and ovicides, but also as deterrents against adults and oviposition. Neem powder from the Neem tree acts as a repellent but also is 100% toxic to mosquito larvae at low concentrations (Singh et al, 2012). Plants such as eucalyptus and citronella have essential oils and extracts that are commonly used as a base for mosquito repellent (Tyagi, 2016). Although this repellent is relatively short lasting, plant-based toxins are environmentally sustainable yet remain volatile to mosquitoes.

The predominant problem with chemical control methods is the widescale development of insecticide resistance (IR). Resistance to all 4 classes of insecticides has been detected in *Aedes* mosquitoes in Africa, Asia and the Americas (Moyes et al., 2017). IR has developed due to several causes, including increased insecticide detoxification and target-site mutations. There may even be more resistance in *Ae. aegypti* than is known, as data on this is missing from large areas of Africa. The geographical expansion of *Ae. albopictus* insecticide resistance is known even less, with the exception of throughout southeast Asia. It is crucial to monitor resistance of both species as they can differ in their rates of IR. *Ae. aegypti* were found to be resistant to pyrethroids in four states in Malaysia, yet *Ae. albopictus* remained largely susceptible. Worryingly, *Ae. albopictus* within the city of Kuala Lumpur had developed moderate resistance (Ishak et al., 2015).

### 1.5.4. Genetic control

There are several methods of genetic manipulation, which can replace or reduce the vector capacity of a biting insect. Methods such as the sterile insect technique

(SIT) and release of a dominant-lethal gene (RIDL) are male specific, focusing on suppression through release of sterile males, which reduce the offspring produced by wild females.

With genetic control methods, insects are generally prepared in a laboratory setting and are constantly released to suppress a population. SIT involves irradiating males to make them infertile; these males will then be released to compete with the wild males. It is argued that the irradiation can make the SIT males weaker and less competitive compared to wild males (Lux et al., 2002), however in some circumstances SIT has proven to be a very successful pest control method. The use of SIT over a period of 20 years has led to the eradication of the screwworm fly in North and Central America, which carried the screwworm parasite which had devastating effects on livestock (Wyss, 2000). Screwworm was also eradicated in Libya within three years of implementing SIT; however, it is estimated that 40 million sterile flies were being released every week to maintain this. This is one drawback to SIT: the mass production that is required and constant releases, making this method very labour-intensive. Nevertheless, it has proven to be locally successful against *Aedes* mosquitoes in recent times; the release of 1000 irradiated *Ae. albopictus* pupae weekly in Italy over a three year period led to sterile males composing 68% of the wild population (Bellini et al., 2013).

The release of genetically-modified mosquitoes was pioneered by Biotech company Oxitec, who created male *Ae. aegypti* mosquitoes that possess a self-limiting gene which results in mosquito death before adulthood (formerly termed RIDL)(Alphey, 2002; Thomas et al., 2000). The self-limiting gene within OX513A mosquitoes is suppressed while rearing in a laboratory by the use of tetracycline; males are then released into the wild, where the gene becomes active (Heinrich and Scott, 2000; Phuc et al., 2007). OX513A males will then mate with wild females, and the self-limiting gene will be inherited by any offspring, meaning they will not reach adulthood and the population will be suppressed as a result. RIDL has proven to be successful with up to 93% reduction of local mosquito populations in the Cayman Islands, Panama and Brazil (Carvalho et al., 2015; Harris et al., 2012). Further releases in the city of Piracicaba in Brazil have shown a reduction of larvae up to 82% within 8 months of implementation (Oxitec, 2018). As with SIT, RIDL requires mass rearing of mosquitoes at an industrial level that

then need to be transported to sites for release, as the gene is self-limiting. For example, Oxitec have completed a mass rearing facility in Piracicaba that will supply the demand of 60 million mosquitoes a week for releases (Oxitec, 2018).

Vector control methods that are self-sustaining once within the environment are attractive as they do not require continual release of modified mosquitoes. Synthetic gene-drive systems are being developed using driving endonuclease genes (DEGs), which contain a 'selfish gene' that propels through a population (Chan et al., 2011; Hammond et al., 2016; Windbichler et al., 2011). DEGs include homing endonuclease genes (HEGs) and CRISPR-Cas9 systems, which are found in many single celled organisms, including bacteria. These DEGs encode for an endonuclease that causes a double-stranded break on the homologous chromosome, inducing the cellular repair process. The cell uses the chromosome carrying the DEG as a template to repair the double-stranded break, and the selfish gene is copied to the damaged chromosome (Godfray et al., 2017). Using DEGs for vector control would focus on targeting lethal genes to mosquitoes; current models for *Anopheles gambiae* control indicate releasing 2-3 HEGs that target female fertility genes could result in population elimination, reducing malaria transmission (Deredec et al., 2011). However, unlike the lethal gene in RIDL mosquitoes that can be 'turned off' by using tetracycline, these DEGs cannot be stopped once introduced into a population. Also, for effective suppression, models indicate there has to be at least 75% of transmission of the selfish gene to the progeny (Deredec et al., 2011). In addition, continual transmission of gene drive systems has been shown to result in nuclease-induced mutations at the target site, resulting in restored functionality of the target gene (Hammond et al., 2017).

The main issue with genetic modification of pests and release into the environment is the negative public view of anything genetically modified. Governments and health bodies must ensure there is sufficient communication with the community about the positive effects of releases, which can be time consuming. This can involve town meetings, pamphlets through doors and good branding, such as Oxitec naming their releases the 'Friendly' *Aedes aegypti* project (Neuhaus, 2018; Oxitec, 2018). In addition, mass rearing of insects can be expensive and this option may not be available for poorer countries that are often

hit the hardest by arboviruses. Alternatively, there are less-expensive, more environmentally friendly control methods that can be implemented.

### 1.5.5. Biological control

Biological control of mosquitoes involves using naturally occurring toxins or mosquito predators to suppress populations. This includes using the natural insect-repellent properties of plants, introducing predatory mosquitoes, copepods and fish into larval breeding sites and release of entomopathogenic fungi. Insecticidal toxins from *Bacillus thuringiensis israelensis* (Bti), a bacteria found naturally in soils, specifically target larval stages of mosquitoes. Bti is widely used for aerial spraying across the United States and is particularly useful for treating standing water bodies (EPA, 2017a). Use of Bti has proven successful against *Aedes* mosquitoes and could be used to suppress *Anopheles* malaria-carrying mosquitoes as well, but with long-term use there is the risk of development of resistance (Benelli et al., 2016; Dambach et al., 2014).

Another biological control method involves introducing predatory fish, copepods and even mosquitoes into breeding sites. Larvivorous fish have been introduced into more than 60 countries for the purpose of mosquito control. *Gambusia affinis* has played an important role in biological control since its first introduction 100 years ago; they are tolerant to insecticides and larvicides and thrive in permanent water bodies. Combining several biological methods has resulted in successful mosquito suppression; for example, using larvivorous fish *G. affinis* followed by Bti in California prevented an expected resurgence of *Culex* mosquitoes (Huang et al., 2017). However, *Gambusia* were introduced to Australia in 1925 for mosquito control and proved to be highly invasive, having a detrimental impact on native fish, frogs and invertebrates (Gomon et al, 2019). In addition,behaviour of mosquitoes can change in response to these predatory fish; *Culex* mosquitoes have been shown to sense when the fish are present and choose to lay eggs elsewhere (Huang et al., 2017). In addition, *Aedes* mosquitoes can utilise artificial containers with varying water levels for breeding, where larvivorous fish cannot live.

The use of predatory mosquitoes and copepods has proven more successful for *Aedes* control. *Toxorhynchites* are large mosquitoes whose larvae predates on smaller species of mosquitoes, such as *Aedes*. In addition, these ‘elephant

mosquitoes' do not consume a blood meal, meaning their release will not affect disease transmission (Benelli et al., 2016). There is evidence they can locate cryptic breeding sites, which are likely to be used by *Aedes*, reducing the quantity of larvae. There are many species of *Toxorhynchites*, some of which are adapted for a sylvatic environment, where others are suited for urban environments. Weekly release of the urban species *Tx. amboinesis* resulted in successful *Ae. aegypti* reduction in New Orleans, USA, however this does involve weekly laborious releases to be effective (Huang et al., 2017). Release of predatory larvivorous copepods of the genus *Mesocyclops* and *Macrocyclops* resulted in successful decrease of DENV transmission due to *Ae. aegypti* reduction in Vietnam, however has not been so successful in other areas due to lack of community participation (Lazaro et al., 2015).

Entomopathogenic fungi can be used to target the adult stage of mosquitoes; these are fungi that produce infective spores which release toxins, resulting in mosquito death. The conidia spores of *Metarhizium* fungi are likely to be ingested by mosquitoes, whereas blastospores upregulate adhesion molecules to attach and penetrate the outer cuticle of mosquitoes (Huang et al., 2017). Once internalised, rapid death of the mosquito occurs. Entomopathogenic fungi can be applied directly to breeding sites or sprayed, much like fogging with chemical insecticides.

### 1.5.6. *Wolbachia* as a control method

One novel control method that bridges the gap between biological and genetic control is the use of *Wolbachia pipientis*, an endosymbiotic bacteria found in up to 52% of terrestrial arthropods (Weinert et al., 2015). *Wolbachia* has been considered for vector control due to i) its ability to shorten a mosquito lifespan, ii) the discovery it can reduce replication and transmission of RNA viruses in insect vectors and iii) release of *Wolbachia*-infected males can suppress existing populations infected with a different strain due to bidirectional incompatibility (Bian et al., 2010; Mains et al., 2016; Min and Benzer, 1997; Moreira et al., 2009; Sinkins et al., 1995; Teixeira et al., 2008; Walker et al., 2011). In addition to this, once *Wolbachia* is established it ensures its propagation through a population by manipulating the host reproduction in its favour, making it an attractive self-propagating method for limiting arbovirus transmission.

*Wolbachia*-infected female mosquitoes have been released in over 12 countries globally, including in Australia, Brazil, Vietnam, Indonesia and Malaysia (WMP, 2018). The intent of the releases is to replace the native population with *Wolbachia*-infected mosquitoes that cannot transmit arboviruses. A high percentage of *Wolbachia*-infected mosquitoes were retained in the population two years following releases. There was a low frequency of uninfected mosquitoes, which were likely due to immigration of mosquitoes from other populations (Hoffmann et al., 2014). This novel vector control method has showed very promising results and research continues into investigating the diversity of *Wolbachia* and the mechanism of pathogen inhibition.

Each vector control method has their advantages and limitations (Table 1.1); the effectiveness of physical, chemical and biological control methods can be increased when applied in a co-operative manner. Genetic control and use of *Wolbachia* differs to the aforementioned control methods, in that they rely on invasion and suppression/replacement of existing populations. However, the increasing spread of arboviruses means the current control methods are

| Control method | Stage of intervention | Methods used | Advantages | Disadvantages |
|---|---|---|---|---|
| Physical | Prevent colony establishment/bite | Remove breeding sites<br>Long sleeved clothing<br>Bed nets | Reduce bites during the day and when asleep<br>Effective against night time biters like Anopheles | Can't remove all breeding sites<br>Bed nets need community-wide use to be effective<br>Bed nets ineffective against day biters like Aedes |
| Chemical | Eradicate existing colony | Insecticides & larvicides<br>Indoor residual spraying<br>Outdoor fogging<br>Apply to breeding sites | Can prevent further disease transmission during epidemics | Widespread insecticide resistance<br>Often applied once epidemic has already begun |
| Genetic | Suppress existing colony | Male lethality<br>SIT<br>RIDL | SIT successfully eradicated screwworm, continues to be effective<br>RIDL reduced mosquito populations where implemented | Self-limiting: requires continual releases and mass-rearing facilities<br>Not ideal for poorer countries<br>Need public approval and environmental assessment for release of GM mosquitoes |
| Biological | Eradicate/suppress existing colony | Plant toxins<br>Predatory mosquitoes<br>Larvivorous fish | Environmentally friendly<br>Very effective in combination with other control methods<br>Predatory mosquitoes can locate cryptic breeding sites | Can't put larvivorous fish in artificial containers<br>Requires constant surveillance of breeding sites and releases<br>Larvivorous fish can replace native fish |
| *Wolbachia* | Suppress/replace existing colony | CI-based suppression<br>Replace population with *Wolbachia*-infected mosquitoes that don't transmit viruses | Self-sustaining; only few weeks of introduction until invades population<br>No GM involved<br>Naturally found in mosquitoes | Have to monitor *Wolbachia* infection following release<br>Replacement will still have biting mosquitoes<br>Can't be used in combination with chemical control |

**Table 1.1. Advantages and disadvantages of vector control methods**
Comparison of vector control methods. Table outlines when each control method is implemented (Stage of Intervention), method of implementation and the advantages and disadvantages of each.

ineffective, and there is a need for targeted *Aedes* mosquito control. This is where *Wolbachia* is an ideal candidate, as the release of *Wolbachia*-infected *Aedes* mosquitoes will replace and reduce the vector efficiency of existing populations.

## 1.6 *Wolbachia pipientis*

### 1.6.1. Biology of *Wolbachia*

*Wolbachia* are gram-negative bacterial endosymbionts of the genus *Rickettsia*, which are found widespread in arthropods and nematodes. *Wolbachia* reside within cells of their host, mainly in reproductive tissues, and do not replicate outside of cells (Rasgon et al., 2006). They are mainly transmitted vertically to offspring through the cytoplasm of eggs, but also can be transferred horizontally (Werren et al., 1995). *Wolbachia* was first discovered in *Culex pipiens* mosquitoes by Hertig and Wolbach in 1924, and given the subsequent species name *Wolbachia pipientis* (Werren, 1997). There have been many more discoveries uncovering the vast diversity of *Wolbachia* strains within this species, however it has proved challenging to arrange these strains phylogenetically.

To date, *Wolbachia* has been categorised into sixteen evolutionary lineages (supergroups), named from A to O, which indicates the huge diversity of strains within this species (Gerth and Bleidorn, 2016; Glowska et al., 2015). Those found in A and B are found in terrestrial arthropods and are the most abundant in nature, found across a wide range of hosts including parasitic wasps, weevils, planthoppers and beetles, to name a few (Werren, 1997). Whole genome sequencing (WGS) indicates the A and B supergroups have a monophyletic lineage, suggesting the ability to adapt to a wide range of arthropod hosts has a single origin (Gerth et al., 2014). In fact, their last common ancestor is predicted to be 200 million years ago (Gerth and Bleidorn, 2016). *Wolbachia* in the C and D supergroups are found in filarial nematodes and commonly have a mutualistic relationship with their host. Only two families of nematodes are known to harbour *Wolbachia* infections; Onchocercidae (filarial nematodes) and Pratylenchidae (plant parasitic nematodes) (Brown et al., 2016; Lefoulon et al., 2016). WGS indicates these mutualist strains have a paraphyletic origin, with possible host-switches from arthropods-nematodes or vice versa occurring several times through their evolution (Gerth et al., 2014). However, Wolbachia supergroups are not

limited to specific hosts; those in supergroup F have been found in arthropods and nematodes (Gerth et al, 2014).

### 1.6.2. Reproductive manipulation

*Wolbachia* are well known as reproductive parasites, employing four strategies across genera to ensure their propagation; parthenogenesis, feminisation, male-killing and cytoplasmic incompatibility (Werren et al., 2008). These reproductive manipulations result in the production of female offspring, which pass on the *Wolbachia* infection. Parthenogenesis occurs in species in which eggs can develop asexually, such as order Hymenoptera (wasps, ants) and mites (Pannebakker et al., 2004; Weeks and Breeuwer, 2001). Feminisation has been observed in Hemiptera, Isopoda Lepidoptera insect orders; in Lepidoptera, *Wolbachia* suppresses expression of the Masc gene, which normally induces development of males (Cordaux et al., 2004; Fukui et al., 2015). *Wolbachia*-induced male killing has been observed in arthropod orders of Diptera, Coleoptera, and Lepidoptera (Werren et al., 2008). *Wolbachia* target the male chromatin in *Drosophila bifasciata*, resulting in errors in chromatid segregation and eventual arrest of male development (Riparbelli et al., 2012). This mechanism of male killing is similar to that of cytoplasmic incompatibility, which will be explained next. It is therefore not surprising that some strains of *Wolbachia* can induce male-killing in one species, yet cause CI when transferred to another species, and vice-versa (Hurst et al., 2000; Sasaki and Ishikawa, 2000).

*Wolbachia* is mainly spread vertically from female mosquitoes to offspring via the ovaries and ensures its propagation and survival within an insect population by inducing cytoplasmic incompatibility (CI) in mosquitoes. This manipulation results in the arrest of development of offspring from a cross with a *Wolbachia*-infected male and uninfected female. Meanwhile, *Wolbachia*-infected females can spread the symbiont to their offspring, regardless of male-infection status (Sinkins, 2004). This skews the mosquito population towards being infected with *Wolbachia* (Figure 1.8.).

It is generally accepted that *Wolbachia*-induced CI follows a modification-rescue pattern, whereby male sperm is modified and is rescued in the early embryo when *Wolbachia* is present. It is thought *Wolbachia* induces a defect in early mitosis

resulting in a delay of male pronuclei development, including the breakdown of the nuclear envelope and activation of mitosis by Cdk1. Due to this delay, during metaphase the male chromosomes are only semi-condensed, whereas female chromosomes are fully condensed. This results in incorrect separation during anaphase with male chromosomes incorrectly separated or excluded entirely from the new zygote, resulting in arrest of egg development (Werren et al., 2008). A recent study has shown *Wolbachia*-encoded operon *cidA-cidB*, a deubiquitating enzyme, can induce CI in *D.melanogaster* in a toxin/anti-toxin manner. This model proposes cidB as a toxin to the fertilised egg, with cidA acting as the anti-toxin. It is theorised cidA is rapidly degraded in an incompatible cross; therefore cidB remains toxic to the egg. However, in a compatible cross, the female provides more cidA, neutralising the toxic cidB (Beckmann et al., 2017). Indeed, cidA has been shown to be capable of rescuing the CI phenotype in *Drosophila* ((Shropshire et al., 2018). However, the rescue factor required for CI rescue must differ between *Wolbachia* strains, as bidirectional incompatibility can occur; for example, when a female and male with two different *Wolbachia* strains mate, cytoplasmic incompatibility occurs (Bordenstein and Werren, 2007). This indicates the mechanism of CI has diverged between *Wolbachia* strains and cannot be explained simply by one mechanism.

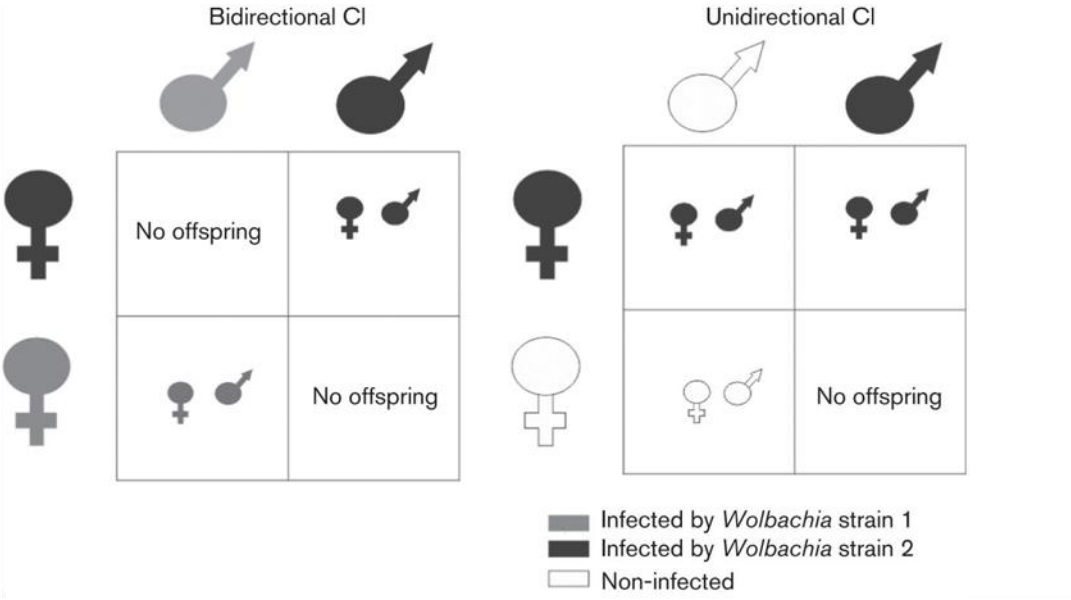


Figure 1.7. **Uni and Bi-directional cytoplasmic incompatibility.**
In crosses with two different *Wolbachia* strains, there is no viable offspring (Bidirectional CI). Females can produce *Wolbachia*-infected progeny with uninfected males or males infected with the same strain (Unidirectional CI). (Rainey et al., 2014)

### 1.6.3. *Wolbachia* in *Drosophila*

The attractiveness of *Wolbachia* as a tool for arbovirus control exploded when it was shown to have pathogen-inhibition abilities, initially with viruses in *Drosophila* and later in *Aedes* mosquitoes. Several species of *Drosophila* naturally harbour *Wolbachia*, including *Drosophila melanogaster* and *Drosophila simulans*. The nomenclature given to *Wolbachia* tends to arise from its native host, for example *w*Mel is the *Wolbachia* strain found in *D. melanogaster*. *D.melanogaster* infected with *w*Mel or *w*MelPop had increased longevity when infected with pathogenic RNA viruses Cricket paralysis virus (CrPV), DCH and FHV, compared to *Wolbachia*-uninfected flies (Hedges et al., 2008; Teixeira et al., 2008). Interestingly, *Wolbachia* did not offer the same protection against DNA virus insect iridescent virus 6 (IIV6) (Teixeira et al., 2008). Further study in *Drosophila* showed a high density of *Wolbachia* was required for viral blockage; in *D.simulans* only high density *Wolbachia* strains *w*Mel, *w*Ri and *w*Au provided antiviral protection from DCV and FHV (Osborne et al., 2009). A comprehensive study of wMel-like variants (wMelCS and wMelPop) revealed a higher density compared to wMel, leading to stronger viral inhibition and decreased lifespan (Chrostek et al., 2014). The discovery of *Wolbachia*-mediated pathogen inhibition in *Drosophila* prompted more research into the presence of the bacteria in biting vectors of arboviruses, and the potential for reducing disease transmission.

### 1.6.4. *Wolbachia* in *Aedes*

*Ae. albopictus* naturally harbors a superinfection of two low-density *Wolbachia* strains in the wild, *w*AlbA and *w*AlbB (Ahmad et al., 2017; Kitrayapong et al., 2002). On the contrary, *Ae. aegypti* is not naturally infected. *Wolbachia* has been artificially transinfected into *Ae. aegypti* by a process known as cytoplasmic transfer, whereby cytoplasm from a *Wolbachia*-infected egg is transferred to an uninfected *Ae. aegypti* egg (Ant et al., 2018; Fraser et al., 2017; McMeniman et al., 2009; Moreira et al., 2009; Xi et al., 2005b). This process is performed on hundreds to thousands of eggs until a *Wolbachia*-positive larvae/adult is detected, from which a *Wolbachia*-infected *Ae. aegypti* colony is established. The density and virus-inhibition ability of *Wolbachia* strains differs between natural hosts and those recently transinfected.

*w*MelPop is a virulent, high density *Wolbachia* strain that was artificially created using laboratory strains of *D. melanogaster*, noted for its ability to half host lifespan (Min and Benzer, 1997; Woolfit et al., 2013). When transinfected into *Ae. aegypti*, *w*MelPop provided strong protection from a range of pathogens including DENV, CHIKV and *Plasmodium* (Moreira et al., 2009). However, the high density of *w*MelPop led to fitness costs for the mosquito, such as life shortening and increased egg mortality (McMeniman et al., 2009). Despite these costs, *w*MelPop is still considered for vector control; this life shortening could result in less mosquitoes surviving long enough to complete the virus incubation period required for virus transmission, and increased egg mortality means there could be less viable mosquito eggs remaining following a dry season. The latter is a particularly important aspect for vector control; eggs that were laid by mosquito populations that are subsequently eradicated can remain viable for several months, hatching once again with rainfall. A recent semi-field study has shown *w*MelPop can reduce egg viability to less than 5% (Ritchie et al., 2015). However, field releases in Australia and Vietnam showed that while *w*MelPop can invade and persist at 80% frequency in wild populations during active releases, once releases stop the percentage of infected adults drops drastically (Nguyen et al., 2015). This is likely due to immigration from other mosquitoes but importantly loss of *w*MelPop-infected mosquitoes due to deleterious fitness costs. For field releases to have continued success, the *Wolbachia* strain continued must not hinder the fitness costs of the mosquito.

Research into the pathogen-inhibition abilities of other *Wolbachia* strains showed that density and pathogen-inhibition ability varies depending on the infected host. *w*AlbA and *w*AlbB (*w*AlbA/B) remain relatively low density in *Ae. albopictus* and have no effect on DENV and CHIKV replication in their native host (Blagrove et al., 2013; Blagrove et al., 2012). *w*AlbB reaches higher densities when transinfected into *Ae. aegypti*, and when challenged with DENV has reduced titres and increased longevity, compared to *Wolbachia*-uninfected mosquitoes (Ant et al., 2018; Bian et al., 2010). The low density of *w*AlbA/B in *Ae. albopictus* is likely due to years of co-evolution, whereas the superinfection in the novel *Ae. aegypti* host has the opportunity to reach higher densities. However, some *Wolbachia* strains confer protection from pathogens in native and novel hosts alike.

The *w*Mel strain from *Drosophila* provides protection from RNA viruses in native and novel mosquito hosts. When transinfected into *Ae. aegypti* and *Ae. albopictus* cleared of their natural infection, *w*Mel provides strong antiviral protection against DENV and CHIKV (Blagrove et al., 2013; Blagrove et al., 2012; Walker et al., 2011). Although the related *w*MelPop offered a stronger pathogen-inhibition phenotype in *Ae. aegypti*, *w*Mel provides good protection without the high fitness costs. The variation in pathogen-inhibition strength between different *Wolbachia*-host interactions has raised questions about the mechanism responsible for viral inhibition.

## 1.7. *Wolbachia*-mediated pathogen inhibition

### 1.7.1. Density

Studies have shown that higher density *Wolbachia*-strains confer the strongest pathogen inhibition. *Wolbachia* density generally increases when it is transinfected into a novel host, such as *w*AlbB reaching higher densities in *Ae. aegypti* and *Ae. polynesiensis* than in native *Ae. albopictus* (Bian et al., 2010; Bian et al., 2013). However, high density *Wolbachia* strains can also occur in native hosts; strong pathogen blocker *w*MelPop grows to high density in native and novel hosts, conferring antiviral protection in *Drosophila* and *Aedes* alike (Chrostek et al., 2013; Moreira et al, 2009). This may be explained by the particularly virulent and fast-replicating nature of *w*MelPop, which is not usually seen with other strains (Kambris et al, 2009; Chrostek et al, 2018).

Viruses follow a specific path through mosquito tissues to complete replication, therefore it may be considered that the density of *Wolbachia* in tissues such as the midgut and salivary gland impact pathogen inhibition. Indeed, *Wolbachia* and DENV only appear to co-habitat cells when *Wolbachia* is at a low density (Lu et al., 2012), indicating virus may be excluded from cells at high density. However, no correlation has been found between high density in tissues and viral inhibition in *D. simulans* and *Ae. aegypti* (Amuzu and McGraw, 2016; Osborne et al., 2012). *Wolbachia* density appears to be more important for pathogen inhibition than tissue specificity. For instance, *w*AlbB in Aa23 (*Ae.albopictus*) cells reduces CHIKV titres, and density within the cell line is much higher than those naturally found in host somatic tissues (Raquin et al., 2015).

### 1.7.2. Immune priming

One proposed mechanism of *Wolbachia*-mediated pathogen inhibition is that of immune priming; activation of immune pathways which in turn reduces viral titre. When transinfected into novel hosts, *Wolbachia* has been shown to upregulate immune genes resulting in transcription of AMPs; *w*Mel, *w*MelPop and *w*AlbB in *Ae. aegypti* resulted in the upregulation of many immune genes involved in the Imd and Toll pathways, including Cecropins and Defensin (Bian et al., 2010; Kambris et al., 2009). Pan et al showed *w*AlbB in *Ae. aegypti* resulted in higher levels of ROS, which led to activation of AMP transcription (Defensin, Cecropin) via the Toll pathway. When challenged with DENV, knockdown of the AMP Defensin resulted in an increase in virus titre, indicating an antiviral role (Pan et al., 2012).

However, pathogen inhibition still occurs in *Drosophila* with native and novel *Wolbachia* strain infections without immune gene upregulation (Chrostek et al., 2014; Wong et al., 2011). In addition, there is no immune gene upregulation in *Ae. albopictus* cleared of their natural *Wolbachia* infection and transinfected with *w*Mel (Blagrove et al, 2012). Despite the lack of immune upregulation, *D.melanogaster* and *Ae.albopictus* infected with *w*Mel exhibit pathogen inhibition (Rances et al 2012). This indicates immune priming is not the fundamental mechanism of *Wolbachia*-mediated virus inhibition. However, it cannot be ruled out that immune upregulation in recently transinfected hosts can have an additive effect on virus inhibition, as shown in Pan et al. It is theorised that the elevated immune gene expression in *Ae. aegypti* is due to introduction of a novel symbiont into the mosquito, as it is not observed in native hosts of *Wolbachia*.

It has been considered that RNAi, the predominant antiviral pathway in insects, plays a role in *Wolbachia*-mediated virus inhibition. However, C636 cells have a dysfunctional RNAi response (Brackney et al., 2010), but when infected with *w*Mel still inhibit DENV (Frentiu et al., 2010). In addition to this, in *Drosophila* with mutated components of the siRNA pathway WNV, DCV and FHV are inhibited (Glaser and Meola, 2010; Hedges et al., 2012). However, *Wolbachia* does induce changes in the miRNA component of the RNAi pathway and this has been shown to have an antagonistic role to DENV. *w*MelPop in *Ae. aegypti* induces expression of aae-mIR-2940, an miRNA that suppresses expression of a DNA methyltransferase (AaDnmt2) gene that may be involved in host defence, gene and lifespan

regulation (Hussain et al., 2011; Zhang et al., 2013). Importantly, DENV was shown to induce AaDnmt2, with an increased expression reducing *Wolbachia* density (Zhang et al., 2013), indicating an antagonistic relationship between bacteria and virus. On the other hand, miRNA and piRNA pathways are not required for antiviral defence in *Drosophila* cells and flies (Petit et al., 2016; Rainey et al., 2016). In light of this, the induction of miRNAs in *Wolbachia*-infected *Ae. aegypti* may be due to the fact it is a novel infection, much like the induction of other immune pathways. This indicates there are other mechanisms at the heart of *Wolbachia*-mediated antiviral defense.

### 1.7.3. Manipulation of cell processes

*Wolbachia* and viruses both require a host cell to replicate in, therefore it can be theorised that they are in competition for host cell resources and this is how pathogen inhibition may inadvertently occur. *Wolbachia* infection interferes with homeostasis of iron, cholesterol and with autophagy and apoptosis; all which may be antagonistic to viral replication. Autophagy is a cellular process that delivers damaged/unused organelles to lysosomes for digestion, releasing resources to be used for other processes. It is implemented during times of cell stress, or in response to invading pathogens (Klionsky and Emr, 2000). *Wolbachia* has been shown to interfere with autophagy in both mutualist and parasitic associations. The autophagosomal marker ATG8a was shown to be associated with *Wolbachia* infection in the mutualistic infection in nematode *Brugia malayi* (Voronin et al., 2012). Increased ATG8a levels were also observed in *w*AlbB-infected C636 cells and *w*MelPop-infected *D.melanogaster* (Voronin et al., 2012). DENV also manipulates autophagy, inducing autophagosomes to co-localise and degrade lipid droplets, releasing fatty acids. These fatty acids are oxidised and transformed into ATP, creating a metabolically pro-viral environment for viral replication (Heaton and Randall, 2011). However, if *Wolbachia* infection has already hijacked the autophagy pathway, DENV may not be able to create this favourable environment.

In addition, *Wolbachia* alters the lipidome of infected cells, which may result in a decrease of fatty acids available for degradation. *Wolbachia*-infected *Ae. albopictus* cells had reduced sphingolipids relative to uninfected cells (Molloy et al., 2016), which have previously been shown to be induced in DENV-infected insect cells (Perera et al., 2012). The lipidome of the intracellular membranes is

crucial for DENV replication as the virus constructs intracellular replication complexes with these membranes (Perera et al., 2012). There appears to be a fine line between *Wolbachia* inducing autophagy and avoiding lysosomal degradation; activation of autophagy using Rapamycin results in a decrease in *Wolbachia*. This indicates *Wolbachia* may have evolved a mechanism to avoid lysosomal degradation, which may involve modulation of key autophagy proteins to delay or block autophagosome maturation (Voronin et al., 2012). This would in turn negatively impact DENV replication, as they require mature autophagosomes to lyse lipid droplets.

Lipid droplets are ER-derived organelles that store protein and lipids. Aag2 (*Ae. aegypti*) cells infected with *w*MelPop have an accumulation of lipid droplets, relative to uninfected cells. It is perhaps not surprising that *Wolbachia* interfere with ER-derived organelles, as electron microscopy has shown they are closely associated with and alter the structure of the ER (White et al., 2017). In addition, *Wolbachia*-infected cells have higher levels of esterified cholesterol, and lower free cholesterol (Geoghegan et al., 2017). Viruses require cholesterol for many stages of their replication, and the lack of free cholesterol may hinder this. To confirm the importance of cholesterol for DENV replication, Aag2 wMelPop cells were treated with cyclodextrin 2HPCD, which facilitates trafficking of cholesterol that was previously esterified. This treatment resulted in a reduction of *Wolbachia*-mediated DENV inhibition, indicating more cholesterol was available for viral replication (Geoghegan et al., 2017).

The importance of cholesterol for virus replication was highlighted in *Drosophila*, when dietary cholesterol supplementation reversed *Wolbachia*-mediated inhibition of DCV in a dose-dependent manner (Caragata et al., 2013). Cholesterol supplementation had no effect on DCV in uninfected flies, presumably as there was free cholesterol present already for viral replication, which would reach a plateu. However, the same result was not observed with DENV in mosquito cells. Interestingly, treatment of Aag2 *w*MelPop cells with cholesterol did not rescue DENV inhibition, and supplementation of cholesterol to Aag2 uninfected cells inhibited DENV replication (Geoghegan et al., 2017). This indicates i) that cholesterol added to *Wolbachia*-infected cells is esterified rapidly and ii) that overloading a cell with cholesterol can inhibit viral replication much like depletion

of cholesterol can. The difference in result with cholesterol supplementation may be due to DENV and DCV being genetically distinct viruses, with slightly different usage of cholesterol in their replication process. Despite the differences in result, there is strong evidence that *Wolbachia* modulates cholesterol within cells and this is detrimental to virus replication.

Another cell resource that is manipulated by *Wolbachia* and viruses is iron. Excess levels of iron can be toxic to cells, as it can react with hydrogen peroxide ($H_20_2$) to produce highly reactive radicals (Fenton's Reaction), resulting in damage of cellular organelles. The protein transferrin is upregulated by the cell in times of redox stress, acting as an iron store and is also implicated in NF-KB activation of insect immunity against bacteria (Kremer et al., 2009). It is thought *Wolbachia* upregulate bacterioferritin, the bacterial iron store, to combat potential redox stress (Brownlie et al., 2009). This stress may be due to the induction of autophagy, which results in accumulation of iron. *Wolbachia* bacterioferritin is upregulated in parasitoid wasp *A. tabida* and *D. simulans* when overloaded with iron (Gill et al., 2014). This may be antagonistic to DENV and CHIKV replication, as virus infection results in downregulation of transferrin (Tchankouo-Nguetcheu et al., 2010). This indicates storage of iron by *Wolbachia* may be antagonistic to flavivirus replication.

There is mounting evidence that *Wolbachia* alters host cell components and resources, which may in turn be antagonistic to viral replication. Figure 1.8 summarises the possible ways *Wolbachia* may be interfering with viral replication within a cell. Immune priming only occurs in novel hosts and is not necessary for viral inhibition, therefore there must be another underlying mechanism of inhibition. This inhibition is not likely to be at the entry, assembly or egress stages, as replication of SFV that was transinfected into cells was still inhibited (Rainey et al., 2016). The multiple changes *Wolbachia* induces in a host cell may inadvertently restrict the replication of arboviruses, and provide a novel way to prevent disease transmission from mosquitoes.

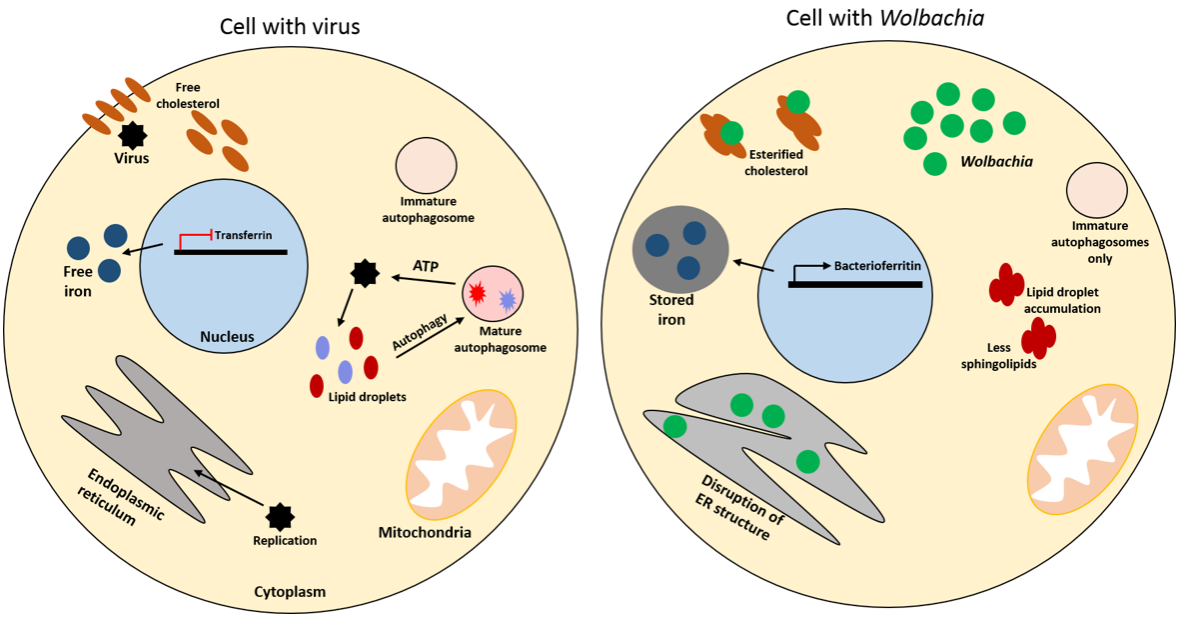


Figure 1.8.

**Schematic showing how *Wolbachia* and viruses may be competing for host cell resources.** Without *Wolbachia*, viruses have access to iron, lipid droplets, cholesterol, and sites for replication (endoplasmic reticulum). With *Wolbachia*, the structure of the ER is disrupted, iron is stored, more cholesterol is esterified and the lipidome is reduced. *Wolbachia* may also be disrupting the maturity of autophagosomes, preventing virus-induced autophagy.

## 1.8. Aims of this study

Much progress has been made in investigating *Wolbachia* and its use in *Ae. aegypti* as a vector control method, to prevent the spread of arboviruses. This study aims to;

1) Add to the current evidence of the mechanism by which *Wolbachia* may be interfering with viral replication, by studying its effects on redox homeostasis and perturbation of the endoplasmic reticulum.

2) Characterise novel transinfections of *Wolbachia* strains in *Ae. aegypti* and report on the differences in fitness and viral inhibition between each strain.

3) Further subject *Wolbachia*-infected *Ae. aegypti* to cyclical heat-temperature stress to assess the stability of transinfected mosquitoes in the field.

# Chapter 2

## Materials and methods

## 2.1. *Aedes aegypti*

### 2.1.1. General rearing

All mosquito colonies were reared on a 12-hour light/dark cycle at 27ºC and 70% relative humidity. Eggs were stimulated to hatch by submerging in water and adding 1g/L bovine liver powder (MP Biomedicals, California, USA). Larvae were fed tropical fish pellets (Tetramin, Tetra, Germany) and adults were provided with a 5% sucrose meal ad libitum. Blood meals were provided using the artificial Hemotek feeding system (Hemotek, UK) using defibrinated sheep blood (TSC Biosciences, UK). Eggs were collected on damp filter paper (Whatman plc, GE Healthcare, UK) and desiccated for 5-10 days prior to further hatching. These conditions were used for mosquito rearing unless stated otherwise.

### 2.1.2. Cyclical heat-treatment

Eggs of *Ae.aegypti* WT, *w*AlbB, *w*Mel and *w*Au were hatched, separated into experimental groups and larvae reared at a density of 200 per 500mL of water. At the L1 larvae stage, the cyclical heat-treatment group were moved to a Panasonic MLR-352-H Plant Growth Incubator Chamber (Panasonic, Osaka, Japan) and exposed to the temperature regime selected based on data from *Ae. aegypti* larval breeding sites in Trinidad and environmental temperatures in Malaysia in April 2017 (Hemme et al, 2009; Accuweather.com). Water temperature from Trinidad was selected to represent a typical tropical region where *Aedes* mosquitoes are found. Water temperatures were monitored using a data logger (Hobo Water Temperature Pro V2, USA) placed in the water. Mosquitoes in the control group were maintained as stated in general rearing section.

### 2.1.3. Strain creation of novel transinfections

Strain creation was performed by Thomas Ant. Briefly, *Wolbachia* was transinfected into *Ae. aegypti* wild-type mosquitoes that had been colonised from Selangor State, Malaysia in the 1960s. *w*AlbA, *w*AlbB and *w*Mel *Ae. aegypti* lines were generated by transfer of cytoplasm from triple-infected *Ae. albopictus*. Cytoplasm was injected into eggs using a microinjector as previously described (Blagrove et al., 2012). Female $G_0$ survivors following injection were back-crossed with wild-type males, blood fed and separated for oviposition. The $G_0$ females were then analysed for *Wolbachia* by PCR. Eggs from *Wolbachia*-

negative females were discarded. Eggs from *Wolbachia*-positive females were hatched and assessed for *Wolbachia* transmission. A triple-infected *Ae. aegypti* line with *w*AlbA, *w*AlbB and *w*Mel was created by transfer from a triple-infected *Ae. albopictus* (origin Indonesia) donor. However, maternal inheritance of all three strains was not 100%, therefore colonies were identified with single strain infection, leading to the creation of each line. The *w*Au line was created by embryonic transfer from *Drosophila simulans* (origin Australia) embryos straight into *Ae. aegypti* embryos. The *w*Au*w*AlbB line was created by transfer of *w*Au from *Ae. aegypti* into the single-infected *w*AlbB *Ae. aegypti* line.

#### 2.1.4. Dissection of *Ae. aegypti* tissue

Adult flies were briefly anaesthetised on ice before sampling of whole bodies or dissection of tissues. Tissues were dissected in a drop of PBS on ice using a dissection microscope. Typically 5 salivary glands, midguts and pairs of ovaries were combined for one technical replicate for RNA extraction. For DNA extraction and quantification of *Wolbachia* (wsp) in ovaries following cyclical heat-treatment, 3 pairs of ovaries were combined.

## 2.2. Maternal inheritance

### 2.2.1. In novel transinfections

Maternal inheritance of *Wolbachia* in novel transinfection lines was assessed by crossing females from each *Wolbachia* line to wild-type males in groups of 20 males and 20 females. Females were provided a blood meal and then separated for oviposition. Eggs laid were then hatched and DNA was extracted from a selection of 10 pupae per cross (resulting in 200 pupae per line) using the phenol:chloroform method. *Wolbachia* presence was then checked by PCR (WSpec and qWSP primers as noted in Appendix 1).

### 2.2.2. Following cyclical heat stress

Maternal transmission of *Wolbachia* in *Ae. aegypti* exposed to cyclical heat stress was assessed by backcrossing heat-treated females with heat-treated males, while females reared under normal conditions were mated with their male counterparts. Females were fed a blood-meal at 5 days old and individualised on damp filter paper inside an up-turned plastic cup, for oviposition. Filter papers were left for two days then collected for desiccation. Once dry, eggs were

hatched in plastic container at control temperatures. 6-10 L4 larvae were selected from each individualised female and DNA was extracted using STE buffer. *Wolbachia* presence was assessed by PCR with strain-specific primers and qPCR with general wsp primers.

## 2.3. Cytoplasmic incompatibility

Cytoplasmic incompatibility induction and rescue was assessed with wild-type mosquitoes and between novel transinfected lines. As above, 20 males and 20 females of each line were allowed to mate and a blood-meal was provided for oviposition. Eggs were collected on damp filter paper and desiccated for 5 days at 27ºC and 70% humidity. Eggs were hatched and larvae counted at L2-L3 stage to determine hatch rate. Females that did not lay eggs were dissected to check for successful mating by presence of spermathecae and those non-mated were excluded from hatch rate analysis.

## 2.4. Assessing mosquito fitness

### 2.4.1. Adult longevity

50 males and 50 females were set up in 24.5x24.5x24.5cm insect rearing cages and reared under general conditions. Four replicates were set up for each line. Cages were blood-fed once a day from day 5 onwards and filter paper was provided for oviposition. Adult mortality was monitored daily for a total length of 70 days.

### 2.4.2. Fecundity

5-day old mated females were fed defibrinated sheeps blood using a Hemotek. 20 fully engorged females were selected per line and placed in up-turned cups on top of filter paper, using an aspirator. 5% sucrose-soaked cotton wool was made available via a hole in the top of the cup. 3 days after the blood meal the filter paper was dampened and left overnight. Filter paper was then replaced the next day and process repeated again. Eggs were counted on each filter paper using a hand-counter and dissection microscope.

### 2.4.3. Egg survival

Egg survival following desiccation was measured by feeding 7-day old mosquitoes and collecting eggs 3 and 4 days post-feed on three separate damp filter cones

in a cage. Egg papers were stored at 27ºC and 70% humidity. 5, 10, 15, 20, 35 and 50-days post oviposition a section of approximately 200-300 eggs was cut from each egg paper and hatched. Eggs were counted using a hand-counter and dissection microscope. Hatch rates were assessed 10 days later by counting larvae using a Pateur pipette and hand-counter.

## 2.5. Virus propagation

Virus was added to 80% confluent C636 cells at an MOI of 0.1 in Schneiders media (Pan Biotech, Germany) with 5% Fetal bovine serum and 25mM HEPES. Cells were transferred to a 28ºC incubator (no $CO_2$). SFV was left for 48 hours to replicate, DENV and ZIKV were left for 5 days. Supernatant was then harvested and spun down to remove cell debris. Virus was quantified by plaque assay or FFA on vero cells.

## 2.6. Virus quantification

### 2.6.1. Fluorescent Focus Assay (FFA)

Infectious virions of Dengue virus were quantified by Fluorescent focus assay (FFA). Vero e6 cells were plated out in 96-well glass-bottom plates (Corning, NY, USA) overnight at a density of 1x10^5. Samples were 10-fold serially diluted in DMEM 2% FBS. Media was removed from vero cells and replaced with 50 µl of each sample dilution. The plate was placed in a 37ºC 5% CO2 incubator for 1 hour, with rocking every 15 minutes. Following this, 150 µl of overlay medium (0.8% carboxymethylcellulose, 5% FBS, 1% penstrep in DMEM 2mM L-glutamine) was gently added on top of the sample, to prevent migration of virus particles. Cells were then left for 48 hours for virus to replicate, then washed with PBS and fixed in ice cold methanol for 30 minutes. Cells were washed with 200 µl PBS (RT) and permeabilised with 150 µl of 0.1% Trixon X-100 in PBS for 5 minutes at RT. Permeabilisation solution was removed and 50 µl of primary antibody solution was added to each well at a dilution of 1:500 in 0.2% BSA PBS. Primary antibody for Dengue virus was MAB8705 Anti-Dengue Virus Complex Antibody clone D3-2H2-9-21, Millipore. Primary antibody for Zika virus was MAB10216 Anti-Flavivirus Virus Complex Antibody clone D1-4G2-4-15 (Millipore, USA). Cells were left for 1 hour at RT in a dark moist chamber, rocking gently. Cells were then washed three times with 0.2% BSA PBS and 50 µl of secondary fluorescent antibody was added to each well (Goat anti-mouse Alexa Fluor 488, A-11001,

Thermo Fisher; 1:400 in 0.2% BSA PBS). Samples were left for 1 hour at RT on a rocker, in a moist chamber, in the dark. Cells were then washed three times with 0.2% BSA PBS again and left in PBS for fluorescent plaque counting.

### 2.6.2. QRT-PCR

Virus RNA was quantified by qRT-PCR. Virus RNA was exracted using Trizol reagent (Sigma-Aldrich, MI, USA) unless otherwise stated, using manufacturers guidelines. cDNA was synthesised using the All-In-One cDNA Synthesis SuperMix (Biotools, TX, USA). Primers used to quantify Dengue by qPCR were the NS5-F and NS5-R set, ZIKV 835 and ZIKV 911c for Zika virus and SFV4-F and SFV4-R for Semliki Forest virus. Levels of target gene were normalised to the RpS17 house-keeping gene using the Pfaffl method (relative expression).

### 2.6.3. Plaque assay

Briefly, virus was 10-fold serially diluted and plated onto a vero monolayer for 48 hours. Vero cells were then fixed with 10% formalin and stained with 10% toluidine blue. Cells were rinsed with ddH20 and plaques were then visible to count. Wells were counted with 10-100 plaques visible with three replicates for each dilution.

## 2.7. Virus challenge

### 2.7.1. Oral feedings

5-day-old females were fed infectious blood-meals containing 800 µldefibrinated sheeps blood, 400 µl of virus suspension and 5mM of phagostimulant ATP. Semliki Forest Virus was sub-type C (1112041v), Dengue virus was serotype 2 (New Guinea C Strain), Zika virus was strain MP1751, all acquired from Public Health England Culture Collections. The final concentration of Semliki Forest Virus in the blood meal was 1x10^8. The final concentration of Dengue virus in the blood meal was 8.3x10^7 FFU/ml. The final concentration of Zika virus in the blood meal was 1.6x10^8 FFU/ml. Engorged females were anaesthatised on ice and placed into cardboard cups, with access to 5% sucrose-soaked cotton wool, and placed in a climactic chamber at 27$^{o}$C and 70% humidity until sampling. Sucrose was replenished every 2-3 days.

### 2.7.2. Intrathoracic injection

20 5-day-old females of each line were anaesthatised on ice and injected with SFV in the thorax using a pulled glass capillary needle and a Nanoject II

(Drummond Scientific, USA) hand-held microinjector. Injected mosquitoes placed in cups with netting and maintained under general rearing conditions for ten days. Whole-bodies of females were then homogenised with glass beads in Trizol (Sigma-Aldrich, MA, USA) on a Precellys 24 homogeniser (VWR) and RNA was extracted according to manufacturers guidelines.

### 2.7.3. Salivation

12 days post-feed females were salivated by inserting the proboscis into a 10 µl pipette tip containing mineral oil and placing a drop of 1% pilocarpine nitrate on to the thorax (to stimulate salivation). Collected saliva was ejected into tubes with Dulbecco's Modified Eagle Medium (DMEM) with 2% fetal bovine serum (FBS) and processed for Fluorescent Focus Assay (FFA). Salivary glands were then dissected where applicable and RNA extracted using the QIAamp Viral RNA Mini Kit (Qiagen, Hilden, Germany) according to the manufacturers guidelines.

## 2.8. DNA extraction

DNA was extracted from cells and mosquitoes using STE buffer (10uM Tris HCL pH 8, 100mm NaCl, 1mm EDTA), unless otherwise specified. Cells were spun down at 2000g for 4 minutes and resuspended in 100 µl STE in an Eppendorf tube. Mosquitoes were homogenised in 100 µl STE using a hand-held pestle. Samples were then boiled for 10 minutes at 95$^{o}$C. Eppendorfs were then put on ice for two minutes, and spun down at 2000g for 4 minutes to pellet cell debris. Supernatant was diluted 1 in 10 in ddH20 for further processing.

## 2.9. RNA extraction

RNA was extracted using TRIzol Reagent (Sigma-Aldrich, CA, USA). Briefly, cell pellet/mosquito were suspended in 500 µl TRIzol reagent and pipetted up and down/homogenised using a hand-held homogeniser and left for 5-15 minutes. 150 µl of chloroform was added to samples and mixed vigorously, samples were left to stand for three minutes at RT. Samples were spun 12,000g for 10 minutes at 4$^{o}$C. Top aqueous phase was pipetted off and dispensed into 250 µl of isopropanol. Samples were mixed and left for 10 minutes at RT. Samples were then spun at 10,000g for 10 minutes at 4$^{o}$C, forming a pellet.

## 2.10. cDNA synthesis

cDNA was synthesised using the All-In-One cDNA Synthesis SuperMix (Biotools, TX, USA) according to manufacturers instructions, unless otherwise stated. cDNA for quantification of ER chaperones in cell lines was created using Superscript II (Invitrogen, CA, USA) according to manufacturers instructions. For creating cDNA, RNA was diluted to 100ng/µl with ddH20 and no more than 6 µl of RNA was used in every reaction.

## 2.11. Polymerase chain reaction (PCR)

### 2.11.1. Primer design

Primers for thioredoxin peroxidase (TPX), calnexin, BiP and Xbp1 splicing were designed using PubMed Primer Design tool, with sequences spanning exons and products produced <500 base pairs. Primers were tested for efficiency by diluting *Ae. aegypti* cDNA 1:5 for a series of dilutions and calculating the efficiency from CT values (Appendix 2). Primers for DUOX and NOXM were taken from Pan et al (2012). Primers for Defensin C, Cecropin D and Cecropin G were designed by Thomas Ant. Primers for *Serratia* quantification were taken from Wei et al (2017).

### 2.11.2. Quantification of nucleic acid

Quantity and quality of nucleic acid was measured using the NanoDrop 1000™ spectrophotometer (Thermo Scientific, UK) according to manufacturer's instructions. Samples were blanked against a sample of the buffer they were diluted in. Concentrations were measured at 260nm and 280nm and given as ng/µl.

### 2.11.3. Standard PCR

*Wolbachia* was quantified from extracted DNA using general or strain-specific primers. Each reaction was set up with 10 µl of 1x Taqmaster mix (Vazyme), 8 µl ddH20, 0.5 µl Primer F, 0.5 µl Primer R, 1 µl DNA. Samples were cycled following the program listed in table 2.1 on a Veriti 96-well thermal cycler (Applied Biosystems). Primers used are listed in Appendix 1.

| Temperature | Time | |
|---|---|---|
| 94°C | 2 min | |
| 94°C | 30 sec | X 35 |
| 55°C | 30 sec | |
| 68°C | 45 sec | |
| 68°C | 7 min | |

Table 2.1. Cycling conditions for standard PCR

### 2.11.4. Agarose gel electrophoresis

Following standard PCR, samples were run on a 1% agarose gel made with 1X TAE buffer, stained with SYBR safe DNA Gel Stain (ThermoScientific, UK) at a concentration of 1:10,000. Once gels were set they were loaded into a gel tank (Fisher Scientific, UK) filled with 1X TAE. Samples were run at 100-120V for the desired distance and visualised using a UV light transilluminator.

## 2.12. Quantitative PCR (QPCR) & Reverse transcriptase quantitative PCR (RT-qPCR)

Quantification of *Wolbachia*, *Serratia* and gene expression was performed on a Rotor Gene Q (Qiagen). Each reaction contained; 2 µl of DNA for qPCR or cDNA for RT-qPCR (diluted 1:10 in ddH20), 5 µl 2x QuantiNova SYBR, 2 µl H20, 0.5 µl Primer F, 0.5 µl Primer R. Samples were cycled on conditions listed in table 2.2. Primers used are listed in Appendix 1.

| Step | Temperature | Time | Comments | |
|---|---|---|---|---|
| Initial denaturation | 95°C | 15 min | Template separates | |
| Denaturation | 95°C | 15 sec | | X 40 |
| Annealing | 60°C | 20 sec | | |
| Extension | 65°C | 5-20 sec | 5 sec per 100bp | |
| Data acquisition | - | - | Fluorescence data collected after every cycle | |
| Melting curve | 65 - 95°C | 1 sec hold per 0.3°C | Creates melt curve for primer specificity | |

Table 2.2. Cycling conditions of qPCR and RT-qPCR for *Wolbachia* and gene expression

## 2.13. Insect cell culture

### 2.13.1. Passaging Aag2 and Aa23 cells

Aag2 and Aa23 cells were maintained in Schneiders media (Pan Biotech, Germany) supplemented with 10% fetal bovine serum and 1% penstrep, maintained at 28$^{o}$C. Cells were grown in 25cm$^{2}$ Nunc tissue culture flasks (no filter) (ThermoFisher, UK) until confluent. Cells were then plated out for experiments or passaged into a new flask. Protocol for passage of cells is; remove old media, replace with fresh complete media, tap cells to remove from bottom and pipette cells up and down, put cells in new flask at a ratio of 3ml cells and 2ml new media.

### 2.13.2. Endoplasmic reticulum chaperone experiment

1x10^6 cells were plated overnight on poly-l-lysine coated 24-well plates. Media was then removed and cells washed 1x with PBS, Thapsigargin (Sigma Aldrich, USA) was added in complete media (10 µg/ml) to cells for 18 hours. Dengue virus 2 was then added at MOI 1 (titre 5x10^6 FFU/ml) for 5 days. Supernatant was then sampled for fluorescent focus assay of infectious virus and cells were spun down for RNA extraction using Trizol.

## 2.14. SFV Rluc

### 2.14.1. SFV Rluc infection

SFV Rluc was obtained (Siu et al., 2011) and grown on BHK cells for 3-5 days until cytopathic effects were observed, then titrated by plaque assay using BHK cells. Infection of Aag2 and Aa23 cells was performed in 24-well plates; 3.5x10^5 were plated out overnight on poly-l-lysine coated plates and infected at MOI 5 for 24 hours. Samples were harvested in 100 µl of passive lysis buffer (Promega, UK), left on a rocker for 20 minutes and luciferase was read on a Glomax Multi+ Microplate Multimode reader (Promega, UK) as outlined in Rainey et al (2016).

### 2.14.2. SFV Rluc Replicon

SFV Rluc replicon was transfected into cells as detailed in Rainey et al (2016). Briefly, replicon plasmid was grown in E.coli competent cells and plated onto agar plates containing Ampicillin and Kenamycin overnight shaking at 37$^{o}$C. Colonies were then selected and sampled into LB broth for growth overnight.

Plasmid DNA was purified using a Maxiprep kit (Qiagen, UK) and in vitro transcription of replicon was performed. Replicon was then transfected into cells using Dharmafect (Dharmacon, UK) for 24 hours, then harvested for luciferase measurement.

## 2.15. Fluorescent imaging

### 2.15.1. Fluorescent in-situ hybridisation

Ovaries were dissected in PBS from 5-day old females and fixed in Carnoy's fixative (chloroform:ethanol:acetic acid, 6:3:1) at 4ºC overnight. Samples were rinsed in PBS and transferred to a 6% hydrogen peroxide solution in ethanol for 72 hours at 4ºC for bleaching. Cells were plated out overnight at a density of 1x10^5 per 96-well glass-bottom plate (Corning, New York, USA). Media was then removed and cells were fixed with ice cold 10% formalin for 30 minutes at room temperature (RT). All samples were then incubated in the hybridisation buffer; 50% formamide, 25% 20xSSC, 0.2% (w/v) Dextran Sulphate, 2.5% Herring Sperm DNA, 1% (w/v) tRNA, 1% Denhardts solution, 0.015% (w/v) DTT and 100ng/ml of each probe ((Moreira et al., 2009)**)**. Probe sequences are as follows – General *Wolbachia* probes used; W2 (green) 5'-CTTCTGTGAGTACCGTCATTATC-(AlexaFluor 488)-3', W3 (green) 5'- AACCGACCCTATCCCTTCGAATA-(AlexaFluor 488)-3', which target *Wolbachia*-specific 16s rRNA, designed by Moreira et al, 2009**.** *w*AlbB (red) 5'-TAGGCTTGCGCACCTTGCAGC-(Cyanine3)-3' designed for this study. Samples were hybridised overnight in a damp container at 37ºC. Following this, samples were washed twice in a solution with 5% 20xSSC, 0.015% DTT and twice in 2.5% 20xSSC, 0.015% DTT for 20 minutes per wash at 55ºC. Ovaries were then placed on a slide with a drop of VECTASHIELD Antifade Mounting Medium with DAPI (Vector Laboratories, California, USA). Cells were kept in 96-well plates and stained for 20 minutes with Hoechst 33342 (ThermoFisher, MA, USA) at a concentration of 1 µg/ml in PBS. Cells were then washed with PBS and left in PBS for visualisation to prevent drying out. All samples were visualised on a Zeiss LSM 880 confocal microscope (Zeiss, Oberkochen, Germany).

### 2.15.2. CellRox Green imaging for oxidative stress

3x10^5 cells were plated on poly-l-lysine coated 96-well plates overnight to adhere. Media was then removed and complete media added with 200 µM TBHP,

100 µM CHPx, 5000 nM of NAC or no treatment, for 2 hours. Media was then removed and cells washed once with PBS. For oxidative stress detection, cells were then stained with 1000nM of CellRox Green (Invitrogen, California) and Hoechst in Schneiders for 30 minutes. Cells were then imaged on a Zeiss LSM 880 confocal microscope (Zeiss, Germany).

### 2.15.3. Image-IT Bodipy for lipid peroxidation

3x10^5 cells were plated on poly-l-lysine coated 96-well plates overnight to adhere. Media was then removed and complete media added with 200 µM TBHP or 100 µM CHPx for 2 hours. Media was then removed and cells washed once with PBS. Cells were then stained with 50 nM of BODIPY reagent (ThermoFisher, UK) and Hoechst in Schneiders for 30 minutes. Cells were then imaged on a Zeiss LSM 880 confocal microscope (Zeiss, Germany).

## 2.16. Flow cytometry

2x10^6 cells were plated on poly-l-lysine coated 12-well plates overnight to adhere. Cells were then stained using appropriate FISH/CellRox/Image-IT Bodipy protocol. Cells were then resuspended in PBS, diluted to 1x10^6 cells per ml and strained through 50 µM filters (Celltrics, Sysmex, Germany) into tubes for flow cytometry analysis. Tubes were run on a BD accuri C6 flow cytometer (BD Biosciences) or BD FACSAria III. 30,000 events were collected and results were analysed using FlowJo software (FlowJo, Oregon).

## 2.17. Protein analyses

### 2.17.1. Protein extraction

Cells were washed 2x with PBS and resuspended in 50 µl passive lysis buffer. Samples were then briefly vortexed and sonicated for five 30 second intervals in a sonicator water bath. Cells were then spun down at 3000g for 4 minutes to pellet debris.

### 2.17.2. Quantification via BCA assay

10 µl of each sample was taken for protein quantification via BCA assay, according to manufacturer's instructions. Controls were pre-diluted BCG samples (ThermoFisher, UK). Once BCA reagent had been added to samples, plates were left at RT for 30 minutes to allow the reaction to proceed. Samples were then run on a Labsystems Multiscan Ascent plate reader.

### 2.17.3. Protein separation via SDS-page electrophoresis

Protein samples were prepared with the same amount of protein in each at a total of 10 µl (2.5 µl 6 x LDL sample loading buffer, 7.5 µl protein sample). 1 µl of BOLT sample reducing agent (Invitrogen) was added and samples were boiled at 95$^{o}$C for 10 minutes, then placed on ice for 2 minutes. Samples were loaded onto pre-made Mini Protean TGC stain-free gels (Bio-Rad) with 10 or 12 wells. Gels were loaded into a Bio-Rad gel tank and 1xTGS buffer was used to fill the tank. Gels were then run at 100V until the samples had migrated to the bottom of the gel.

### 2.17.4. Western blotting

Blotting was performed on PVDF membranes as provided with the Bio-Rad Trans-blot turbo transfer system. Membrane and stack paper was pre-wet in Bio-Rad transfer buffer and the membrane was then prepared for blotting by placing in Methanol until translucent. Blots were then transferred using the Bio-Rad Trans-blot turbo transfer system for 7 minutes. Membranes with samples were then blocked in milk powder (Marvel) for 2 hours at RT.

### 2.17.5. Western hybridisation

Calnexin antibody (ab75801, Abcam) and Actin antibody (ab8224, Abcam) were diluted in milk powder at a concentration of 1:2000 and 1:500 respectively and left on membrane rocking overnight at 4$^{o}$C. The next day, membranes were washed several times with milk powder and secondary Rabbit HRP antibody (170-6515, Bio-Rad) was added at a concentration of 1:500 for 2 hours rocking at RT. Membranes were again washed several times in milk powder.

### 2.17.6. Western signal detection

Bands were stained using Pierce ECL western blotting substrate (ThermoFisher, UK), with 1 ml placed on each membrane for several minutes. Blots were then visualised using a transilluminator.

## 2.18. Hydrogen peroxide assay

Hydrogen peroxide levels were measured in whole bodies of *Ae. aegypti* using the Amplex Red Hydrogen Peroxide Kit (ThermoFisher, MA, USA) according to the manufacturers instructions. 3 females were pooled per technical replicate in PBS containing 2 mg/ml of catalase inhibitor 3-amino-1,2,3-trizole. Samples were

then filtered through a 10K molecular weight cut off (Corning Spin- XUF; Corning Life Science) (Pan et al., 2012). The elution was tested on the Amplex Red Hydrogen Peroxide Kit and protein measured by BCA assay. Fluorescence intensity was measured at Excitation/Emission 550/590 using a microplate reader (BMG Labtech). $H_20_2$ was normalised to protein.

## 2.19. *Serratia marcescens* challenge

### 2.19.1. *S. marcescens* culture

*S. marcescens* as used in (Diaz-Albiter et al., 2012) was grown overnight in LB nutrient broth at 37ºC with constant shaking. The optical density (OD) was then measured on a spectrophotometer to assess *S. marcescens* growth, using LB media as a blank.

### 2.19.2. Oral challenge

For challenge in a blood meal, defibrinated sheeps blood was spun down at 1000G for 10 minutes at 4ºC to separate plasma and red blood cells. Plasma was then heat inactivated at 56ºC for 1 hour. *Serratia* (OD 0.17) was resuspended in plasma and fed to mosquitoes on a Hemotek for 45 minutes. For challenge in a sucrose meal, Serratia (OD 0.1) was diluted 1 in 150 in 5% Sucrose in ddH20. Cotton wool was soaked in this solution and left on the mosquito cages for feeding *ad libitum* 12 hours before time points begun. For oral challenges, individual mosquitoes (5-7) were sampled per time point, DNA extracted by STE and *S. marcescens* presence quantified using primers cited in (Wei et al., 2017), listed in Appendix 1.

### 2.19.3. Thoracic injection

*S. marcescens* was grown overnight and diluted to OD 0.4 in LB broth. *S.marcescens* was then heat-inactivated at 100ºC for 90 minutes; LB broth was treated the same for media-only control. 10-day old *Ae. aegypti* WT and wMel were first injected with media-only and then heat-inactivated Serratia using a capillary needle and Nanoject II (Drummond Scientific, PA, USA). Mosquitoes were then transferred to 27ºC and 70% humidity until sampled in pools of 3 at each time point for RNA extraction and qRT-PCR of immune genes listed in Appendix 1.

## 2.20. Statistical analysis

Data were checked for normality on GraphPad Prism using the Shapiro-Wilk normality test. If data was normally distributed, Students T-test was performed. If data was not normal, the non-parametric Mann-Whitney test was performed. When multiple lines were being compared with novel transinfections, One-Way Anova was performed on R studio. Statistics of positive/negative virus points was tested using a one-tailed Fishers exact test. Graphs were created on R studio, Microsoft Excel and Graphpad Prism.

# Chapter 3

## Towards a better understanding of the mechanism of *Wolbachia*-mediated pathogen inhibition

# 3.1. Introduction

*Wolbachia*-infected female *Aedes* mosquitoes are currently being released in order to replace the wild population, with the aim of the resulting vectors being unable to spread arboviruses. This vector replacement strategy relies on *Wolbachia*-mediated pathogen inhibition, which has been widely studied in several insect species and yet the precise mechanism is not known. There is evidence that *Wolbachia* interferes with host cells in several ways that could directly or indirectly impact the arbovirus life cycle.

## 3.1.1. Redox homeostasis

*Wolbachia* are intracellular endosymbionts, therefore their presence within a cell can cause many perturbations in cell processes. One such perturbation is disruption of redox homeostasis, but its role in *Wolbachia*-mediated pathogen inhibition remains uncertain. Reactive oxygen species (ROS) are highly-reactive oxygen-derived species including superoxide anion ($O_2$), hydroxyl radical ($OH\cdot$) and hydrogen peroxide ($H_20_2$), the latter of which is easily transformed to $OH\cdot$. Under normal cell conditions, ROS are produced as a by-product of mitochondrial oxidative phosphorylation, but can also be up-regulated in times of stress or pathogen detection (Caragata et al., 2016; Mikonranta et al., 2014).

Although most studies of ROS have focused on mammalian systems, redox homeostasis remains an important aspect of immunity in eukaryotic cells of insects, particularly in the gut (Ha et al., 2005b). Dual oxidases (DUOX, NOXM) are enzymes whose sole function is to produce ROS, generating superoxide anion and hydrogen peroxide via the reduction of oxygen. *Drosophila* Duox (dDuox) has an important role in suppression of microbial growth within the gut; *Drosophila* with dDuox silenced had higher mortality rates when fed a microbe-contaminated meal than their control counterparts (Ha et al., 2005a). Silencing of Duox in *Ae. aegypti* midguts also leads to increased gut flora, highlighting the importance ROS play in shaping the microbial composition of the gut (Oliveira et al., 2011).

While ROS can protect the host from colonisation of unwelcome microbes, it can also inadvertently facilitate the development of the malaria parasite, *Plasmodium*. Following blood-meal ingestion by a female mosquito, a peritrophic

matrix (PM) forms to protect the gut epithelial cells and bacteria from the breakdown of the pro-oxidant heme. In *Anopheles gambiae*, a heme-peroxidase and Duox catalyse the cross-linking in the protein layer of the PM, which in turn protects the gut and also the *Plasmodium* parasite from immune elicitors (Kumar et al., 2010). However, ROS can also detrimentally affect parasite development; an *An. gambiae* strain selected that was refractory to *Plasmodium* infection had higher levels of ROS and increased parasite melanisation (Kumar et al., 2003).

There is evidence that *Wolbachia* infection perturbs redox homeostasis in a novel host which can also lead to pathogen inhibition; *Aedes polynesiensis*, a primary vector of lympathic filariasis caused by filarial worms, cleared of its native *Wolbachia* infection and transinfected with *w*AlBb showed a reduced ability to regulate oxidative stress (Andrews et al., 2012). This was particularly apparent following a blood meal, as the *Ae. polynesiensis* line with the native *Wolbachia* strain retained high levels of ROS following a blood meal, whereas the *w*AlbB-line experienced a drop in ROS. Despite this decrease in oxidative stress, when challenged with filarial worms the *w*AlbB-line had significantly less worms reaching an infective stage (Andrews et al., 2012). Perhaps the long co-evolution of filarial worms with this host has led to adaptation of the worms to oxidative stress, and this new perturbation with *w*AlbB indirectly disrupted the development.

The *Wolbachia* strains *w*MelCS, *w*Ri and *w*Au which protect *Drosophila* from *Drosophila* C Virus by extending survival have 1.5-2 fold more $H_20_2$ than their counterpart flies cleared of *Wolbachia* infection (Wong et al., 2015). However, there was no investigation into how this higher $H_20_2$ protected against viral infection. Artificial transinfection of *w*AlbB in *Ae. aegypti* has resulted in higher levels of $H_20_2$, which indirectly activated the Toll pathway and led to DENV inhibition (Pan et al., 2012). Despite this finding, *Wolbachia*-mediated pathogen inhibition has been shown to occur in *Drosophila* Toll and Imd-pathway mutants, showing this is not crucial for inhibition (Rancès et al., 2013). However, *Wolbachia*-induced ROS may be causing damage to another part of the cell required for viral replication.

### 3.1.2. Disruption of viral replication

Cell components particularly liable to oxidative damage include lipids, which are large components of cell membranes; oxidative stress can disrupt the function of lipids and permeability of membranes, potentially creating toxic by-products in the process (Niki, 2008). Oxidative damage of lipids could be detrimental to virus replication, as lipids such as cholesterol and sphingomyelin play roles in virus entry, replication, glycoprotein transport and finally budding, particularly with Alphaviruses (Ng et al., 2008). Analysis of the lipid profile of *Wolbachia*-infected Aa23 cells showed less sphingolipids than in uninfected cells (Molloy et al., 2016). Cholesterol trafficking is also disrupted in Aag2 *w*MelPop cells, with cholesterol accumulating in a similar way that is observed in cells with the Niemann-pick lipid storage disorder in humans (Geoghegan et al., 2017). In-fact, recovery of cholesterol homeostasis in *w*MelPop cells by treatment with 2-hydroxypropyl-ß-cyclodextrin resulted in a recovery of DENV replication, which had previously been inhibited (Geoghegan et al., 2017).

Depletion of cholesterol has also been shown to disrupt the lateral organisation of Alphavirus glycoproteins on the virus envelope, crucial for early entry events (Sousa et al., 2011). There is evidence *Wolbachia* is interfering at the stage of viral replication; replication of an SFV replicon that was transfected straight into *Wolbachia*-infected *Drosophila* JW18 cells, bypassing entry, was still inhibited (Rainey et al., 2016). There is also evidence that DENV viral RNA is rapidly degraded in *w*Mel-infected Aag2 cells, compared to uninfected cells (Thomas et al., 2018). There is accumulated evidence that *Wolbachia* is interfering with viral replication, possibly in more than one way.

### 3.1.3. Unfolded protein response

*Wolbachia* has also been shown to interfere with expression of proteins involved in protein folding in the endoplasmic reticulum (Geoghegan et al., 2017). Proteomic analysis of *w*MelPop-infected Aag2 cells and *w*Mel-infected *Ae. aegypti* midguts revealed upregulation of proteins involved in the unfolded protein response (UPR) in the presence of *Wolbachia*. The function of the ER is to fold proteins correctly and assist in their transportation to the golgi apparatus (Schwarz and Blower, 2016). Misfolding of proteins can lead to an accumulation and therefore ER stress, which can activate the UPR via three pathways; IRE1α,

PERK or ATF6 (Hollien, 2013). These pathways can result in the upregulation of chaperones such as BiP and Calnexin, which work to correctly fold the misfolded proteins (Fig.3.1.1). Upregulation of proteins involved in quality control of glycoproteins as they enter the ER has been observed (Geoghegan et al., 2017) in the presence of *Wolbachia*. This may be interfering directly with virus replication as viruses manipulate the ER machinery in a timely manner to enable their replication, in both mammalian and insect cells. In mammalian cells, DENV serotype 2 has been shown to induce transient upregulation and suppression of the PERK pathway via phosphorylation of eIF2α very early in infection, indicating the virus takes control of this pathway (Peña and Harris, 2011). DENV also alleviates ER stress 24-36 hours post-infection by activating the IRE1-Xbp1 pathway, which correlates with the stage of the virus replication cycle involving

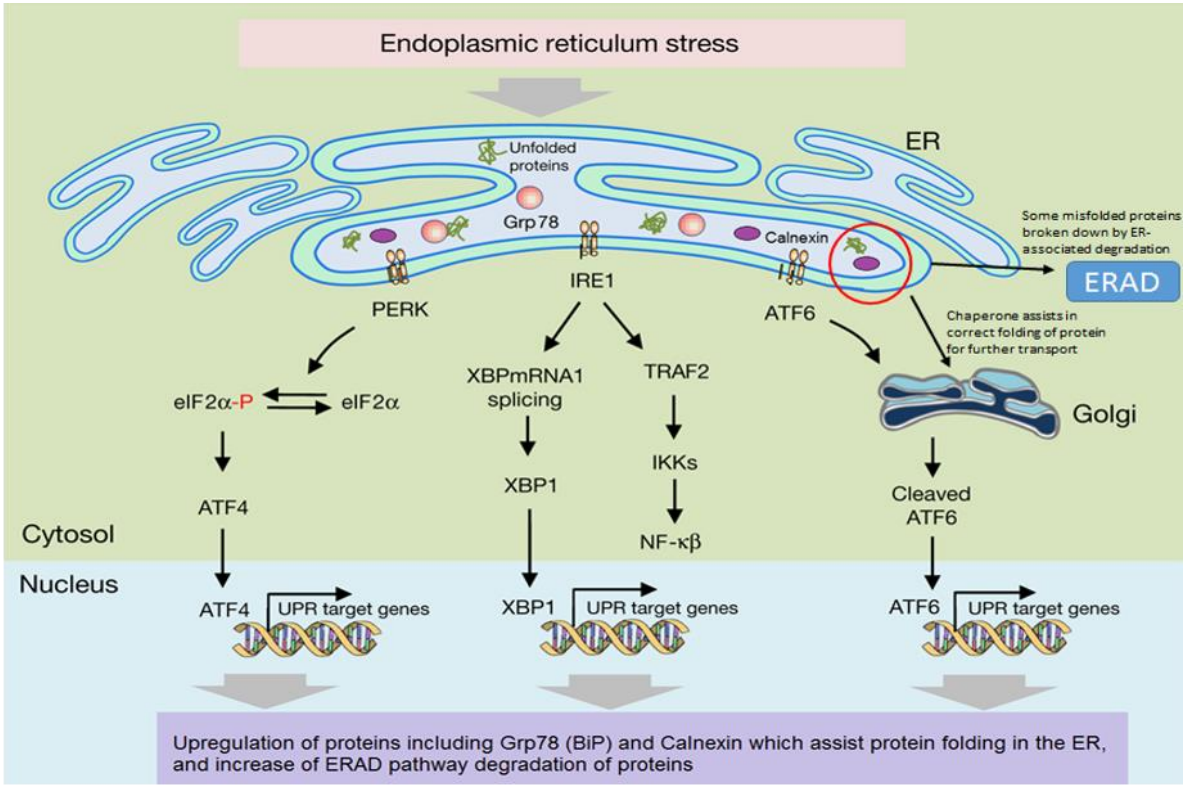


Fig. 3.1.1. **Schematic representation of the unfolded protein response (UPR) and ER-associated protein degradation pathway (ERAD) in eukaryotic cells.**

Misfolded proteins can accumulate in the endoplasmic reticulum (ER) causing ER stress. The unfolded protein response can then be activated by one of three arms of the pathway; PERK, IRE1 and ATF6. This activation results in transcription of UPR-target genes including chaperone proteins Grp78(BiP) and Calnexin, which either assist in correct folding and transport of proteins to the golgi apparatus, or deliver misfolded proteins for degradation by the ERAD pathway. Figure adapted from (Iranpour et al., 2016).

viral protein synthesis (Peña and Harris, 2011). This DENV2-induced splicing of Xbp1 is stronger than is observed with DENV1 infection, indicating activation of the UPR differs between virus serotypes (Umareddy et al., 2007). The Xbp1 gene is also spliced in response to DENV2 infection at 24 hours post-infection in *Ae. albopictus* C636 cells, resulting in an increase in BiP/GRP78, which subsequently alleviates oxidative stress (Chen et al., 2017). If *Wolbachia* is established within an insect cell and has already modified the UPR pathways, this means any invading virus may not be able to activate and suppress the pathways to allow virus replication.

The aforementioned proteomic data adds to other evidence that *Wolbachia* infection perturbs the ER. Using electron microscopy *Wolbachia* has been shown to be closely associated with the ER in *Drosophila* cells and alters morphology of the organelle, with an increase in cisternae, swelling and extensions observed, relative to uninfected cells (White et al., 2017). This same study revealed 36 and 41 genes that reduced or increased *Wolbachia* titre respectively, revealing the multifactorial processes that can affect *Wolbachia* replication. Knock-down of ER membrane protein Ubc6 resulted in a four-fold reduction in *Wolbachia* titre; Ubc6 is a component of the endoplasmic-reticulum-associated degradation of mis-folded proteins (ERAD) pathway, which is also activated by ER stress (White et al., 2017). This provides evidence that the ER is a crucial structure involved in the maintenance of *Wolbachia* titre, possibly via the degradation of misfolded proteins by the ERAD pathway, providing an amino acid source.

It is clear that *Wolbachia* infection can perturb many processes, some of which may be interlinked. Cells from native hosts (*Ae. albopictus* Aa23) and novel hosts (*Ae. aegypti* Aag2) of *Wolbachia* were used to investigate *Wolbachia*-mediated pathogen inhibition. The density of *Wolbachia* strains *w*MelPop and *w*Au in *Aedes* cells was quantified using qPCR, confocal fluorescent in-situ hybridisation (FISH) and flow cytometry FISH. Levels of ROS and lipid peroxidation were then measured in cell lines to assess any *Wolbachia*-mediated perturbation of redox homeostasis. To investigate the stage at which *Wolbachia* blocks virus replication in *Aedes* cells, a SFV replicon was transinfected into cells and genomic and sub-genomic RNA was quantified. In addition, the perturbations of UPR-related genes was investigated, with and without DENV.

## 3.2. Results

### 3.2.1. Characterisation of *Wolbachia*-infected cell lines

The cell lines chosen for investigating *Wolbachia*-mediated pathogen inhibition both carried high density *Wolbachia*: Aag2 with *w*MelPop (*Ae. aegypti*) and Aa23 with *w*Au (*Ae. albopictus*). The Aag2 and Aa23 cell lines were derived from *Ae. aegypti* and *Ae. albopictus* eggs with developing embryos within them, respectively (O'Neill et al., 1997; Peleg, 1968). The Aa23 *w*MelPop cell line would have been desirable for these experiments but was not used due to instability, which is discussed later in this chapter. These cell lines were characterised for *Wolbachia* density using qPCR (*Wolbachia*: host genome ratio), fluorescent in situ hybridisation (FISH) and flow cytometry. QPCR of the *Wolbachia* wsp gene normalised to the endogenous cell homothorax (hth) gene revealed the density of *Wolbachia* in *w*MelPop (490/ host genome) and *w*Au (408/ host genome) did not significantly differ - both strains were present at a similar high density (Fig.3.2.1A). While qPCR analysis of *Wolbachia* gives a general measurement of density, it gives an overall picture rather than details of density variation between cells.

FISH of *Wolbachia* using a wsp probe allows visualisation of individual bacteria between cells (Fig. 3.2.1B). Using FISH, it is clear while *w*MelPop appears to infect almost every cell in Aag2 cells, *w*Au tends to aggregate in very high-density cells interspersed throughout (Fig.3.2.1). The confocal visualisation of FISH confirmed the slightly higher density of *w*MelPop relative to *w*Au as seen with qPCR. The density of each *Wolbachia* within individual cells may impact the pathogen inhibition, depending if it is a cell-autonomous process or not. Taking multiple pictures of confocal images is laborious and time-consuming, with the added element of user bias that may select sections with more *Wolbachia* presence. In addition, cells can clump together and this makes selection of individual cells for analysis troublesome.

In order to improve *Wolbachia* density quantification, we sought to develop flow cytometry FISH (FLOW-FISH), to analyse hundreds of cells for *Wolbachia* presence in an accurate manner. Cells were stained using the FISH protocol and strained through a filter for running in the flow cytometer; cells were then analysed for

green fluorescence, indicating *Wolbachia*. A cohort of each cell type was heated to 37ºC for 1 hour as a positive control for identification of dead cells. Aa23 –ve and *w*Au cells were then plotted on a scatterplot for forward scatter (size) and side scatter (granularity) (Fig.3.2.2). Analysis of the dead-cell control revealed most cells were concentrated towards the side scatter axis (not shown). However, these cells were inactivated by heat, whereas those used for FISH are fixed to inactivate them. Nevertheless, with this in mind, cells along the side scatter axis were avoided and cells along the axis of forward scatter were gated (boundaries placed in FlowJo to select populations of cells) for further analysis (cells of interest).

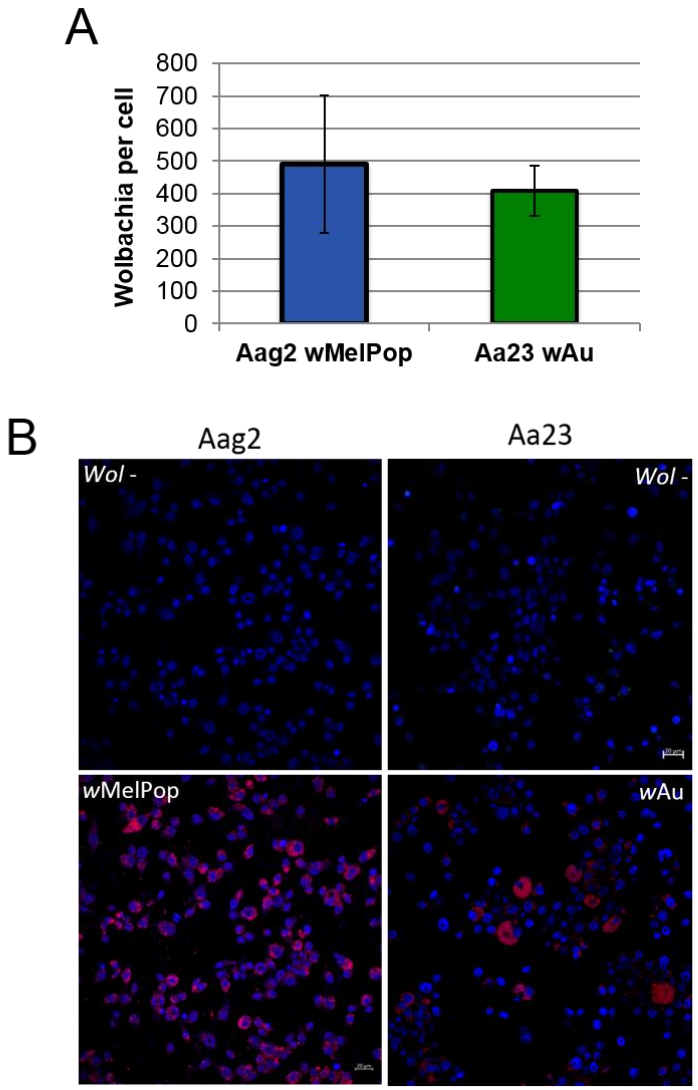


**Fig. 3.2.1.** *Wolbachia* density in Aag2 *w*MelPop and Aa23 *w*Au cells as assessed by qPCR and FISH.

DNA was extracted from Aag2 wMelPop and Aa23 wAu cells and qPCR was performed for *Wolbachia* wsp gene normalised to hth **(A)**. Results represent cells from three independent 25cm$^2$ flasks of cells. The same cells were also stained for fluorescent in-situ hybridisation (FISH) with a wsp-binding probe, and visualised on a confocal microscope **(B)**. Images are representative of six pictures.

These gated cells of interest were then plotted against green fluorescence, with Aa23 –ve cells acting as an uninfected control, setting the baseline for auto-fluorescence. It was then possible to identify *Wolbachia*-positive *w*Au cells and the percentage infected could be observed within the scatterplot (Fig.3.2.2). To confirm the accuracy of this method, Aa23 –ve and *w*Au cells were mixed and run through the flow cytometer, with the results showing an almost even split of uninfected and infected cells, indicating correct identification of both cell types (Fig.3.2.2). Plotting data as a histogram showed differentiation of the two cell types as observed by two peaks, with the *w*Au cells skewed to higher green fluorescence (Fig.3.2.2). When green fluorescence is plotted against cell count and samples are overlaid, we can see a similar number of Aa23 –ve cells were analysed per replicate, but in one of the Aa23 wAu samples there were more cells present relative to the other two (Fig.3.2.2).

The same protocol was carried out on Aag2 –ve and *w*MelPop cells, however far less cells of interest were identified in the *w*MelPop cells (Fig.3.2.3A). Further analysis suggested *Wolbachia* was present in 62.7% of cells (Fig.3.2.3A), however plotting of cell count on a histogram revealed the very low count of *w*MelPop cells present (Fig.3.2.3.B). The mean and median green fluorescence was plotted in a bar chart for both Aag2 *w*MelPop and Aa23 *w*Au cells, showing similar results in both cell lines (Fig.3.2.2&3). By using data obtained from scatterplots of three replicates showing percentage of cells infected with *Wolbachia*, as indicated by green fluorescence, the average percentage of cells infected could be calculated; a significant difference of 62% in Aag2 *w*MelPop and 81% in Aa23 *w*Au (Fig.3.2.3B, $p=<0.05$). This may not corroborate with the qPCR and confocal FISH data, which indicated higher density and percentage of cells infected in the Aag2 *w*MelPop cells, however the cells for FLOW-FISH were taken at a different time and *Wolbachia* infection is known to fluctuate within cells. It is therefore prudent to continually check *Wolbachia* density in cells used for experiments as this may have changed. Data from FLOW-FISH indicates this method could be used to assess percentage of cells infected with *Wolbachia*, but differentiation of cells into high and low infected would require additional experiments with positive controls for each type.

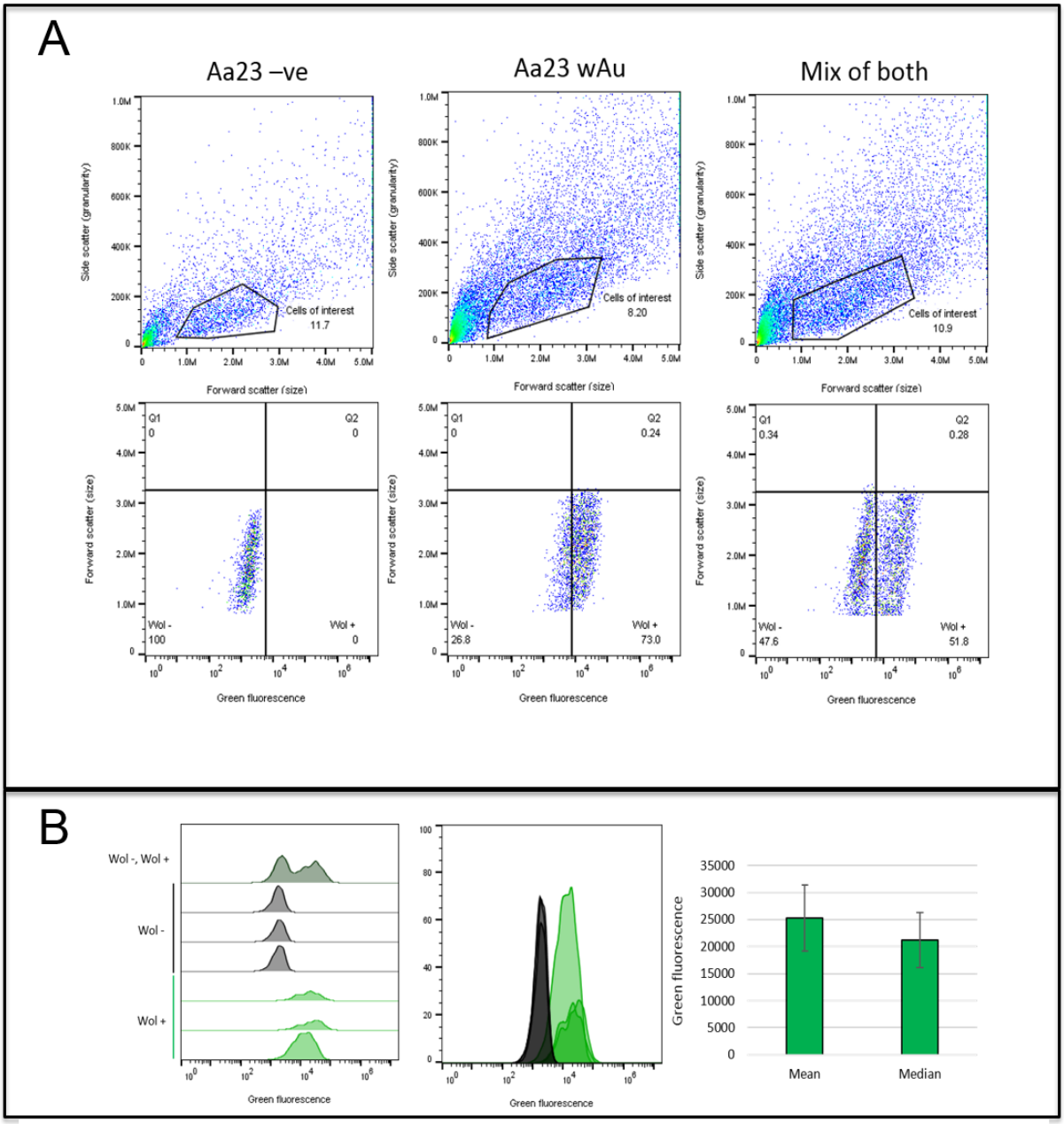


**Fig. 3.2.2.** Flow cytometry analysis of Aa23 *w*Au cells

Cells were stained using basic FISH protocol and run through a flow cytometer to quantify green fluorescence (*Wolbachia*). Cells of interest were gated on a scatterplot of forward scatter (size) and side scatter (granularity) **(A – top row)**. Gated cells were then plotted against green fluorescence and positive/negative quartiles set **(A – bottom row)**. Data gathered is represented in histograms **(B)** showing cell count plotted against green fluorescence **(left, middle).** Mean and median green fluorescence was calculated for Aa23 *w*Au cells **(right)**. Three independent 25cm$^2$ flasks were used for each replicate. Error bars represent standard deviation.

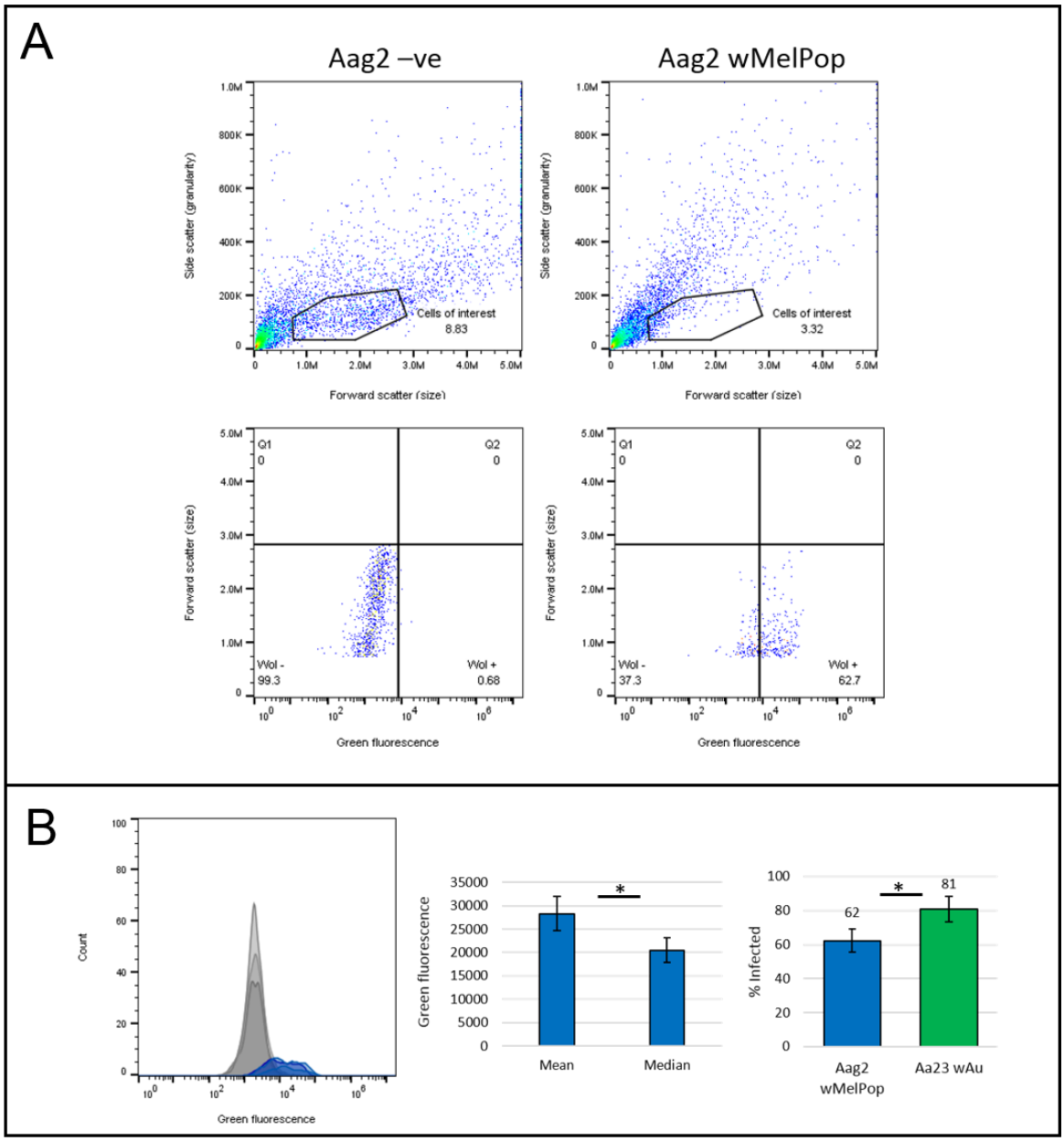


**Fig. 3.2.3.** Flow cytometry analysis of Aag2 *w*MelPop cells

Cells were stained using basic FISH protocol and run through a flow cytometer to quantify green fluorescence (*Wolbachia*). Cells of interest were gated on a scatterplot of forward scatter (size) and side scatter (granularity) **(A – top row)**. Gated cells were then plotted against green fluorescence and positive/negative quartiles set **(A – bottom row)**. Data gathered is represented in histograms **(B)** showing cell count plotted against green fluorescence **(left)**. Mean and median green fluorescence was calculated for Aag2 wMelPop cells **(middle)**. Percentage of cells infected with *Wolbachia* in Aag2 *w*MelPop and Aa23 *w*Au cells was calculated **(right)**. Three independent 25cm$^2$ flasks were used for each replicate. Error bars represent standard deviation. T-tests were performed for significance, represented by asterisks.

## 3.2.2. *w*MelPop-infected *Aedes* cells are under oxidative stress

*Wolbachia*-induced oxidative stress was measured in Aag2 (*Ae. aegypti*) and Aa23 (*Ae. albopictus*) cells, in order to assess if any results were a species-wide effect. The CellRox Green probe was used to measure oxidative stress as it fluoresces when oxidised by any free radical, rather than a specific ROS such as $H_20_2$. This kit is compatible with eukaryotic cells, however the efficacy in insect cells was tested by using an inducer of oxidative stress. Aag2 uninfected cells were treated with tert-butyl hydroperoxide (TBHP) to induce oxidative stress as a positive control (Brennan et al., 2008). TBHP was tested on Aag2 –ve cells for toxicity, by adding concentrations of 0, 10, 100 and 200uM of TBHP for 2.5 or 4.5 hours. Cells were then tested for viability using trypan blue, revealing no significant difference in viability up to 200uM regardless of incubation time, therefore the highest concentration was used (Fig.3.2.4.A).

CellRox Green was then added to Aag2 uninfected, *w*MelPop and TBHP-treated cells at a concentration of 1000nm and visualised using a confocal microscope. Aag2 *w*MelPop cells did appear to be experiencing oxidative stress, with green fluorescence observed in many of the cells much like the positive control (Fig.3.2.5). The same result was observed in Aa23 *w*MelPop cells (Fig.3.2.6). However, there is noticeable cell detritus in the Aa23 *w*MelPop line, with green fluorescence occurring in patches outside of cells, indicating the cells may have burst, possibly due to apoptosis.

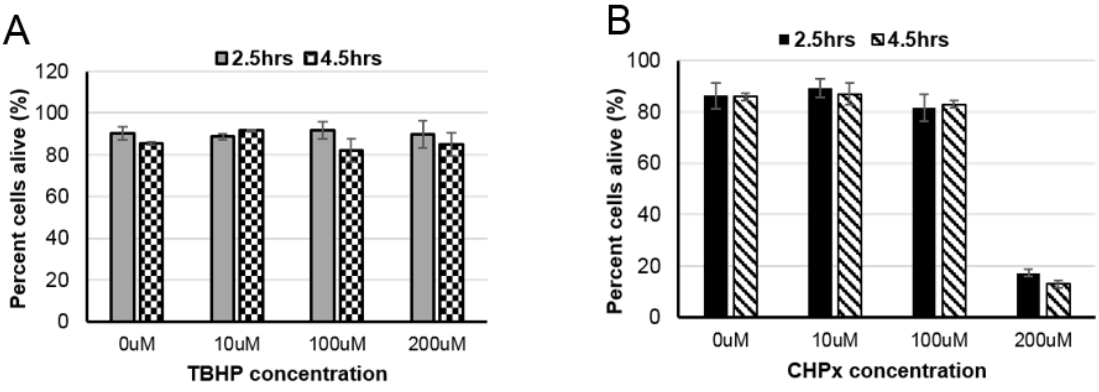


**Fig. 3.2.4.** Toxicity testing of tert-butyl hydroperoxide and cumene hydroperoxide on Aag2 Wol -ve cells

Aag2 uninfected cells were treated with tert-butyl hydroperoxide (TBHP) and cumene hydroperoxide (CHPx) at concentrations of 0, 10, 100 and 200uM for 2.5 and 4.5 hours. Cells were harvested and tested for cell viability using trypan blue. Data represents mean values of three replicates, error bars are standard error.

The antioxidant N-acetyl-cysteine (NAC), a free-radical scavenger (Kerksick and Willoughby, 2005), was tested as a negative control in Aa23 cells. Cumene hydroperoxide (CHPx) was also tested as an alternative positive control; CHPx induces oxidative stress via peroxidation of lipids that are found within the cell (Weiss and Estabrook, 1986). CHPx toxicity was tested on Aag2 –ve cells at concentrations of 0, 10, 100 and 200uM, revealing a significant reduction in cell viability at 200uM only (Fig.3.2.4.B). Therefore, cells were treated with 100uM of

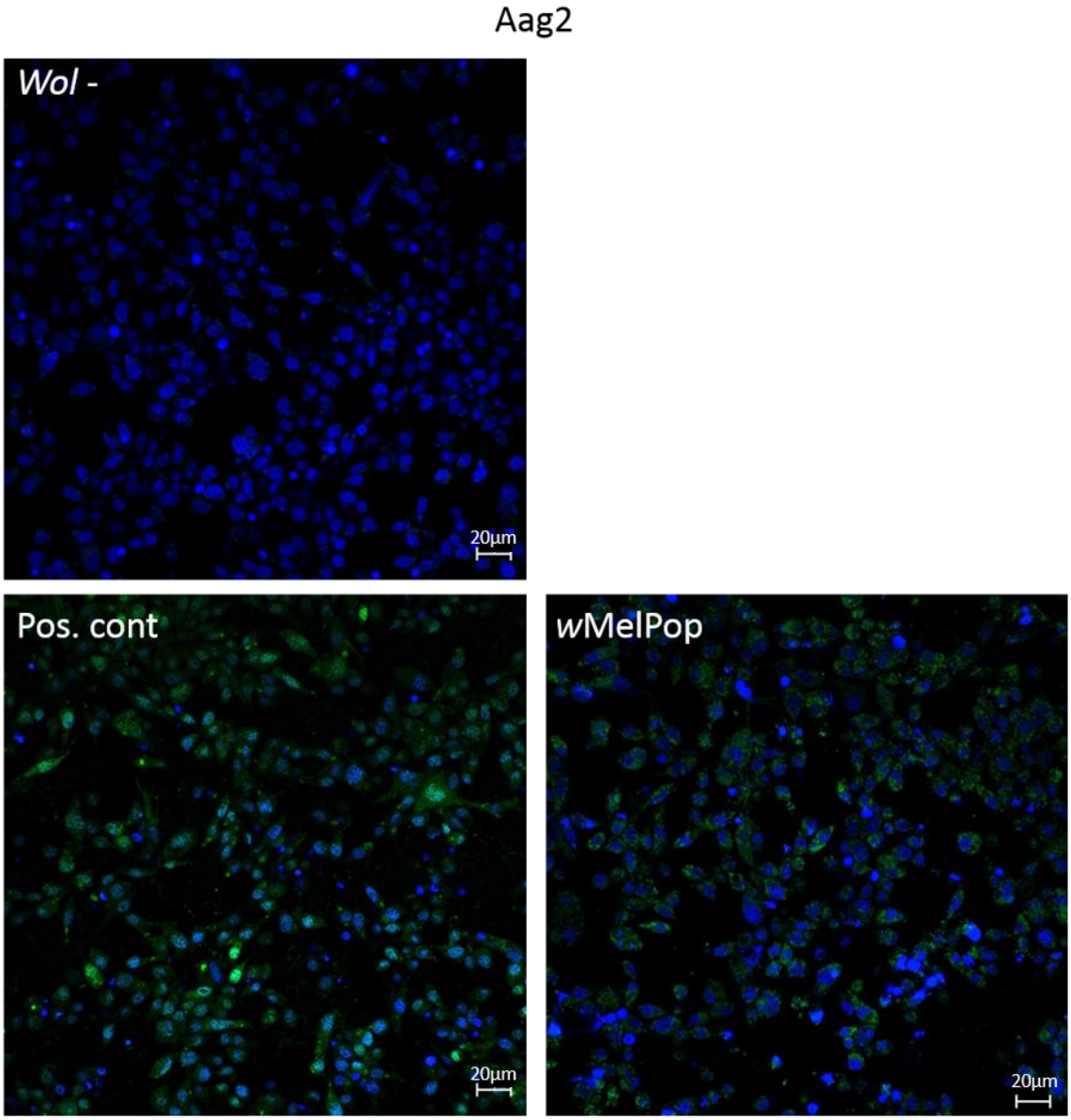


**Fig. 3.2.5.** CellRox Green staining of oxidative stress in Aag2 *w*MelPop cells

Aag2 uninfected and wMelPop-infected cells were stained for oxidative stress using CellRox **(green)** and nucleus with Hoechst **(blue)**. Positive control was obtained by treating Aag2 uninfected cells with 200 µM TBHP for 2 hours prior to staining. Images were gained using a confocal and represent six images captured.

CHPx and 5000uM NAC for 2 hours. NAC did reduce oxidative stress as indicated by the reduction of faint regions of green fluorescence observed in the Aa23 untreated cells (Fig.3.2.6 – Neg. cont). CHPx did induce oxidative stress in Aa23 cells, but it appeared to alter the cell morphology, therefore TBHP was used for future experiments (Fig.3.2.6 – Pos. cont). In order to avoid user bias of selecting regions under oxidative stress by microscopy and to provide a thorough characterisation of the whole cell line, CellRox Green in cells was then measured by flow cytometry.

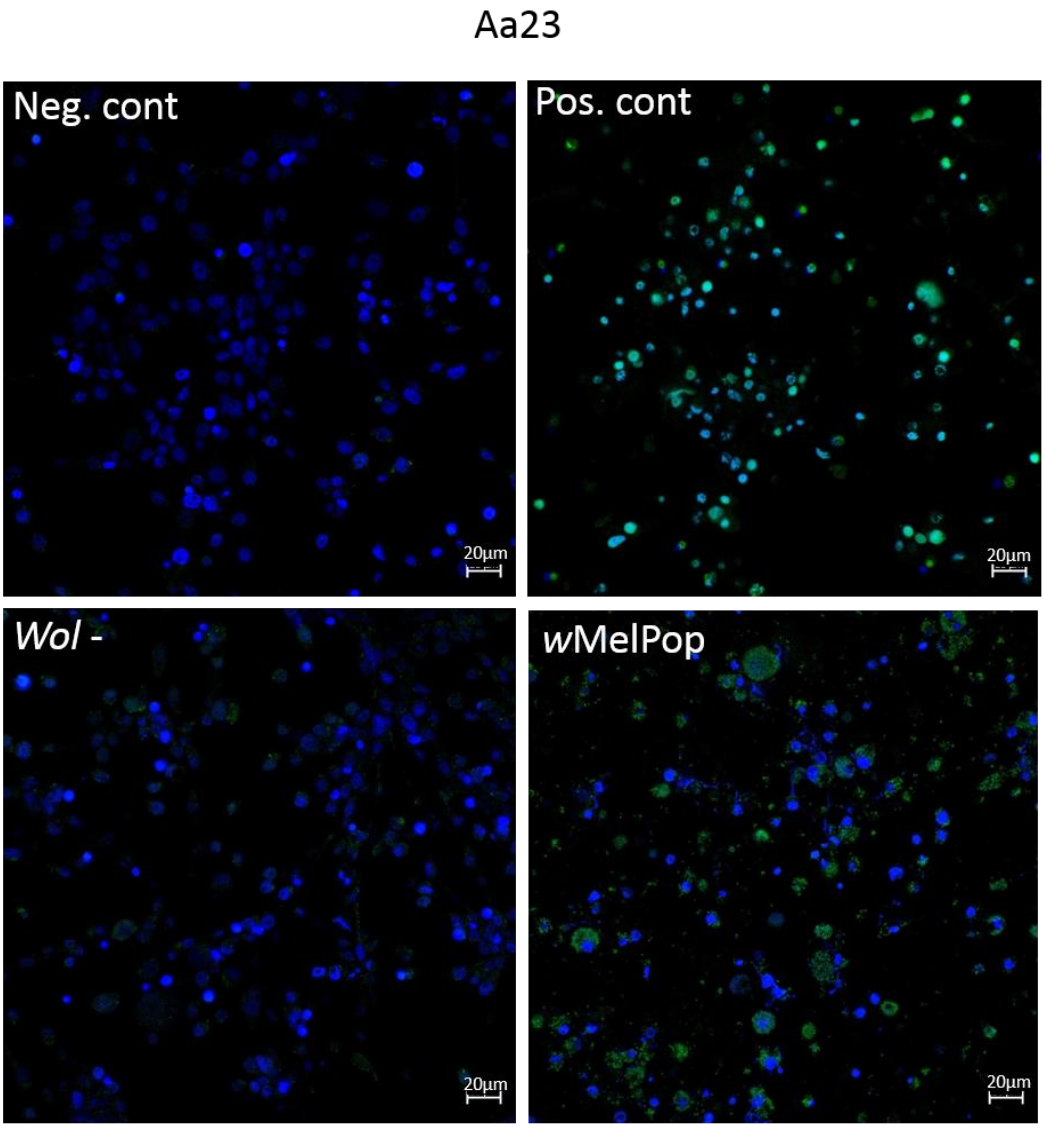


**Fig. 3.2.6.** CellRox Green staining of oxidative stress in Aa23 *w*MelPop cells
Aa23 uninfected and wMelPop-infected cells were stained for oxidative stress using CellRox **(green)** and nucleus with Hoechst **(blue).** Positive and negative controls were obtained by treating Aa23 uninfected cells with 100 µM CHPx and 5000 nM NAC for 2 hours prior to staining, respectively. Images were gained using a confocal and represent six images captured.

### 3.2.3. Flow cytometry confirms higher oxidative stress in Aag2 *w*MelPop cells

Flow cytometry enables thousands of cells to be measured for several parameters without human bias. Aag2 *w*MelPop and Aa23 *w*Au cells were stained with CellRox Green and run through a flow cytometer, to measure oxidative stress. For these experiments, Aa23 *w*MelPop was substituted for another high density strain Aa23 *w*Au, due to the instability of the *w*MelPop cell line. The flow cytometry data confirmed that Aag2 *w*MelPop cells were under oxidative stress, as the histogram plot of cells skewed towards the right, indicating higher CellRox Green and more oxidative stress (Fig.3.2.7.A.). These data also confirm the TBHP positive control worked accurately, with a peak which has moved to the right compared to uninfected cells. The median CellRox fluorescence of each sample confirmed the *w*MelPop cells had a significantly higher fluorescence compared to uninfected (Fig.3.2.7.B, $p=<0.01$). However, the Aa23 *w*Au cells showed a different result, with the histogram skewed towards less oxidative stress much like the uninfected cells (Fig.3.2.7.C). Quantification of the median CellRox fluorescence confirmed no difference between *w*Au and uninfected cells (Fig.3.2.7.D.).

### 3.2.4. Analysis of lipid peroxidation in Aag2 *w*MelPop cells

As the Aag2 *w*MelPop cells were observed to be experiencing oxidative stress, lipid peroxidation was investigated as a potential direct or indirect consequence of this. Lipids are an important component of cell membranes, which are susceptible to oxidative damage. Arboviruses use the cell membrane to enter the cell and can also use components of the membrane as their outer capsid following replication, therefore the composition of the lipids is important for the completion of viral replication. To measure lipid peroxidation the BODIPY 581/591 C11 reagent was applied to live cells; when added to cells, BODIPY localises to membranes and upon oxidation by lipid hydroperoxides, fluorescence shifts from 590 nm (red) to 510 nm (green). Use of BODIPY reagent was optimised by testing concentrations of 5, 10 and 50 μM on Aag2 uninfected cells treated with 100 μM CHPx for two hours (Fig.3.2.8). While the 5 μM of BODIPY appeared too low, single BODIPY molecules were observed at 10 μM, although it did not appear representative of the cell line. Lipid peroxidation was represented better with 50 μM of BODIPY. Initial tests using CHPx (Fig.3.2.9A) and TBHP (Fig.3.2.9B & C) as positive controls

were variable; using a confocal microscope BODIPY was observed fluorescing green shades with both treatments, however this was patchy throughout the cell line.

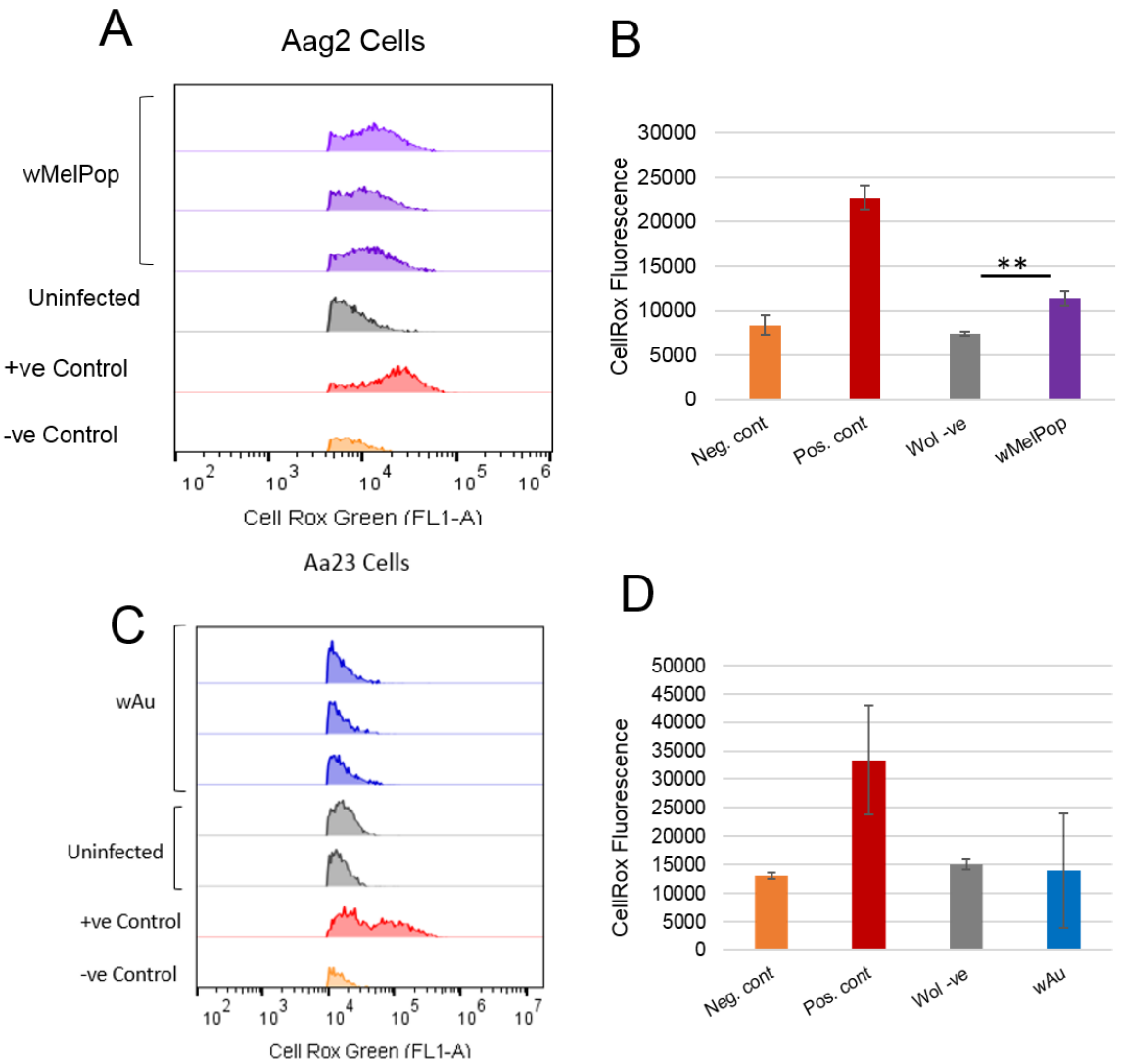


**Fig. 3.2.7.** Analysis of CellRox Green staining in Aag2 and Aa23 cells by flow cytometry

Aag2 *w*MelPop and Aa23 *w*Au cells and their uninfected counterparts were stained for oxidative stress using CellRox Green. Representative samples of Aag2 **(A)** and Aa23 **(C)** cells were plotted as a histogram with green fluorescence on the x axis, showing more fluorescence in cells towards the right of the axis. Median CellRox fluorescence for three replicates of Aag2 cells **(C)** and Aa23 cells **(D)** were averaged and displayed as bar charts. Uninfected cells were treated with TBHP for 2 hours as a positive control. Cells were then run through a flow cytometer and analysed on FlowJo software. T-tests were used for significance, represented by asterisks.

When Aag2 uninfected and *w*MelPop cells were assessed for lipid peroxidation by confocal microscopy, there were variable results depending on the area being scanned. Both cell lines had areas fluorescing green, while other sections remained a bright red (Fig.3.2.9D & E). Green fluorescence is also very susceptible to bleaching, which may bias analysis on the confocal. As with the CellRox analysis, BODIPY-labelled cells were run through a flow cytometer, to measure the red and green fluorescence accurately. The density pseudocolour plots show a representation of two independent replicates performed on a flow cytometer in which the green and red were fluoresced by the same laser (Fig.3.2.10A). The pseudoplot of the CHPx-treated Aag2 cells shows a shift towards higher green fluorescence, indicating lipid peroxidation of the BODIPY reagent. TBHP has been shown to induce lipid peroxidation in mouse erythrocytes using as low as 5uM (Roy and Sil, 2012), however the flow cytometry data confirmed that TBHP treatment of cells did not induce lipid peroxidation in insect cells (Fig.3.2.10A).

CHPx was therefore taken forward as a positive control, as it is a specific inducer of lipid peroxidation. While there was not a large difference between Aag2 uninfected and *w*MelPop cells, some *w*MelPop cells did show a shift towards less fluorescence, possibly indicating yellowing as has been seen in the confocal images. A dotplot that represents one replicate of Aag2 uninfected (orange), *w*MelPop (purple) and CHPx (red) shows the slight shift of *w*MelPop to less red fluorescence, but not higher green fluorescence as with the positive control. Nevertheless, when the ratio of red to green BODIPY reagents was quantified, *w*MelPop cells did have a significantly lower ratio than uninfected cells, indicating lipid peroxidation (Fig.3.2.10.C, $p=<0.05$). For the third replicate of this experiment, a flow cytometer was sourced which excited the green and red on independent lasers. The previous replicates were run on a flow cytometer which fluoresced red and green using the same laser, therefore some cross-over could occur in the results. By using a flow cytometer with independent lasers for red and green, this bias was avoided. Data from this experiment shows a red:green ratio that is similar in Aag2 uninfected and *w*MelPop cells, yet the CHPx positive control still remained a low ratio as in the previous experiments (Fig.3.2.10.E). It seems likely therefore that the third replicate provided the most accurate results, showing no difference in lipid peroxidation in *Wolbachia*-infected cells.

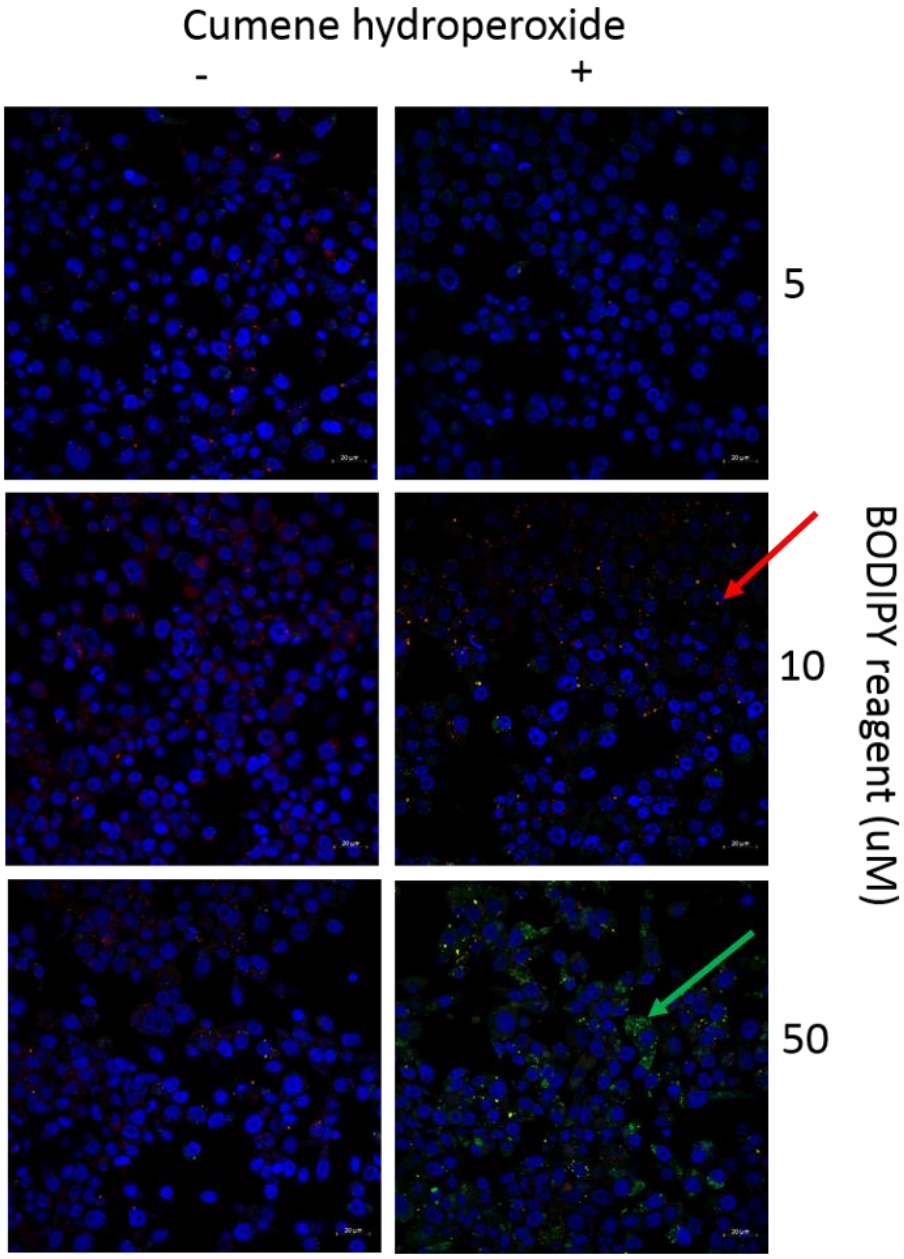


**Fig. 3.2.8.** Initial testing of BODIPY reagent on Aag2 uninfected cells

Aag2 uninfected cells were treated with cumene hydroperoxide (CHPx) to induce lipid peroxidation. BODIPY reagent was added to cells at concentrations of 5,10 and 50 μM for 30 minutes. BODIPY fluorescence changes from red to green when peroxidised (indicated by red and green arrows).

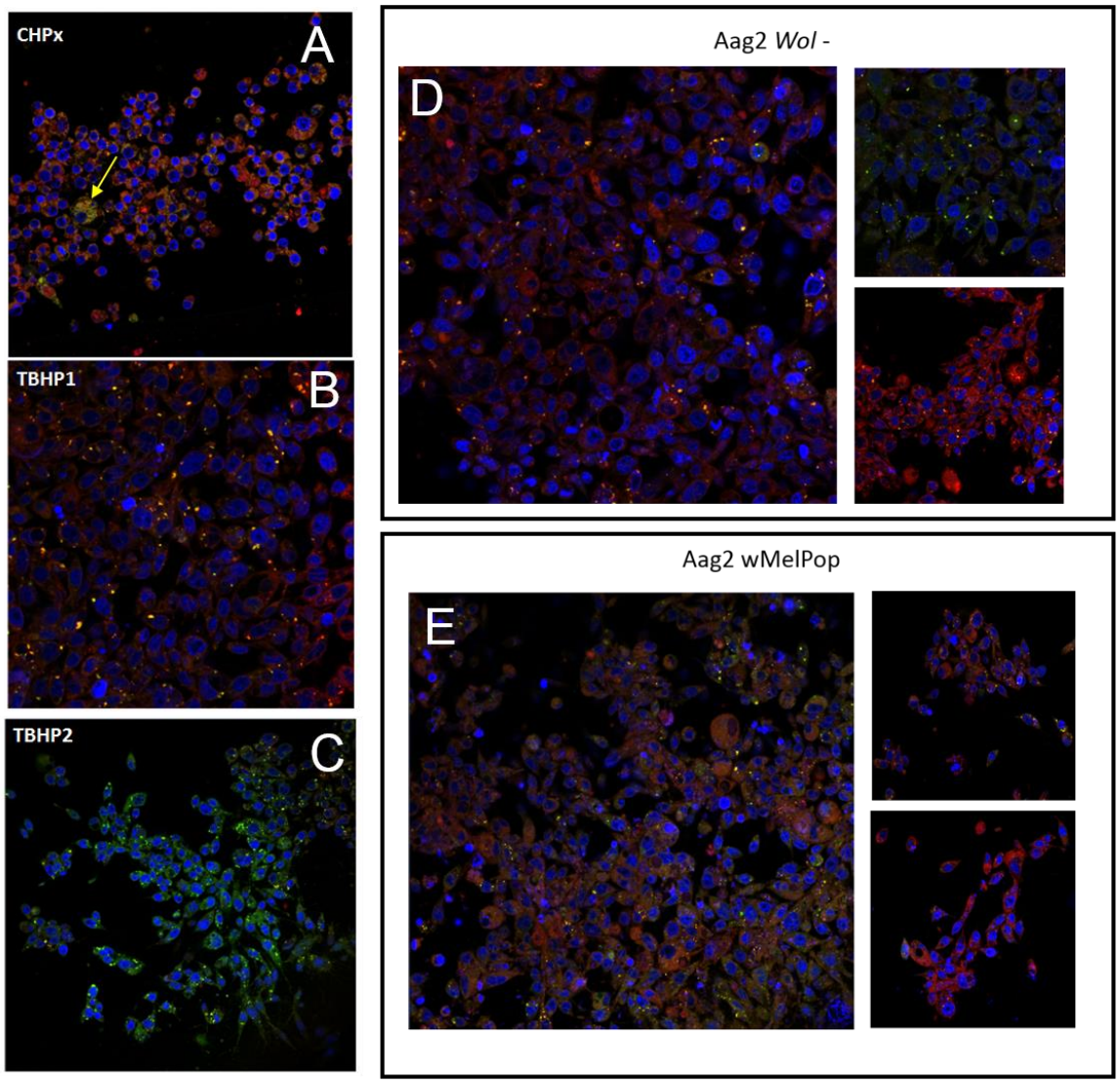


**Fig. 3.2.9.** Confocal imaging of BODIPY in Aag2 cells

Aag2 uninfected cells were treated with 100 µM of CHPx **(A)** or 200µM of TBHP **(B, C)** for 2 hours and lipid peroxidation visualised with staining of 50 µM BODIPY reagent for 30 minutes, visualised using a confocal microscope. Lipid peroxidation was then visualised in Aag2 *Wolbachia*-uninfected cells **(D, Aag2 Wol-)** and Aag2 *w*MelPop cells **(E, *w*MelPop)**. BODIPY reagent fluoresces green when peroxidised. Yellowing of BODIPY shown with yellow arrow in **A**.

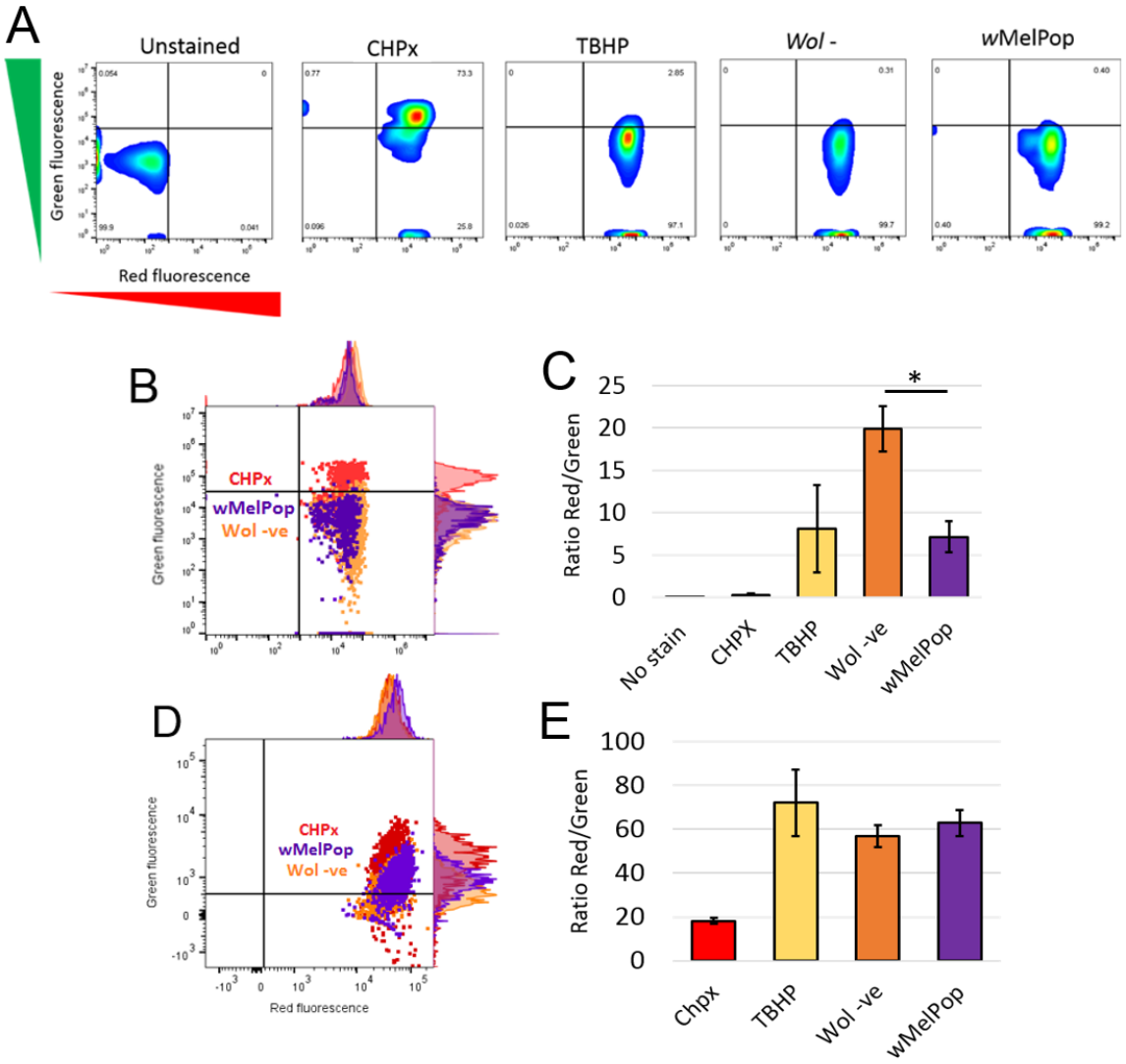


**Fig. 3.2.10.** Flow cytometry analysis of BODIPY in Aag2 cells

Pseudoplots are shown representing one sample of each treatment type **(A)**. Unstained (Aag2 Wol -ve with no BODIPY), CHPx and TBHP positive control, Aag2 Wol -ve and *w*MelPop with BODIPY. BODIPY changes from red to green fluorescence when peroxidised. Dot plot shows a representative sample of data from two independent replicates, plotted against red and green fluorescence **(B)** with the ratio of red:green calculated from all samples **(C)**. Dot plot of representative samples run in the third replicate on a flow cytometer with independent lasers for green and red fluorescence is shown in **(D)**. Red:green ratio of all samples in this replicate is shown in **(E)**. Data was analysed on FlowJo software. Bars represent mean ratio of red/green with standard error. T-tests were used for significance, represented by an asterisk.

### 3.2.5. *Wolbachia* inhibits viral replication in *Aedes* cells

As the presence of *Wolbachia* in Aag2 cells did not appear to be altering lipid peroxidation which could impact viral binding or capsid formation, it was then investigated if viral replication was indeed being directly inhibited instead. Firstly, a range of Aag2 (*w*MelPop, *w*Au) and Aa23 (*w*AlbB, *w*MelPop, *w*Au, *w*Mel) cell lines were challenged with a modified Semliki forest virus which has a Renilla luciferase reporter inserted into the genome, for quantification of replicated virus (Fig. 3.2.11A)(Rainey et al., 2016). SFV was chosen for these experiments as it is a well-studied model alphavirus. Cells were infected with SFV (RLuc) at MOI 5 for 24 hours, following which samples were read for luciferase units. Results from two independent replicates show SFV levels several ten-folds less in *Wolbachia*-infected cell lines relative to their uninfected counterparts (Fig.3.2.11C). The Aag2 *w*Au cells were only challenged once as the cells subsequently lost the *Wolbachia* infection. This result confirmed general inhibition of SFV by a variety of *Wolbachia* strains in cell lines from two host species, however it does not tell us at which stage the inhibition is occurring.

To achieve this, cells were transinfected with a SFV replicon, thereby bypassing entry into cells. The structural genes of this replicon were replaced with Firefly luciferase (sub-genomic region), and Renilla luciferase remained embedded among the non-structural proteins (genomic region) (Fig.3.2.11B). Separation of the genomic and sub-genomic regions allows direct quantification of each section of the viral genome; quantification of the sub-genomic section which would normally be structural proteins required for composition of new virions reveals if viral replication is actively occurring. The SFV replicon was transfected into Aa23 *w*AlbB, *w*Mel and *w*MelPop cells for 24 hours and samples were quantified for Renilla and Firefly luciferase. Results show significantly inhibition of genomic (Fig.3.2.11D) and sub-genomic (Fig.3.2.11E) replication, indicating *Wolbachia* is inhibition active replication of SFV. Renilla and Firefly luciferase were used as SFV readouts as they directly correlate with genome replication. This is consistent with results found in *Drosophila* JW18 cells (Rainey et al., 2016). Aag2 cells were not used in the replicon experiment as they were unstable, however previous experiments in the lab have shown similar inhibition of sub-genomic virus (not shown).

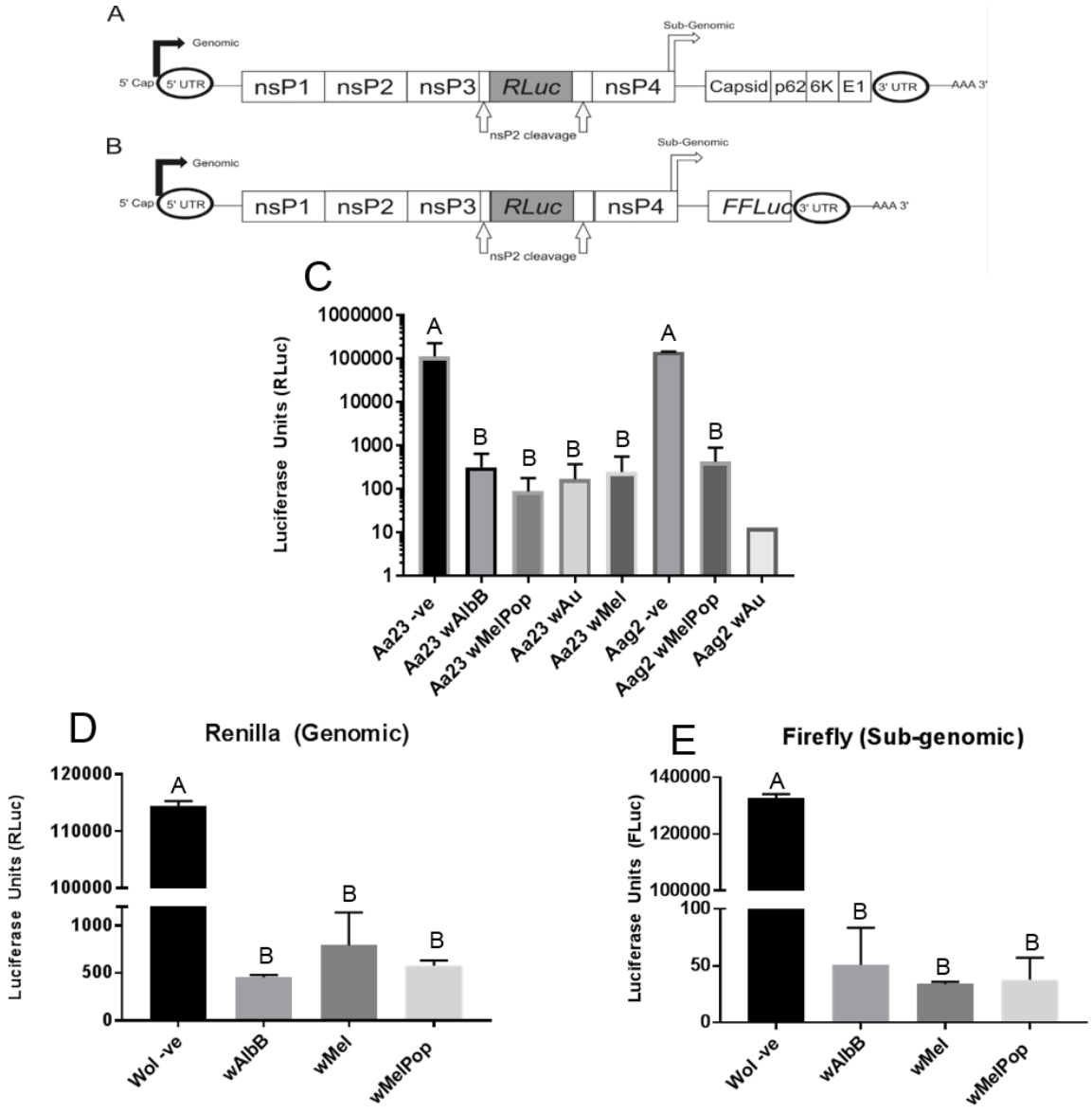


**Fig. 3.2.11.** Virus and replicon studies in Aedes cells

Schematic diagram of SFV4(3H)-RLuc reporter gene with Rennilla luciferase (RLuc) reporter inserted at the nsP3/4 junction **(A)**. Genome is split into genomic section containing non-structural proteins and sub-genomic region with structural proteins (capsid, p62, 6K, E1). Replicon schematic representation with the structural proteins replaced with Firefly luciferase (FFLuc) **(B)**. *Aedes* cells were infected with SFV-Rluc from (A) and luciferase units read after 24 hours **(C)**. SFV replicon was transinfected into Aa23 cells and genomic RLuc **(D)** and sub-genomic FFLuc **(E)** levels were measured. Results in (C) represent mean of two independent replicates, each with three technical replicates, except Aag2 wAu which represents one biological replicate. Results in D & E represent mean of one replicate, with three technical replicates. Standard error is shown. T-test was performed for significance, represented by letters above bars (e.g. A & B are statistically different).

### 3.2.6. Investigating *Wolbachia*-induced perturbation of the ER and arbovirus inhibition

Previous proteomic analysis of *Wolbachia*-infected and uninfected midguts revealed protein differences in proteins involved with the endoplasmic reticulum (ER) (Geoghegan et al., 2017). One ER-related proteomic hit was Calnexin (putative calnexin 99a), a chaperone involved in the unfolded protein response (UPR) of the ER. Calnexin is upregulated to assist the folding of misfolded proteins which may be aggregating in the ER. Calnexin protein was 1.35 and 1.16 higher in Aag2 *w*MelPop cells and *Ae. aegypti w*Mel midguts relative to their uninfected counterparts (Geoghegan et al., 2017). To follow up this proteomic data, gene transcripts of Calnexin, another UPR chaperone BiP and splicing of the Xbp1 gene were initially measured in *Ae. aegypti w*Mel and *w*Au midguts. However, there were conflicting results depending on the replicate and between *Wolbachia* strains (Appendix 3), therefore we decided to use cell lines to investigate ER perturbations as there are less variables to account for.

Calnexin, Bip and Xbp1 splicing was assessed in Aag2 uninfected and *w*MelPop cells. Both cell lines had controls treated with thapsigargin (thaps), which induces ER stress in a calcium-dependent manner (Oslowski and Urano, 2011). Following treatment, cell viability was tested with trypan blue staining, showing no differences than non-treated cells. Expression of ER-related genes was also measured following the addition of DENV-2 at MOI 1 to Aag2 uninfected and *w*MelPop cells for 5 days.

Levels of DENV were measured in the cells by RT-qPCR and in the cell supernatant by fluorescent focus assay (FFA). RT-qPCR quantifies RNA levels of DENV, whereas FFA measures live infectious virions. Non-infected Aag2 Wol –ve cells were used as negative controls. Under normal conditions, Aag2 *w*MelPop cells had around ten-fold less DENV RNA (Fig.3.2.12.A) and infectious virions (FFU) (Fig.3.2.12.B) compared to Aag2 *Wol* –ve cells. Previous studies have shown a 6-12 fold reduction in DENV density in Aag2 *w*MelPop relative to Aag2 uninfected cells (Geoghegan et al., 2017; Hussain et al., 2013) The addition of thaps to Aag2 *Wol* –ve cells resulted in less DENV RNA and no infectious virions (Fig.3.2.12.A&B). On the other hand, addition of thaps to *w*MelPop cells resulted in an increase in DENV RNA but again no infectious virions. Inducing ER stress in *w*MelPop cells by using thaps appears

to have allowed the DENV genome to replicate; qPCR of *Wolbachia* density revealed a significant decrease of *w*MelPop when treated with thaps (data not shown), showing inducing ER stress results in a drop in *Wolbachia* density.

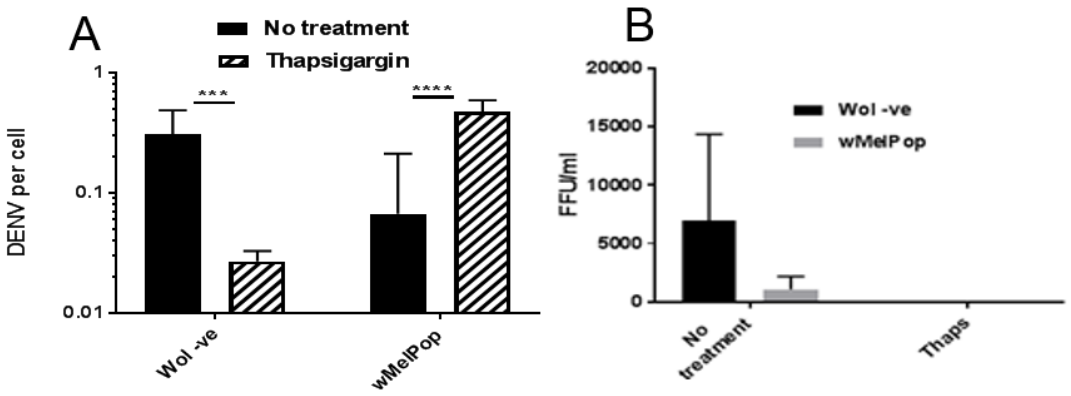


**Fig. 3.2.12.** DENV replication in Aag2 -ve and wMelPop cells during ER stress

ER stress was induced in cells with thapsigargin treatment for 18 hours, after which DENV was added at MOI 1 and left to replicate for 5 days. Cells were harvested, spun down and RNA was extracted to quantify DENV RNA **(A)**. Infectious virions from the supernatant of the same cells was quantified by fluorescent focus assay (fluorescent focus units/ml). Data represents mean of five replicates with standard error. Statistics performed were students T-test. Asterisks represent extremely significant differences (*** = p = 0.0001 to 0.001; **** = p = <0.0001).

Gene expression of chaperones Calnexin and BiP were then quantified in Aag2 *Wol*-ve and *w*MelPop cells by RT-qPCR, both with and without thaps treatment and DENV. Under normal cell line conditions, significantly more Calnexin and BiP expression was measured in *w*MelPop cells compared to *Wol* –ve cells (Fig.3.2.13.A&B), a result which corroborates the proteomic results. When both cell lines were treated with thaps, the *Wol* –ve cells increased expression of both genes to similar levels found in *w*MelPop, resulting in significantly higher expression in the case of BiP (Fig.3.2.13.A&B). Protein levels of calnexin were also quantified by western blot, confirming the same pattern as observed with gene expression data (Fig.3.2.13.C), although this only represents one replicate of samples. This indicates inducing ER stress in uninfected Aag2 cells mimics the *w*MelPop infection. However, an independent experiment quantifying expression of Calnexin protein levels in Aag2 uninfected and *w*MelPop cells showed the opposite result; there was significantly less Calnexin in *w*MelPop cells relative to

uninfected cells (Fig.3.2.13.E). This variability could be a result of differences in condition / confluence of cells between replicates.

Addition of DENV to cell lines under normal conditions led to downregulation of Calnexin and BiP relative to their non-virus counterparts. However, *w*MelPop cells retained significantly higher expression than in *Wol* –ve cells (Fig.3.2.13.A&B). When DENV was added to thaps-treated cells, the opposite result was observed; *w*MelPop cells had significantly less expression of Calnexin. These *w*MelPop cells also had higher levels of DENV RNA compared to the non-treated cells, but still no infectious virions produced (Fig.3.2.12.A&B). DENV being able to replicate coincided with a drop in *Wolbachia* density, which also explains the decrease in Calnexin.

The IRE1 pathway of the UPR can activate splicing of the Xbp1 gene, which results in upregulation of chaperones to assist in protein folding. Splicing of the Xbp1 gene was quantified by RT-qPCR; this was achieved using primers specific for the non-modified Xbp1 gene, the spliced form and the unspliced form. The spliced and unspliced forms were normalised to the control gene and the ratio calculated. There were no differences in Xbp1 splicing between *Wol* –ve and *w*MelPop cells under normal cell conditions and when treated with thaps; however there was significantly less spliced Xbp1 in *w*MelPop cells compared to Wol –ve when DENV was added (Fig.3.2.13.C).

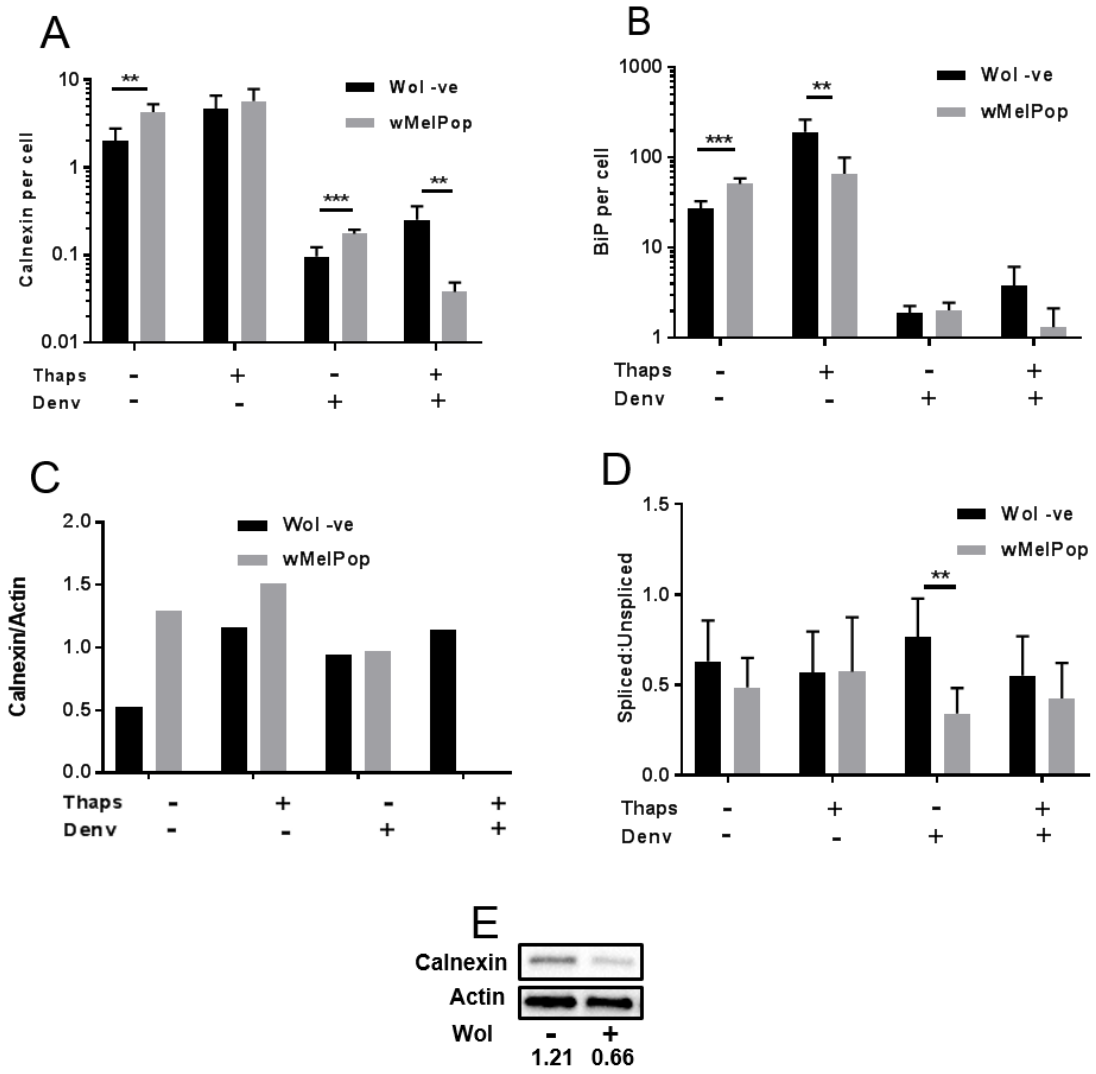


**Fig. 3.2.13.** Gene expression of ER-related genes in Aag2 -ve and *w*MelPop cells

ER stress was induced in cells with thapsigargin treatment for 18 hours, after which DENV was added at MOI 1 and left to replicate for 5 days. Cells were harvested, spun down and RNA was extracted to quantify gene expression of Calnexin **(A)**, BiP **(B)** and Spliced:unspliced ratio of Xbp1 **(D)**. Protein expression of Calnexin from one sample for each treatment is shown **(C)**. Protein was processed by western blot and analysed on Image J. The ratio of calnexin to actin is displayed. Another independent replicate showing calnexin protein expression in Aag2 Wol -ve and *w*MelPop cells is also shown **(E)**. Calnexin:actin ratio is displayed below blot. Bar graphs A,B & D represent the mean of five replicates, with standard error. C and E represent one preliminary replicate. T-test was performed for significance, marked by asterisks.

## 3.3. Discussion

### 3.3.1. Different *Wolbachia* strains may block arboviruses by different mechanisms

The work presented in this chapter suggests that although the fundamental stage at which viruses are blocked may be conserved between *Drosophila* and mosquitoes, the mechanism in which this is achieved may differ between *Wolbachia* strains. Infection of *Aedes* cells derived from two species with SFV RLuc showed strong inhibition of virus by all strains measured. The Aag2 *w*Au cells were not used for further experiments as the *Wolbachia* infection was lost, and Aag2 *w*MelPop cells were unstable at the time of the replicon experiments. Transfection of the SFV replicon into Aa23 *w*AlbB, *w*Mel and *w*MelPop cells showed sub-genomic SFV production was inhibited despite the virus bypassing entry, indicating replication was inhibited. This is the same result as observed in *Drosophila* JW18 cells (Rainey et al., 2016), suggesting virus replication is one of the stages at which *Wolbachia* is inhibition across different species and viruses.

One hypothesis for the mechanism of *Wolbachia*-mediated viral inhibition involves induction of reactive oxygen species (ROS), resulting in expression of antimicrobial peptides which inhibit DENV (Pan et al., 2012). Data shown in this chapter revealed Aag2 *w*MelPop cells are indeed under oxidative stress, as measured by CellRox Green reagent. On the other hand, the high-density *w*Au strain in Aa23 cells is not inducing oxidative stress, yet both cell lines strongly blocked SFV Fluc. This supports the theory that oxidative stress is only present in naturally naïve hosts of *Wolbachia*, whereas in those hosts with a long evolutionary history with the endosymbiont there is not usually induction of oxidative stress (Zug and Hammerstein, 2015). However, it may be speculated that novel transinfections such as *w*AlbB in *Ae. aegypti*, which previously experienced oxidative stress, may evolve and adapt over time to the novel host, leading to less oxidative stress. The Aa23 cells are *Ae. albopictus* which is naturally superinfected with *w*AlbA and *w*AlbB, and *w*Au from *D.simulans* was transinfected into the cell line. Although this is not a natural *Wolbachia*-host association, perhaps the cells were primed for infection with *Wolbachia* and therefore oxidative stress did not occur. Data here supports other evidence that there was no difference in ROS hydrogen peroxide in

Aa23 cell lines infected with several *Wolbachia strains*, relative to uninfected cells (Molloy and Sinkins, 2015).

In addition, whether a *Wolbachia*-host relationship is commensal or parasitic may alter the oxidative state of the cells. *w*MelPop is a high-density, fast replicating *Wolbachia* strain which has detrimental fitness effects on its host, indicating a parasitic relationship (McMeniman et al., 2009; Min and Benzer, 1997; Moreira et al., 2009). On the other hand, *w*Au is also high density but does not impose the same deleterious effects in its native host, *D.simulans*. Treatment of *w*MelPop-infected *D.melanogaster* with paraquat to induce oxidative stress leads to a reduction in *w*MelPop density (Monnin et al., 2016). On the other hand, inducing oxidative stress in *w*Ri-infected *D.simulans* led to no change in *Wolbachia* density (Monnin et al., 2016). *w*Ri and *w*Au are closely related *Wolbachia* strains that both singly naturally infect *D.simulans* in the wild, and both appear to have a commensal relationship with their natural host. These results indicate *w*MelPop is a parasitic symbiont, as the oxidative stress observed in Aag2 *w*MelPop cells may be a host-defense to maintain the *Wolbachia* density at an appropriate level for cells to function. Despite this, the Aag2 *w*MelPop cell line still has a propensity to crash, indicating the *Wolbachia* and host are an unstable combination. To investigate the ROS-mediated theory further, Aag2 Wol –ve cells could have been induced to oxidative stress and any subsequent effect this may have on arbovirus inhibition could be measured. There is evidence flaviviruses induce oxidative stress during infection in a timely manner and this positively affects replication of positive strand RNA (Gullberg et al., 2015). In fact, antioxidant treatment can reduce replication of negative strand RNA; flaviviruses may induce oxidative stress as a proxy to control their genome replication. If *Wolbachia* is in control of redox homeostasis, this may render viral replication impossible. Nevertheless, it appears ROS is not induced in all *Wolbachia*-infected cell lines and is likely not the fundamental mechanism of inhibition.

Despite the oxidative stress experienced by *w*MelPop-infected Aag2 cells, this did not alter levels of lipid peroxidation as measured by Bodipy reagent. *Rickettsia rickettsii* is an intracellular bacterium of the same genus as *Wolbachia* which is causes Rocky Mountain spotted fever in humans. Infection of human endothelial cells with *R. rickettsia* resulted in higher levels of intracellular perodixes relative

to uninfected cells (Silverman and Santucci, 1988). In the same infection, it was also observed that this increase of peroxides coincided with dilation of membranes of the endoplasmic reticulum, however there was no causal link established. This indicates members of the *Rickettsia* genus are capable of altering lipid peroxidation and morphology of the ER, the latter of which has already been shown for *Wolbachia*. However, in Aag2 *w*MelPop cells there was no difference in lipid peroxidation detected when samples were analysed on the flow cytometer which used separate lasers for red and green fluorescence. The two replicates on the flow cytometer that used a combined laser for both colours showed misleading results when analysed. This could be avoided with the use of controls that are 100% red or green, however this was not possible with the Image-IT kit. It was theorised that lipid peroxidation could impact cell membrane permeability and fluidity which is important for viral entry and exit, however other work in this chapter and other studies suggest *Wolbachia* is interfering with viral replication, rather than binding and entry to cells (Rainey et al., 2016; Thomas et al., 2018).

One aspect that must be considered when analysing *Wolbachia*-infected *Aedes* cells by flow cytometry is the propensity for clumping. This is important as cells are strained through a molecular cut-off sieve to ensure single cells are run on the flow cytometer, preventing potential blockages and for accurate single-cell analysis. However, under a microscope it is clear some *Wolbachia*-infected cells tend to clump together, and it is possible some of these cells were excluded from further analysis. Furthermore, it may be these cells are highly infected with *Wolbachia*, therefore this could skew the results. For future flow cytometry experiments, cells could be treated with trypsin to de-clump the cells, ensuring this does not have a detrimental effect to the cell line. The Aa23 and Aag2 cell lines also comprise various sizes of heterogenous cells, which must be considered when performing cell exclusion with gating during analysis. Ideally for these experiments, the same *Wolbachia* strain would have been investigated in both cell types, Aag2 and Aa23. As Aa23 *w*Au and Aag2 *w*MelPop were compared, this means it cannot be ruled out that each *Wolbachia* strain would operate differently in the other respective host. If the same *Wolbachia* strain is used in both cell lines, this would outrule the effect of host background on any result. However, due to the propensity of high-density cell lines to crash, this was not possible.

### 3.3.2. *Wolbachia* infection perturbs UPR chaperone expression

Previous proteomic data showed upregulation of Calnexin in *w*MelPop cells and *w*Mel midguts related to uninfected counterparts, indicating *Wolbachia* presence is modifying ER homeostasis. Gene expression of chaperones Calnexin and BiP was indeed significantly higher in *w*MelPop cells relative to *Wol* –ve cells, consistent with the proteomic data. Although BiP was not a hit identified in the proteomics, it was investigated as it is a UPR chaperone similar to Calnexin. This data indicates *Wolbachia* presence results in perturbation of UPR-related chaperone expression.

Thapsigargin was chosen to disrupt ER homeostasis as it does so in a calcium dependent manner; this would particularly affect expression of Calnexin as it is a calcium-binding protein (Michalak et al., 2002). Addition of thapsigargin to *Wol* –ve cells resulted in an increased expression of both genes similar to those found in *w*MelPop cells; this indicates induction of ER stress may mimic the *w*MelPop infection. Addition of DENV only resulted in significant reduction of both chaperones in both cell lines, indicating the virus is manipulating the UPR. In the case of Calnexin, *w*MelPop still retained significantly higher expression compared to WT, even with virus added. However, when *w*MelPop cells were perturbed with thapsigargin treatment and DENV was added, there was a significant decrease in Calnexin expression relative to WT. QPCR analysis of the *Wolbachia* wsp gene showed a significant reduction in *w*MelPop density due to the thapsigargin treatment, which would explain the decrease in Calnexin expression, however not the fact that it dropped to significantly less than in *Wol* –ve cells. Additionally, the drop in *Wolbachia* density also explains the increased DENV RNA measured in thapsigargin-treated *w*MelPop cells relative to non-treated cells. The *Wolbachia* density data was not shown as it was obtained by quantification of wsp from cDNA, not DNA. It is known that wsp is a single copy gene in DNA, however this may have been multiplied an unknown amount during the reverse-transcriptase process when creating cDNA. Therefore, as the *Wolbachia* density appeared to be several ten-fold less when treated with thaps, we concluded there is a decrease in relative density, but were not able to present this absolutely. This result adds to evidence that *Wolbachia* require an intact ERAD-pathway in order to maintain their density (White et al., 2017). *Wolbachia* may use amino acids derived from broken-down misfolded proteins for replication, as the bacterium lacks the metabolic pathways for amino acid synthesis. A previous study has shown that establishment of a

*Wolbachia* infection *in Ae. albopictus* naturally naïve cells co-incided with activation of the proteasome, indicating a degree of controlled intracellular degradation to free resources (Fallon and Witthuhn, 2009). To this end, it would benefit *Wolbachia* to be in control of the UPR pathway, which in turn could interfere with virus replication.

To further elucidate the quantification of these chaperones it would be ideal to perform protein quantification by western blot, thereby giving a picture of gene expression and subsequent amount of each protein present in midguts. Attempts were made to quantify Calnexin and Troponin H (BiP) in *Ae. aegypti* midguts, however the appearance of many non-specific protein bands on the blots made this process difficult. This may be due to the fact that *Drosophila*-based antibodies were used, as there are very few mosquito-specific antibodies available. While the Calnexin antibody worked in Aag2 cells, within the mosquito midgut there are many more factors and proteins to interfere with the assay. Protein quantification of Aag2 *w*MelPop cells revealed around half the expression of Calnexin as was found in Wol –ve cells, which is the opposite of the proteomic results. It is also the opposite result as measured by qPCR in the DENV experiment. This may be due to the fact that when Calnexin protein levels are low, gene expression is high as there is a demand for the chaperone, and vice versa. This indicates that *Wolbachia*-mediated manipulation of the ER may be a dynamic process that experiences cycles of chaperone production. However, to test this hypothesis further replicates would need to be performed, during which both the protein and the gene expression were measured. To add to this, measurements could be taken during various time points of cell growth, whilst also monitoring the *Wolbachia* density.

## 3.4. Conclusion

Data in this chapter highlights the important of investigating the mechanism of *Wolbachia*-induced arbovirus inhibition using various strains of the bacterium and in different hosts. The effect *Wolbachia* has on cells differs depending if they are derived from a host naturally infected with *Wolbachia*, or naturally naïve. An added complexity of investigating pathogen inhibition is that *Wolbachia* and viruses are inducing multiple, complex biological perturbations simultaneously, making pin-pointing of the exact process by which inhibition occurs troublesome. It is likely *Wolbachia* is manipulating the host cell in several ways that are unfavourable for virus replication, however it is clear that the close association of the bacterium with the ER is not by chance. The ER is also the site of flavivirus replication, therefore competition in this organelle between bacterium and virus is a plausible hypothesis for pathogen inhibition. To elucidate this, further work could be done investigating gene and protein expression of UPR-related molecules at different time points during virus infection, with flaviviruses and alphaviruses, in *Wolbachia* infected and uninfected cell lines/mosquitoes.

# Chapter 4

## Characterising novel transinfections of *Wolbachia* in *Ae. aegypti*

## 4.1. Introduction

Following the discovery that transinfection of *Wolbachia* into the naturally naïve *Ae. aegypti* results in pathogen inhibition, *Wolbachia*-infected females have been released as a form of vector control, with the intention of replacing wild populations. To date, these releases have focused mainly on the *w*Mel *Wolbachia* strain, which provides strong but incomplete inhibition of Dengue, Chikungunya and Zika viruses. Releases of *w*Mel in Australia have proven successful, with continued invasion and spread of *Wolbachia* through the field population. Since the release of *Wolbachia*-infected mosquitoes, there has been reportedly reduced dengue transmission (O'Neill et al., 2018). In a laboratory setting *w*Mel has exhibited incomplete virus inhibition, and when challenged with Dengue-viraemic blood from patients, can fail to prevent virus transmission (Ferguson et al., 2015). This leaves scope for *w*Mel-infected mosquitoes to still transmit arboviruses following release into the field.

Considering *Wolbachia* are a highly diverse genus of alpha proteobacteria comprised of up to 16 supergroups, there may be other strains which can provide more complete pathogen inhibition and are better suited for use in dengue control. *Aedes albopictus*, the secondary vector of Dengue virus, is naturally predominantly infected with *Wolbachia* strains *w*AlbA and *w*AlbB together, termed a 'superinfection'. However, single-strain infections can also occur. A survey of *Ae. albopictus* in Thailand revealed that of the 100% *Wolbachia*-positive mosquitoes, 99.4% were the *w*AlbA/B superinfection, leaving 6 that harboured *w*AlbA only (Kittayapong et al., 2002). On the other hand, analysis of Malaysian *Ae. albopictus* revealed that while all females had the *w*AlbA/B superinfection, a proportion of the males had lost the *w*AlbA infection (Noor Afizah et al., 2015). Further analysis revealed *w*AlbA decreased in density and was eventually lost in *Ae. albopictus* males with increasing age, after which *w*AlbB density increased (Tortosa et al., 2010). This highlights the importance of monitoring transinfected *Wolbachia* in *Ae. aegypti* in both males and females over time in order to identify a stable strain for eventual releases, but also that these two strains can exist independently without the other.

The multiple findings of *Ae. albopictus* without superinfection indicates there may be competition between the two strains, despite being the predominant natural infection type. The increased *w*AlbB density in *Ae. albopictus* males when *w*AlbA is absent supports this theory. Perhaps in unfavourable conditions one strain fairs better than the other, and is retained in a subset of mosquitoes. This was observed with the transinfection of superinfected cytoplasm from *Ae. albopictus* into *Ae. aegypti*, in which resulting progeny were predominantly infected with *w*AlbB only. In fact, the only *w*AlbA-infected line was lost due to lack of egg-hatching, although the authors admit this may have been due to procedure error (Xi et al., 2006). Two old colonies were found to carry *w*AlbA-only (their original colonization was hypothesized to pre-date the global spread of the superinfection), indicating it is a viable mosquito line (Sinkins et al., 1995).

The *w*AlbA/B superinfection does not inhibit DENV-2 replication in *Ae. albopictus*, but does restrict dissemination/presence of the virus in the salivary glands, albeit only at lower viral innoculum concentrations (Mousson et al., 2012). However, when *w*AlbB is transinfected into *Ae. aegypti* it significantly reduces DENV replication in the midgut and reduces the percentage of mosquitoes with virus in the head to less than 40% (Bian et al., 2010). Although *w*AlbB in *Ae. aegypti* provides more protection than the superinfection in the native host, there is still imperfect inhibition. It could be hypothesised that *w*AlbA may also increase in density in *Ae. aegypti* without *w*AlbB present, possibly providing strong pathogen inhibition. In addition, *w*AlbA alone provides cytoplasmic incompatibility against superinfected *Ae. albopictus* much like *w*AlbB does, indicating it could be used for population replacement (Sinkins et al., 1995).

*Wolbachia* strain *w*Au is naturally found in *Drosophila simulans* and is closely related to the *w*Mel strain. Within its natural host *w*Au reaches high densities and offers protection against pathogenic viruses; 90% of *w*Au-infected *D.simulans* survived up to 30 days following injection of *Drosophila* C Virus (DCV) and Flock House Virus (FHV), compared to a median of 8 days survival in *Wolbachia*-uninfected flies (Osborne et al., 2009). Further analysis revealed that although there were significantly lower titres of DCV in *w*Au-infected flies at 2 days post-infection, titres increased to similar levels as in the uninfected flies after 30 days. Despite this recovery in titre, the initial reduction in virus reveals that *w*Au

possesses the ability to interfere with virus replication. In this study, *D. simulans* with *w*Ri also survived significantly longer than uninfected flies when challenged with DCV and FHV, although not as long as *w*Au flies. When transinfected into *Ae. aegypti, w*Ri establishes a density lower than *w*Mel. Although *w*Ri-infection results in significantly lower titres of DENV following oral-challenge compared to their uninfected counterparts, there is still virus present at levels up to 10^7 DENV per head, unlike *w*Mel-infected mosquitoes which had only a few low positives (Fraser et al., 2017). While in this case *w*Mel remained the strongest pathogen blocker, it is vital to explore other *Wolbachia* strains in an attempt to find one with similar fitness advantages and complete viral blockage.

It is hypothesised that the increased fitness *w*Au exhibits on its native host accounts for its successful spread through populations, as this particular strain does not induce cytoplasmic incompatibility, yet *w*Au has previously spread and increased in frequency throughout field *D. simulans* populations in Australia (Kriesner et al., 2013). The *w*Au strain represents a good candidate for transinfection into *Ae. aegypti* for arbovirus control; it reaches higher density than *w*Mel in its native host and provides stronger protection against pathogenic viruses, whilst increasing host fitness. We hypothesised due to its close relationship with *w*Mel we would observe much the same fitness advantages as with *w*Mel infection, but with complete viral blockage.

Novel transinfections were created in *Ae. aegypti* using *Wolbachia* strains *w*AlbA and *w*Au in an attempt to discover the best host-symbiont combination for pathogen inhibition. Fitness traits of these novel lines were characterised, including survival, egg fecundity/viability and reproductive manipulation, compared to *w*Mel and *w*AlbB-infected *Ae. aegypti*. Importantly, lines were challenged with model Alphavirus Semliki Forest virus and Flaviviruses dengue virus and Zika virus, to assess their pathogen inhibition potential. The impact of novel *Wolbachia* transinfections on the immune system was assessed by measuring levels of reactive oxygen species (ROS) and antimicrobial peptides (AMPs) in each line. In addition, *w*Mel mosquitoes were challenged with pathogenic bacteria *Serratia marcescens* to investigate the induction of AMPs and their role in bacterial defence. A novel superinfection of *w*Au*w*AlbB was also created in *Ae. aegypti*,

which was shown to cause unidirectional cytoplasmic incompatibility, adding an alternative method for spread of *w*Au through field populations.

## 4.2. Results

### 4.2.1. Creation of novel *Wolbachia* transinfections in *Ae. aegypti*

*Wolbachia*-infected lines were created in the same host background of *Ae. aegypti* with strains *w*AlbA, *w*AlbB, *w*Mel and *w*Au. This was achieved by transfer of embryonic cytoplasm from *Wolbachia*-infected eggs of each donor species into *Ae. aegypti* eggs using a needle (Fig.4.2.1.A). The donor organism for *w*Au was *Drosophila simulans*, leading to stable transinfections in *Ae. aegypti* and complete maternal transmission of *Wolbachia* (Fig.4.2.1.B). An *Ae.albopictus* triple infected line was created with *w*Mel, *w*AlbA and *w*AlbB, and this cytoplasm was transferred to *Ae. aegypti*. Within the novel host, the three strains were not completely maternally inherited (Ant and Sinkins, 2018). This resulted in the subsequent creation of *Ae. aegypti* with single infections of *w*AlbA, *w*AlbB and *w*Mel (Fig.4.2.1.B).

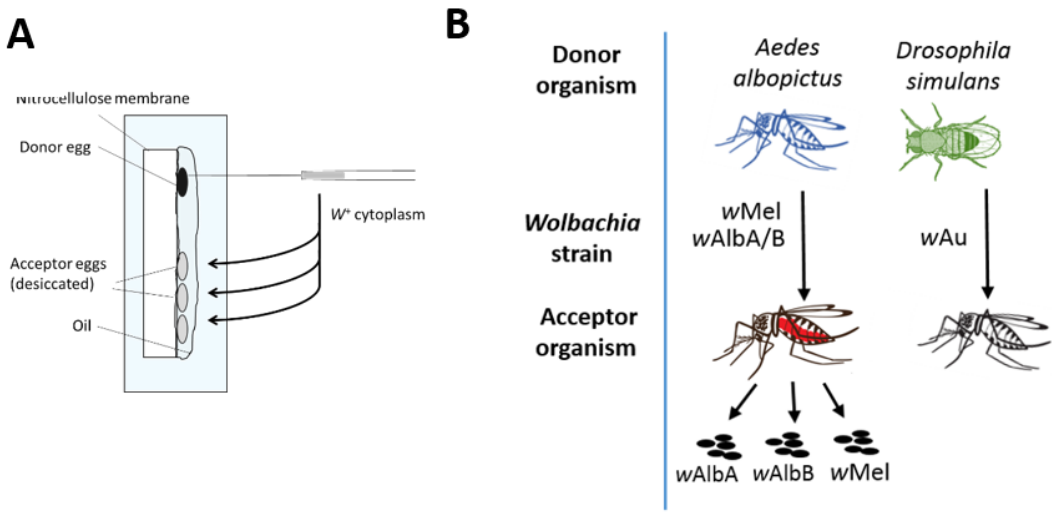


**Fig.4.2.1.** Creation of novel *Wolbachia* transinfections in *Ae. aegypti*

Novel transinfections were created by embryonic transfer of cytoplasm from a *Wolbachia*-infected host into the naïve *Ae. aegypti* using a needle **(A)**. This process was repeated hundreds of times until *Wolbachia* positive mosquitoes were detected to start a colony. *Wolbachia* strains were taken from *Ae. albopictus* (*w*AlbA*w*AlbB), *D.melanogaster* (*w*Mel), *D.simulans* (*w*Au) and transferred to *Ae. aegypti* **(B)**. *w*AlbA*w*AlbB *Ae. aegypti* were blood fed and laid eggs with incomplete maternal transmission leading to creation of single-strain infected colonies.

### 4.2.2. All *Wolbachia*-infected lines assessed induce CI except *w*Au

Mating crosses were performed on all the novel transinfected lines and with wild type (WT) uninfected mosquitoes to assess whether these lines induce cytoplasmic incompatibility (CI), a manipulation required for successful invasion of field populations. Cages were set up with crosses of 20 males and 20 females of each line and left for several days to allow mating, then females were blood-fed and individualised for oviposition. Following this, the number of eggs that hatched were counted. All *Wolbachia*-infected lines induced unidirectional CI with WT mosquitoes except *w*Au, as crosses with *w*Au-infected males and WT females still led to 91.4% hatch rate (Table 4.2.1.). This is consistent with reports that *w*Au does not cause CI in its native host, *Drosophila simulans* (Turelli and Hoffmann, 1995). The *w*AlbA, *w*AlbB and *w*Mel lines all exhibit not only unidirectional incompatibility with WT mosquitoes, but also with each other *Wolbachia* strain, indicating bidirectional incompatibility.

| | | Female line | | | | |
|---|---|---|---|---|---|---|
| | | *w*AlbA | *w*AlbB | *w*Mel | *w*Au | wt |
| Male line | *w*AlbA | 89.2 (1541) | 0 (774) | 0 (644) | 0 (499) | 0 (488) |
| | *w*AlbB | 0 (663) | 89.4 (954) | 0 (821) | 0 (663) | 0 (1321) |
| | *w*Mel | 0 (1254) | 0 (667) | 90.4 (416) | 0 (451) | 0 (974) |
| | *w*Au | 91.4 (680) | 75.3 (237) | 92.7 (402) | 92.4 (637) | 91.4 (810) |
| | wt | 83.7 (771) | 79.4 (527) | 87.6 (669) | 87.6 (296) | 87.3 (225) |

Eggs are from a single-cage cross of 20 males and 20 females. Females were blood-fed and individualized for oviposition. Numbers show percentage hatch rates with total numbers of eggs counted in parentheses.

https://doi.org/10.1371/journal.ppat.1006815.t001

**Table 4.2.1.**: Crossing patterns in all *Ae. aegypti* lines

### 4.2.3. *w*AlbA and *w*Au have the highest *Wolbachia* density in whole body and tissues

The density of *Wolbachia* in the whole body of female mosquitoes was quantified at least five generations after creation of the strains. Females were sampled at 1,5,10 and 15 days post-eclosion (d.p.o.) for DNA extraction and *Wolbachia* quantification by qPCR. *Wolbachia* density increased in all lines over time (Fig. 4.2.2.A). *w*AlbA and *w*Au showed similar high densities of over 100 *Wol*/ host genome at 1 d.p.o., which steadily increased up to around 1000 *Wol*/ host genome in both lines after 15 d.p.o. *w*Mel had the third highest density, several logs lower than those in *w*AlbA and *w*Au, and *w*AlbB had the lowest density at all time points observed. A similar trend in density was observed when we dissected and performed qPCR on tissues to investigate *Wolbachia* tropism in the novel

transinfections. *w*Au and *w*AlbA had higher densities than wAlbB and wMel in the ovaries, midgut and salivary glands (Fig. 4.2.2.B). Of the tissues examined, *Wolbachia* density in midguts across all lines was the lowest in comparison to ovaries and salivary glands.

Given the discovery that *w*AlbA reached a much higher density when transinfected in *Ae. aegypti* compared to those found in the natural *Ae. albopictus* host, the effect of host-species on density was further investigated. An *Ae. aegypti* line transinfected with *w*AlbA and *w*AlbB was also created due to imperfect maternal transmission of the triple-infected line, and compared with wild-type *Ae. albopictus* with the same infection. Strain-specific qPCR was performed on whole bodies of each species, revealing that *w*AlbA and *w*AlbB both reach higher densities in the *Ae. aegypti* host, with a significant difference observed with *w*AlbA (Fig.4.2.2.C). In the native *Ae. albopictus* host, *w*AlbB outnumbered *w*AlbA at a ratio of 1:7, whereas in *Ae. aegypti* this was reversed as *w*AlbA outnumber *w*AlbB 15:1. To further investigate differences in tissue distribution in each host, midguts, ovaries and salivary glands were dissected for strain-specific qPCR. In the native *Ae. albopictus* host, *w*AlbA and *w*AlbB were highest density in the ovaries, with small amounts in the midguts and salivary glands (Fig.4.2.2.D). On the other hand, in the novel *Ae. aegypti* host, both strains were found at similar densities across all three tissues, indicating a broad colonisation of the host. Due to deleterious effects observed on survival, the *Ae. aegypti w*AlbA*w*AlbB line was not brought forward for further characterisation.

### 4.2.4. *w*AlbA and *w*Au infection impacts survival rate and egg hatch

High density *Wolbachia* strains such as *w*MelPop have proven to have deleterious effects on host fitness in *Ae. aegypti*, therefore it was investigated whether the high-density *w*AlbA and *w*Au novel transinfections had a negative effect on survival and fecundity. Four cages were set up containing 25 females at 1 day post-eclosion for each line and the number of deaths was recorded daily for each line. Survival curves show all lines generally had good survival up to 20 d.p.o, after which the *w*Au and *w*AlbA lines have a steady and significant decline in survival compared to WT mosquitoes ($p=0.001$), with all females dead at 60 d.p.o (Fig. 4.2.3.A). *w*AlbA mosquito survival in particular started to decline sharply in survival from 20 to 40 d.p.o. *w*Mel and *w*AlbB-infected mosquitoes both had longer survival than *w*AlbA

and *w*Au lines, with a small number of mosquitoes surviving past 60 d.p.o. Despite this, *w*AlbB experienced a slight but significant decrease in survival relative to WT mosquitoes. *w*Mel-infected mosquitoes had the best survival rate, which was not significantly different to WT.

In order for *Wolbachia* to be able to spread through a population, female fecundity must not be too heavily impacted, otherwise the invasion threshold frequency will be too high. As *Wolbachia* is mostly vertically transmitted from mother to offspring, infection with a *Wolbachia* strain that negatively impacts egg

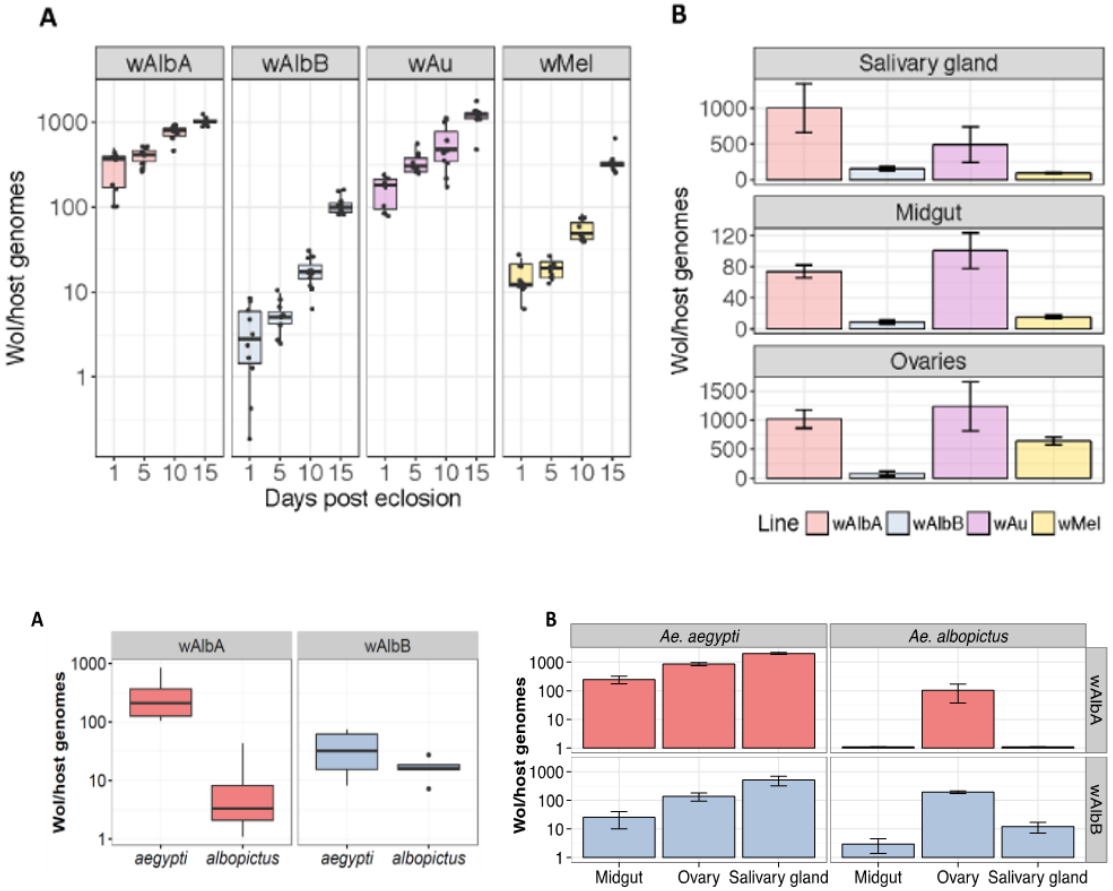


**Fig.4.2.2** *Wolbachia* density and tissue tropism in transinfected *Ae. aegypti*.

Quantification of *Wolbachia* density by qPCR in whole bodies of females and tissues at various time points, *Wolbachia* surface protein (wsp) gene was normalised to hth. **(A)** Time course of whole-body density in novel transinfections. Boxes represent 10 biological replicates, each replicate with 5 pooled females within. Mean *Wolbachia* density in tissues is shown **(B),** whereby 5 salivary glands, midguts of pairs of ovaries were combined for 5 biological replicates. Error bars represent standard error. **(C)** *w*AlbA and *w*AlbB strain specific densities in the whole-body of superinfected (*w*AlbA*w*AlbB) *Ae. aegypti* and *Ae. albopictus* females 5 days post-eclosion. 5 females were pooled for 5 biological replicates, whiskers show upper and lower quartiles. **(D)** Mean *w*AlbA and *w*AlbB strain specific densities in dissected tissues of superinfected *Ae. aegypti* and *Ae. albopictus*. Error bars represent standard error. Statistic analysis performed was two-tailed Students t-test.

production will hinder spread of the symbiont. The number of eggs produced from 20 individualised females per line following a blood-meal were counted. There was a slight variation in numbers of eggs produced per line with average egg numbers ranging from 87-95 per female, however egg number in *Wolbachia*

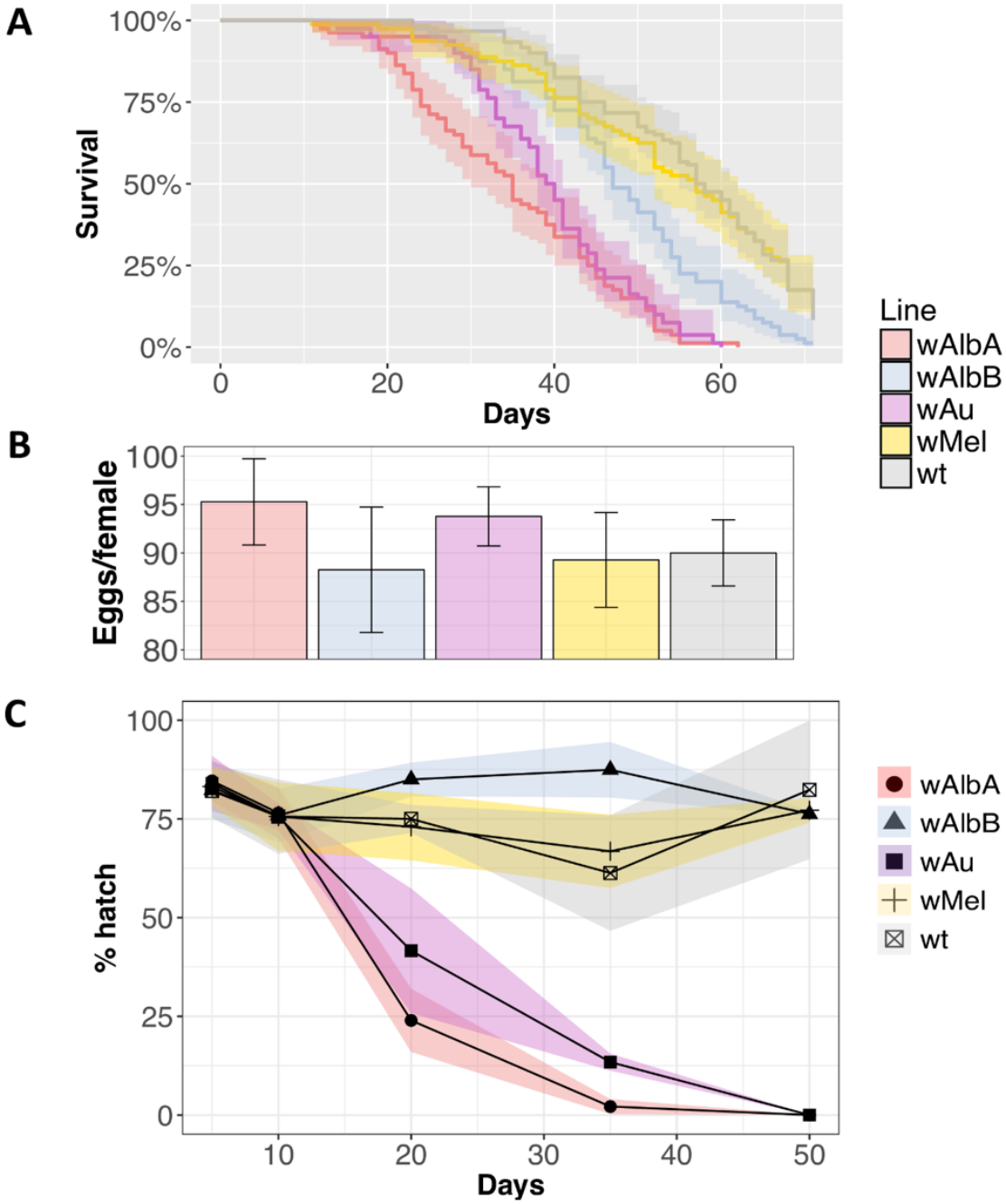


**Fig.4.2.3.** Measurement of fitness traits in novel transinfections in *Ae. aegypti*.

(A) Survival curve of *Wolbachia*-infected lines and uninfected (WT). Curves represent percentage survival with 95% confidence interval shown by shaded area. Data shown represents 4 replicate cages per line with 25 initial females in each. (B) Fecundity measured by eggs laid per female during the first gonotrophic cycle. 20 females were individualised for oviposition and eggs laid were counted. Bars represent mean egg count per female with standard deviation. ANOVA was performed for significance. (C) Percentage hatch of eggs dessicated for 5,10,20,35 and 50 days. Egg number varied per time point from 200-500. Lines represent percentage hatch with 95% confidence intervals shown in shaded area.

transinfected lines were not significantly different to uninfected WT mosquitoes (Fig. 4.2.3.B).

Another important aspect of fitness to assess in novel *Wolbachia* transinfections is egg quiescence; the ability of eggs to hatch following drying. *Aedes* mosquitoes in the wild experience wet but also dry seasons of weather, with very little rainfall, which is required to stimulate egg hatching. Uninfected WT *Aedes* eggs have therefore adapted the ability to withstand extended desiccation, meaning they can remain dormant until the wet season arrives. If *Wolbachia* reduces the ability of eggs to withstand desiccation, it could result in loss of the symbiont within the mosquito population. Females of each transinfected line were fed a blood-meal and laid eggs onto egg cones, which were then dried for 5,10, 20, 35 and 50 days, then put into water for hatching. The percentage hatch rate was calculated from the counting of 200-500 eggs per line, per time point. *w*AlbA and *w*Au eggs experienced a sharp drop in egg hatch following more than 10 days of dessication (Fig. 4.2.3.C). Less than 50% of *w*AlbA and *w*Au eggs hatched following 15-18 days desiccation. On the other hand, *w*Mel and *w*AlbB-infected eggs experienced no significant difference in egg hatch at 50 days desiccation compared to 5 days, much like uninfected WT eggs.

### 4.2.5. All *Wolbachia* transinfections exhibit pathogen inhibition except *w*AlbA

The success of releasing *Wolbachia*-infected *Ae. aegypti* as a vector replacement strategy relies on *Wolbachia*-mediated pathogen inhibition to reduce the transmission of arboviruses. The novel lines were challenged with model *Alphavirus* SFV and Flaviviruses DENV and ZIKV to investigate broad virus-inhibition abilities of each *Wolbachia* strain across two genera. Firstly, females from each line were challenged with SFV via thoracic injection and virus quantified by RT-qPCR in the whole-bodies of mosquitoes 10 days post-injection. As expected, the high density *w*Au strain exhibited the strongest pathogen inhibition, with significantly lower levels of SFV relative to WT mosquitoes (Fig. 4.2.4.A, $p=<0.01$). The moderate density *w*AlbB and *w*Mel strains also exhibited strong pathogen inhibition with SFV levels several logs lower than those found in WT ($p=0.05$). Surprisingly, there was no viral inhibition observed in the high density *w*AlbA line.

The lines that had shown pathogen-inhibition abilities with SFV were then challenged with blood-feedings of DENV and ZIKV. Due to the technical difficulties of challenging multiple lines simultaneously, *w*AlbA-infected mosquitoes were not challenged with flaviviruses as they showed no inhibition of the model alphavirus SFV. Following oral challenge of virus, blood-fed females were incubated for 12 days and individual females were sampled for qRT-PCR of virus presence/levels. As well as checking for virus in whole abdomens, salivary glands were dissected to check for transmission potential. There were no DENV-positive salivary glands in any of the 18 *w*Au mosquitoes sampled (Fig. 4.2.4.B), despite DENV detection in

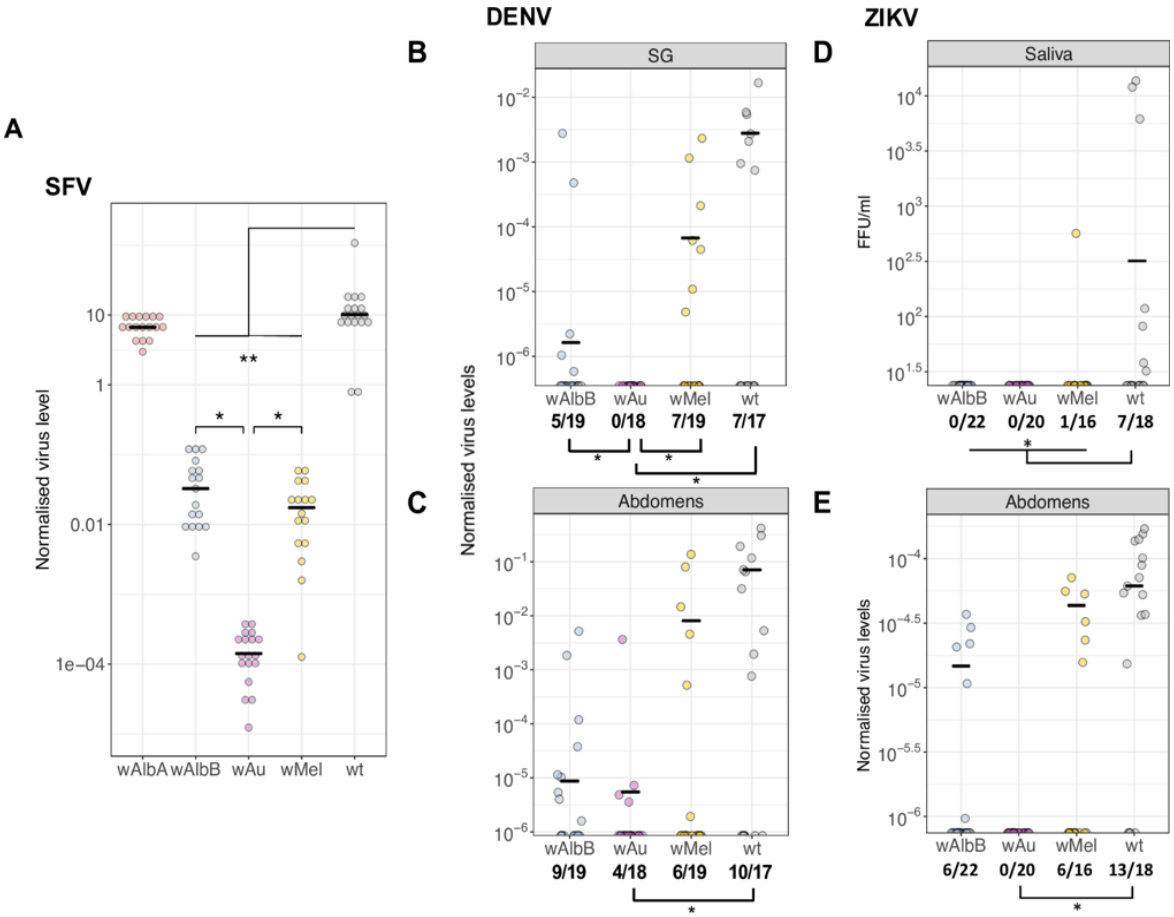


**Fig.4.2.4.** Virus inhibition in novel transinfections in *Ae. aegypti*.

(**A**) Genome copies of Semliki Forest Virus (SFV) following thoracic injection into *Wolbachia*-infected and uninfected (WT) *Ae. aegypti*. At 10 days post-injection RNA was extracted from females and virus was quantified by qRT-PCR, normalised to RPS17. Statistic analysis performed was one-way ANOVA with Dunnett's post-hoc test. 5-day old females were also challenged with Dengue-2 (**B & C**) and Zika (**D & E**) viruses and incubated for 12 days. Females were then salivated (ZIKV only) and RNA was extracted from dissected salivary glands and abdomens for virus quantification by qRT-PCR. Zika titres in saliva were quantified by fluorescent focus units (FFU). Numbers under each graph indicate proportion of mosquitoes infected with respective virus. Statistics of positive/negative infectivity was assesse by one-tailed Fischer's exact test. Black lines indicates median of positive samples.

22.2% of *w*Au abdomens (Fig. 4.2.4.C). DENV was detected in 31.6% and 36.8% of *w*Mel abdomens and salivary glands respectively, which was not significantly lower than WT infection of 58.8% and 41.1%. *w*AlbB also exhibited partial DENV-inhibition with 26.3% infection in SG and 47.3% infection of abdomens. *w*Au proved to be the strongest DENV blocker in the lines tested, with infection rate significantly lower than WT mosquitoes in abdomens and SG, the latter of which is important for transmission.

The novel lines were also orally challenged with ZIKV in order to check broad inhibition of Flaviviruses. Although quantifying viral RNA in the salivary glands is a good indication of risk of transmission, females were also salivated and virus presence detected by FFA. *w*Au completely blocked ZIKV as no virus was detected in abdomens or saliva (Fig. 4.2.4.D&E). In addition, although there was ZIKV detected in 27.7% and 37.5% of *w*AlbB and *w*Mel abdomens, both lines had a significantly lower infection rate in the saliva relative to 39% in WT, with no virus detected in any *w*AlbB saliva and only one positive *w*Mel saliva sample (Fig.4.2.4.D&E).

### 4.2.6. *w*AlbA transinfection results in high expression of antimicrobial peptides

Previous studies have shown transinfection of *Ae. aegypti* with *Wolbachia* can result in upregulation of immune genes including antimicrobial peptides (AMPs) and ROS. There is evidence that *Wolbachia*-induced ROS $H_20_2$ can result in increased expression of AMP defensin C, which can inhibit replication of DENV in *Ae. aegypti* (Pan et al., 2012). Considering *Wolbachia*-induced immunity may play a role in virus inhibition, levels of $H_20_2$, expression of ROS-related Nox/Duox genes (NOXM, DUOX) and antioxidant gene Thioredoxin peroxidase (TPX) were measured in the novel transinfection lines. In addition, expression of AMPs cecropin d (CECD), cecropin G (CECG) and defensin C (DEFC) was quantified.

As studies before have shown that high levels of $H_20_2$ occur only in novel transinfections in *Ae. aegypti*, $H_20_2$ levels were measured over several generations post-creation to assess if results were consistent or due to the novel nature of *Wolbachia* infection. 3, 5-day old females were pooled for 6 replicates per line and $H_20_2$ was measured using the Amplex Red Hydrogen Peroxide Kit. At generation

7 (G7) there were significantly higher levels of $H_20_2$ across all *Wolbachia*-infected lines assessed relative to WT (Fig. 4.2.5.A). However, by G8 $H_20_2$ levels in *w*AlbA and *w*AlbB had decreased to levels similar to WT, with only *w*Mel significantly higher. By G10, despite a higher mean $H_20_2$ level in *w*Mel compared to WT, this difference was not significant.

As there was a stabilisation of $H_20_2$ level with more advanced generations, immune gene expression was quantified at G15, in order to gain insight into *Wolbachia* strain effect on immunity. RNA was extracted from 3 pooled females at 5 days post-eclosion for 6 replicates per line and each gene of interest quantified by qRT-PCR, normalised to housekeeping gene RPS17. Expression of ROS-related gene DUOX was similar in all *Wolbachia*-infected lines relative to WT except for *w*Mel, which had significantly lower expression levels (Fig. 4.2.5.B). *w*Mel-infected mosquitoes also had lower levels of antioxidant TPX, however this was only significantly lower compared to other *Wolbachia* lines *w*AlbB and *w*Au, not uninfected WT. Levels of NOXM were very similar across all *Wolbachia*-infected lines compared to WT, with a small but significant decrease in *w*AlbA expression compared to *w*Mel. Analysis of AMP expression showed *w*AlbA-infected mosquitoes had significantly higher expression of CECD and DEFC relative to all other *Wolbachia* lines and uninfected WT (Fig. 4.2.5.B). Similar expression of CECG was observed across all lines except *w*AlbB, in which surprisingly we found no detectable expression of this gene.

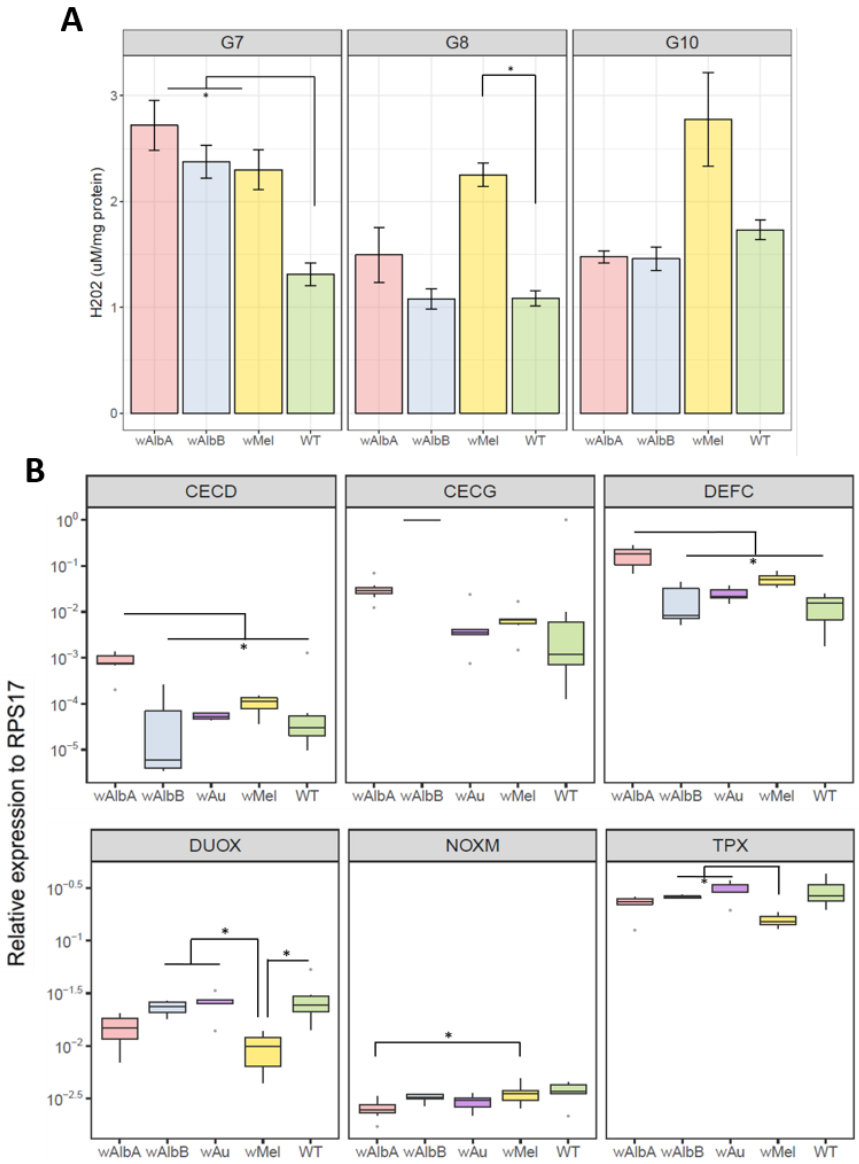


**Fig.4.2.5.** Hydrogen peroxide and immune gene expression in novel transinfections in *Ae. aegypti*.

(**A**) Hydrogen peroxide (H202) in female mosquitoes 7, 8 and 10 generations post-creation of the lines. H202 levels were measured using the Amplex Red Hydrogen Peroxide Kit. Each bar represents mean H202 level and standard error of 6 biological replicates, each with 3 pooled females per replicate. (**B**) Expression of Antimicrobial peptides (CECD, CECG, DEFC) and ROS-related genes (DUOX, NOXM, TPX) in novel transinfections at generation 15, normalised to RPS17. Boxplots represent 6 biological replicates, each with 3 pooled females per replicate. The centre of the boxplot represents median gene expression, the edges show the upper/ lower quartiles, the whiskers show the upper/lower extremes and grey dots represent outliers. Statistics performed were Students T-test and One-way Anova performed on R.

### 4.2.7. Assessing *Wolbachia*-induced AMP expression in response to challenge with *Serratia marcescens*

As one ROS-related theory of *Wolbachia*-mediated pathogen inhibition relies on the upregulation of AMPs, the role of AMPs in defense against pathogenic bacteria was also investigated. Studies have shown transinfection of *Wolbachia* into novel hosts such as *Ae. aegypti* can lead to upregulation of AMPs, Toll and Imd pathway (Kambris et al., 2009; Moreira et al., 2009). Upregulation of AMPs and the Toll pathway has been shown to be important in the mosquito defence against DENV (Pan et al., 2012; Xi et al., 2008). Previously in this chapter, the *w*Mel line showed higher levels of $H_20_2$ and AMPs DEFC and CECG, compared to WT. This line also showed good virus inhibition and was taken forward for challenges of pathogenic bacteria *Serratia marcescens*, to investigate if upregulated AMP expression also inhibits pathogenic bacteria. Due to time constraints, only the *w*Mel line was used for these challenges.

The ability of *Ae. aegypti w*Mel and WT to clear *S.marcescens* following oral challenge was assessed by exposure to an infected blood or sucrose meal. A blood meal is digested within the midgut, whereas a sucrose meal is delivered to the crop of the mosquito. For sucrose exposure, mosquitoes were allowed to feed ad libitum on infected cotton-wool for 12 hours until the experiment began. For blood-meal, females fed on heated sheeps blood for 60 minutes then placed in a cage until samples at experimental timepoints. DNA was extracted for 5-6 individual females per time point (0, 24, 48, 72, 100 hours) and qPCR performed for *S. marcescens* quantification. There was no difference in clearance of *S. marcescens* following blood-meal exposure between WT and *w*Mel mosquitoes, with both lines exhibiting the same decline in *S. marcescens* after 72 hours, resulting in very little bacteria present at 100 hours (Fig.4.2.6.). Following exposure to a sucrose-infected meal, *w*Mel did have higher levels of *S. marcescens* at 0, 24 and 48 hours post-exposure relative to WT, however both lines had the same level of *S. marcescens* at the end of the experiment. *S. marcescens* in WT mosquitoes appeared to experience an initial drop at 24 hours, but was able to replicate and increase in number by 72 hours.

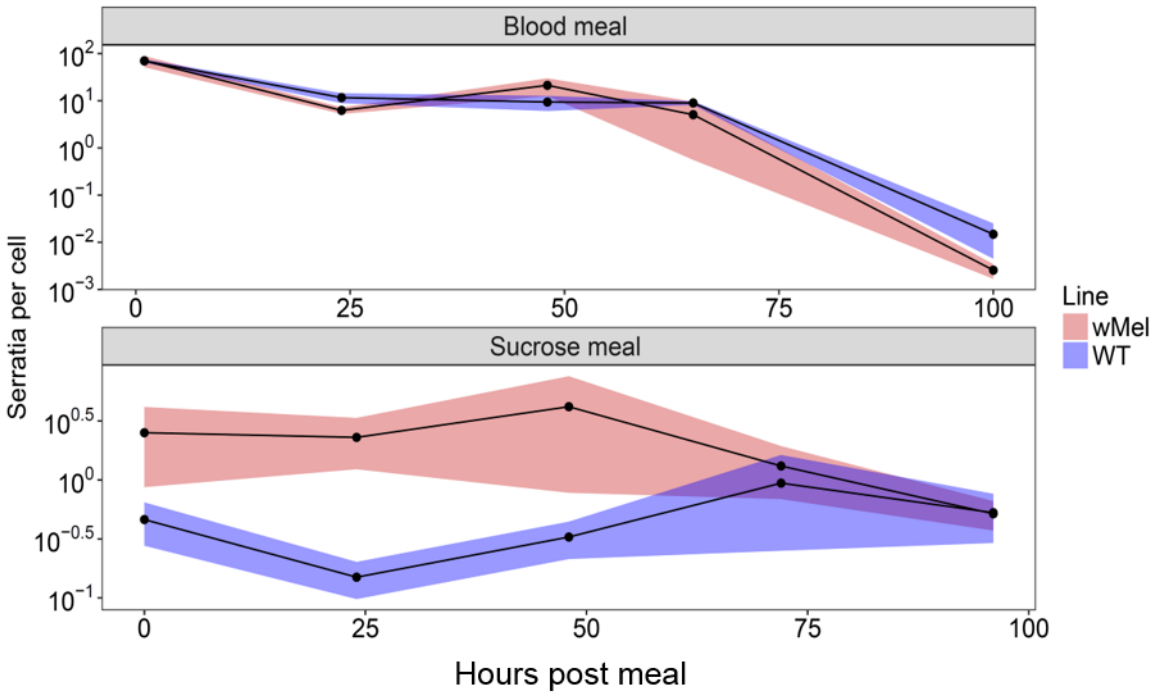


**Fig.4.2.6.** *S. marcescens* in WT and *w*Mel *Ae. aegypti* following exposure to infected blood or sucrose meal.

5 day old wild type and *w*Mel *Ae. aegypti* females were fed live *S. marcescens* at an optical density (OD) of 2 via a blood meal (top) or provided as a sucrose meal (bottom). For sucrose feeding mosquitoes fed ad libitum on infected cotton wool for 12 hours before time points began. 5-7 mosquitoes were samples per time point, DNA was extracted and qPCR performed to quantify *S. marcescens*. Lines show *S. marcescens* per host cell (reference gene hth) with the shaded areas representing 95% confidence intervals.

As the *w*Mel and WT lines appeared to be able to clear *S. marcescens* infection at a similar rate following oral exposure, the lines were also challenged with the bacteria by intrathoracic injection. Levels of $H_20_2$ and AMPs DEFC and CECG were measured prior to injection, showing significantly higher levels of $H_20_2$ and 4-6 fold higher expression of AMPs in *w*Mel mosquitoes relative to WT (Fig.4.2.7.A&B). Mosquitoes were injected with a media-only control, in order to measure AMP response to general injury. There was no change in AMP expression in WT mosquitoes following an injury only (Fig.4.2.7.C). On the other hand, *w*Mel mosquitoes had significantly higher expression of both AMPs relative to WT at both time points. This indates *w*Mel mosquitoes are primed for AMP defense regardless of the recognition of a pathogen. Mosquitoes were then injected with heat-killed *S. marcescens*, as previous injections with live *S. marcescens* proved fatal to mosquitoes. Using heat-killed *S. marcescens* could still initiate a receptor-mediated immune response. Following *S. marcescens* injection, expression of

DEFC in WT mosquitoes increased similarly to wMel at 48 hours, however this decreased by 96 hours, whereas wMel retained significantly higher levels of DEFC (Fig.4.2.7.D). Both lines also had increased expression of CECG at the 48 hour time point, again decreasing by 96 hours, with no significant difference observed between the lines. This data indicates *Wolbachia*-uninfected mosquitoes can mount an AMP response to pathogenic bacteria to similar levels found in *w*Mel

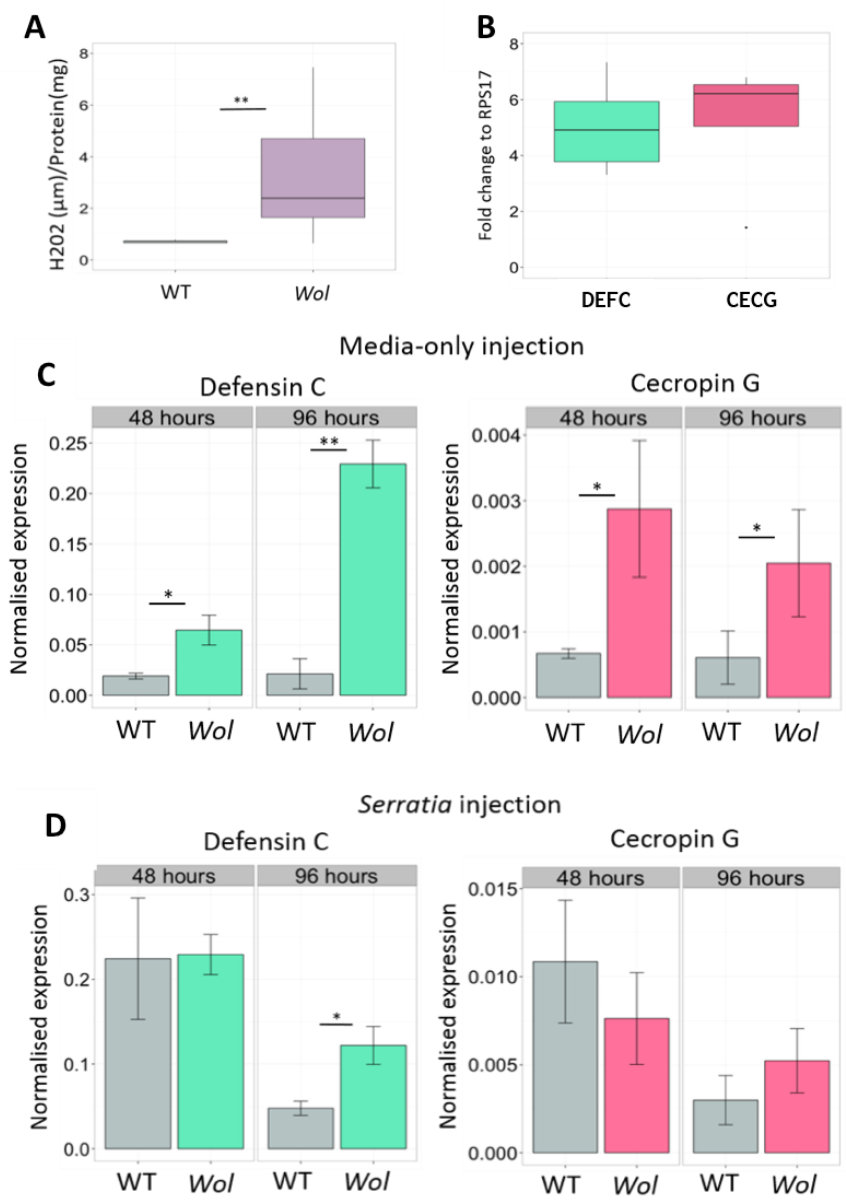


**Fig.4.2.7.** $H_2O_2$ and AMP expression following challenge with *Serratia marcescens*.

$H_2O_2$ was measured in whole females using Amplex Red Hydrogen Peroxide Kit **(A)**. Expression of antimicrobial peptides Defensin C (DEFC, green) and Cecropin G (CECG, pink) was quantified in whole females by extracting RNA and performing RT-qPCR for the genes of interest, referenced to rps17 **(B)** Whiskers of box plots represent upper and lower quartiles, with median line shown. Mosquitoes were injected with media **(C)** or heat-inactivated *S.marcescens* **(D)** using a Nanoject and collected for RT-qPCR at 48 and 96 hours post-injection. All data represents mean of 5-6 biological replicates each with 3 pooled females. Error bars are standard deviation. T-tests were performed for significance, represented by asterisks (p=<0.05).

mosquitoes, however this induced immune response remains higher for longer in *Wolbachia*-infected mosquitoes.

### 4.2.8. A *w*Au/*w*AlbB superinfection in *Ae. aegypti* causes unidirectional cytoplasmic incompatibility

*w*Au is the strongest virus blocker in *Ae. aegypti* and is stable under heat stress (see: Chapter 5), but it does not cause cytoplasmic incompatibility. Despite this, *w*Au has been able to spread through field populations of *Drosophila*, however to ensure rapid invasion it would be ideal to combine this strain with another that causes CI. Cytoplasm was transferred from *w*Au-infected *Ae. aegypti* into *w*AlbB-infected *Ae. aegypti* to create a *w*Au/*w*AlbB superinfection. Crosses with WT mosquitoes showed that the *w*Au/*w*AlbB does indeed cause CI, with 0% hatch rate from a cross with *Wolbachia*-infected males and uninfected females (Fig. 4.2.9.A). Analysis of *Wolbachia* density in the *w*Au*w*AlbB line by qPCR revealed a similar density to the *w*Au line, indicating it would be a good viral blocker (Fig. 4.2.9.B). This increase in density was confirmed to be due to higher *w*Au levels with *Wolbachia*-specific PCR, and also the discovery that *w*AlbB significantly decreased in density in the superinfected line, relative to the single-infection line (Fig. 4.2.9.C).

FISH probes were designed to differentiate between *w*Au and *w*AlbB strains when in superinfection. A general *Wolbachia* probe targeting the wsp gene was used to identify *w*Au (and by proxy, *w*AlbB). A supergroup B-specific probe was designed to identify wAlbB-only, by aligning 16s sequences of supergroup A (*w*Au) and supergroup B (*w*AlbB) strains and identifying a region of difference in the sequence. Testing of the specificity of the probes was carried out using Aa23 *w*Au and *w*AlbB-infected cells, which were combined in culture and analysed for FISH. Results showed the supergroup B (red) probe was able to identify *w*AlbB (Fig.4.2.8.B) whereas *w*Au (wsp) fluoresced in green (Fig.4.2.8.A). The high density of *w*Au relative to *w*AlbB was then visualised in the ovaries of mosquitoes with FISH (Fig.4.2.9.D). In the single-infected ovaries, *w*AlbB are visually at a higher density compared to the superinfected ovaries, whereby *w*AlbB is compacted into smaller areas. On the other hand, *w*Au retains its high density in the single infected line and also the superinfection.

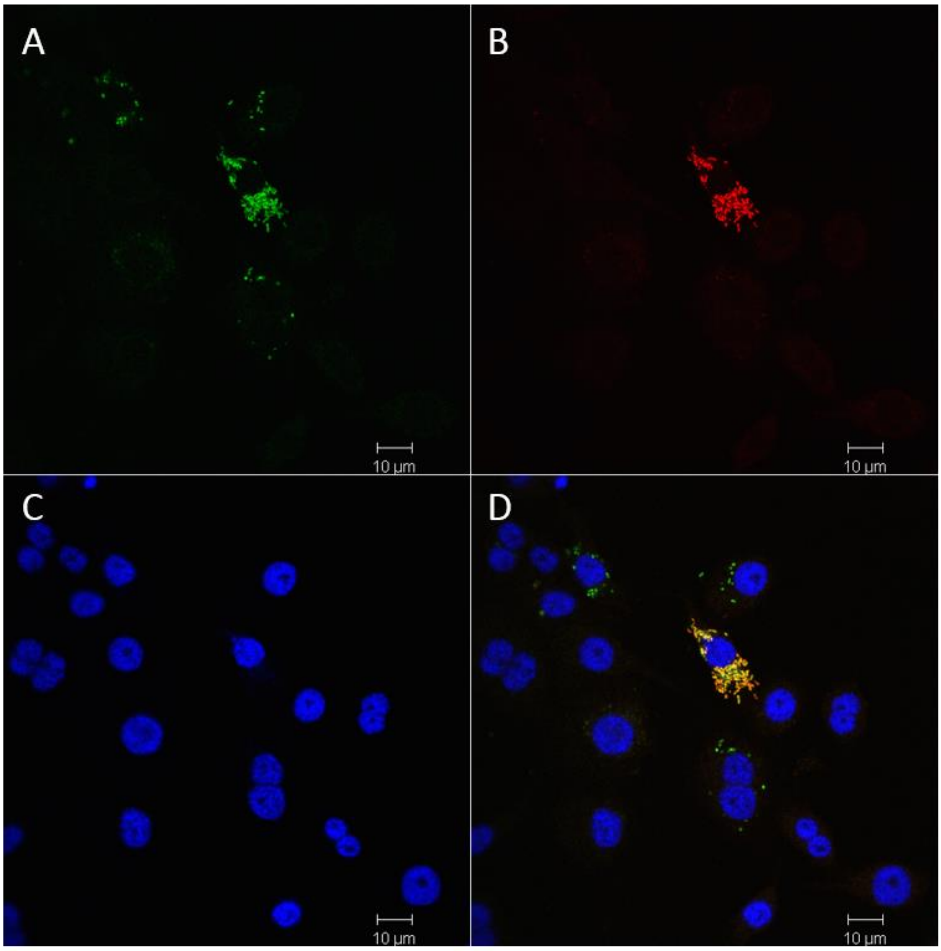


**Fig.4.2.8.** Testing FISH probes to identify superinfection in cells.

Aa23 cells infected with either *w*Au or *w*AlbB *Wolbachia* strains were cultured separately then combined at a 50:50 ratio to test the ability of FISH probes to differentiate between strains. A general wsp FISH probe was used to identify *w*Au **(A)**(green) and a supergroup-specific 16s probe was designed to identify *w*AlbB **(B)**(red). The nucleus of cells was stained with VectaShield containing DAPI **(C)**(blue). Combination of panels **(D)** shows one cell with yellowing colour, indicating *w*AlbB fluorescing with the specific 16s probe and the general wsp probe. The other cells are wAu-only as they do not fluoresce red.

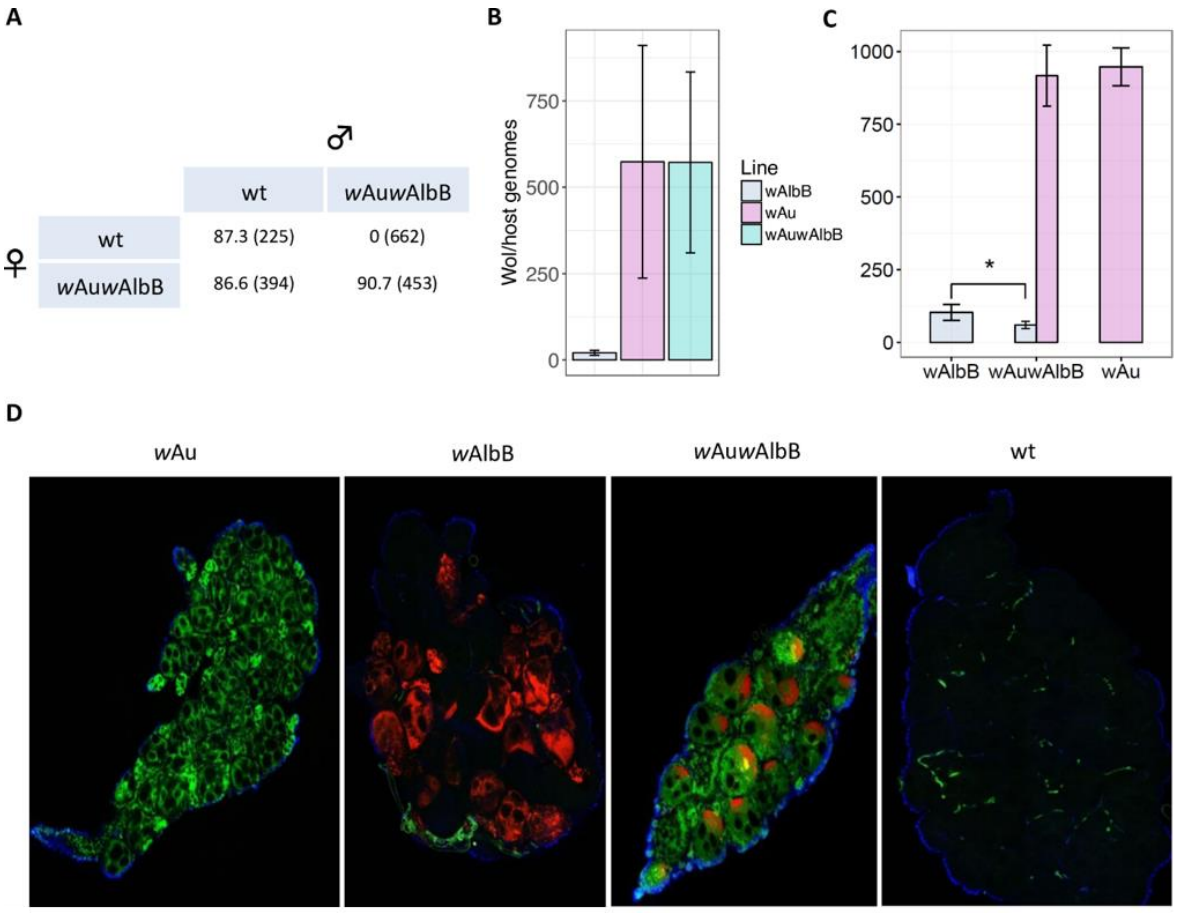


**Fig.4.2.9.** Generation of *w*Au*w*AlbB superinfection in *Ae. aegypti*.

**(A)** Mating crosses between *w*Au*w*AlbB superinfection and *Wolbachia*-uninfected mosquitoes. Numbers represent percentage of eggs that hatched, with number of eggs counted in brackets. **(B)** Quantification of general *Wolbachia* density in whole bodies of 10-day old females by qPCR of wsp gene relative to hth. Each bar consists of 10 biological replicates, each containing pools of 5 females. **(C)** Quantification of specific *Wolbachia* in the ovaries of each strain. Each bar represents 5 biological replicates, each with 10 pairs of pooled ovaries. Error bars on graphs represent standard deviation. Statistical analysis performed was one-way ANOVA. **(D)** FISH of *Wolbachia* in ovaries of *w*Au, *w*AlbB, *w*Au*w*AlbB and WT lines. Probes show specific *Wolbachia* location of *w*Au (green) and *w*AlbB (red). Blue stain is nuclear dye DAPI.

## 4.3. Discussion

*Wolbachia* strains *w*AlbA and *w*Au were transferred into *Ae. aegypti* with the intention of discovering a combination that provided complete arbovirus inhibition, without detrimental fitness effects as found with *w*MelPop. Our results show that the high-density strains *w*AlbA and *w*Au do have a detrimental affect on the fitness of *Ae. aegypti* compared to uninfected WT mosquitoes. Surprisingly, although being high density in *Ae. aegypti*, *w*AlbA offered no pathogen inhibition, indicating the mechanism of *Wolbachia*-induced virus inhibition is more important than density. Data from this study shows that although the high-density strain *w*Au provides complete virus inhibition, the detrimental effects on host fitness and lack of CI means it is not the best option for vector control compared to medium-strength strains *w*AlbB and *w*Mel.

### 4.3.1. *w*Au provides complete viral inhibition in *Ae. aegypti* but detrimentally affects fitness

When transinfected into *Ae. aegypti*, *w*Au provides very strong pathogen-inhibition across the *Alphavirus* and *Flavivirus* genii, by both oral challenge and thoracic injection. This inhibition was particularly apparent in salivary glands and saliva analysed following DENV and ZIKV infection, as no viral infection was detected in any *w*Au-infected mosquitoes. This is consistent with research in native host *D. simulans*, whereby *w*Au also provided the strongest reduction in viral titre following injection with highly pathogenic Flock House Virus (Martinez et al., 2014). However, *w*Au is at a much higher density in *Ae. aegypti* than in *D.simulans*, in which the density is similar to *w*Mel infection. *w*Au and *D.simulans* have likely developed a mutualistic relationship over years of evolution, which keeps the density at an advantageous level to the host; providing pathogen inhibition and increased fitness. Whilst *w*Au in *Ae. aegypti* provides complete pathogen inhibition, there is a detrimental effect on survival and egg dessication due to the high density.

Release of *w*Au-infected mosquitoes for population replacement would require a fitness advantage to succeed, as it does not induce CI. Despite this lack of reproductive manipulation, *w*Au was able to increase its spread in *D.simulans* in Australia from 1999-2008, suggesting it conferred a fitness advantage (Hoffman et al., 1996; Kriesner et al., 2013). However, another native strain *w*Ri which does

cause CI has rapidly replaced *w*Au in this region (Kriesner et al., 2013). If *w*Au-infected mosquitoes were released, the same scenario could occur, rendering the releases useless.

Despite the detrimental fitness effects *w*Au has on *Ae. aegypti* fitness, they are not as extreme as experienced with *w*MelPop infection. *w*MelPop impacts survival of *Ae. aegypti* mosquitoes more than *w*Au, with most dead at 40 days post-eclosion, compared to 60 days for *w*Au (McMeniman et al., 2009). In addition, there is a significant drop in *w*MelPop egg hatch following egg quiescence after only 3 days of drying. On the other hand, *w*Au eggs start to drop in egg hatch after 20 days. Despite this, *w*MelPop-infected *Ae. aegypti* have been shown to be successful at suppressing local populations of mosquitoes. In semi-field conditions, *w*MelPop invades *Ae. aegypti* to a high frequency and following subsequent drying of eggs, the local population is suppressed due to egg mortality (Ritchie et al., 2015). In light of this, *w*Au-infected *Ae. aegypti* could be used in a similar manner to suppress local populations. On the other hand, wAu-infected Ae. aegypti could be released in areas without a dry season such as the tropical rain belt, therefore the egg mortality would not be an issue. Given there are so many strains of *Wolbachia* with different phenotypes, there is scope for selecting certain strains for different areas based on their characteristics.

### 4.3.2. *w*Mel and *w*AlbB retain a strong pathogen-inhibition phenotype

When investigating pathogen-inhibition of high density strains, checking virus presence in the whole body or abdomen can be sufficient, due to the almost complete inhibition of virus replication. However, with moderate-density strains, investigation into specific tissues for transmission can give a better indication of inhibition potential, as virus may be able to replicate to a certain degree in the midgut, but does not get transmitted to salivary glands for transmission. Although analysing whole-bodies of mosquito gave an overall picture of strain inhibition following SFV injection, once oral challenges of DENV and ZIKV were established salivary glands and saliva were analysed in order to gain an accurate analysis of transmission potential. The importance of this is highlighted with the ZIKV challenge, whereby 6/22 *w*AlbB mosquitoes had detectable ZIKV in the abdomen, yet none were positive with salivation. In addition, virus in the saliva was

quantified using fluorescent focus assay (FFA), which quantifies infectious virions, rather than using RNA, which can also detect non-infectious viral RNA.

Although mosquitoes were not salivated following DENV oral-challenge, dissection and quantification of virus in salivary glands can be a good indicator of transmission, as the SG and saliva from the ZIKV feed had similar results. DENV inhibition in *w*AlbB and *w*Mel was not as efficient as with ZIKV, with only *w*Au having significantly less infection than WT. However, if FFA had been performed on dissected salivary glands it may have more accurately represented infectious virus. This may have resulted in a different outcome as several of the *w*AlbB and *w*Mel positive for DENV had titres several logs lower than those found in WT; these titres may be below a threshold for effective transmission. Overall, *w*AlbB and *w*Mel show good, but not complete, pathogen-inhibition of Alphaviruses and Flaviviruses. *w*Mel and *w*AlbB are described as only 'good' virus inhibiters as some virus is still able to replicate in the abdomen, despite the fact that a lot of virus is prevented from being transmitted via the salivary glands. This means if some *Wolbachia* was to be lost in the salivary glands, there may still be potential for virus transmission.

### 4.3.3. *Wolbachia* superinfections allow the combination of desirable characteristics for vector control

The creation of the *w*Au*w*AlbB strain gave insights into the possibility of combining the *w*Au strain for virus inhibition and *w*AlbB for inducing CI. Although the line was not challenged with virus, the high density of the strain indicates it would be a good blocker, considering these strains alone provide good viral blockage. A *w*Mel*w*AlbB superinfected line has been challenged with DENV, resulting in significantly less virus in the salivary glands relative to single *w*Mel infection (Joubert et al., 2016). It could therefore be hypothesised that the *w*Au*w*AlbB superinfection could block virus better than *w*AlbB alone. As this superinfection causes unidirectional CI, if released it may be able to invade a population quickly and negate any detrimental fitness effects imposed by *w*Au infection, as seen in the single infected line. However, the fitness of the superinfection would have to be characterised to have an accurate assessment of release potential, as parameters such as egg viability are particularly important. Females of the *w*Mel*w*AlbB superinfection did have slightly reduced lifespan compared to the

single infected lines, but a decline was not seen until 40 days post eclosion (Joubert et al., 2016). The high density of *w*Au and low density of *w*AlbB in the ovaries of the superinfection compared to *w*Au would also need to be monitored over time, as there may be potential for *w*AlbB infection to be lost. Perhaps a *w*Au*w*Mel superinfection would ensure a more even distribution in the ovaries, as in the single infected line *w*Mel is higher density than *w*AlbB.

The transfer of the *w*AlbA*w*AlbB superinfection into *Ae. aegypti* resulted in *w*AlbA reaching a higher density in its new host compared to levels reached in its native *Ae. albopictus* host. This indicates the strain and host have a long history of co-evolution, resulting in a suppression of *w*AlbA density. This would be beneficial to the host, as the *w*AlbA-infected *Ae. aegypti* were so high density that it detrimentally affected fitness. On the other hand, *Wolbachia* in *Ae. albopictus* was mostly restricted to somatic tissues, which is necessary for maternal transmission. This means we cannot assume a *Wolbachia* strain that is low density in its native host will remain low in a novel host, but also highlights that *Wolbachia* density should be measured over a long period of time to assess if the host adapts and suppresses growth of the bacteria.

### 4.3.4. High density *w*AlbA exhibited no pathogen inhibition indicating mechanism is crucial

Perhaps the most surprising discovery is that the high-density *w*AlbA strain provided no protection against SFV infection. Although injection of virus is not truly biologically representative of natural infection due to bypassing the midgut barrier, we first injected all strains with virus to be sure virus could establish, as previous oral infections had not been successful. These injections still provide a useful assessment of each strains potential to block viruses, as even the moderate density *w*AlbB and *w*Mel strains had significantly less SFV in their whole bodies compared to WT. It was theorised that *w*AlbA would have inhibition similar to *w*Au, however SFV levels were similar to those found in WT mosquitoes. It could therefore be predicted that *w*AlbA would also not provide the expected pathogen inhibition of flaviviruses that is usually observed with high-density strains. However, there is preliminary data showing wAlbA does have the capacity to reduce ZIKV presence in *Ae. aegypti* saliva following oral challenge, relative to uninfected mosquitoes (not shown, unpublished). This in turn highlights the

importance of oral viral challenges as they are biologically accurate and represents how *Wolbachia* truly interacts with viruses, but also that even though a strain is high density, the mechanism of inhibition is not always the same strength.

In this study, *Wolbachia* density was quantified using qPCR primers for *Wolbachia* surface protein, under the assumptions they bind to each strain at the same efficiency. However, this may not be the case; in order to investigate density further, strain-specific qPCR primers and TaqMan probes could be designed for qPCR, making the quantificiation very specific and reliable. Using general wsp primers in this study gave an observation of general relative densities, but could be improved for future work.

The high fitness costs of *w*AlbA in *Ae. aegypti* is consistent with a high-density *Wolbachia* strain, with reduced survival and percentage egg hatch following drying. Creation of the single *w*AlbA line occurred by chance, with indirect maternal transmission of *w*AlbA and *w*AlbB occurring from an *Ae. albopictus* egg. Previous transinfections of *w*AlbA and *w*AlbB superinfected embryos into uninfected *Ae. albopictus* and *Ae. aegypti* have resulted in only wAlbB establishing in the new host (Xi et al., 2005a; Xi et al., 2005b). Perhaps those embryos that had wAlbA transferred had high larval death and did not reach eclosion stage, therefore the line was never created. Given the high fitness costs associated with *w*AlbA, it is not surprising that it is often lost during cytoplasmic transfer.

The lack of pathogen-inhibition with *w*AlbA infection indicates the mechanism of inhibition, rather than general *Wolbachia* density, is important. Analysis of antimicrobial peptide genes showed *w*AlbA had significantly higher expression of CECD and DEFC relative to all lines, as no other *Wolbachia*-infected lines differed in expression compared to WT. It was therefore hypothesised that this up-regulation of AMPs was not a critical component of the mechanism of virus inhibition, as knockdowns of DEFC in *w*AlbB-infected *Ae. aegypti* have resulted in increased DENV (Pan et al., 2012). This same study showed that *w*AlbB induced ROS $H_20_2$, which resulted in the AMP upregulation. $H_20_2$ levels in our novel lines was indeed significantly higher than WT mosquitoes at G7, but this did stabilise to non-significant levels by G10. This indicates that the introduction of *Wolbachia*

did initially perturb redox homeostasis, but this levelled out with stabilisation of the line. This adds to other studies which show no induction of ROS with *Wolbachia* infection, yet provide pathogen inhibition (Molloy and Sinkins, 2015).

Transinfection of *Wolbachia* into a novel host such as *Ae. aegypti* is likely to be a turbulent process that impacts immune upregulation and production of ROS as a defence mechanism. *D. melanogaster* naturally infected with *w*Mel and *w*MelPop show no upregulation of AMPs Defensin and Cecropin, however novel transinfections in mosquitoes do (Kambris et al., 2010; Wong et al., 2011). To investigate if upregulated AMPs in novel transinfections provide additional protection from pathogenic bacteria, mosquitoes were challenged with gram-negative bacteria *S. marcescens*. *w*Mel-infected mosquitoes were chosen for these experiments as they had previously shown the highest induction of $H_20_2$ relative to WT. Females were challenged both orally via a blood or sugar meal and intrathoracically with a needle, as it has been shown that the route of challenge is crucial for *Wolbachia*-mediated bacterial protection (Gupta et al., 2017). As no difference was observed in reduction of *Serratia* between *w*Mel and WT mosquitoes following oral challenge, expression of AMPs was not measured. Although *w*Mel mosquitoes did begin the sucrose challenge with higher levels of *S. marcescens*, this may have been due to other uncontrollable factors such as the size of sucrose meal taken or time feeding on the cotton, as mosquitoes were allowed to feed ad libitum. *w*MelPop-infected *Ae. aegypti* do experience limited blood-feeding success and even have an observed 'bendy' proboscis, which may explain this (Turley et al., 2009). Multiple attempts were made to inject mosquitoes with live *S.marcescens*, in order to monitor growth of the bacteria as well as AMP expression. However, with a high optical density (OD) this proved fatal to the mosquito, whereas lower OD resulted in no establishment of the pathogen bacteria. In order to inject live bacteria without fatalities a less virulent strain could have been selected, however due to time constraints mosquitoes were injected with heat-killed *S.marcescens*.

Results showed that WT mosquitoes were capable of mounting an AMP response similar to *w*Mel mosquitoes 48 hours post injection, however AMP expression remained higher in *w*Mel mosquitoes 96 hours post injection. It could therefore be hypothesised that this elevated AMP expression in *Wolbachia*-infected mosquitoes

aids in defence against pathogens. As the experiments performed involved heat-killed *S.marcescens*, it was not possible to observe the effect AMP expression had on suppression of bacterial growth. However, results from oral challenges suggest no additional capacity of *w*Mel mosquitoes to clear *S.marcescens* than WT, which is in agreement with other studies showing *Wolbachia* provide little to no antibacterial protection (Wong et al., 2011). Even *Ae. aegypti* infected with the highly virulent *w*MelPop did not survive longer than WT mosquitoes when challenged with a broad spectrum of extra and intracellular bacteria (Ye et al., 2013). To add to this experiment it would have been interesting to challenge *w*AlbA-infected mosquitoes with *S.marcesens*, as these mosquitoes had significantly higher basal expression of AMPs relative to all other lines. However, due to fitness problems at the time of the experiment these mosquitoes were not included.

In addition, analysis of ROS-related genes did not provide clear results relating to *Wolbachia* infection. Gene transcripts of Dual oxidase 2 (DUOX) and NOX enzyme (NOXM) were quantified, which are involved in NADPH-related production of ROS (Kawahara et al., 2007). DUOX has previously been shown to be highly upregulated in the carcass of *w*AlbB-infected *Ae. aegypti* relative to uninfected (Pan et al., 2012). Analysis of *Wolbachia*-infected lines showed no upregulated expression of DUOX or NOXM relative to WT. In fact, there was significantly less expression of DUOX in *w*Mel compared to WT. Gene expression of antioxidant Thioredoxin Peroxidase 4 (TPX) was also quantified, as previous proteomics analysis of wMel midguts showed 5x more TPX protein relative to WT (Geoghegan et al., 2017). Pan et al (2012) hypothesised that *Wolbachia* infection resulted in an upregulation of ROS-related genes, which consequently resulted in higher expression of antioxidant genes, to prevent toxicity. *w*AlbB and *w*Au had significantly higher expression of DUOX than *w*Mel, and also the same trend with TPX, indicating there may be an attempt to restore redox homeostasis. However, *Wolbachia*-uninfected mosquitoes also had higher DUOX than *w*Mel, therefore it is likely not a side effect of *Wolbachia* infection. Overall, there were no discernable differences between the *Wolbachia*-infected lines and WT mosquitoes regarding ROS-related genes. Analysis of a wider selection of ROS/antioxidant related genes may have elucidated this further, however this has been performed in *Ae. albopictus* (Aa23) *Wolbachia*-infected cells with no difference in gene expression (Molloy and

Sinkins, 2015). Redox homeostasis within relatively novel transinfections is likely to be a turbulent process which may indirectly affect virus replication, however this is not observed in all *Wolbachia* infections in *Ae. aegypti*.

## 4.4. Conclusion

*Wolbachia* is a highly diverse genus of intracellular bacteria, of which only a small selection of strains have been investigated to limit arbovirus transmission by *Aedes* mosquitoes. Our work in this chapter shows *w*Mel and *w*AlbB remain good choices for field releases, as they provide a fine balance of pathogen inhibition and no detrimental fitness effects. However, the discovery that *w*AlbA infection, without *w*AlbB, is high density and yet does not provide pathogen inhibition shows we cannot reliably predict how different strains will perform when transinfected into a novel host. The superior pathogen inhibition observed for *w*Au means that, ideally in combination with another strain that increases mosquito fitness or using an additional way to increasing its relative fitness (such as use of biopesticides to which it provides protection), it could represent a very useful new strain for future field releases.

# Chapter 5

## Effect of cyclical high temperature rearing on *Wolbachia* in *Ae. aegypti*

## 5.1. Introduction

The success of *Wolbachia* as a method for limiting arbovirus transmission by *Aedes* mosquitoes relies on its ability to manipulate host reproduction, ensuring its spread through a population, while maintaining viral inhibition. While *Wolbachia* may maintain a relatively constant density under laboratory conditions, environmental conditions may differ markedly in the field once mosquitoes are released. *Wolbachia* has been shown to be affected by various stresses in a variety of insect species.

The microbial communities within insects is diverse and can be affected by the environmental conditions around it, including temperature. *D. melanogaster* which normally harbor *Acetobacter*, *Wolbachia* and *Leuconostoc* genera of bacteria, have a higher abundance of *Acterobacter* at a higher rearing temperature (31$^{o}$C), whereas *Wolbachia* is the dominant bacteria at a lower temperature (13$^{o}$C) (Moghadam et al., 2017). Although the *w*Mel strain in *D. melanogaster* may proliferate better at low temperatures, this may not to be the case for all strains of *Wolbachia*. The highest abundance of three co-existing strains of *Wolbachia* in the *Leptopilina heterotoma* wasp occurred at the highest rearing temperature (26$^{o}$C), rather than the lowest temperature (14$^{o}$C) (Mouton et al., 2007).

While *Wolbachia* may thrive at intermediate temperatures, it may be adversely affected at extremely high temperatures. Treatment of the Asian citrus psyllid (louse) at 40$^{o}$C for 24 hours resulted in a reduction in *Wolbachia* Surface Protein (wsp) density as analysed by qPCR (Hussain et al., 2017). However, a general wsp PCR assay was used for *Wolbachia* detection, therefore it does not tell us which strain in the *Wolbachia* genus is being affected by the temperature.

Rather than rearing the mosquitoes at a constant temperature, which would be rare in the field, studies have reared them at fluctuating temperatures and monitored the effects. *Ae. aegypti* with *w*Mel, *w*MelPop-CLA and *w*AlbB strains reared at 12 hour at 26$^{o}$C then 12 hours at 32$^{o}$C, 26-34.5$^{o}$C or 26-37$^{o}$C, showed some interesting effects on *Wolbachia* at the highest temperature cycle only. Within this temperature range, *w*Mel and *w*MelPop-CLA had reduced whole body

density, egg hatch, partial loss of cytoplasmic incompatibility and complete loss of maternal transmission. Interestingly, *w*AlbB was only affected by a slight loss of maternal transmission in the highest temperature regime (Ross et al., 2017). *w*MelPop-CLA is a variant of *w*MelPop that showed reduce pathogenesis when transinfected back into *D.melanogaster* following 35 months of cell passage in *Aedes* cell lines (McMeniman et al., 2008). *Ae. aegypti* with *w*Mel have also been subjected to even higher heat treatments, similar to heatwave temperatures that are experienced in Cairns, Australia, where current releases of *Wolbachia*-infected mosquitoes are taking place. Eggs and larvae were subjected to fluctuating temperatures between 30-40$^{o}$C for various timescales during development. *Wolbachia* density did decrease at these higher temperatures, however 4-7 days post-eclosion the densities recovered (Ulrich et al., 2016). This may indicate that the mosquitoes experienced more of a heat-shock at such high temperatures, which they were able to recover from, rather than a gradual exposure to higher temperatures.

In order to gain a realistic view of how *Wolbachia* responds to fluctuating temperatures in the field, *Wolbachia*-infected larvae were reared at temperatures that represent the highest *Ae. aegypti* larval breeding sites in several locations in Trinidad. Hemme et al (2009) recorded the water temperature ~20cm below the surface in breeding containers in March, May and October of 2005. This study was chosen for water temperatures as Trinidad lies in the tropical rainforest belt, which is a main area of mosquito burden. The mosquitoes were exposed to the maximum and minimum May temperatures observed, in order to expose *Wolbachia* to the higher end of conditions that will be encountered naturally. These temperatures were cross-referenced with those experienced in April (2017) in Kuala Lumpur, Malaysia, *w*here *w*AlbB-infected *Ae. aegypti* are currently being released (Fig.5.1.1.). Kuala Lumpur is a hotspot for DENV transmission therefore represents an area where *Aedes* mosquitoes are active. Temperature data from April was chosen as there were the maximum range of fluctuations observed. Mosquitoes were subjected to this temperature cycle over two generations, in order to monitor the ongoing effect. *Wolbachia* density was quantified in whole bodies and tissues such as midguts, salivary glands and ovaries, the latter of which is important for maternal transmission of the symbiont. Further to this, heat-

treated mosquitoes were challenged with SFV, a well-studied model alphavirus, and virus inhibition was measured.

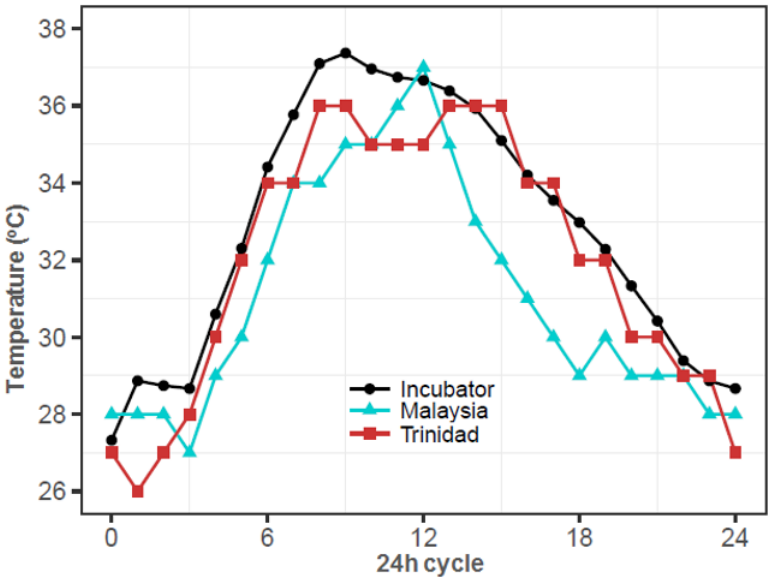


**Fig.5.1.1.** Plot of temperatures measured in Malaysia, Trinidad breeding sites and experimental incubator.

Data represents 24 hour cycles of temperature observed in a typical April day in Malaysia (teal line), water larval breeding sites in Trinidad (red line) and the temperatures larvae were reared in for the experiments (black line). Malaysia range is calculated from mean temperatures over a day in April (2017) in Kuala Lumpur as recorded on accuweather.com. Range of temperatures from Trinidad was determined from water temperature data found ~20cm from the surface in various *Ae. aegypti* breeding sites at several sites in May 2005 (Hemme et al., 2009). The temperatures chosen for the experiment represented the extreme highs and lows of the Malaysia and Trinidad datasets. Larvae were reared at these cycling temperatures until pupation.

## 5.2. Results

### 5.2.1. *Wolbachia* density significantly decreases in *w*Au and *w*Mel females over two generations of heat-treatment

The density of *Wolbachia* within the whole body of female and male mosquitoes was quantified by qPCR in order to assess whether any of the three strains were affected by heat-treatment. Quantification of *Wolbachia* wsp gene in whole bodies revealed *w*Au and *w*Mel decrease significantly in females after one and two generations of heat-treatment (Fig.5.2.1.A&B). Additional replicates also supported this result (Fig.5.2.1.D&E). *w*AlbB density remained unaffected in females and males across all generations with heat-treatment (Fig.5.2.1.A,B&C). Density of *w*Au in males was largely unaffected following one generation of heat-treatment (Fig.5.2.1.A&D), however after two generations of heat-treatment experienced a significant reduction (Fig.5.2.1.B). *w*Mel males experienced a significant reduction in density in two replicates after one generation of heat-treatment (Fig.5.2.1.A&E), however not in the third replicate (Fig.5.2.1.E). The control *w*Mel density in the third replicate was lower than those found in the other two replicates, therefore this replicate was not taken forward for further experiments. *Wolbachia* density in control *w*Au and *w*Mel females and males does appear to be similar in Fig.5.2.1.A, however the data represents relative quantification of *Wolbachia* compared to a reference gene, rather than absolute quantification. This means the comparison that is important is the relative drop in density within a strain when exposed to heat-treatment, rather than between strains. For more accurate absolute quantification, a plasmid with known *Wolbachia* copies could be used as a standard curve. Overall, *w*Mel and *w*Au showed susceptibility to heat-treatment, whereas *w*AlbB retained a consistent density throughout.

### 5.2.2. *w*Mel and *w*Au density is affected by heat-treatment in tissues important for viral replication

Following on from the observation that *w*Au and *w*Mel densities decrease in the whole body of females after heat-treatment, midguts and salivary glands were dissected to check tissue-specific density. The midgut and salivary glands are important tissues for viral replication and transmission of viruses, therefore it was hypothesised a decrease in *Wolbachia* density may impact pathogen inhibition.

*Wolbachia* density in *w*Mel midguts decreases significantly after one ($p$=0.04, t-test) and two ($p$=0.002, mann whitney) generations of heat-treatment (Fig.5.2.2.A). An additional replicate of G2 *w*Mel midguts also shows a significant reduction in density ($p$=0.02, t-test)(Fig.5.2.2.C). A significant decrease was also

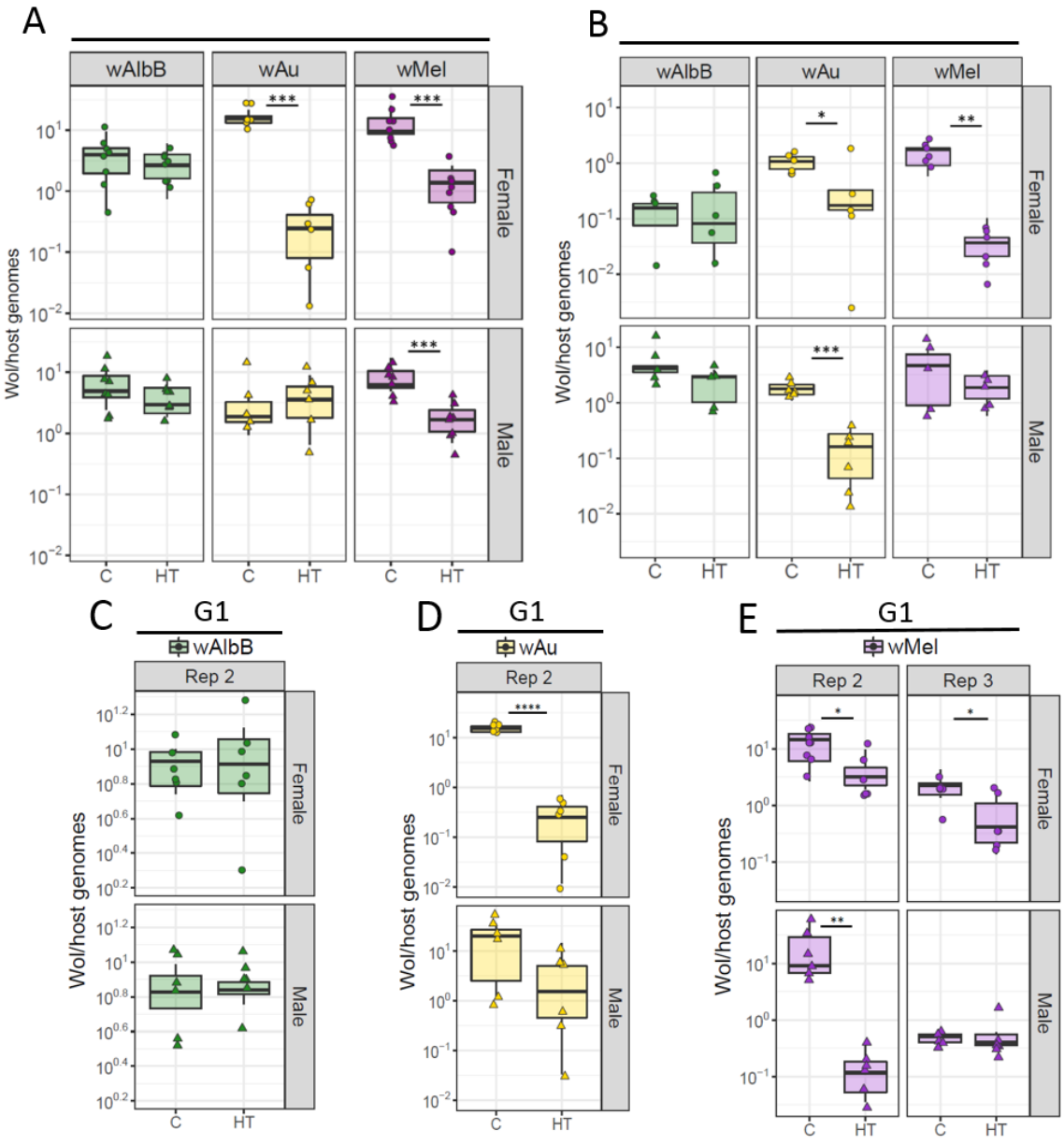


**Figure 5.2.1.** *Wolbachia* density in whole body after one and two generations of heat-treatment

Females and males were sampled 5 days post-eclosion and DNA was extracted for qPCR of *Wolbachia* wsp gene normalised to reference gene hth. Results represent one biological experiment after one generation **(G1)** of heat treatment **(A)** and two generations **(G2) (B)**. Additional experiments following one generation of heat-treatment are shown for *w*AlbB **(C)** *w*Au **(D)** and *w*Mel **(E)**. Boxplots represent 6 biological replicates, with each point representing one mosquito. Black line in the middle of boxplots represents the median and whiskersrepresent the upper and lower quartiles. Statistic analysis performed was t-test and mann-whitney test.

observed in *w*Au midguts over both generations ($p$=0.004, mann whitney; $p$=0.01, t-test), whereas *w*AlbB maintains a relatively constant density with heat-treatment across two generations (Fig.5.2.2.A). *w*Au density decreases significantly in the salivary glands after one ($p$=0.001, t-test) and two generations of heat treatment (Fig.5.2.2.B). *w*Mel remained at a stable density in salivary glands despite the heat-treatment, much like *w*AlbB. However, the density of *Wolbachia* in salivary glands is very low in *w*Mel compared to *w*Au, and with the significant drop in midgut density this may result in some virus being able to replicate and be transmitted by a mosquito, following exposure to similar temperatures in the field.

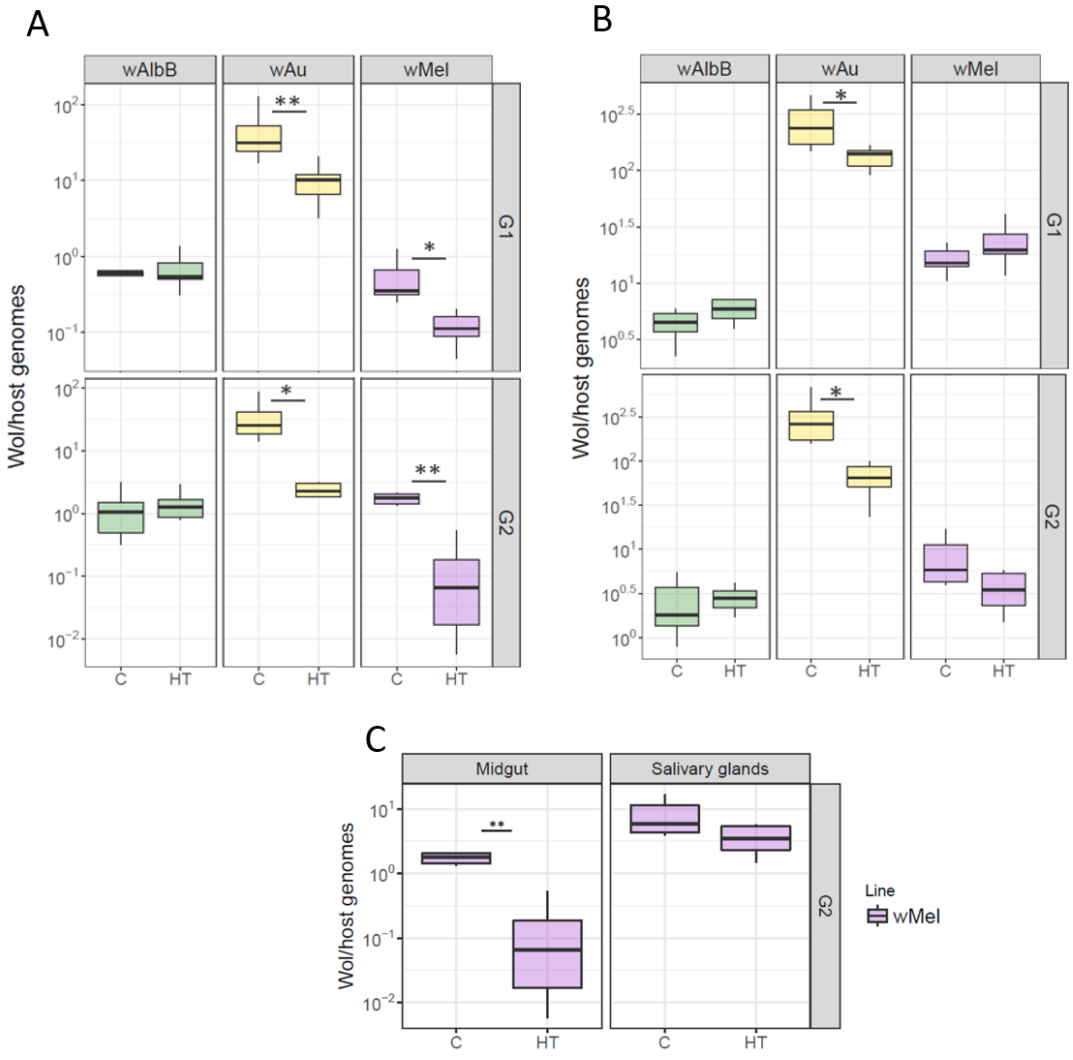


**Figure 5.2.2.** *Wolbachia* density in midguts and salivary glands after one and two generations of heat-treatment

Midguts **(A)** and salivary glands **(B)** were dissected and pooled 5 days post-eclosion and DNA was extracted for qPCR of *Wolbachia*. **(C)** represents additional G2 *w*Mel experiment. Results represent one experiment with 5-6 biological replicates of 3 pooled tissues. wsp gene was normalised to hth reference gene. Mann-whitney and t-tests were performed to test for significance, represented by an asterisk.

### 5.2.3. *Wolbachia* retains virus inhibition following two generations of heat-treatment

As a reduction in *Wolbachia* density was observed in tissues important for viral replication and transmission, it was hypothesised that this may reduce the strength of pathogen inhibition. Control and heat-treated mosquitoes were challenged with a blood meal containing the model arbovirus SFV. After 14 days, individual females were sampled for RNA, and RT-qPCR was performed to identify SFV-infected mosquitoes. Above 80% of WT mosquitoes in both treatments were infected with SFV, indicating the vector was susceptible to viral infection (Fig.5.2.3.A). *w*AlbB and *w*Mel strongly blocked SFV infection under control conditions, with only 15% and 14% of mosquitoes infected, respectively. However, the wAu line showed complete blockage of SFV infection. With the heat-treatment, there was a 9-11% increase in SFV-infected mosquitoes in the *w*AlbB and *w*Mel lines, while *w*Au increased only by 5% (Fig.5.2.3.A). However, infection of heat-treated WT mosquitoes also resulted in 9% increase in infection, indicating this is not due to *Wolbachia*.

The quantity of SFV was then measured in whole bodies of females to investigate if heat-treatment resulted in higher viral titres in the *Wolbachia*-infected mosquitoes. WT mosquitoes had a wide range of SFV levels, from 0.0001 to 10 virus genomes per host cell (Fig.5.2.3.B). Although the heat-treated WT had more SFV-positive mosquitoes compared to control, there was not a significantly higher viral titre ($p=0.054$). SFV levels in *w*AlbB control and heat-treated mosquitoes were all lower than 0.1 per host cell, as was the one virus-positive heat-treated *w*Au female. The majority of SFV-infected *w*Mel mosquitoes were also lower than 0.1 virus per host cell, with the exception of one control mosquito and 4 heat-treated mosquitoes (Fig.5.2.3.B). The majority of *Wolbachia*-infected mosquitoes, regardless of heat-treatment status, remained uninfected.

In order to gain more insight into the transmission potential of mosquitoes that were positive for virus by RT-qPCR, heat-treated mosquitoes were challenged with SFV again and the bodies were dissected into two parts, head and abdomen. Quantification of virus in the head gives an indication of virus dissemination throughout organs not essential for replication. Following 14 days incubation post-

feed, RT-qPCR was performed on heads and abdomens. A high percentage of WT mosquitoes were infected in the head and abdomen, indicating the virus was again permissive to replication in these mosquitoes (Fig.5.2.4.). With regards to abdomen infection, control and heat-treated WT mosquitoes had similar quantities of SFV relative to rps17. In *Wolbachia*-infected lines, for the most part SFV remained several logs lower than those found in WT, below 0.0001 SFV/rps17 (Fig.5.2.4.). However, one notable exception to this is one female *w*AlbB HT,

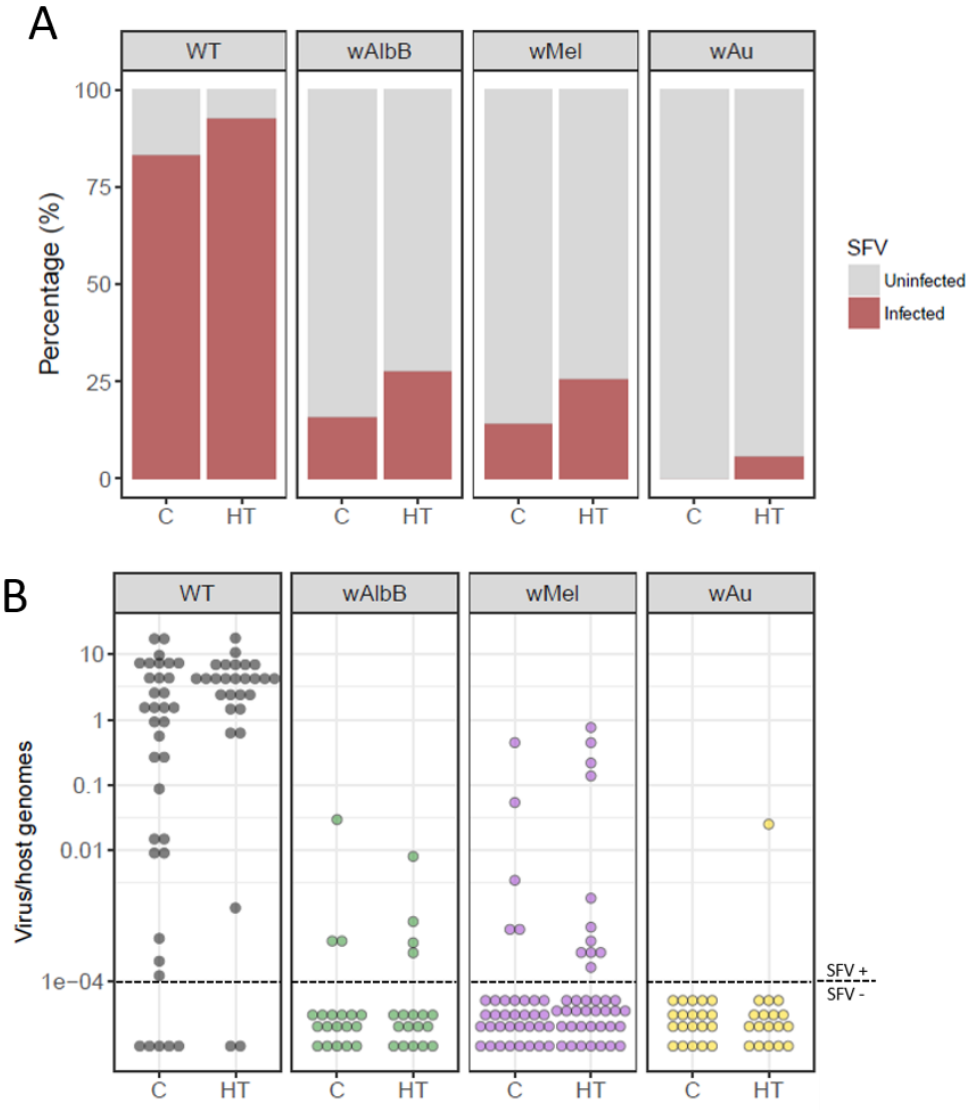


**Figure 5.2.3.** Detection of SFV in *Ae.aegypti* orally challenged with virus, following two generations of heat-treatment.

5 day old females were challenged with SFV in a blood meal and placed in an incubator for 14 days. RNA was extracted from females and RT-qPCR was performed to quantify SFV copies to rps17. Data represents percentage of each line/treatment with SFV detected and uninfected **(A)**. Quantification of SFV genome relative to rps17 with each dot representing one female **(B)**. Dotted line represents cut-off with uninfected females below. Significance was tested using Fishers exact test.

which had 0.01 SFV/rps17. This female that had 0.01 SFV/rps17 in the abdomen also had the same titre in the head, indicating high viral dissemination. Aside from this data point, SFV in *Wolbachia*-infected lines remained below 0.0001 virus/host genomes. *w*AlbB, *w*Mel and *w*Au-infected mosquitoes exhibited similar strength inhibition of SFV under control conditions; it may be expected that wAu would provide stronger inhibition, however previous work has shown similar results between strains with SFV Fluc (Chapter 3). In addition, RT-qPCR picks up viral RNA rather than infectious virions only; there may have been a more noticeable difference if fluorescent focus assay for infectious virions was performed. There was no statistical difference in the quantity of SFV in heat-treated mosquitoes in heads or abdomens in the *Wolbachia*-infected lines. However, heat-treated WT mosquitoes did have significantly higher titres of SFV relative to control mosquitoes (p=0.04).

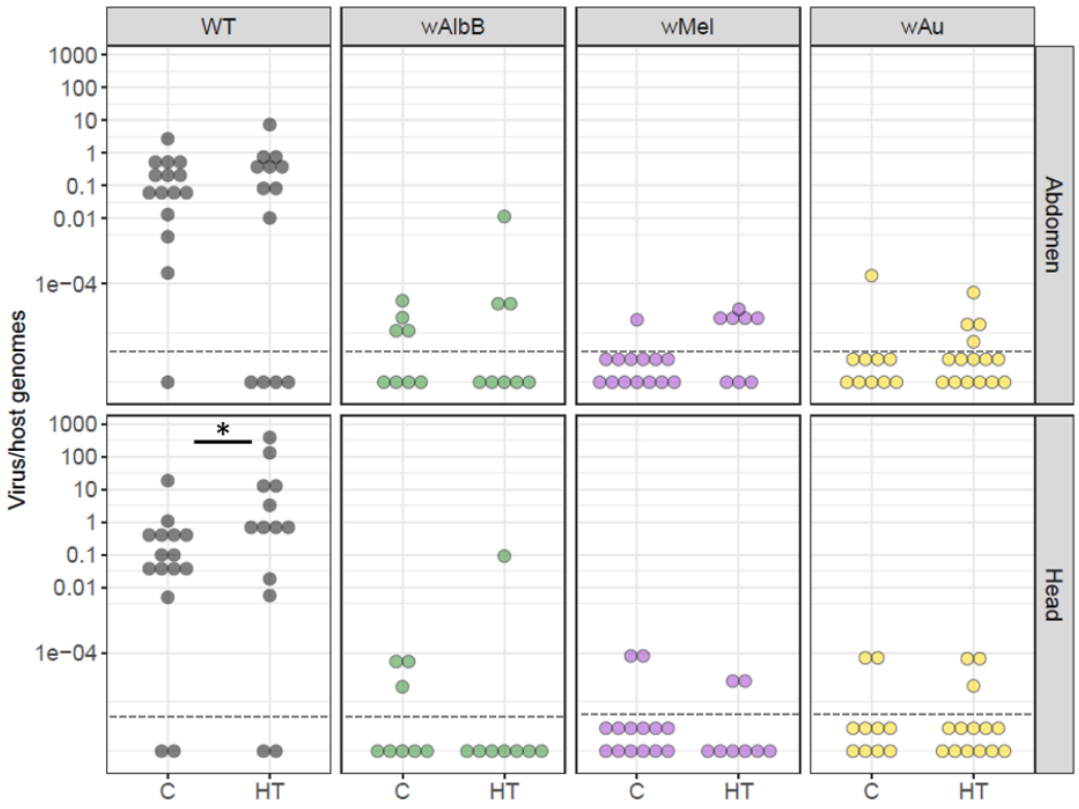


**Figure 5.2.4.** Detection of SFV in the head and abdomen of *Ae. aegypti* orally challenged with SFV, following one generation of heat-treatment

5 day old females were challenged with SFV in a blood meal and placed in an incubator for 14 days. Females were cut in two parts (head, thorax/abdomen) and RNA was extracted for RT-qPCR of SFV normalised to rps17. Data represents quantification of SFV levels with each dot representing tissues from one female. Dotted line represents cut-off with uninfected females below. Statistical analysis was performed using a one-tailed Fisher's exact test comparing number of virus positive and negative samples. Significance represented by asterisk (p=<0.05).

### 5.2.4. *Wolbachia wMel* and *wAu* significantly decrease in density in ovaries following heat-treatment

*Wolbachia* is maternally transmitted via the ovaries; therefore density was quantified in these organs following heat-treatment. Pairs of ovaries were dissected and pooled to quantify *Wolbachia* density by qPCR, and also visualised with FISH using a general *Wolbachia* probe. After one generation of heat-treatment, *w*Au and *w*Mel significantly decrease in ovaries as visualised by FISH (Fig.5.2.5.A) and further quantified by qPCR (Fig.5.2.5.B). As with the midgut and salivary glands, *w*AlbB in the ovaries does not appear to be affected by the heat-treatment regime, maintaining a stable density (Fig.5.2.5.A&B). After two generations of heat-treatment, *w*Au and *w*Mel again significantly decrease in the ovaries, however *w*AlbB significantly increases in density (Fig.5.2.6.A&B). The control *Wolbachia* density of *w*Au and *w*AlbB does appear higher in G2 compared to G1, however this is relative quantification of wsp to reference gene hth, therefore should not be analysed as a total *Wolbachia* number. Rather, the comparison of control and heat-treated ovaries within experiments is important.

### 5.2.5. Heat-treatment results in significant maternal leakage of *w*Mel, whereas *w*AlbB retains complete transmission

As *Wolbachia* density was shown to significantly decrease in *w*Mel and *w*Au ovaries following heat-treatment, it was then investigated if maternal transmission of the bacteria was impacted. Females were individualised to lay eggs following a blood meal and families of larvae were reared separately. After three days, 4-5 larvae were selected from each family and PCR was performed for *Wolbachia* presence. The percentage of *Wolbachia*-positive larvae from each family was calculated and all families per treatment were combined and averaged. *w*AlbB retained 100% maternal transmission following one generation of heat-treatment over two biological replicates (Fig.5.2.7.A&B). *w*Au maternal transmission decreased significantly to 80% in the first replicate ($p=0.0031$), and again to 90% in the second replicate ($p=0.4$). However, wMel experienced a significant decrease in maternal transmission in both replicates ($p=<0.0001$), with only 30% and 13% of larvae infected with *Wolbachia*, respectively (Fig.5.2.7.A&B).

*Wolbachia* density was then additionally quantified in the larvae samples by qPCR to assess whether the density was very low in the *w*Mel samples and therefore undetectable by PCR or if *w*Mel was absent. The qPCR results confirmed that the maternal leakage observed was due to the complete loss of *w*Mel in 3 of the 6 heat-treated families sampled (Fig.5.2.7.A). Two families of the heat-treatment retained a similar density to those found in control families, and family C had one *w*Mel-positive larvae. When analysed as one group, the *Wolbachia* density in larvae from heat-treated females are significantly lower than those of controls

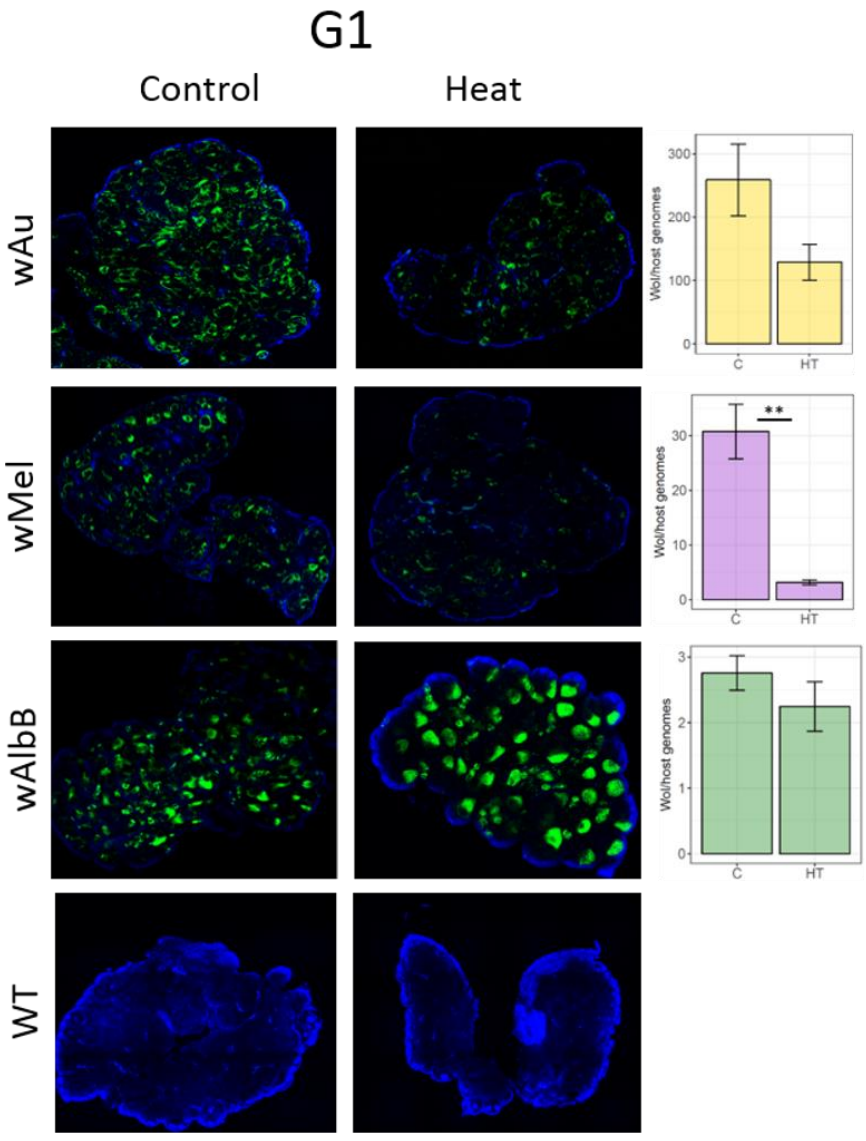


**Figure 5.2.5.** *Wolbachia* density in ovaries after one generation of heat-treatment

Pairs of ovaries were dissected 5 days post-eclosion and stained by fluorescent in-situ hybridisation (FISH). Green = *Wolbachia* with FISH probe, Blue = nucleus stained by DAPI. Corresponding qPCR of *Wolbachia* density in ovaries is shown next to FISH images. Mean *Wolbachia* density is shown in bar chart, with error bars representing standard error. Results represent one experiment, with 6 biological replicates of 3 pairs of pooled ovaries. Ovaries were STE extracted for DNA and relative qPCR for wsp was performed, normalised to reference gene hth. C = Control, HT = Heat-treatment. T-tests were performed for significance, represented by asterisks.

(*p*=<0.0001, mann-whitney). The density of heat-treated *w*Au larvae also significantly decreases compared to controls (*p*=0.005, mann-whitney), with the exception of one high density family (Fig.5.2.7.B). There was a trend of higher density in *w*AlbB in heat-treated larvae compared to the control in all families except one (Fig.5.2.7.E). When the larvae from each family are combined, there is a significant increase in *w*AlbB density in the heat-treated larvae (*p*=0.0002, mann-whitney).

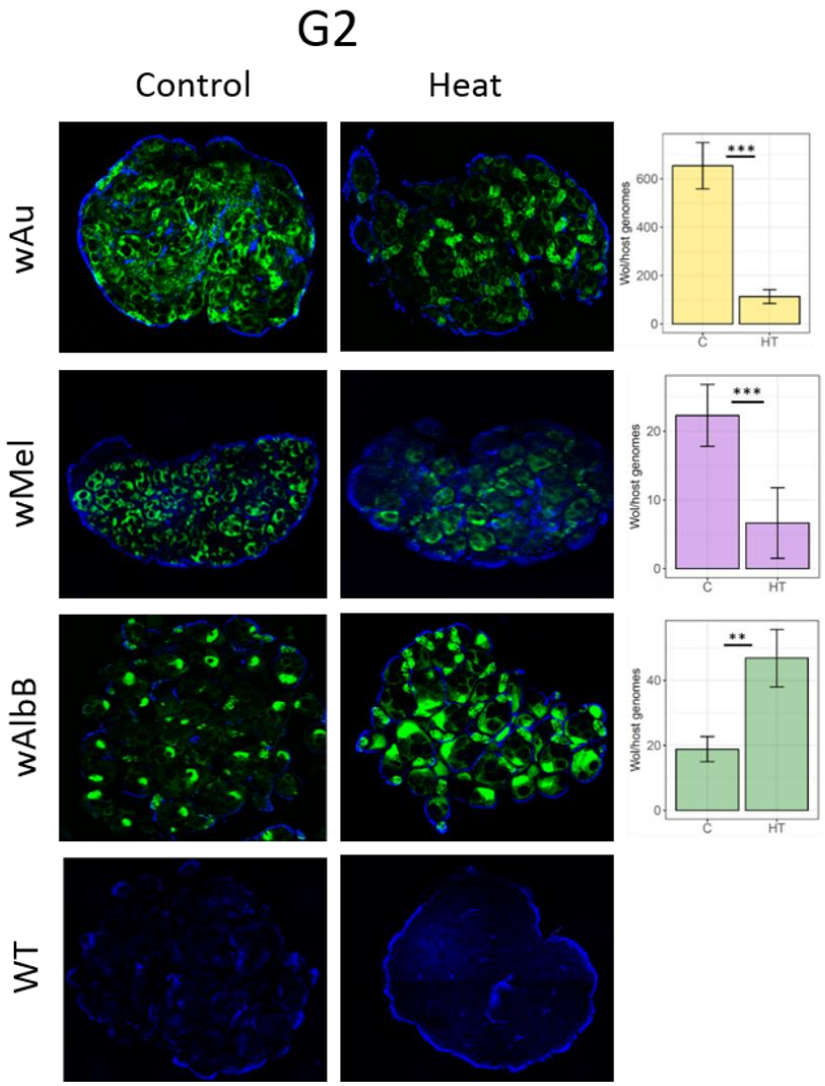


**Figure 5.2.6.** *Wolbachia* density in ovaries after two generations of heat-treatment

Pairs of ovaries were dissected 5 days post-eclosion and stained by fluorescent in-situ hybridisation (FISH). Green = *Wolbachia* with FISH probe, Blue = nucleus stained by DAPI. Corresponding qPCR of *Wolbachia* density in ovaries is shown next to FISH images. Mean *Wolbachia* density is shown in bar chart, with error bars representing standard error. Results represent one experiment, with 6 biological replicates of 3 pairs of pooled ovaries. Ovaries were STE extracted for DNA and relative qPCR for wsp was performed, normalised to reference gene hth. C = Control, HT = Heat-treatment. T-tests were performed for significance, represented by asterisks.

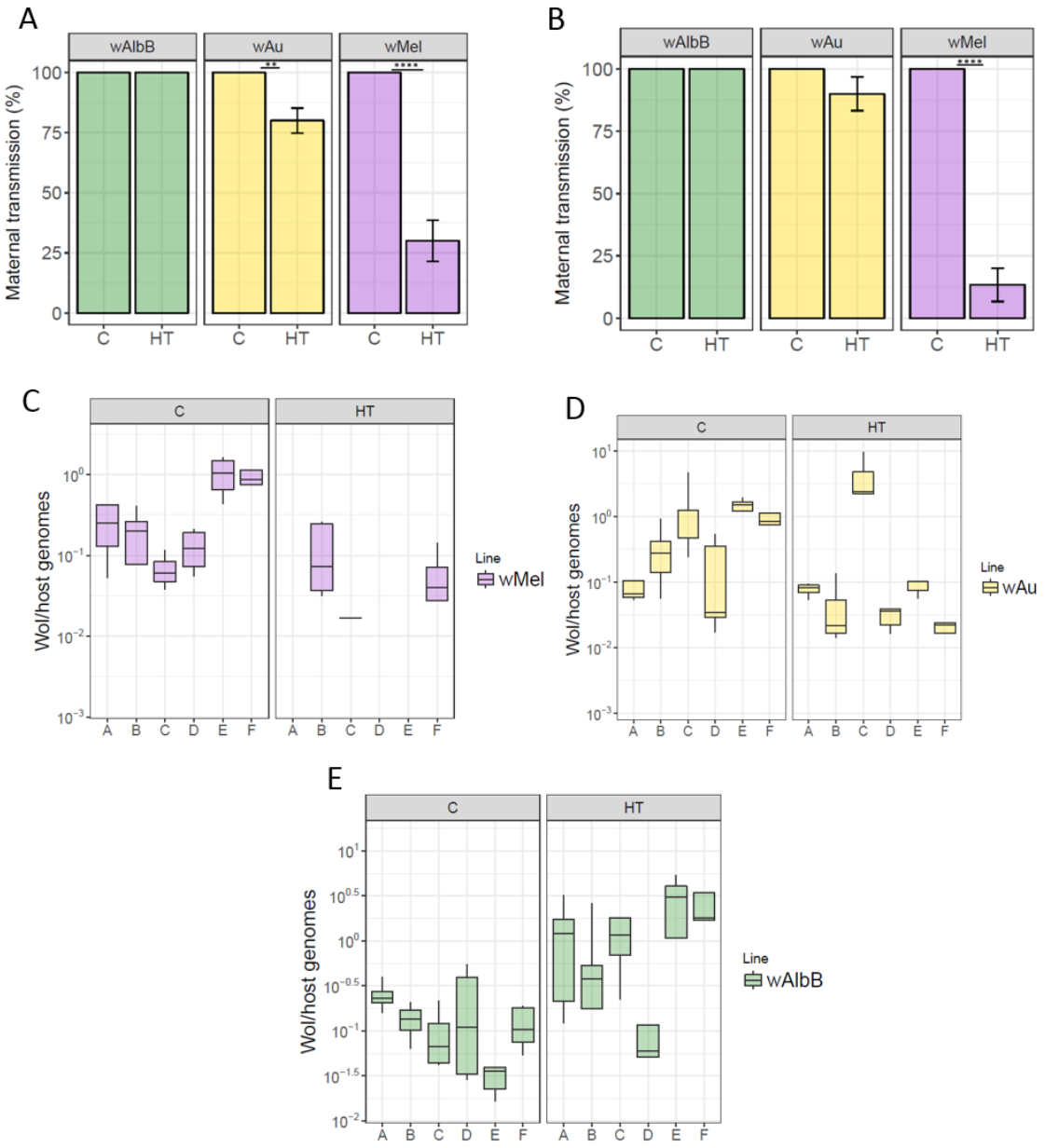


**Figure 5.2.7.** Maternal transmission of *Wolbachia* following one generation of heat-treatment

Females were blood fed and individualised in order to collect eggs from each mother. 5-6 larvae were selected from 4-6 females and PCR was performed for *Wolbachia* presence. Percentage of *Wolbachia*-positive larvae was averaged across the five families for one **(A)** and two **(B)** independent experiments. Additional qPCR of wsp in the larvae tested revealed the density of *Wolbachia* *w*Mel **(C)**, *w*Au **(D)** and *w*AlbB **(E)** across 6 families (A-F). Significance was performed by Students t-test.

## 5.3. Discussion

### 5.3.1. Maternal transmission of *w*Mel and *w*Au decreases following exposure to cyclical heat stress

*Wolbachia w*Mel-infected females have previously been released in multiple sites across the world in an attempt to replace the current mosquito population and reduce their ability to transmit arboviruses. Data here showed *Wolbachia* density of *w*Mel and the closely related *w*Au strains are significantly affected by a fluctuating temperature regime similar to those experienced in the field in the equatorial zone, which could hinder vector control regimes. Despite this discovery, the World Mosquito Program reports *w*Mel is stable in field *Ae. aegypti* in North Queensland, Australia, since its introduction in 2011 (O'Neill et al., 2018). This indicates *w*Mel may be suitable for releases in areas that do not experience temperatures fluctuating as extreme as those found in Trinidad and Malaysia, however other strains such as *w*AlbB are more suitable to unpredictable environments.

The density of *w*Au and *w*Mel-infected females is consistently significantly reduced over two generations of heat-treatment, whereas *w*AlbB density was not reduced. The consistent decrease in density is associated with a significant drop observed in the ovaries, where most of *Wolbachia* is located. The fact that the density of *w*AlbB is unaffected in the whole bodies and specifically in the ovaries supports this. The decrease in *Wolbachia* density in the ovaries has a marked effect on maternal transmission rates, particularly with *w*Mel heat-treated mosquitoes, in which almost 75% of progeny lose *Wolbachia* infection. Maternal transmission of *w*Au is less affected, with an almost 25% loss of *Wolbachia* infection, presumably as *w*Au is still at a high density in the ovaries following heat-treatment when compared to *w*Mel control ovaries. However, if this experiment was continued for several generations using heat-treated mosquitoes, perhaps the *w*Au would decrease to even lower levels and maternal transmission significantly more affected.

This imperfect maternal transmission has implications for releases; even if there is perfect maternal transmission, there is an estimated invasion threshold of 20-30%, which must be reached during initial releases in order for *Wolbachia* to

successfully invade a population (Jiggins, 2017). However, if *w*Mel mosquitoes show reduced rates of maternal transmission at high temperatures experienced in the field, this threshold would need to be higher, and clearly the equilibrium frequency reached would be below 100%. *w*Au would be difficult to spread due to its imperfect maternal transmission at high temperature, no induction of CI and deleterious fitness costs imposed on the mosquito host. On the other hand, *w*AlbB mosquitoes retained perfect maternal inheritance, which means that in combination with its low fitness costs this strain would require a lower invasion threshold to spread.

After one generation of heat-treatment, in males *w*Mel decrease in density but return to similar levels as the control by the second generation; the *w*Au males experience the same drop in density but this time in the second generation. As we attributed the significant drop in *Wolbachia* density in females largely to the loss in the ovaries, this may explain why there is not a consistent drop of density in males, as the density in the reproductive organs is likely to be lower. Despite these variable results across generations, it is clear that *w*Au and *w*Mel in males can significantly decrease in density when exposed to field-like temperature regimes, expected to impact CI, whereas *w*AlbB remains at a stable density. To investigate this further we could have set up CI crosses, in which our heat-treated males could be assessed for their ability to induce CI with wild type females. In fact, it has been shown elsewhere that *w*Mel males do lose the ability to induce CI when the larvae are reared at 12-hour diurnal cycles between 26ºC and 37.5ºC, whereas *w*AlbB males retained the CI-inducing phenotype (Ross and Hoffmann, 2018). This data clearly suggests *w*AlbB is more thermo-stable at higher temperatures than *w*Mel and *w*Au *Wolbachia* strains.

### 5.3.2. *w*AlbB is stable and can increase in density at high temperatures

Data here shows that *w*AlbB replicates to higher levels with high temperatures, as *Wolbachia* density increased in the ovaries following two generations of our temperature regime. After one generation, the density in the ovaries was largely unaffected, but following two generations we found a significant increase in density as quantified by qPCR, and visually with FISH. Investigating this further revealed *w*AlbB larvae from this generation were at a significantly higher density

than those reared at control temperatures. A similar phenomenon has been observed in *w*AlbB-infected *Anopheles stephensi*, whereby *w*AlbB density increased significantly when reared above 24ºC, compared to those reared at lower temperatures (Murdock et al., 2014)). In addition, *w*AlbB strongly reduced *Plasmodium* oocyst number at the highest temperature (28ºC), compared to having no effect at the lowest temperature (20ºC), presumably due to the difference in density. Altogether, these results suggest *w*AlbB can thrive at higher temperatures, making it a strong candidate for releases in areas with extended periods of daytime temperature peaks in the high thirties (celcius). The *w*MelPop strain of *Wolbachia* has also been shown to replicate to higher levels and therefore reduce mosquito survival at higher temperatures, due to its pathogenicity (Reynolds et al., 2003). Although *w*AlbB retains a moderate density compared to *w*MelPop in *Ae. aegypti*, it may be worthwhile to check if multiple rounds of heat-treatment results in a high density *w*AlbB that could potentially be detrimental to host fitness.

### 5.3.3. Alphavirus inhibition is conserved despite density drop

Despite experiencing a significant reduction in density, heat-treated *w*Mel and *w*Au mosquitoes still exhibited strong inhibition of SFV over two independent experiments. *w*Au in particular maintained an almost perfect inhibition, with only one positive heat-treated female; this is perhaps not surprising, as the heat-treated *w*Au females were still at a higher density than moderate blockers of wMel control, even in individual tissues. We hypothesised an increase in virus in *w*Mel mosquitoes as *Wolbachia* density significantly decreased in the midgut in both generations; this is where arboviruses experience their first bottleneck, as they have to pass the midgut barrier for further replication and dissemination.

The number of SFV-positive *w*Mel females doubled in the first experiment following heat-treatment compared to control, however the same increase occured in *Wolbachia*-uninfected females, meaning this cannot be attributed solely due to reduction in *Wolbachia* density. As the mechanism of *Wolbachia*-mediated pathogen inhibition is not currently known, it cannot be assumed that a decrease in certain tissues means a loss of the inhibition phenotype. It has been suggested that virus inhibition is indeed a tissue-specific effect, as higher densities of *Wolbachia* in *Drosophila* tissues correlated with a more protective effect

against *Drosophila* C Virus (Osborne et al., 2012). In addition, immunofluorescence of *w*MelPop-infected *Ae. aegypti* injected with DENV showed cellular exclusion of the virus when *Wolbachia* was present in tissues (Moreira et al., 2009). On the other hand, levels of DENV-3 RNA have been shown to not be correlated with *Wolbachia* density in specific tissues such as fat body, midgut, salivary glands and malphigian tubules, indicating *Wolbachia*-mediated inhibition is a systemic effect (Amuzu and McGraw, 2016). While it is clear that high density strains of *Wolbachia* protect strongly against arboviruses, the importance of *Wolbachia* exclusion of virus in specific tissues in this process remains unclear.

Further investigation into titre of SFV in the abdomen and head revealed a significantly higher virus titre in the head of wild type heat-treated mosquitoes, relative to control. This is similar to results obtained by (Ulrich et al., 2016), who observed an increase in DENV dissemination in wild type *Ae. aegypti* when reared at higher temperatures. Heat-treated mosquitoes were challenged with DENV-2 at a titre of 1 x 10^6 in the blood meal, however after performing FFA on salivary glands 14 days post-feed there was no detectable infection in wild type females and therefore any results observed in *Wolbachia*-infected lines could not be compared. As in the previous SFV challenges, (Ulrich et al., 2016) also struggled to investigate heat-treatment on DENV infection in *w*Mel due to a lack of virus-positive females. Due to the potent viral inhibition induced by *Wolbachia*, to investigate any effects temperature could have on this phenotype an experiment would have to be performed on a much larger scale, in order to get enough virus-positive females in the *Wolbachia*-positive strains to perform statistical analysis. Studies have also shown that the extrinsic incubation period (EIP) of arboviruses (the period required within the arthropod vector to travel from midgut to salivary gland for transmission) reduces when mosquitoes are reared at higher temperatures, resulting in a higher percentage of mosquites infected (Mbaika et al., 2016; Xiao et al., 2014). With regards to *Wolbachia*-mediated pathogen inhibition, if a strain is released into field populations that reduces in density at higher temperatures, combined with a shorter EIP, this could result in the commencement of arbovirus transmission once again.

### 5.3.4. *Wolbachia* strains should be robustly tested before field release

This research highlights that *Wolbachia* strains can vary in their response to environmental stressors, and should be assess thoroughly if used for vector control. A recent study has shown that infection with *Wolbachia* can alter the thermal preference of *D.melanogaster*; while uninfected flies preferred environments of 24.4ºC, those infected with *w*Mel preferred temperatures 1.2ºC lower, and with *w*MelPop 4ºC lower (Truitt et al., 2018). Although it is a small temperature change with regards to *w*Mel infection, this may have a huge impact on *Wolbachia* titre within the fly, and indicates that *Wolbachia* may be influencing behaviour of infected flies for its own benefit. The affect of temperature on *Wolbachia* strains may be exacerbated in the novel *Ae. aegypti* host, leading to our observed drastic decrease in *w*Mel density.

Efforts have been made to create a 'heat-resistant' *w*Mel strain that can be deployed to the field, in which *w*Mel-infected females reared under cyclical stress (12 hour intervals of 26ºC and 36.5ºC/37.5ºC) were mated to *w*Mel males reared at 26ºC, with any resulting hatched larvae selected for the next generation (Ross and Hoffmann, 2018). Despite repeating this heat-treatment selection for eight generations, *w*Mel density was still lost by the seventh generation, indicating it is not stable at high temperatures despite constant selection. This study also found field-caught *w*Mel mosquitoes and the laboratory *w*Mel colony used responded similarly to the heat-treatment, giving confidence that our results do represent what could happen to *Wolbachia* in the field (Ross and Hoffmann, 2018).

Despite our results, *w*Mel should not be completely ruled out for releases; perhaps this strain will be better suited (given its low fitness costs) for releases in areas with lower average temperature regimes, wheras *w*AlbB will be more useful in much warmer, equatorial areas. Although *w*Au provides perfect virus inhibition on its own, in order for it to be used for releases it should be paired with another *Wolbachia* strain capable of inducing CI. Superinfection of *w*Mel and *w*AlbB in *Ae. aegypti* is an ideal combination for releases, as together they have been shown to provide stronger inhibition of DENV than alone, and the heat stability of *w*AlbB means that even if *w*Mel was lost in some mosquitoes, *w*AlbB-only would still be

able to provide pathogen inhibition (Joubert et al., 2016). This work highlights the importance of investigating the stressors imposed upon *Wolbachia*-infected mosquitoes in order to assess their robustness in the field.

## 5.4. Conclusion

*Wolbachia* is a diverse genus containing many strains that reach different densities in the *Ae. aegypti* host. Under laboratory conditions, *Wolbachia* remains at a relatively constant density and induces complete maternal transmission. These data show *Wolbachia* strains are differentially affected by environmental stressors, specifically temperatures which are likely to occur in the field. The loss of complete maternal transmission of *w*Mel and *w*Au mosquitoes following exposure to high temperatures means these strains may not invade and persistently spread through a wild mosquito population. On the other hand, *w*AlbB remains a constant density and maintains robust virus inhibition, indicating it is the ideal choice for releases. This study highlights the importance of measuring the impact of environmental stressors on novel *Wolbachia* transinfections to ensure successful invasion in the wild and prevention of arbovirus transmission.

# Chapter 6

## Discussions, Future Work and Conclusions

## 6.1. Discussion

Arboviruses are increasingly becoming a huge economic and health burden. With increased movement and global warming, mosquitoes are able to infect more people worldwide than ever before. This was evident by the recent outbreaks of Zika and chikungunya. Therefore, new, effective control strategies are increasingly required. *Wolbachia* provides an opportunity to control both mosquito populations and the spread of arboviruses.

The data within this thesis adds to the expanding information on how *Wolbachia* impacts the homeostasis of the cells it inhabits and the effect this can have on arbovirus replication. Here, predominant results from each chapter and the direction for future work are discussed.

### 6.1.1. Chapter 3: Towards a better understanding of the mechanism of *Wolbachia*-mediated pathogen inhibition

In this chapter it was shown that two high-density *Wolbachia* strains in two species of *Aedes* cells exhibit different states of redox stress. This work confirms other evidence that redox stress is not exhibited in native hosts of *Wolbachia* (Molloy & Sinkins, 2015). In addition, data from this chapter adds to the evidence that *Wolbachia* requires an intact protein degradation pathway in the endoplasmic reticulum to retain high density, as disruption of ER homeostasis using thapsigargin reduced *Wolbachia* density. Chaperone expression in Aag2 *w*MelPop cells was also shown to be significantly different compared to uninfected cells, even when Dengue virus was added. These differences in chaperone expression are of particular interest as it may be related to the method by which *Wolbachia* influence the protein-degradation pathway, and therefore block virus replication.

To continue this work, gene expression of chaperones should be quantified in cells and mosquitoes at several stages of Dengue infection, as studies have shown that viruses can manipulate the unfolded-protein response in a time-dependent manner. In addition, chaperone expression should be measured in response to several viruses across the Flavivirus and Alphavirus genus to assess if any manipulations are universal. It would also be beneficial to optimise checking protein expression of chaperones, however this has associated technical challenges due to the lack of mosquito-specific antibodies commercially available.

### 6.1.2. Chapter 4: Characterising novel transinfections of *Wolbachia* in *Ae. aegypti*

The creation of novel transinfections with *w*Au and *w*AlbA in *Ae. aegypti* revealed interesting results; 1) *w*Au provides complete virus inhibition of all arboviruses tested and 2) despite being a similar density as *w*Au, *w*AlbA did not exhibit pathogen inhibition of SFV. The creation of the *Ae. aegypti w*Au line adds to the knowledge of how different *Wolbachia* strains replicate when transinfected in novel hosts, and suggests that by exploring other strains in the genus there may be a discovery of a strain which provides complete virus inhibition without major detrimental fitness effects. The discovery that *w*AlbA provided no inhibition of SFV was surprising, but also indicates that the mechanism of pathogen-inhibition is not as clear cut as was previously thought - that inhibition is not necessarily directly related to density. While it is true that high-density strains typically provide the best inhibition, *w*AlbA in *Ae. aegypti* goes against this dogma.

In order to investigate the lack of *w*AlbA pathogen inhibition it would be ideal to further challenge this line with Flaviviruses such as DENV and ZIKV, to monitor if it is a genus-wide effect. In addition, tissues such as midguts and salivary glands could be dissected from a strong-pathogen inhibition line and *w*AlbA during infection, making comparisons of gene expression and possible ER perturbations. Further characterisation of the *w*AlbA line was not possible due to an insectary overnight overheating problem which resulted in the loss of many lines. However, proteomic data from *w*AlbA and *w*Au midguts is currently being analysed within the lab and may provide notable hits which differ between the two that could be potentially manipulated in *w*Au mosquitoes to monitor if there is a loss of pathogen inhibition.

### 6.1.3. Chapter 5: Effect of cyclical high temperature rearing on *Wolbachia* in *Ae. aegypti*

Data from this chapter revealed that *w*Mel and *w*Au *Wolbachia* strains were not as stable at a higher temperature range as *w*AlbB. There is currently evidence that *w*Mel drops in density at extreme high temperatures, however this study is the first analysis of *Wolbachia* density and transmission following larval exposure to temperatures that have been recorded in the field. Here we show strong evidence that maternal transmission of *w*Mel is drastically reduced following the

temperature cycle, which has major implications for the fate of mosquito release programs that are currently on-going. These data also show that another weakness of *w*Au is the slight instability of the strain in response to heat, as well as the other detrimental fitness effects discussed in Chapter 4. This chapter unequivocally shows that *w*AlbB should retain a stable density when exposed to high temperatures and should currently be the preferred choice for releases in very hot equatorial zone.

The discovery that *w*AlbB increased in density following heat-stress is a point of interest that requires further study. It may be that following releases, *w*AlbB may increase in density in the field population following exposure to very hot temperatures and provide complete virus inhibition. To continue this work, larvae could again be exposed to the temperature regime and gene expression quantified at various stages of development; such as immune genes, those involved in apoptosis and regulation of the endoplasmic reticulum. This may provide some insight into the establishment of *Wolbachia* replication rate, i.e. what factors result in a strain being maintained at high or low density.

## 6.2. Conclusions of this study

The aim of this study was to further understand *Wolbachia*-mediated arbovirus inhibition in *Aedes* mosquitoes and how it can optimally be used for arbovirus control. Data reported here confirms that *Wolbachia* remains a viable option for reducing the transmission of arboviruses and shows that multiple strains colonise novel hosts differently. It also highlights the importance of assessing the properties of different strains that are proposed for releases, as demonstrated when *w*Mel was exposed to heat-treatment. Data here also hints that there may be different mechanisms of viral inhibition between *Wolbachia* strains, important to bear in mind when performing future work on the mechanisms of virus inhibition. Overall, this thesis shows it is beneficial to investigate multiple *Wolbachia* strains to identify the optimal strains for field releases (which may vary between regions) and elucidate a complete picture of the mechanism of virus inhibition.

# Appendices

| *Wolbachia* qPCR | | | | |
|---|---|---|---|---|
| FORWARD | | | REVERSE | |
| AAEL011643 qHTH F | TGGTCCTATATTGGCGAGCTA | | AAEL011643 qHTH R | TCGTTTTTGCAAGAAGGTCA |
| MG547559.1 qWSP F | GCATCTTTTATAGCTGGTGG | | MG547559.1 qWSP R large | GGAGTGATAGGCATATCTTCAAT |

| *Wolbachia* PCR | | | | |
|---|---|---|---|---|
| FORWARD | | | REVERSE | |
| MK053601.1 Wspec F | CATACCTATTCGAAGGGATAG | | MK053601.1 Wspec R | AGCTTCGAGTGAAACCAATTC |
| MG765532.1 wAlbA F | GTAGTATTTACCCCAGCAG | | MG765532.1 wAlbA R | ATCTGCACCAGTAGTTTCG |
| KX650069.1 wAlbB F | GCAATACCTATGCCGTTTA | | KX650069.1 wAlbB R | GACGAAGGGGATAGGTTAATATC |
| DQ235409.1 wAu wMel (81F) | TGGTCCAATAAGTGATGAAGAAAC | | DQ235409.1 wAu R | AGTAACCTGTCTGGTTGAATC |
| | | | wMel R KX650072.1 | CAGCCTGTCCGGTTGAATT |

| Immune gene qRT-PCR | | | | |
|---|---|---|---|---|
| FORWARD | | | REVERSE | |
| AAEL004175 RPS17 F | CACTCCCAGGTCCGTGGTAT | | AAEL004175 RPS17 R | GGACACTTCCGGCACGTAGT |
| AAEL000598 Cecropin D F1 | GCTAGGTCAAACCGAAGCAG | | AAEL000598 Cecropin D R1 | TCCTACAACAACCGGGAGAG |
| AAEL003832 Defensin C F1 | TTGTTTGCTTCGTTGCTCTTT | | AAEL003832 Defensin C R1 | ATCTCCTACACCGAACCCACT |
| XR_002499766.1 Cecropin G F1 | TCACAAAGTTATTTCTCCTGATCG | | XR_002499766.1 Cecropin G R1 | GCTTTAGCCCCGCTACAAC |
| AAEL002309 TPX4 R3 | AAGTGCCATGTCGATTGGGT | | AAEL002309 TPX4 R3 | CTCGGAGACACTCGGTAGGA |
| AAEL007562 DUOX 2 F | CGTGGCGGAGTATTTCAGT | | AAEL007562 DUOX 2 R | GCAAATTCATCAGCAACCAC |
| AAEL010179 NOXM F | TCCACAATACGGTTTCGCTA | | AAEL010179 NOXM R | GCCGTCCAACAGAAATTGTA |

| Pathogen qPCR | | | | |
|---|---|---|---|---|
| FORWARD | | | REVERSE | |
| MK334655.1 Serratia F1 | ACGTTCATCAATTGACGTTACTCGCA | | MK334655.1 Serratia R1 | AACCGCCTGCGTGCGCTTA |
| KP699763.1 SFV4 F | CGCATCACCTTCTTTTGTG | | KP699763.1 SFV4 R | CCAGACCACCCGAGATTT |
| MG721058.1 DENV NS5 F | ACAAGTCGAACAACCTGGTCCAT | | MG721058.1 DENV NS5 R | GCCGCACCATTGGTCTTCTC |
| MH900227.1 ZIKV 835 F | TTGGTCATGATACTGCTGATTGC | | MH900227.1 ZIKV 911c R | CCTTCCACAAAGTCCCTATTGC |

| ER Gene expression | | | | |
|---|---|---|---|---|
| FORWARD | | | REVERSE | |
| AAEL017349 BiP F1 | CCCATGACCAAGGACAACCA | | AAEL017349 BiP R1 | CTTCTGGGGTCAGACGGTTC |
| AAEL015100 Calnexin F2 | CAAGGACAAGCAACCGCATC | | AAEL015100 Calnexin R2 | GGAGGCGTAAACTCGGTGAA |
| AAEL005558_C2F2 | GGAAGCACAGACGACACTGA | | AAEL005558_C2R2 | ACAGGGTCGCTACCTTTTCT |
| AAEL005558_UF2 | ATCCGCCCAAACCCCTCA | | AAEL005558_UR2 | CCATCTTGTCCTGACTCAGTGT |
| AAEL005558_SF2 | GAGCGACGACTCAACGATCT | | AAEL005558_SR2 | TCCATTAAAGATCCCTGCTGCT |

| FISH probes | | | | |
|---|---|---|---|---|
| FORWARD | | | REVERSE | |
| MH732670.1 W2 Alexa Fluor 488 | CTTCTGTGAGTACCGTCATTATC | | MH732670.1 W3 Alexa Fluor 488 | AACCGACCCTATCCCTTCGAATA |
| KF725077.1 wAlbB | GCATCTTTTATAGCTGGTGG | | | |

**Appendix 1.** List of primers and probes used in this study.
Primer and probe sequences are listed with gene accession number.

| BiP1 F1R1 | | | |
|---|---|---|---|
| Dilution | CT | | Average |
| 1 | 22.25 | 22.08 | 22.16 |
| 0.30103 | 24.72 | 24.44 | 24.58 |
| -0.39794 | 26.62 | 26.45 | 26.53 |
| -1.09691 | 28.52 | 28.43 | 28.47 |
| | 29.82 | 29.68 | 29.75 |
| | | efficiency | 116.15 |

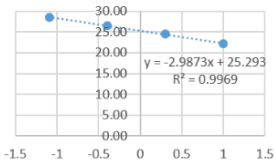


| C2 F2R2 | |
|---|---|
| Dilution | Average CT |
| 1 | 22.34 |
| 0.30103 | 24.68 |
| -0.39794 | 26.70 |
| -1.09691 | 28.84 |
| -1.79588 | 31.27 |
| Efficiency (%) | 107.6054517 |

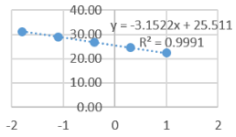


| CALNEX F1R1 | | | |
|---|---|---|---|
| Dilution | CT | | Average |
| 1 | 27.99 | 27.84 | 27.91 |
| 0.30103 | 29.93 | 30.04 | 29.99 |
| -0.39794 | 31.74 | 32.29 | 32.02 |
| -1.09691 | 35.35 | 35.09 | 35.22 |
| H20 | | 39.19 | 39.19 |
| | | Efficiency | 95.85592 |

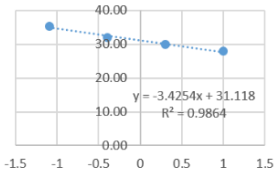


| U F2R2 | |
|---|---|
| Dilution | Average CT |
| 1 | 23.10 |
| 0.30103 | 25.10 |
| -0.39794 | 27.10 |
| -1.09691 | 29.42 |
| -1.79588 | 31.49 |
| Efficiency (%) | 114.4432241 |

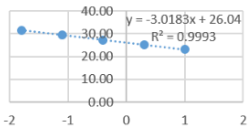


| TPX - F3R3 | | | |
|---|---|---|---|
| Dilution | CT | | Average CT |
| 1 | 23.13 | 23.26 | 23.20 |
| 0.30103 | 24.85 | 24.98 | 24.91 |
| -0.39794 | 27.03 | 27.17 | 27.10 |
| -1.09691 | 29.35 | 29.77 | 29.56 |
| | | Efficiency | 117.90% |

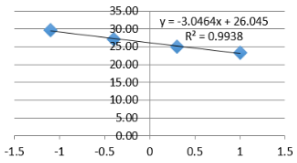


| S F2R2 | |
|---|---|
| Dilution | Average CT |
| 1 | 22.26 |
| 0.30103 | 24.17 |
| -0.39794 | 26.26 |
| -1.09691 | 28.42 |
| -1.79588 | 30.21 |
| | 122.37072 |
| Efficiency (%) | 22 |

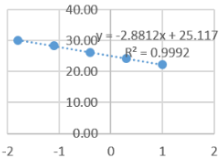


**Appendix 2.** Efficiency of primers designed for this study.
cDNA from *Ae. aegypti* WT was diluted 1:5 for a series of dilutions and the qPCR was performed to gain CT values. CT values were then plotted to calculate the efficiency.

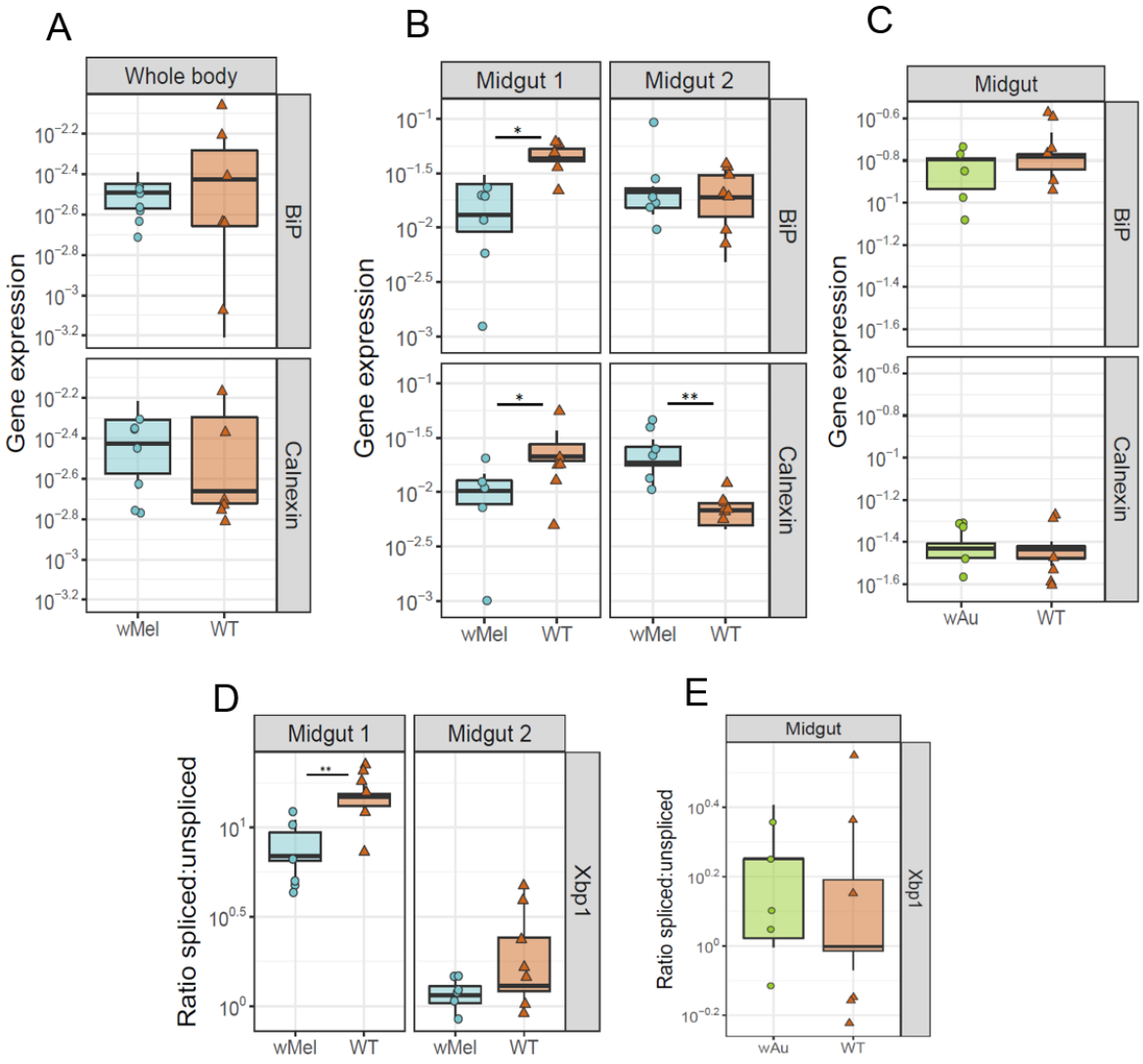


**Appendix 3.** Gene expression of ER-related genes in *Ae. aegypti* *w*Mel and *w*Au mosquitoes

RNA was extracted from *w*Mel and *w*Au mosquitoes for qRT-PCR of BiP, Calnexin and Xbp1 splicing. BiP and Calnexin expression was quantified in individual female whole bodies of *w*Mel **(A)**, two independent replicates of *w*Mel midguts **(B)** and one replicate of *w*Au midguts **(C)**. The ratio of spliced:unspliced Xbp1 gene was quantified in wMel midguts (D) and wAu midguts (E). Five midguts were pooled per data point for five replicates. Statistics performed was students T-test.

# List of References


Acosta, E. G., V. Castilla, and E. B. Damonte, 2009, Alternative infectious entry pathways for dengue virus serotypes into mammalian cells: Cell Microbiol, v. 11, p. 1533-49.

Acosta, E. G., V. Castilla, and E. B. Damonte, 2012, Differential requirements in endocytic trafficking for penetration of dengue virus: PLoS One, v. 7, p. e44835.

Ahmad, N. A., I. Vythilingam, Y. A. Lim, N. Z. Zabari, and H. L. Lee, 2017, Detection of *Wolbachia* in *Aedes albopictus* and Their Effects on Chikungunya Virus: Am J Trop Med Hyg, v. 96, p. 148-156.

Allard, A., B. M. Althouse, L. Hébert-Dufresne, and S. V. Scarpino, 2017, The risk of sustained sexual transmission of Zika is underestimated: PLoS Pathog, v. 13, p. e1006633.

Acosta-Ampudia, Y., D. M. Monsalve, Y. Rodríguez, Y. Pacheco, J. M. Anaya, and C. Ramírez-Santana, 2018, Mayaro: an emerging viral threat?: Emerg Microbes Infect, v. 7, p. 163.

Alphey, L., 2002, Re-engineering the sterile insect technique: Insect Biochem Mol Biol, v. 32, p. 1243-7.

Amuzu, H. E., and E. A. McGraw, 2016, *Wolbachia*-Based Dengue Virus Inhibition Is Not Tissue-Specific in *Aedes aegypti*: PLoS Negl Trop Dis, v. 10, p. e0005145.

Andrews, E. S., P. R. Crain, Y. Fu, D. K. Howe, and S. L. Dobson, 2012, Reactive oxygen species production and *Brugia pahangi* survivorship in *Aedes polynesiensis* with artificial *Wolbachia* infection types: PLoS Pathog, v. 8, p. e1003075.

Ant, T. H., C. S. Herd, V. Geoghegan, A. A. Hoffmann, and S. P. Sinkins, 2018, The *Wolbachia* strain *w*Au provides highly efficient virus transmission inhibition in *Aedes aegypti*: PLoS Pathog, v. 14, p. e1006815.

Ant, T. H., and S. P. Sinkins, 2018, A *Wolbachia* triple-strain infection generates self-incompatibility in *Aedes albopictus* and transmission instability in *Aedes aegypti*: Parasit Vectors, v. 11, p. 295.

Barletta, A. B., M. C. Nascimento-Silva, O. A. Talyuli, J. H. Oliveira, L. O. Pereira, P. L. Oliveira, and M. H. Sorgine, 2017, Microbiota activates IMD pathway and limits Sindbis infection in *Aedes aegypti*: Parasit Vectors, v. 10, p. 103.

Barrera, R., A. M. Bingham, H. K. Hassan, M. Amador, A. J. Mackay, and T. R. Unnasch, 2012, Vertebrate hosts of *Aedes aegypti* and *Aedes mediovittatus* (Diptera: Culicidae) in rural Puerto Rico: J Med Entomol, v. 49, p. 917-21.

Barrett, A. D. T., 2018, The reemergence of yellow fever: Science, v. 361, p. 847-848.

Bawo, L. L., A. D. Harries, T. Reid, M. Massaquoi, R. Jallah-Macauley, J. J. Jones, C. S. Wesseh, J. Enders, and L. Hinneh, 2012. Coverage and use of insecticide-treated bed nets in households with children under five years in Liberia. Public Health Action, v.2, p. 112-116.

Beckmann, J. F., J. A. Ronau, and M. Hochstrasser, 2017, A *Wolbachia* deubiquitylating enzyme induces cytoplasmic incompatibility: Nat Microbiol, v. 2, p. 17007.

Bellini, R., A. Medici, A. Puggioli, F. Balestrino, and M. Carrieri, 2013, Pilot field trials with *Aedes albopictus* irradiated sterile males in Italian urban areas: J Med Entomol, v. 50, p. 317-25.

Benedict, M. Q., R. S. Levine, W. A. Hawley, and L. P. Lounibos, 2007, Spread of the tiger: global risk of invasion by the mosquito *Aedes albopictus*: Vector Borne Zoonotic Dis, v. 7, p. 76-85.

Benelli, G., C. L. Jeffries, and T. Walker, 2016, Biological Control of Mosquito Vectors: Past, Present, and Future: Insects, v. 7., p.52.

Bian, G., Y. Xu, P. Lu, Y. Xie, and Z. Xi, 2010, The endosymbiotic bacterium *Wolbachia* induces resistance to dengue virus in *Aedes aegypti*: PLoS Pathog, v. 6, p. e1000833.

Bian, G., G. Zhou, P. Lu, and Z. Xi, 2013, Replacing a native *Wolbachia* with a novel strain results in an increase in endosymbiont load and resistance to dengue virus in a mosquito vector: PLoS Negl Trop Dis, v. 7, p. e2250.

Blagrove, M. S., C. Arias-Goeta, C. Di Genua, A. B. Failloux, and S. P. Sinkins, 2013, A *Wolbachia w*Mel transinfection in *Aedes albopictus* is not detrimental to host fitness and inhibits Chikungunya virus: PLoS Negl Trop Dis, v. 7, p. e2152.

Blagrove, M. S., C. Arias-Goeta, A. B. Failloux, and S. P. Sinkins, 2012. *Wolbachia* strain *w*Mel induces cytoplasmic incompatibility and blocks dengue transmission in *Aedes albopictus*: Proc Natl Acad Sci U S A, v. 109, p. 255-60.

Blair, C. D., 2011, Mosquito RNAi is the major innate immune pathway controlling arbovirus infection and transmission: Future Microbiol, v. 6, p. 265-77.

Bolling, B. G., N. Vasilakis, H. Guzman, S. G. Widen, T. G. Wood, V. L. Popov, S. Thangamani, and R. B. Tesh, 2015, Insect-specific viruses detected in laboratory mosquito colonies and their potential implications for experiments evaluating arbovirus vector competence: Am J Trop Med Hyg, v. 92, p. 422-8.

Bordenstein, S. R., and J. H. Werren, 2007, Bidirectional incompatibility among divergent *Wolbachia* and incompatibility level differences among closely related *Wolbachia* in Nasonia: Heredity (Edinb), v. 99, p. 278-87.

Bosio, C. F., B. J. Beaty, and W. C. Black, 1998, Quantitative genetics of vector competence for dengue-2 virus in *Aedes aegypti*: Am J Trop Med Hyg, v. 59, p. 965-70.

Brackney, D. E., J. C. Scott, F. Sagawa, J. E. Woodward, N. A. Miller, F. D. Schilkey, J. Mudge, J. Wilusz, K. E. Olson, C. D. Blair, and G. D. Ebel, 2010, C6/36 *Aedes albopictus* cells have a dysfunctional antiviral RNA interference response: PLoS Negl Trop Dis, v. 4, p. e856.

Brennan, L. J., B. A. Keddie, H. R. Braig, and H. L. Harris, 2008, The endosymbiont *Wolbachia pipientis* induces the expression of host antioxidant proteins in an *Aedes albopictus* cell line: PLoS One, v. 3, p. e2083.

Brown, A. M., S. K. Wasala, D. K. Howe, A. B. Peetz, I. A. Zasada, and D. R. Denver, 2016, Genomic evidence for plant-parasitic nematodes as the earliest *Wolbachia* hosts: Sci Rep, v. 6, p. 34955.

Brown, J. E., B. R. Evans, W. Zheng, V. Obas, L. Barrera-Martinez, A. Egizi, H. Zhao, A. Caccone, and J. R. Powell, 2014, Human impacts have shaped historical and recent evolution in *Aedes aegypti*, the dengue and yellow fever mosquito: Evolution, v. 68, p. 514-25.

Brownlie, J. C., B. N. Cass, M. Riegler, J. J. Witsenburg, I. Iturbe-Ormaetxe, E. A. McGraw, and S. L. O'Neill, 2009, Evidence for metabolic provisioning by a common invertebrate endosymbiont, *Wolbachia pipientis*, during periods of nutritional stress: PLoS Pathog, v. 5, p. e1000368.

Brustolin, M., S. Pujhari, C. A. Henderson, and J. L. Rasgon, 2018, *Anopheles* mosquitoes may drive invasion and transmission of Mayaro virus across geographically diverse regions: PLoS Negl Trop Dis, v. 12, p. e0006895.

Caminade, C., J. Turner, S. Metelmann, J. C. Hesson, M. S. Blagrove, T. Solomon, A. P. Morse, and M. Baylis, 2017, Global risk model for vector-borne transmission of Zika virus reveals the role of El Niño 2015: Proc Natl Acad Sci U S A, v. 114, p. 119-124.

Caragata, E. P., E. Rancès, L. M. Hedges, A. W. Gofton, K. N. Johnson, S. L. O'Neill, and E. A. McGraw, 2013, Dietary cholesterol modulates pathogen inhibition by *Wolbachia*: PLoS Pathog, v. 9, p. e1003459.

Caragata, E. P., F. O. Rezende, T. C. Simões, and L. A. Moreira, 2016, Diet-Induced Nutritional Stress and Pathogen Interference in *Wolbachia*-Infected *Aedes aegypti*: PLoS Negl Trop Dis, v. 10, p. e0005158.

Carvalho, D. O., A. R. McKemey, L. Garziera, R. Lacroix, C. A. Donnelly, L. Alphey, A. Malavasi, and M. L. Capurro, 2015, Suppression of a Field Population of *Aedes aegypti* in Brazil by Sustained Release of Transgenic Male Mosquitoes: PLoS Negl Trop Dis, v. 9, p. e0003864.

CDC, 2014, Dengue Epidemiology, Centers for Disease Control and Prevention. < https://www.cdc.gov/dengue/epidemiology/index.html>. Accessed on 22/09/2018.

CDC, 2015, Transmission of Japanese Encephalitis Virus.< https://www.cdc.gov/japaneseencephalitis/transmission/index.html>. Accessed on 22/09/2018.

CDC, 2017a, Areas with Risk of zika, Centre for Disease Control.< https://wwwnc.cdc.gov/travel/page/zika-travel-information>. Accessed on 22/09/2018.

CDC, 2017b, History Timeline Transcript: Yellow Fever, Centre for Disease Control and Prevention.< https://www.cdc.gov/travel-training/local/HistoryEpidemiologyandVaccination/HistoryTimelineTranscript.pdf >.Accessed 29/09/2018.

Chan, Y. S., D. A. Naujoks, D. S. Huen, and S. Russell, 2011, Insect population control by homing endonuclease-based gene drive: an evaluation in *Drosophila melanogaster*: Genetics, v. 188, p. 33-44.

Charles, A. S., and R. C. Christofferson, 2016, Utility of a Dengue-Derived Monoclonal Antibody to Enhance Zika Infection In Vitro: PLoS Curr, v. 8.

Chen, T. H., Y. H. Chiang, J. N. Hou, C. C. Cheng, E. Sofiyatun, C. H. Chiu, and W. J. Chen, 2017, XBP1-Mediated BiP/GRP78 Upregulation Copes with Oxidative Stress in Mosquito Cells during Dengue 2 Virus Infection: Biomed Res Int, v. 2017, p. 3519158.

Chrostek, E., Marialva, M.S.P., Esteves, S.S., Weinert, L.A., Martinez, J., Jiggins, F.M., Teixeira, L, 2013. *Wolbachia* Variants Induce Differential Protection to Viruses in *Drosophila melanogaster*: A Phenotypic and Phylogenomic Analysis. PLoS Genetics, p. e1003896.

Chrostek, E., M. S. Marialva, R. Yamada, S. L. O'Neill, and L. Teixeira, 2014, High anti-viral protection without immune upregulation after interspecies *Wolbachia* transfer: PLoS One, v. 9, p. e99025.

Chrostek, E. & Teixeira, L, 2018. Within host selection for faster replicating bacterial symbionts. PLoS One, v.13, 1. p. e0191530.

Clements, A., 1992, The Biology of Mosquitoes: Development, Nutrition and Reproduction: CABI Publishing; New Ed edition. London, Chapman & Hall.

Connor, B., and W. B. Bunn, The changing epidemiology of Japanese encephalitis and New data: the implications for New recommendations for Japanese encephalitis vaccine, 2017. Tropical Diseases, Travel Medicine and Vaccines. V.3, 14.

Cook, S., S. N. Bennett, E. C. Holmes, R. De Chesse, G. Moureau, and X. de Lamballerie, 2006, Isolation of a new strain of the flavivirus cell fusing agent virus in a natural mosquito population from Puerto Rico: J Gen Virol, v. 87, p. 735-48.

Cook, S., G. Moureau, R. E. Harbach, L. Mukwaya, K. Goodger, F. Ssenfuka, E. Gould, E. C. Holmes, and X. de Lamballerie, 2009, Isolation of a novel species of flavivirus and a new strain of Culex flavivirus (Flaviviridae) from a natural mosquito population in Uganda: J Gen Virol, v. 90, p. 2669-78.

Cordaux, R., A. Michel-Salzat, M. Frelon-Raimond, T. Rigaud, and D. Bouchon, 2004, Evidence for a new feminizing *Wolbachia* strain in the isopod Armadillidium vulgare: evolutionary implications: Heredity (Edinb), v. 93, p. 78-84.

Costa, A., E. Jan, P. Sarnow, and D. Schneider, 2009, The Imd pathway is involved in antiviral immune responses in *Drosophila*: PLoS One, v. 4, p. e7436.

Cui, S., Y. Pan, Y. Lyu, Z. Liang, J. Li, Y. Sun, X. Dou, L. Tian, D. Huo, L. Chen, X. Li, and Q. Wang, 2017, Detection of yellow fever virus genomes from four imported cases in China: Int J Infect Dis, v. 60, p. 93-95.

Dambach, P., V. R. Louis, A. Kaiser, S. Ouedraogo, A. Sié, R. Sauerborn, and N. Becker, 2014, Efficacy of *Bacillus thuringiensis var. israelensis* against malaria mosquitoes in northwestern Burkina Faso: Parasit Vectors, v. 7, p. 371.

Deilgat, M., J. Geduld, and M. Drebot, 2014, CHIKUNGUNYA OUTBREAK IN THE CARIBBEAN 2013-2014: Can Commun Dis Rep, v. 40, p. 7-12.

Dejnirattisai, W., P. Supasa, W. Wongwiwat, A. Rouvinski, G. Barba-Spaeth, T. Duangchinda, A. Sakuntabhai, V. M. Cao-Lormeau, P. Malasit, F. A. Rey, J. Mongkolsapaya, and G. R. Screaton, 2016, Dengue virus sero-cross-reactivity drives antibody-dependent enhancement of infection with Zika virus: Nat Immunol, v. 17, p. 1102-8.

Delisle, E., C. Rousseau, B. Broche, I. Leparc-Goffart, G. L'Ambert, A. Cochet, C. Prat, V. Foulongne, J. B. Ferre, O. Catelinois, O. Flusin, E. Tchernonog, I. E. Moussion, A. Wiegandt, A. Septfons, A. Mendy, M. B. Moyano, L. Laporte, J. Maurel, F. Jourdain, J. Reynes, M. C. Paty, and F. Golliot, 2015, Chikungunya outbreak in Montpellier, France, September to October 2014: Euro Surveill, v. 20.

Deredec, A., H. C. Godfray, and A. Burt, 2011, Requirements for effective malaria control with homing endonuclease genes: Proc Natl Acad Sci U S A, v. 108, p. E874-80.

Deubel, V., J. P. Digoutte, X. Mattei, and D. Pandare, 1981, Morphogenesis of yellow fever virus in *Aedes aegypti* cultured cells. II. An ultrastructural study: Am J Trop Med Hyg, v. 30, p. 1071-7.

Diaz-Albiter, H., Sant'Anna, MR., Genta, FA., Dillon, RJ, 2012, Reactive oxygen species-mediated immunity against *Leishmania mexicana* and *Serratia marcescens* in the sand phlebotomine fly *Lutzomyia longipalpis*. Journal Biol Chem, v. 287, 28. p. e376095.

Di Francesco, J., R. Choeung, B. Peng, L. Pring, S. Pang, R. Duboz, S. Ong, S. Sorn, A. Tarantola, D. Fontenille, V. Duong, P. Dussart, V. Chevalier, and J. Cappelle, 2018, Comparison of the dynamics of Japanese encephalitis virus circulation in sentinel pigs between a rural and a peri-urban setting in Cambodia: PLoS Negl Trop Dis, v. 12, p. e0006644.

Dom, N. C., A. H. Ahmad, and R. Ismail, 2013, Habitat characterization of *Aedes* sp. breeding in urban hotspot area, Procedia-Social and Behavioral Sciences, p. 100-109.

Dong, S., V. Balaraman, A. M. Kantor, J. Lin, D. G. Grant, and N. L. Held, 2017, Chikungunya virus dissemination from the midgut of *Aedes aegypti* is associated with temporal basal lamina degradation during bloodmeal digestion, Public Library of Science: Neglected Tropical Diseases. p. e0005976.

ECDC, 2015, Microcephaly in Brazil potentially linked to the Zika virus epidemic, European Centre for Disease Control. < https://ecdc.europa.eu/en/publications-data/rapid-risk-assessment-microcephaly-brazil-potentially-linked-zika-virus-epidemic >. Accessed on 29/09/2018.

ECDC, 2016, *Aedes aegypti* - Factsheet for experts, European Centre for Disease Prevention and Control.< https://ecdc.europa.eu/en/disease-vectors/facts/mosquito-factsheets/*Aedes*-aegypti>. Accessed on 29/09/2018.

EPA, 2017a, Bti for Mosquito Control, United States Environmental Protection Agency.< https://www.epa.gov/mosquitocontrol/bti-mosquito-control>. Accessed on 20/09/2018.

EPA, 2017b, Controlling adult mosquitoes, United States Environmental Protection Agency.< https://www.epa.gov/mosquitocontrol/controlling-adult-mosquitoes>. Accessed on 20/09/2018.

Esu, E., A. Lenhart, L. Smith, and O. Horstick, 2010, Effectiveness of peridomestic space spraying with insecticide on dengue transmission; systematic review: Trop Med Int Health, v. 15, p. 619-31.

Fallon, A. M., and B. A. Witthuhn, 2009, Proteasome activity in a naïve mosquito cell line infected with *Wolbachia pipientis w*AlbB: In Vitro. Cell Dev Biol Anim, v. 45, p. 460-6.

Faull, K. J., and C. R. Williams, 2015, Intraspecific variation in desiccation survival time of *Aedes aegypti* (L.) mosquito eggs of Australian origin: J Vector Ecol, v. 40, p. 292-300.

Ferguson, N. M., D. T. Kien, H. Clapham, R. Aguas, V. T. Trung, T. N. Chau, J. Popovici, P. A. Ryan, S. L. O'Neill, E. A. McGraw, V. T. Long, l. T. Dui, H. L. Nguyen, N. V. Chau, B. Wills, and C. P. Simmons, 2015, Modeling the impact on virus transmission of *Wolbachia*-mediated inhibition of dengue virus infection of *Aedes aegypti*: Sci Transl Med, v. 7, p. 279ra37.

Fernandez-Garcia, M. D., M. Mazzon, M. Jacobs, and A. Amara, 2009, Pathogenesis of flavivirus infections: using and abusing the host cell: Cell Host Microbe, v. 5, p. 318-28.

Ferreira, Á., H. Naylor, S. S. Esteves, I. S. Pais, N. E. Martins, and L. Teixeira, 2014, The Toll-dorsal pathway is required for resistance to viral oral infection in *Drosophila*: PLoS Pathog, v. 10, p. e1004507.

Franz, A. W., A. M. Kantor, A. L. Passarelli, and R. J. Clem, 2015, Tissue Barriers to Arbovirus Infection in Mosquitoes: Viruses, v. 7, p. 3741-67.

Fraser, J. E., J. T. De Bruyne, I. Iturbe-Ormaetxe, J. Stepnell, R. L. Burns, H. A. Flores, and S. L. O'Neill, 2017, Novel *Wolbachia*-transinfected *Aedes aegypti* mosquitoes possess diverse fitness and vector competence phenotypes: PLoS Pathog, v. 13, p. e1006751.

Frentiu, F. D., J. Robinson, P. R. Young, E. A. McGraw, and S. L. O'Neill, 2010, *Wolbachia*-mediated resistance to dengue virus infection and death at the cellular level: PLoS One, v. 5, p. e13398.

Friedrich-Jänicke, B., P. Emmerich, D. Tappe, S. Günther, D. Cadar, and J. Schmidt-Chanasit, 2014, Genome analysis of Mayaro virus imported to Germany from French Guiana: Emerg Infect Dis, v. 20, p. 1255-7.

Fukui, T., M. Kawamoto, K. Shoji, T. Kiuchi, S. Sugano, T. Shimada, Y. Suzuki, and S. Katsuma, 2015, The Endosymbiotic Bacterium *Wolbachia* Selectively Kills Male Hosts by Targeting the Masculinizing Gene: PLoS Pathog, v. 11, p. e1005048.

Geoghegan, V., K. Stainton, S. M. Rainey, T. H. Ant, A. A. Dowle, T. Larson, S. Hester, P. D. Charles, B. Thomas, and S. P. Sinkins, 2017, Perturbed cholesterol and vesicular trafficking associated with dengue inhibition in *Wolbachia*-infected *Aedes aegypti* cells: Nat Commun, v. 8, p. 526.

Gerth, M., and C. Bleidorn, 2016, Comparative genomics provides a timeframe for *Wolbachia* evolution and exposes a recent biotin synthesis operon transfer: Nat Microbiol, v. 2, p. 16241.

Gerth, M., M. T. Gansauge, A. Weigert, and C. Bleidorn, 2014, Phylogenomic analyses uncover origin and spread of the *Wolbachia* pandemic: Nat Commun, v. 5, p. 5117.

Gill, A. C., A. C. Darby, and B. L. Makepeace, 2014, Iron necessity: the secret of *Wolbachia*'s success?: PLoS Negl Trop Dis, v. 8, p. e3224.

Glaser, R. L., and M. A. Meola, 2010, The native *Wolbachia* endosymbionts of *Drosophila melanogaster* and *Culex quinquefasciatus* increase host resistance to West Nile virus infection: PLoS One, v. 5, p. e11977.

Glowska, E., A. Dragun-Damian, M. Dabert, and M. Gerth, 2015, New *Wolbachia* supergroups detected in quill mites (Acari: Syringophilidae): Infect Genet Evol, v. 30, p. 140-6.

Godfray, H. C. J., A. North, and A. Burt, 2017, How driving endonuclease genes can be used to combat pests and disease vectors: BMC Biol, v. 15, p. 81.

Gomon, M.F., & Bray, D.J. 2019. Gambusia holbrooki in Fishes of Australia.< http://fishesofaustralia.net.au/home/species/3636> Accessed on 25/01/19.

Gould, E., J. Pettersson, S. Higgs, R. Charrel, and X. de Lamballerie, 2017, Emerging arboviruses: Why today?: One Health, v. 4, p. 1-13.

Grandadam, M., V. Caro, S. Plumet, J. M. Thiberge, Y. Souarès, A. B. Failloux, H. J. Tolou, M. Budelot, D. Cosserat, I. Leparc-Goffart, and P. Desprès, 2011, Chikungunya virus, southeastern France: Emerg Infect Dis, v. 17, p. 910-3.

Gullberg, R. C., J. Jordan Steel, S. L. Moon, E. Soltani, and B. J. Geiss, 2015, Oxidative stress influences positive strand RNA virus genome synthesis and capping: Virology, v. 475, p. 219-29.

Gupta, V., R. B. Vasanthakrishnan, J. Siva-Jothy, K. M. Monteith, S. P. Brown, and P. F. Vale, 2017, The route of infection determines *Wolbachia* antibacterial protection in *Drosophila*: Proc Biol Sci, v. 284, 1856.

Gómez, M. M., F. V. S. Abreu, A. A. C. D. Santos, I. S. Mello, M. P. Santos, I. P. Ribeiro, A. Ferreira-de-Brito, R. M. Miranda, M. G. Castro, M. S. Ribeiro, R. D. C. Laterrière Junior, S. F. Aguiar, G. L. S. Meira, D. Antunes, P. H. M. Torres, D. Mir, A. C. P. Vicente, A. C. R. Guimarães, E. R. Caffarena, G. Bello, R. Lourenço-de-Oliveira, and M. C. Bonaldo, 2018, Genomic and structural features of the yellow fever virus from the 2016-2017 Brazilian outbreak: J Gen Virol. v. 4, p. 536-548.

Ha, E. M., C. T. Oh, Y. S. Bae, and W. J. Lee, 2005a, A direct role for dual oxidase in *Drosophila* gut immunity: Science, v. 310, p. 847-50.

Ha, E. M., C. T. Oh, J. H. Ryu, Y. S. Bae, S. W. Kang, I. H. Jang, P. T. Brey, and W. J. Lee, 2005b, An antioxidant system required for host protection against gut infection in *Drosophila*: Dev Cell, v. 8, p. 125-32.

Halstead, S. B., 2017, Dengvaxia sensitizes seronegatives to vaccine enhanced disease regardless of age: Vaccine, v. 35, p. 6355-6358.

Hammond, A., R. Galizi, K. Kyrou, A. Simoni, C. Siniscalchi, D. Katsanos, M. Gribble, D. Baker, E. Marois, S. Russell, A. Burt, N. Windbichler, A. Crisanti, and T. Nolan, 2016, A CRISPR-Cas9 gene drive system targeting female reproduction in the malaria mosquito vector *Anopheles gambiae*: Nat Biotechnol, v. 34, p. 78-83.

Hammond, A. M., K. Kyrou, M. Bruttini, A. North, R. Galizi, X. Karlsson, N. Kranjc, F. M. Carpi, R. D'Aurizio, A. Crisanti, and T. Nolan, 2017, The creation and selection of mutations resistant to a gene drive over multiple generations in the malaria mosquito: PLoS Genet, v. 13, p. e1007039.

Han, Y. H., Y. J. Luo, Q. Wu, J. Jovel, X. H. Wang, R. Aliyari, C. Han, W. X. Li, and S. W. Ding, 2011, RNA-based immunity terminates viral infection in adult *Drosophila* in the absence of viral suppression of RNA interference: characterization of viral small interfering RNA populations in wild-type and mutant flies: J Virol, v. 85, p. 13153-63.

Harris, A. F., A. R. McKemey, D. Nimmo, Z. Curtis, I. Black, S. A. Morgan, M. N. Oviedo, R. Lacroix, N. Naish, N. I. Morrison, A. Collado, J. Stevenson, S. Scaife, T. Dafa'alla, G. Fu, C. Phillips, A. Miles, N. Raduan, N. Kelly, C. Beech, C. A. Donnelly, W. D. Petrie, and L. Alphey, 2012, Successful suppression of a field mosquito population by sustained release of engineered male mosquitoes: Nat Biotechnol, v. 30, p. 828-30.

Hassing, R. J., I. Leparc-Goffart, S. N. Blank, S. Thevarayan, H. Tolou, G. van Doornum, and P. J. van Genderen, 2010, Imported Mayaro virus infection in the Netherlands: J Infect, v. 61, p. 343-5.

Hawley, W. A., C. B. Pumpuni, R. H. Brady, and G. B. Craig, 1989, Overwintering survival of *Aedes albopictus* (Diptera: Culicidae) eggs in Indiana: J Med Entomol, v. 26, p. 122-9.

Heaton, N. S., and G. Randall, 2011, Dengue virus and autophagy: Viruses, v. 3, p. 1332-41.

Hedges, L. M., J. C. Brownlie, S. L. O'Neill, and K. N. Johnson, 2008, *Wolbachia* and virus protection in insects: Science, v. 322, p. 702.

Hedges, L. M., R. Yamada, S. L. O'Neill, and K. N. Johnson, 2012, The small interfering RNA pathway is not essential for *Wolbachia*-mediated antiviral protection in *Drosophila melanogaster*: Appl Environ Microbiol, v. 78, p. 6773-6.

Heinrich, J. C., and M. J. Scott, 2000, A repressible female-specific lethal genetic system for making transgenic insect strains suitable for a sterile-release program: Proc Natl Acad Sci U S A, v. 97, p. 8229-32.

Heukelbach, J., C. Henrique Alencar, A. A. Kelvin, W. Kleber de Oliviera, and L. Pamplona de Goes Cavalcanti, 2016, Zika virus outbreak in Brazil, The Journal of Infection in Developing Countries, p. 116-120.

Hoffman, A. A., D. Clandy, and J. Duncan, 1996, Naturally-occurring *Wolbachia* infection in *Drosophila simulans* that does not cause cytoplasmic incompatibility, Hereditary, (1), p. 1-8.

Hoffmann, A. A., I. Iturbe-Ormaetxe, A. G. Callahan, B. L. Phillips, K. Billington, J. K. Axford, B. Montgomery, A. P. Turley, and S. L. O'Neill, 2014, Stability of the *w*Mel *Wolbachia* Infection following invasion into *Aedes aegypti* populations: PLoS Negl Trop Dis, v. 8, p. e3115.

Hollien, J., 2013, Evolution of the unfolded protein response: Biochim Biophys Acta, v. 1833, p. 2458-63.

Huang, Y. S., S. Higgs, and D. L. Vanlandingham, 2017, Biological Control Strategies for Mosquito Vectors of Arboviruses: Insects, v. 8, 1. p. e8010021.

Hurst, G. D., A. P. Johnson, J. H. Schulenburg, and Y. Fuyama, 2000, Male-killing *Wolbachia* in *Drosophila*: a temperature-sensitive trait with a threshold bacterial density: Genetics, v. 156, p. 699-709.

Hussain, M., K. S. Akutse, K. Ravindran, Y. Lin, B. S. Bamisile, M. Qasim, C. K. Dash, and L. Wang, 2017, Effects of different temperature regimes on survival of *Diaphorina citri* and its endosymbiotic bacterial communities: Environ Microbiol, v. 19, p. 3439-3449.

Hussain, M., F. D. Frentiu, L. A. Moreira, S. L. O'Neill, and S. Asgari, 2011, *Wolbachia* uses host microRNAs to manipulate host gene expression and facilitate colonization of the dengue vector *Aedes aegypti*: Proc Natl Acad Sci U S A, v. 108, p. 9250-5.

Hussain, M., G. Lu, S. Torres, J. H. Edmonds, B. H. Kay, A. A. Khromykh, and S. Asgari, 2013, Effect of *Wolbachia* on replication of West Nile virus in a mosquito cell line and adult mosquitoes: J Virol, v. 87, p. 851-8.

Ishak, I. H., Z. Jaal, H. Ranson, and C. S. Wondji, 2015, Contrasting patterns of insecticide resistance and knockdown resistance (kdr) in the dengue vectors *Aedes aegypti* and *Aedes albopictus* from Malaysia: Parasit Vectors, v. 8, p. 181.

Izurieta, R., D. DeLacure, A. Izurieta, I. Hoare, and M. Reina Ortiz, 2018, Mayaro virus: the jungle flu, Dovepress, Dovepress.

Jiggins, F. M., 2017, The spread of *Wolbachia* through mosquito populations: PLoS Biol, v. 15, p. e2002780.

Jose, J., J. E. Snyder, and R. J. Kuhn, 2009, A structural and functional perspective of alphavirus replication and assembly: Future Microbiol, v. 4, p. 837-56.

Jose, J., A. B. Taylor, and R. J. Kuhn, 2017, Spatial and Temporal Analysis of Alphavirus Replication and Assembly in Mammalian and Mosquito Cells: MBio, v. 8, p. e02294-16.

Josseran, L., C. Paquet, A. Zehgnoun, N. Caillere, A. Le Tertre, J.-L. Solet, and L. Martine, 2006, Chikungunya Disease Outbreak, Reunion Island, Emerging Infectious Diseases, v.12, 12. p. 1994-1995.

Joubert, D. A., T. Walker, L. B. Carrington, J. T. De Bruyne, D. H. Kien, N. e. T. Hoang, N. V. Chau, I. Iturbe-Ormaetxe, C. P. Simmons, and S. L. O'Neill, 2016, Establishment of a *Wolbachia* Superinfection in *Aedes aegypti* Mosquitoes as a Potential Approach for Future Resistance Management: PLoS Pathog, v. 12, p. e1005434.

Kakumani, P. K., S. S. Ponia, R. K. S, V. Sood, M. Chinnappan, A. C. Banerjea, G. R. Medigeshi, P. Malhotra, S. K. Mukherjee, and R. K. Bhatnagar, 2013, Role of RNA interference (RNAi) in dengue virus replication and identification of NS4B as an RNAi suppressor: J Virol, v. 87, p. 8870-83.

Kambris, Z., A. M. Blagborough, S. B. Pinto, M. S. Blagrove, H. C. Godfray, R. E. Sinden, and S. P. Sinkins, 2010, *Wolbachia* stimulates immune gene expression and inhibits *plasmodium* development in *Anopheles gambiae*: PLoS Pathog, v. 6, p. e1001143.

Kambris, Z., P. E. Cook, H. K. Phuc, and S. P. Sinkins, 2009, Immune activation by life-shortening *Wolbachia* and reduced filarial competence in mosquitoes: Science, v. 326, p. 134-6.

Kawahara, T., M. T. Quinn, and J. D. Lambeth, 2007, Molecular evolution of the reactive oxygen-generating NADPH oxidase (Nox/Duox) family of enzymes: BMC Evol Biol, v. 7, p. 109.

Kerksick, C., and D. Willoughby, 2005, The antioxidant role of glutathione and N-acetyl-cysteine supplements and exercise-induced oxidative stress: J Int Soc Sports Nutr, v. 2, p. 38-44.

Kingsolver, M. B., Z. Huang, and R. W. Hardy, 2013, Insect antiviral innate immunity: pathways, effectors, and connections: J Mol Biol, v. 425, p. 4921-36.

Kitrayapong, P., V. Baimai, and S. L. O'Neill, 2002, Field prevalence of *Wolbachia* in the mosquito vector *Aedes albopictus*: Am J Trop Med Hyg, v. 66, p. 108-11.

Kittayapong, P., K. J. Baisley, R. G. Sharpe, V. Baimai, and S. L. O'Neill, 2002, Maternal transmission efficiency of *Wolbachia* superinfections in *Aedes albopictus* populations in Thailand: Am J Trop Med Hyg, v. 66, p. 103-7.

Klionsky, D. J., and S. D. Emr, 2000, Autophagy as a regulated pathway of cellular degradation: Science, v. 290, p. 1717-21.

Kremer, N., D. Voronin, D. Charif, P. Mavingui, B. Mollereau, and F. Vavre, 2009, *Wolbachia* interferes with ferritin expression and iron metabolism in insects: PLoS Pathog, v. 5, p. e1000630.

Kriesner, P., A. A. Hoffmann, S. F. Lee, M. Turelli, and A. R. Weeks, 2013, Rapid sequential spread of two *Wolbachia* variants in *Drosophila* simulans: PLoS Pathog, v. 9, p. e1003607.

Kumar, S., G. K. Christophides, R. Cantera, B. Charles, Y. S. Han, S. Meister, G. Dimopoulos, F. C. Kafatos, and C. Barillas-Mury, 2003, The role of reactive oxygen species on Plasmodium melanotic encapsulation in *Anopheles gambiae*: Proc Natl Acad Sci U S A, v. 100, p. 14139-44.

Kumar, S., A. Molina-Cruz, L. Gupta, J. Rodrigues, and C. Barillas-Mury, 2010, A peroxidase/dual oxidase system modulates midgut epithelial immunity in *Anopheles gambiae*: Science, v. 327, p. 1644-8.

LaBeaud, A. D., T. Banda, J. Brichard, E. M. Muchiri, P. L. Mungai, F. Mutuku, M, E. Borland, G. Gildengorin, S. Pfeil, C. Teng, Y, K. Long, M. Heise, A. Powers, M, U. Kitron, and C. King, H, 2015, High Rates of O'Nyong Nyong and Chikungunya

Virus Transmission in Coastal Kenya, PLOS Neglected Tropical Diseases, PLOS Neglected Tropical Diseases. v. 9, 2. p. e0003436.

Lazaro, A., W. W. Han, P. Manrique-Saide, L. George, R. Velayudhan, J. Toledo, S. Runge Ranzinger, and O. Horstick, 2015, Community effectiveness of copepods for dengue vector control: systematic review: Trop Med Int Health, v. 20, p. 685-706.

Lefoulon, E., O. Bain, B. L. Makepeace, C. d'Haese, S. Uni, C. Martin, and L. Gavotte, 2016, Breakdown of coevolution between symbiotic bacteria *Wolbachia* and their filarial hosts: PeerJ, v. 4, p. e1840.

Leung, J. Y., M. M. Ng, and J. J. Chu, 2011, Replication of alphaviruses: a review on the entry process of alphaviruses into cells: Adv Virol, v. 2011, p. 249640.

Lindahl, J. F., K. Ståhl, J. Chirico, S. Boqvist, H. T. Thu, and U. Magnusson, 2013, Circulation of Japanese encephalitis virus in pigs and mosquito vectors within Can Tho city, Vietnam: PLoS Negl Trop Dis, v. 7, p. e2153.

Liu, T., Y. Xu, X. Wang, J. Gu, G. Yan, and X. G. Chen, 2017, Antiviral systems in vector mosquitoes: Dev Comp Immunol. v. 83, p. 34-43.

Long, K. C., S. A. Ziegler, S. Thangamani, N. L. Hausser, T. J. Kochel, S. Higgs, and R. B. Tesh, 2011, Experimental transmission of Mayaro virus by *Aedes aegypti*: Am J Trop Med Hyg, v. 85, p. 750-7.

Lu, P., G. Bian, X. Pan, and Z. Xi, 2012, *Wolbachia* Induces Density-Dependent Inhibition to Dengue Virus in Mosquito Cells. PLoS Neglected Tropical Diseases, v. 6, 7. p. e1754.

Lux, S., J. Vilardi, P. Liedo, K. Gaggl, G. Calcagno, and F. Munyiri, 2002, Effects of irradiation on the courtship behavior of medfly (Diptera, Tephritidae) mass reared for the sterile insect technique: Florida Entomologist, v. 85, p. 102-12.

Mains, J. W., C. L. Brelsfoard, R. I. Rose, and S. L. Dobson, 2016, Female Adult *Aedes albopictus* Suppression by *Wolbachia*-Infected Male Mosquitoes: Sci Rep, v. 6, p. 33846.

Martinez, J., B. Longdon, S. Bauer, Y. S. Chan, W. J. Miller, K. Bourtzis, L. Teixeira, and F. M. Jiggins, 2014, Symbionts commonly provide broad spectrum resistance to viruses in insects: a comparative analysis of *Wolbachia* strains: PLoS Pathog, v. 10, p. e1004369.

MATTINGLY, P. F., and L. J. BRUCE-CHWATT, 1954, Morphology and bionomics of *Aëdes* (Stegomyia) pseudoafricanus Chwatt (Diptera, Culicidae), with some notes on the distribution of the subgenus stegomyia in Africa: Ann Trop Med Parasitol, v. 48, p. 183-93.

Mattingly, P. F., and L. J. Brucechwatt, 1954, Morphology and Bionomics of *Aedes*-(Stegomyia)-Pseudoafricanus Chwatt (Diptera, Culicidae), with Some Notes on the Distribution of the Subgenus Stegomyia in Africa, Annals of Tropical Medicine and Parasitology, p. 183-193.

Mbaika, S., J. Lutomiah, E. Chepkorir, F. Mulwa, C. Khayeka-Wandabwa, C. Tigoi, E. Oyoo-Okoth, J. Mutisya, Z. Ng'ang'a, and R. Sang, 2016, Vector competence of *Aedes aegypti* in transmitting Chikungunya virus: effects and implications of extrinsic incubation temperature on dissemination and infection rates: Virol J, v. 13, p. 114.

McClelland, G., 1960, A prelimnary study of the genetics of abdominal color variations in *Aedes aegypti* (L.) (Diptera: Culicidae), Annals of Tropical Medicine and Parasitology, p. 305-320.

McMeniman, C. J., A. M. Lane, A. W. Fong, D. A. Voronin, I. Iturbe-Ormaetxe, R. Yamada, E. A. McGraw, and S. L. O'Neill, 2008, Host adaptation of a *Wolbachia* strain after long-term serial passage in mosquito cell lines: Appl Environ Microbiol, v. 74, p. 6963-9.

McMeniman, C. J., R. V. Lane, B. N. Cass, A. W. Fong, M. Sidhu, Y. F. Wang, and S. L. O'Neill, 2009, Stable introduction of a life-shortening *Wolbachia* infection into the mosquito *Aedes aegypti*: Science, v. 323, p. 141-4.

Medigeshi, G. R., A. J. Hirsch, D. N. Streblow, J. Nikolich-Zugich, and J. A. Nelson, 2008, West Nile virus entry requires cholesterol-rich membrane microdomains and is independent of alphavbeta3 integrin: J Virol, v. 82, p. 5212-9.

Michalak, M., J. M. Robert Parker, and M. Opas, 2002, Ca2+ signaling and calcium binding chaperones of the endoplasmic reticulum: Cell Calcium, v. 32, p. 269-78.

Mikonranta, L., J. Mappes, M. Kaukoniitty, and D. Freitak, 2014, Insect immunity: oral exposure to a bacterial pathogen elicits free radical response and protects from a recurring infection: Front Zool, v. 11, p. 23.

Miller, B. R., and C. J. Mitchell, 1991, Genetic selection of a flavivirus-refractory strain of the yellow fever mosquito *Aedes aegypti*: Am J Trop Med Hyg, v. 45, p. 399-407.

Min, K. T., and S. Benzer, 1997, *Wolbachia*, normally a symbiont of *Drosophila*, can be virulent, causing degeneration and early death: Proc Natl Acad Sci U S A, v. 94, p. 10792-6.

Moghadam, N. N., P. M. Thorshauge, T. N. Kristensen, N. de Jonge, S. Bahrndorff, H. Kjeldal, and J. L. Nielsen, 2017, Strong responses of *Drosophila melanogaster* microbiota to developmental temperature: Fly (Austin), p. 1-12.

Molloy, J. C., and S. P. Sinkins, 2015, *Wolbachia* Do Not Induce Reactive Oxygen Species-Dependent Immune Pathway Activation in *Aedes albopictus*: Viruses, v. 7, p. 4624-39.

Molloy, J. C., U. Sommer, M. R. Viant, and S. P. Sinkins, 2016, *Wolbachia* Modulates Lipid Metabolism in *Aedes albopictus* Mosquito Cells: Appl Environ Microbiol, v. 82, p. 3109-20.

Monnin, D., N. Kremer, C. Berny, H. Henri, A. Dumet, Y. Voituron, E. Desouhant, and F. Vavre, 2016, Influence of oxidative homeostasis on bacterial density and cost of infection in *Drosophila-Wolbachia* symbioses: J Evol Biol, v. 29, p. 1211-22.

Moreira, L. A., I. Iturbe-Ormaetxe, J. A. Jeffery, G. Lu, A. T. Pyke, L. M. Hedges, B. C. Rocha, S. Hall-Mendelin, A. Day, M. Riegler, L. E. Hugo, K. N. Johnson, B. H. Kay, E. A. McGraw, A. F. van den Hurk, P. A. Ryan, and S. L. O'Neill, 2009, A *Wolbachia* symbiont in *Aedes aegypti* limits infection with dengue, Chikungunya, and Plasmodium: Cell, v. 139, p. 1268-78.

Mousson, L., K. Zouache, C. Arias-Goeta, V. Raquin, P. Mavingui, and A. B. Failloux, 2012, The native *Wolbachia* symbionts limit transmission of dengue virus in *Aedes albopictus*: PLoS Negl Trop Dis, v. 6, p. e1989.

Mouton, L., H. Henri, D. Charif, M. Boulétreau, and F. Vavre, 2007, Interaction between host genotype and environmental conditions affects bacterial density in *Wolbachia* symbiosis: Biol Lett, v. 3, p. 210-3.

Moyes, C. L., J. Vontas, A. J. Martins, L. C. Ng, S. Y. Koou, I. Dusfour, K. Raghavendra, J. Pinto, V. Corbel, J. P. David, and D. Weetman, 2017, Contemporary status of insecticide resistance in the major *Aedes* vectors of arboviruses infecting humans: PLoS Negl Trop Dis, v. 11, p. e0005625.

Murdock, C. C., S. Blanford, G. L. Hughes, J. L. Rasgon, and M. B. Thomas, 2014, Temperature alters Plasmodium inhibition by *Wolbachia*: Sci Rep, v. 4, p. 3932.

Myles, K. M., M. R. Wiley, E. M. Morazzani, and Z. N. Adelman, 2008, Alphavirus-derived small RNAs modulate pathogenesis in disease vector mosquitoes: Proc Natl Acad Sci U S A, v. 105, p. 19938-43.

Myllymäki, H., and M. Rämet, 2014, JAK/STAT pathway in *Drosophila* immunity: Scand J Immunol, v. 79, p. 377-85.

Ndoen, E., C. Wild, P. Dale, N. Sipe, and M. Dale, 2011, Dusk to dawn activity patterns of anopheline mosquitoes in West Timor and Java, Indonesia: Southeast Asian J Trop Med Public Health, v. 42, p. 550-61.

Neuhaus, C. P., 2018, Community Engagement and Field Trials of Genetically Modified Insects and Animals: Hastings Cent Rep, v. 48, p. 25-36.

Ng, C. G., I. Coppens, D. Govindarajan, J. Pisciotta, V. Shulaev, and D. E. Griffin, 2008, Effect of host cell lipid metabolism on alphavirus replication, virion morphogenesis, and infectivity: Proc Natl Acad Sci U S A, v. 105, p. 16326-31.

Nguyen, T. H., H. L. Nguyen, T. Y. Nguyen, S. N. Vu, N. D. Tran, T. N. Le, Q. M. Vien, T. C. Bui, H. T. Le, S. Kutcher, T. P. Hurst, T. T. Duong, J. A. Jeffery, J. M. Darbro, B. H. Kay, I. Iturbe-Ormaetxe, J. Popovici, B. L. Montgomery, A. P. Turley, F. Zigterman, H. Cook, P. E. Cook, P. H. Johnson, P. A. Ryan, C. J. Paton, S. A. Ritchie, C. P. Simmons, S. L. O'Neill, and A. A. Hoffmann, 2015, Field evaluation of the establishment potential of *w*MelPop *Wolbachia* in Australia and Vietnam for dengue control: Parasit Vectors, v. 8, p. 563.

NIH, 2017, Zika Virus Vaccines, National Institute of Health. < https://www.niaid.nih.gov/diseases-conditions/zika-vaccines>. Accessed on 20/09/2018.

Niki, E., 2008, Lipid peroxidation products as oxidative stress biomarkers: Biofactors, v. 34, p. 171-80.

Noor Afizah, A., A. Roziah, W. A. Nazni, and H. L. Lee, 2015, Detection of *Wolbachia* from field collected *Aedes albopictus* Skuse in Malaysia: Indian J Med Res, v. 142, p. 205-10.

O'Neill, S. L., M. M. Pettigrew, S. P. Sinkins, H. R. Braig, T. G. Andreadis, and R. B. Tesh, 1997, In vitro cultivation of *Wolbachia* pipientis in an *Aedes albopictus* cell line: Insect Mol Biol, v. 6, p. 33-9.

O'Neill, S. L., P. A. Ryan, A. P. Turley, G. Wilson, K. Retzki, I. Iturbe-Ormaetxe, Y. Dong, N. Kenny, C. J. Paton, S. A. Ritchie, J. Brown-Kenyon, D. Stanford, N. Wittmeier, K. L. Anders, and C. P. Simmons, 2018, Scaled deployment of: Gates Open Res, v. 2, p. 36.

Oliveira, J. H., R. L. Gonçalves, F. A. Lara, F. A. Dias, A. C. Gandara, R. F. Menna-Barreto, M. C. Edwards, F. R. Laurindo, M. A. Silva-Neto, M. H. Sorgine, and P. L. Oliveira, 2011, Blood meal-derived heme decreases ROS levels in the midgut of *Aedes aegypti* and allows proliferation of intestinal microbiota: PLoS Pathog, v. 7, p. e1001320.

Osborne, S. E., I. Iturbe-Ormaetxe, J. C. Brownlie, S. L. O'Neill, and K. N. Johnson, 2012, Antiviral protection and the importance of *Wolbachia* density and tissue tropism in *Drosophila* simulans: Appl Environ Microbiol, v. 78, p. 6922-9.

Osborne, S. E., Y. S. Leong, S. L. O'Neill, and K. N. Johnson, 2009, Variation in antiviral protection mediated by different *Wolbachia* strains in *Drosophila* simulans: PLoS Pathog, v. 5, p. e1000656.

Oslowski, C. M., and F. Urano, 2011, Measuring ER stress and the unfolded protein response using mammalian tissue culture system: Methods Enzymol, v. 490, p. 71-92.

Oxitec, 2018, Friendly *Aedes aegypti* project, Oxitec. < https://www.oxitec.com/friendly-mosquitoes/>. Accessed on 20/09/2018.

Pan, X., G. Zhou, J. Wu, G. Bian, P. Lu, A. S. Raikhel, and Z. Xi, 2012, *Wolbachia* induces reactive oxygen species (ROS)-dependent activation of the Toll pathway to control dengue virus in the mosquito *Aedes aegypti*: Proc Natl Acad Sci U S A, v. 109, p. E23-31.

Pannebakker, B. A., L. P. Pijnacker, B. J. Zwaan, and L. W. Beukeboom, 2004, Cytology of *Wolbachia*-induced parthenogenesis in Leptopilina clavipes (Hymenoptera: Figitidae): Genome, v. 47, p. 299-303.

Paradkar, P. N., L. Trinidad, R. Voysey, J. B. Duchemin, and P. J. Walker, 2012, Secreted Vago restricts West Nile virus infection in *Culex* mosquito cells by activating the Jak-STAT pathway: Proc Natl Acad Sci U S A, v. 109, p. 18915-20.

Paupy, C., H. Delatte, L. Bagny, V. Corbel, and D. Fontenille, 2009, *Aedes albopictus*, an arbovirus vector: from the darkness to the light: Microbes Infect, v. 11, p. 1177-85.

Peleg, J., 1968, Growth of arboviruses in primary tissue culture of *Aedes aegypti* embryos: Am J Trop Med Hyg, v. 17, p. 219-23.

Perera, R., C. Riley, G. Isaac, A. S. Hopf-Jannasch, R. J. Moore, K. W. Weitz, L. Pasa-Tolic, T. O. Metz, J. Adamec, and R. J. Kuhn, 2012, Dengue virus infection perturbs lipid homeostasis in infected mosquito cells: PLoS Pathog, v. 8, p. e1002584.

Petit, M., V. Mongelli, L. Frangeul, H. Blanc, F. Jiggins, and M. C. Saleh, 2016, piRNA pathway is not required for antiviral defense in *Drosophila melanogaster*: Proc Natl Acad Sci U S A, v. 113, p. E4218-27.

Peña, J., and E. Harris, 2011, Dengue virus modulates the unfolded protein response in a time-dependent manner: J Biol Chem, v. 286, p. 14226-36.

Pfeffer, M., and G. Dobler, 2010, Emergence of zoonotic arboviruses by animal trade and migration: Parasit Vectors, v. 3, p. 35.

Phuc, H. K., M. H. Andreasen, R. S. Burton, C. Vass, M. J. Epton, G. Pape, G. Fu, K. C. Condon, S. Scaife, C. A. Donnelly, P. G. Coleman, H. White-Cooper, and L. Alphey, 2007, Late-acting dominant lethal genetic systems and mosquito control: BMC Biol, v. 5, p. 11.

Possas, C., R. Lourenço-de-Oliveira, P. L. Tauil, F. P. Pinheiro, A. Pissinatti, R. V. D. Cunha, M. Freire, R. M. Martins, and A. Homma, 2018, Yellow fever outbreak in Brazil: the puzzle of rapid viral spread and challenges for immunisation: Mem Inst Oswaldo Cruz, v. 113, p. e180278.

Powell, J. R., and W. J. Tabachnick, 2013, History of domestication and spread of *Aedes aegypti*--a review: Mem Inst Oswaldo Cruz, v. 108 Suppl 1, p. 11-7.

Powers, A. M., A. C. Brault, Y. Shirako, E. G. Strauss, W. Kang, J. H. Strauss, and S. C. Weaver, 2001, Evolutionary relationships and systematics of the alphaviruses: J Virol, v. 75, p. 10118-31.

Rainey, S. M., J. Martinez, M. McFarlane, P. Juneja, P. Sarkies, A. Lulla, E. Schnettler, M. Varjak, A. Merits, E. A. Miska, F. M. Jiggins, and A. Kohl, 2016, *Wolbachia* Blocks Viral Genome Replication Early in Infection without a Transcriptional Response by the Endosymbiont or Host Small RNA Pathways: PLoS Pathog, v. 12, p. e1005536.

Rancès, E., T. K. Johnson, J. Popovici, I. Iturbe-Ormaetxe, T. Zakir, C. G. Warr, and S. L. O'Neill, 2013, The toll and Imd pathways are not required for *Wolbachia*-mediated dengue virus interference: J Virol, v. 87, p. 11945-9.

Raquin, V., C. Valiente Moro, Y. Saucereau, F. H. Tran, P. Potier, and P. Mavingui, 2015, Native *Wolbachia* from *Aedes albopictus* Blocks Chikungunya Virus Infection In Cellulo: PLoS One, v. 10, p. e0125066.

Rasgon, J. L., C. E. Gamston, and X. Ren, 2006, Survival of *Wolbachia* pipientis in cell-free medium: Appl Environ Microbiol, v. 72, p. 6934-7.

Receveur, M. C., M. Grandadam, T. Pistone, and D. Malvy, 2010, Infection with Mayaro virus in a French traveller returning from the Amazon region, Brazil, January, 2010: Euro Surveill, v. 15.

Reynolds, K. T., L. J. Thomson, and A. A. Hoffmann, 2003, The effects of host age, host nuclear background and temperature on phenotypic effects of the virulent *Wolbachia* strain popcorn in *Drosophila melanogaster*: Genetics, v. 164, p. 1027-34.

Rezza, G., 2014, Dengue and chikungunya: long-distance spread and outbreaks in naïve areas: Pathog Glob Health, v. 108, p. 349-55.

Riparbelli, M. G., R. Giordano, M. Ueyama, and G. Callaini, 2012, *Wolbachia*-mediated male killing is associated with defective chromatin remodeling: PLoS One, v. 7, p. e30045.

Ritchie, S. A., M. Townsend, C. J. Paton, A. G. Callahan, and A. A. Hoffmann, 2015, Application of wMelPop *Wolbachia* Strain to Crash Local Populations of *Aedes aegypti*: PLoS Negl Trop Dis, v. 9, p. e0003930.

Romo, H., J. L. Kenney, B. J. Blitvich, and A. C. Brault, 2018, Restriction of Zika virus infection and transmission in *Aedes aegypti* mediated by an insect-specific flavivirus: Emerg Microbes Infect, v. 7, p. 181.

Ross, P. A., and A. A. Hoffmann, 2018, Continued Susceptibility of the *w*Mel *Wolbachia* infection in *Aedes aegypti* to Heat Stress Following Field Deployment and Selection: Insects, v. 9, 3. p. e9030078.

Ross, P. A., I. Wiwatanaratanabutr, J. K. Axford, V. L. White, N. M. Endersby-Harshman, and A. A. Hoffmann, 2017, *Wolbachia* Infections in *Aedes aegypti* Differ Markedly in Their Response to Cyclical Heat Stress: PLoS Pathog, v. 13, p. e1006006.

Roy, A., and P. C. Sil, 2012, Tertiary butyl hydroperoxide induced oxidative damage in mice erythrocytes: Protection by taurine: Pathophysiology, v. 19, p. 137-48.

Sasaki, T., and H. Ishikawa, 2000, Transinfection of *Wolbachia* in the mediterranean flour moth, *Ephestia kuehniella*, by embryonic microinjection: Heredity (Edinb), v. 85 ( Pt 2), p. 130-5.

Schnettler, E., M. G. Sterken, J. Y. Leung, S. W. Metz, C. Geertsema, R. W. Goldbach, J. M. Vlak, A. Kohl, A. A. Khromykh, and G. P. Pijlman, 2012, Noncoding flavivirus RNA displays RNA interference suppressor activity in insect and Mammalian cells: J Virol, v. 86, p. 13486-500.

Schultz, M. J., H. M. Frydman, and J. H. Connor, 2018, Dual Insect specific virus infection limits Arbovirus replication in *Aedes* mosquito cells: Virology, v. 518, p. 406-413.

Schwarz, D. S., and M. D. Blower, 2016, The endoplasmic reticulum: structure, function and response to cellular signaling: Cell Mol Life Sci, v. 73, p. 79-94.

Shropshire, J. D., J. On, E. M. Layton, H. Zhou, and S. R. Bordenstein, 2018, One prophage WO gene rescues cytoplasmic incompatibility in: Proc Natl Acad Sci U S A, v. 115, p. 4987-4991.

Silverman, D. J., and L. A. Santucci, 1988, Potential for free radical-induced lipid peroxidation as a cause of endothelial cell injury in Rocky Mountain spotted fever: Infect Immun, v. 56, p. 3110-5.

Simmonds, P., P. Becher, J. Bukh, E. A. Gould, G. Meyers, T. Monath, S. Muerhoff, A. Pletnev, R. Rico-Hesse, D. B. Smith, J. T. Stapleton, and Ictv Report Consortium, 2017, ICTV Virus Taxonomy Profile: Flaviviridae: J Gen Virol, v. 98, p. 2-3.

Singh, B., Singh, P.R., Mohanty, M.K. 2012. Toxicity of a plant based mosquito repellent/killer. Interdicip Toxicol. v. 5, 4. pp. 184- 191.

Sinkins, S. P., 2004, *Wolbachia* and cytoplasmic incompatibility in mosquitoes: Insect Biochem Mol Biol, v. 34, p. 723-9.

Sinkins, S. P., H. R. Braig, and S. L. O'Neill, 1995, *Wolbachia* superinfections and the expression of cytoplasmic incompatibility: Proc Biol Sci, v. 261, p. 325-30.

Siu, R. W., R. Fragkoudis, P. Simmonds, C. L. Donald, M. E. Chase-Topping, G. Barry, G. Attarzadeh-Yazdi, J. Rodriguez-Andres, A. A. Nash, A. Merits, J. K. Fazakerley, and A. Kohl, 2011, Antiviral RNA interference responses induced by Semliki Forest virus infection of mosquito cells: characterization, origin, and frequency-dependent functions of virus-derived small interfering RNAs: J Virol, v. 85, p. 2907-17.

Smit, J. M., B. Moesker, I. Rodenhuis-Zybert, and J. Wilschut, 2011, Flavivirus cell entry and membrane fusion: Viruses, v. 3, p. 160-71.

Sousa, I. P., C. A. Carvalho, D. F. Ferreira, G. Weissmüller, G. M. Rocha, J. L. Silva, and A. M. Gomes, 2011, Envelope lipid-packing as a critical factor for the biological activity and stability of alphavirus particles isolated from mammalian and mosquito cells: J Biol Chem, v. 286, p. 1730-6.

Souza-Neto, J. A., S. Sim, and G. Dimopoulos, 2009, An evolutionary conserved function of the JAK-STAT pathway in anti-dengue defense: Proc Natl Acad Sci U S A, v. 106, p. 17841-6.

Sánchez-San Martín, C., C. Y. Liu, and M. Kielian, 2009, Dealing with low pH: entry and exit of alphaviruses and flaviviruses: Trends Microbiol, v. 17, p. 514-21.

Tchankouo-Nguetcheu, S., H. Khun, L. Pincet, P. Roux, M. Bahut, M. Huerre, C. Guette, and V. Choumet, 2010, Differential protein modulation in midguts of *Aedes aegypti* infected with chikungunya and dengue 2 viruses: PLoS One, v. 5. p. e0013149.

Teixeira, L., A. Ferreira, and M. Ashburner, 2008, The bacterial symbiont *Wolbachia* induces resistance to RNA viral infections in *Drosophila melanogaster*: PLoS Biol, v. 6, p. e2.

Theilacker, C., J. Held, L. Allering, P. Emmerich, J. Schmidt-Chanasit, W. V. Kern, and M. Panning, 2013, Prolonged polyarthralgia in a German traveller with Mayaro virus infection without inflammatory correlates: BMC Infect Dis, v. 13, p. 369.

Thomas, D. D., C. A. Donnelly, R. J. Wood, and L. S. Alphey, 2000, Insect population control using a dominant, repressible, lethal genetic system: Science, v. 287, p. 2474-6.

Thomas, S., J. Verma, M. Woolfit, and S. L. O'Neill, 2018, *Wolbachia*-mediated virus inhibition in mosquito cells is dependent on XRN1-mediated viral RNA degradation and influenced by viral replication rate: PLoS Pathog, v. 14, p. e1006879.

Thomas, S. M., U. Obermayr, D. Fischer, J. Kreyling, and C. Beierkuhnlein, 2012, Low-temperature threshold for egg survival of a post-diapause and non-diapause European aedine strain, *Aedes albopictus* (Diptera: Culicidae): Parasit Vectors, v. 5, p. 100.

Tortosa, P., S. Charlat, P. Labbé, J. S. Dehecq, H. Barré, and M. Weill, 2010, *Wolbachia* age-sex-specific density in *Aedes albopictus*: a host evolutionary response to cytoplasmic incompatibility?: PLoS One, v. 5, p. e9700.

Truitt, A. M., M. Kapun, R. Kaur, and W. J. Miller, 2018, *Wolbachia* modifies thermal preference in *Drosophila melanogaster*: Environ Microbiol. p. e1462-2920 (epub).

Tsetsarkin, K. A., D. L. Vanlandingham, C. E. McGee, and S. Higgs, 2007, A single mutation in chikungunya virus affects vector specificity and epidemic potential: PLoS Pathog, v. 3, p. e201.

Tsetsarkin, K. A., and S. C. Weaver, 2011, Sequential adaptive mutations enhance efficient vector switching by Chikungunya virus and its epidemic emergence: PLoS Pathog, v. 7, p. e1002412.

Turelli, M., and A. A. Hoffmann, 1995, Cytoplasmic incompatibility in *Drosophila* simulans: dynamics and parameter estimates from natural populations: Genetics, v. 140, p. 1319-38.

Turley, A. P., L. A. Moreira, S. L. O'Neill, and E. A. McGraw, 2009, *Wolbachia* infection reduces blood-feeding success in the dengue fever mosquito, *Aedes aegypti*: PLoS Negl Trop Dis, v. 3, p. e516.

Tyagi, B. K., 2016, Advances in Vector Mosquito Control Technologies, with Particular Reference to Herbal Products: Herbal Insecticides, Repellents and Biomedicines: Effectiveness and Commercialization, Springer, New Delhi, p. 1-9.

Ulrich, J. N., J. C. Beier, G. J. Devine, and L. E. Hugo, 2016, Heat Sensitivity of *w*Mel *Wolbachia* during *Aedes aegypti* Development: PLoS Negl Trop Dis, v. 10, p. e0004873.

Umareddy, I., O. Pluquet, Q. Y. Wang, S. G. Vasudevan, E. Chevet, and F. Gu, 2007, Dengue virus serotype infection specifies the activation of the unfolded protein response: Virol J, v. 4, p. 91.

van der Schaar, H. M., M. J. Rust, C. Chen, H. van der Ende-Metselaar, J. Wilschut, X. Zhuang, and J. M. Smit, 2008, Dissecting the cell entry pathway of dengue virus by single-particle tracking in living cells: PLoS Pathog, v. 4, p. e1000244.

Vancini, R., R. Hernandez, and D. Brown, 2015, Progress in Molecular Biology and Translational Science, The Molecular Basis of Viral Infection: Chapter Two - Alphavirus Entry into Host Cells, Elsevier, p. 33-62.

Vancini, R., G. Wang, D. Ferreira, R. Hernandez, and D. T. Brown, 2013, Alphavirus genome delivery occurs directly at the plasma membrane in a time- and temperature-dependent process: J Virol, v. 87, p. 4352-9.

Vega-Rúa, A., C. Schmitt, I. Bonne, J. Krijnse Locker, and A. B. Failloux, 2015, Chikungunya Virus Replication in Salivary Glands of the Mosquito *Aedes albopictus*: Viruses, v. 7, p. 5902-7.

Voronin, D., D. A. Cook, A. Steven, and M. J. Taylor, 2012, Autophagy regulates *Wolbachia* populations across diverse symbiotic associations: Proc Natl Acad Sci U S A, v. 109, p. E1638-46.

Walker, T., P. H. Johnson, L. A. Moreira, I. Iturbe-Ormaetxe, F. D. Frentiu, C. J. McMeniman, Y. S. Leong, Y. Dong, J. Axford, P. Kriesner, A. L. Lloyd, S. A. Ritchie, S. L. O'Neill, and A. A. Hoffmann, 2011, The *w*Mel *Wolbachia* strain blocks dengue and invades caged *Aedes aegypti* populations: Nature, v. 476, p. 450-3.

Wanzira, H., H. Katamba, and D. Rubahika, 2016, Use of long-lasting insecticide-treated bed nets in a population with universal coverage following a mass distribution campaign in Uganda: Malar J, v. 15, p. 311.

Weeks, A. R., and J. A. Breeuwer, 2001, *Wolbachia*-induced parthenogenesis in a genus of phytophagous mites: Proc Biol Sci, v. 268, p. 2245-51.

Wei, G., Y. Lai, G. Wang, H. Chen, F. Li, and S. Wang, 2017, Insect pathogenic fungus interacts with the gut microbiota to accelerate mosquito mortality: Proc Natl Acad Sci U S A, v. 114, p. 5994-5999.

Weinert, L. A., E. V. Araujo-Jnr, M. Z. Ahmed, and J. J. Welch, 2015, The incidence of bacterial endosymbionts in terrestrial arthropods: Proc Biol Sci, v. 282, p. 20150249.

Weiss, R. H., and R. W. Estabrook, 1986, The mechanism of cumene hydroperoxide-dependent lipid peroxidation: the function of cytochrome P-450: Arch Biochem Biophys, v. 251, p. 348-60.

Werren, J. H., 1997, Biology of *Wolbachia*: Annu Rev Entomol, v. 42, p. 587-609.

Werren, J. H., L. Baldo, and M. E. Clark, 2008, *Wolbachia*: master manipulators of invertebrate biology: Nat Rev Microbiol, v. 6, p. 741-51.

Werren, J. H., W. Zhang, and L. R. Guo, 1995, Evolution and phylogeny of *Wolbachia*: reproductive parasites of arthropods: Proc Biol Sci, v. 261, p. 55-63.

White, P. M., L. R. Serbus, A. Debec, A. Codina, W. Bray, A. Guichet, R. S. Lokey, and W. Sullivan, 2017, Reliance of: Genetics, v. 205, p. 1473-1488.

WHO, 2011, West Nile Virus, World Health Organisation.< https://www.who.int/news-room/fact-sheets/detail/west-nile-virus>. Accessed on 20/09/2018.

WHO, 2015, Japanese encephalitis, World Health Organisation. < https://www.who.int/news-room/fact-sheets/detail/japanese-encephalitis>. Accessed on 20/09/2018.

WHO, 2016, Yellow fever factsheet, World Health Organisation. < https://www.who.int/news-room/fact-sheets/detail/yellow-fever>. Accessed on 19/09/2018.

WHO, 2017a, Chikungunya - Italy, World Health Organisation. < https://www.who.int/csr/don/29-september-2017-chikungunya-italy/en/>. Accessed on 19/09/2018.

WHO, 2017b, Chikungunya - Italy, World Health Organisation.< https://www.who.int/csr/don/29-september-2017-chikungunya-italy/en/>. Accessed on 19/09/2018.

WHO, 2017c, Dengue and severe dengue, World Health Organisation.< https://www.who.int/news-room/fact-sheets/detail/dengue-and-severe-dengue>. Accessed on 19/09/2018.

WHO, 2017d, Insecticide-treated mosquito nets: a WHO position statement, IVCC Website < http://www.ivcc.com/sites/ivcc.mrmdev.co.uk/files/content/itnspospaperfinal.pdf>. Accessed on 19/09/2018.

WHO, 2017e, Malaria. < https://www.who.int/malaria/en/>. Accessed on 19/09/2018.

WHO, 2018, Immunization, Vaccines and Biologicals, World Health Organisation, p. Dengue Vaccines.< https://www.who.int/immunization/en/>. Accessed 19/09/2018.

WHO, 2019, Yellow fever outbreak Angola, Democratic Republic of the Congo and Uganda 2016-2017, World Health Organisation.< https://www.who.int/emergencies/yellow-fever/en/>. Accessed on 19/09/2018.

Wielgosz, M. M., R. Raju, and H. V. Huang, 2001, Sequence requirements for Sindbis virus subgenomic mRNA promoter function in cultured cells: J Virol, v. 75, p. 3509-19.

Windbichler, N., M. Menichelli, P. A. Papathanos, S. B. Thyme, H. Li, U. Y. Ulge, B. T. Hovde, D. Baker, R. J. Monnat, A. Burt, and A. Crisanti, 2011, A synthetic homing endonuclease-based gene drive system in the human malaria mosquito: Nature, v. 473, p. 212-5.

WMP, 2018, The World Mosquito Program's project sites around the world., World Mosquito Program.< https://www.worldmosquitoprogram.org/>. Accessed on 20/09/2018.

Wong, Z. S., J. C. Brownlie, and K. N. Johnson, 2015, Oxidative stress correlates with *Wolbachia*-mediated antiviral protection in *Wolbachia-Drosophila* associations: Appl Environ Microbiol, v. 81, p. 3001-5.

Wong, Z. S., L. M. Hedges, J. C. Brownlie, and K. N. Johnson, 2011, *Wolbachia*-mediated antibacterial protection and immune gene regulation in *Drosophila*: PLoS One, v. 6, p. e25430.

Woolfit, M., I. Iturbe-Ormaetxe, J. C. Brownlie, T. Walker, M. Riegler, A. Seleznev, J. Popovici, E. Rancès, B. A. Wee, J. Pavlides, M. J. Sullivan, S. A. Beatson, A. Lane, M. Sidhu, C. J. McMeniman, E. A. McGraw, and S. L. O'Neill, 2013, Genomic evolution of the pathogenic *Wolbachia* strain, *w*MelPop: Genome Biol Evol, v. 5, p. 2189-204.

Wyss, J. H., 2000, Screwworm eradication in the Americas: Ann N Y Acad Sci, v. 916, p. 186-93.

Xi, Z., J. L. Dean, C. Khoo, and S. L. Dobson, 2005a, Generation of a novel *Wolbachia* infection in *Aedes albopictus* (Asian tiger mosquito) via embryonic microinjection: Insect Biochem Mol Biol, v. 35, p. 903-10.

Xi, Z., C. C. Khoo, and S. L. Dobson, 2005b, *Wolbachia* establishment and invasion in an *Aedes aegypti* laboratory population: Science, v. 310, p. 326-8.

Xi, Z., C. C. Khoo, and S. L. Dobson, 2006, Interspecific transfer of *Wolbachia* into the mosquito disease vector *Aedes albopictus*: Proc Biol Sci, v. 273, p. 1317-22.

Xi, Z., J. L. Ramirez, and G. Dimopoulos, 2008, The *Aedes aegypti* toll pathway controls dengue virus infection: PLoS Pathog, v. 4, p. e1000098.

Xiao, F. Z., Y. Zhang, Y. Q. Deng, S. He, H. G. Xie, X. N. Zhou, and Y. S. Yan, 2014, The effect of temperature on the extrinsic incubation period and infection rate of dengue virus serotype 2 infection in *Aedes albopictus*: Arch Virol, v. 159, p. 3053-7.

Yactayo, S., J. E. Staples, V. Millot, L. Cibrelus, and P. Ramon-Pardo, 2016, Epidemiology of Chikungunya in the Americas: J Infect Dis, v. 214, p. S441-S445.

Yamanaka, A., S. Thongrungkiat, P. Ramasoota, and E. Konishi, 2013, Genetic and evolutionary analysis of cell-fusing agent virus based on Thai strains isolated in 2008 and 2012: Infect Genet Evol, v. 19, p. 188-94.

Ye, Y. H., M. Woolfit, E. Rancès, S. L. O'Neill, and E. A. McGraw, 2013, *Wolbachia*-associated bacterial protection in the mosquito *Aedes aegypti*: PLoS Negl Trop Dis, v. 7, p. e2362.

Zanluca, C., V. C. Melo, A. L. Mosimann, G. I. Santos, C. N. Santos, and K. Luz, 2015, First report of autochthonous transmission of Zika virus in Brazil: Mem Inst Oswaldo Cruz, v. 110, p. 569-72.

Zhang, G., M. Hussain, S. L. O'Neill, and S. Asgari, 2013, *Wolbachia* uses a host microRNA to regulate transcripts of a methyltransferase, contributing to dengue virus inhibition in *Aedes aegypti*: Proc Natl Acad Sci U S A, v. 110, p. 10276-81.

Zhang, H., M. U. Rehman, K. Li, H. Luo, Y. Lan, F. Nabi, L. Zhang, M. K. Iqbal, S. Zhu, M. T. Javed, Y. Chamba, and J. K. Li, 2017, Epidemiologic Survey of Japanese Encephalitis Virus Infection, Tibet, China, 2015: Emerg Infect Dis, v. 23, p. 1023-1024.

Zug, R., and P. Hammerstein, 2015, *Wolbachia* and the insect immune system: what reactive oxygen species can tell us about the mechanisms of *Wolbachia*-host interactions: Front Microbiol, v. 6, p. 1201.

Wong, Z. S., L. M. Hedges, J. C. Brownlie, and K. N. Johnson, 2011, *Wolbachia*-mediated antibacterial protection and immune gene regulation in *Drosophila*: PLoS One, v. 6, p. e25430.

Woolfit, M., I. Iturbe-Ormaetxe, J. C. Brownlie, T. Walker, M. Riegler, A. Seleznev, J. Popovici, E. Rancès, B. A. Wee, J. Pavlides, M. J. Sullivan, S. A. Beatson, A. Lane, M. Sidhu, C. J. McMeniman, E. A. McGraw, and S. L. O'Neill, 2013, Genomic evolution of the pathogenic *Wolbachia* strain, *w*MelPop: Genome Biol Evol, v. 5, p. 2189-204.

Wyss, J. H., 2000, Screwworm eradication in the Americas: Ann N Y Acad Sci, v. 916, p. 186-93.

Xi, Z., C. C. Khoo, and S. L. Dobson, 2005, *Wolbachia* establishment and invasion in an *Aedes aegypti* laboratory population: Science, v. 310, p. 326-8.

Xi, Z., C. C. Khoo, and S. L. Dobson, 2006, Interspecific transfer of *Wolbachia* into the mosquito disease vector *Aedes albopictus*: Proc Biol Sci, v. 273, p. 1317-22.

Xi, Z., J. L. Ramirez, and G. Dimopoulos, 2008, The *Aedes aegypti* toll pathway controls dengue virus infection: PLoS Pathog, v. 4, p. e1000098.

Yactayo, S., J. E. Staples, V. Millot, L. Cibrelus, and P. Ramon-Pardo, 2016, Epidemiology of Chikungunya in the Americas: J Infect Dis, v. 214, p. S441-S445Ye, Y. H., M. Woolfit, E. Rancès, S. L. O'Neill, and E. A. McGraw, 2013, *Wolbachia*-associated bacterial protection in the mosquito *Aedes aegypti*: PLoS Negl Trop Dis, v. 7, p. e2362.

Zanluca, C., V. C. Melo, A. L. Mosimann, G. I. Santos, C. N. Santos, and K. Luz, 2015, First report of autochthonous transmission of Zika virus in Brazil: Mem Inst Oswaldo Cruz, v. 110, p. 569-72.

Zhang, G., M. Hussain, S. L. O'Neill, and S. Asgari, 2013, *Wolbachia* uses a host microRNA to regulate transcripts of a methyltransferase, contributing to dengueZug, R., and P. Hammerstein, 2015, *Wolbachia* and the insect immune system: what reactive oxygen species can tell us about the mechanisms of *Wolbachia*-host interactions: Front Microbiol, v. 6, p. 1201.